Handbook T-XV
CIERMMI Women in Science Engineering and Technology

MARROQUÍN-DE JESÚS, Ángel
OLIVARES-RAMÍREZ, Juan Manuel
CRUZ-RAMÍREZ, Marisela
CRUZ-CARPIO, Luis Eduardo

Coordinators

ECORFAN®

ECORFAN®

Coordinators
MARROQUÍN-DE JESÚS, Ángel. PhD
OLIVARES-RAMÍREZ, Juan Manuel. PhD
CRUZ-RAMÍREZ, Marisela. PhD
CRUZ-CARPIO, Luis Eduardo. BsC

Editor in Chief
VARGAS-DELGADO, Oscar. PhD

Executive Director
RAMOS-ESCAMILLA, María. PhD

Editorial Director
PERALTA-CASTRO, Enrique. MsC

Web Designer
ESCAMILLA-BOUCHAN, Imelda. PhD

Web Diagrammer
LUNA-SOTO, Vladimir. PhD

Editorial Assistant
TREJO-RAMOS, Iván. BsC

Translator
DÍAZ-OCAMPO, Javier. BsC

Philologist
RAMOS-ARANCIBIA, Alejandra. BsC

ISBN: 978-607-8695-58-4
ECORFAN Publishing Label: 607-8695
HET Control Number: 2021-10
HET Classification (2021): 251021-1006

Handbooks

Definition of Handbooks

Scientific Objectives

To support the International Scientific Community in its written production of Science, Technology and Innovation in the CONACYT and PRODEP research areas.

ECORFAN-Mexico, S.C. is a Scientific and Technological Company in contribution to the formation of Human Resources focused on the continuity in the critical analysis of International Research and is attached to the RENIECYT of CONACYT with number 1702902, its commitment is to disseminate research and contributions of the International Scientific Community, academic institutions, agencies and entities of the public and private sectors and contribute to the linkage of researchers who perform scientific activities, technological developments and training of specialized human resources with governments, businesses and social organizations.

To encourage the interlocution of the International Scientific Community with other study centres in Mexico and abroad and to promote a wide incorporation of academics, specialists and researchers to the serial publication in Science Niches of Autonomous Universities - State Public Universities - Federal IES - Polytechnic Universities - Technological Universities - Federal Technological Institutes - Teacher Training Colleges - Decentralised Technological Institutes - Intercultural Universities - S&T Councils - CONACYT Research Centres.

Scope, Coverage and Audience

Handbooks is a product edited by ECORFAN-Mexico S.C. in its Holding with repository in Mexico, it is a refereed and indexed scientific publication. It admits a wide range of contents that are evaluated by academic peers by the double-blind method, on topics related to the theory and practice of the CONACYT and PRODEP research areas respectively with diverse approaches and perspectives, which contribute to the dissemination of the development of Science, Technology and Innovation that allow arguments related to decision-making and influence the formulation of international policies in the field of Science. The editorial horizon of ECORFAN-Mexico® extends beyond academia and integrates other segments of research and analysis outside that field, as long as they meet the requirements of argumentative and scientific rigour, in addition to addressing issues of general and current interest of the International Scientific Society.

Editorial Board

Arbitration Committee

Assignment of Rights

By submitting a Scientific Work to ECORFAN Handbooks, the author undertakes not to submit it simultaneously to other scientific publications for consideration. To do so, the author must complete the Originality Form for his or her Scientific Work.

The authors sign the Authorisation Form for their Scientific Work to be disseminated by the means that ECORFAN-Mexico, S.C. in its Holding Mexico considers pertinent for the dissemination and diffusion of their Scientific Work, ceding their Scientific Work Rights.

Declaration of Authorship

Indicate the name of 1 Author and a maximum of 3 Co-authors in the participation of the Scientific Work and indicate in full the Institutional Affiliation indicating the Unit.

Identify the name of 1 author and a maximum of 3 co-authors with the CVU number -PNPC or SNI-CONACYT- indicating the level of researcher and their Google Scholar profile to verify their citation level and H index.

Identify the Name of 1 Author and 3 Co-authors maximum in the Science and Technology Profiles widely accepted by the International Scientific Community ORC ID - Researcher ID Thomson - arXiv Author ID - PubMed Author ID - Open ID respectively.

Indicate the contact for correspondence to the Author (Mail and Telephone) and indicate the Contributing Researcher as the first Author of the Scientific Work.

Plagiarism Detection

All Scientific Works will be tested by the PLAGSCAN plagiarism software. If a Positive plagiarism level is detected, the Scientific Work will not be sent to arbitration and the receipt of the Scientific Work will be rescinded, notifying the responsible Authors, claiming that academic plagiarism is typified as a crime in the Penal Code.

Refereeing Process

All Scientific Works will be evaluated by academic peers using the Double Blind method. Approved refereeing is a requirement for the Editorial Board to make a final decision which will be final in all cases. MARVID® is a spin-off brand of ECORFAN® specialised in providing expert reviewers all of them with PhD degree and distinction of International Researchers in the respective Councils of Science and Technology and the counterpart of CONACYT for the chapters of America-Europe-Asia-Africa and Oceania. The identification of authorship should only appear on a first page, which can be removed, in order to ensure that the refereeing process is anonymous and covers the following stages: Identification of ECORFAN Handbooks with their author occupancy rate - Identification of Authors and Co-authors - PLAGSCAN Plagiarism Detection - Review of Authorisation and Originality Forms-Assignment to the Editorial Board - Assignment of the pair of Expert Referees - Notification of Opinion - Statement of Observations to the Author - Modified Scientific Work Package for Editing - Publication.

ECORFAN CIERMMI Women in Science

Volume XV

The Handbook will offer volumes of selected contributions from researchers who contribute to the scientific dissemination activity of the Colegio de Ingenieros en Energías Renovables de Querétaro A.C. in their areas of research in Engineering and Technology. In addition to having a total evaluation, in the hands of the directors of the Colegio de Ingenieros en Energías Renovables de Querétaro A.C., the quality and timeliness of its chapters, each individual contribution was refereed to international standards (RESEARCH GATE, MENDELEY, GOOGLE SCHOLAR and REDIB), the Handbook thus proposes to the academic community, recent reports on new developments in the most interesting and promising areas of research in the Engineering and Technology.

For future volumes:
http://www.ecorfan.org/handbooks/

MARROQUÍN-DE JESÚS, Ángel. PhD
OLIVARES-RAMÍREZ, Juan Manuel. PhD
CRUZ-RAMÍREZ, Marisela. PhD
CRUZ-CARPIO, Luis Eduardo. BsC

Coordinators

CIERMMI Women in Science T-XV Engineering and Technology *Handbooks*

Colegio de Ingenieros en Energías Renovables de Querétaro A.C – Mexico. October, 2021

DOI: 10.35429/H.2021.6.1.180

Preface

In recent years, society has achieved a better quality of life; this has been possible thanks to scientific and technological advances. Among the advances that have allowed us to move forward is, without a doubt, the development of the vaccine against the SARS-CoV-2 virus. The method used for the synthesis of this vaccine was developed by Ugur Sahin and Öezlem Türeci, founders of BioNTech. Yes, behind the scientific development of greatest impact and relevance in recent years are a man and a woman. This scientific development was possible thanks to both of them, and here it is important to highlight the quality of women in science related to seeing issues from another perspective.

Therefore, the union of their strengths and their differences made it possible to have a vaccine that makes it possible to return to life without confinement, without fear of going out, and with the possibility of enjoying it. Thus, the role of women in science is not only valuable, but fundamental to solve the problems that afflict us today. In this context, I can only thank and congratulate the women who today, thanks to their training, discipline and commitment, are giving us this wonderful work of science. I am sure that more challenges will come, but always counting on them, we will come out ahead. My most sincere appreciation and admiration.

DOMÍNGUEZ-CUELLO, Alma Delia M.D.
Executive Director Querétaro Energy Cluster

Introduction

The Colegio de Ingenieros en Energías Renovables de Querétaro A.C (CIER-QUERÉTARO), and its chapters of Renewable Energy, Industrial Maintenance, Mechatronics and Computer Science, technical sponsors of the International Interdisciplinary Congress on Renewable Energy, Maintenance, Mechatronics and Computer Science, CIERMMI 2021 has as general objective to establish a space for discussion and reflection on issues related to the areas of: renewable energy, industrial maintenance, mechatronics and computer science with the participation of students, professors, researchers and national and international speakers, promoting the formation and consolidation of research networks. Contributing to provide a space for dissemination and discussion of the presentations of students, graduates, academics and researchers, representatives of various higher education institutions, research centers in our country, as well as educational institutions beyond our borders. Promoting the formation of research networks between different institutions. Offering a space for undergraduate, master's, doctoral and postdoctoral students, in which they can present the progress of the research they carry out in their different educational centers. Providing a space in which study groups and members of academic bodies, linked to the curricular program of renewable energy, industrial maintenance, mechatronics and computer science careers, can present the research work developed within their institution and in collaboration with other national or international educational institutions. Establishing a training space for the attendees, through the development of specific lectures and conferences.

This volume, Women in Science T-XV-2021 contains 10 refereed chapters dealing with these issues, chosen from among the contributions, we gathered some researchers and graduate students from the 32 states of our country. We thank the reviewers for their feedback that contributed greatly in improving the book chapters for publication in these proceedings by reviewing the manuscripts that were submitted.

As the first chapter, *Lozano, Galicia and Figueroa* present Biogas Production, through low-cost tubular system for energy in the Tlalmanalco municipality..., as the second chapter, *Cerón, Romero and Martínez*, will talk about Bifunctional catalysts applied to produce biodiesel from waste cooking oil. as third chapter, *Alanis, Ávila, Romero and Natividad*, present Biodiesel production as an alternative to reduce the environmental impact of University food courts, as fourth chapter, *Peña, Hurtado, Romero and Natividad* propose Absorption and reaction of CO2 in capillaries, as fifth chapter, *Villagrán, Siordia, Cuéllar and Patiño* perform Mechanical characterization of the L4 and L5 lumbar vertebrae, as sixth chapter, *Hernández, Mex, Ortiz and Castillo* develop Applied study of training projects as a learning strategy, as seventh chapter, *Antonio, Purata, Vázquez and Trejo* discuss Remediation of soils contaminated by hydrocarbons using a polymeric material (carboxymethylcellulose gel), in eighth chapter, *Cuahuizo, Santacruz and Santacruz* present A review on electrospinning technologies and their potential use in the biomedical industry, as ninth chapter, *Lizárraga, Vázquez. and Bigurra* performed Green infrastructure: an ally to improve urban runoff management in semi-arid areas and as the last chapter, *Santacruz & Santacruz* focus on Microencapsulation of acachul (Ardisia Compressa) extract by spray drying using different polymeric materials as encapsulating agents.

MARROQUÍN-DE JESÚS, Ángel
OLIVARES-RAMÍREZ, Juan Manuel
CRUZ-RAMÍREZ, Marisela
CRUZ-CARPIO, Luis Eduardo

Coordinators

Content

Page

Chapter 1 Biogas Production, through low-cost tubular system for energy in the Tlalmanalco municipality

Capítulo 1 Producción de biogás, por medio de sistemas tubulares de bajo costo, para la generación de energía en el municipio de Tlalmanalco

LOZANO-CAMARGO, Maria Luisa†*, GALICIA-LUIS, Laura and FIGUEROA-DELGADO, Pablo Jesús

Tecnológico de Estudios Superiores del Oriente del Estado de México. Dept. Environmental Engineering, Paraje San Isidro S / N, Barrio de Tecamachalco, Los Reyes La Paz, State of Mexico. CP 56400, Mexico.
Universidad Autónoma Metropolitana-Iztapalapa, Department of Chemistry. Av. Michoacán y la Purísima, Col. Vicentina. CP 09340, Mexico.

1st Author ID: *Maria Luisa Lozano-Camargo* / **ORD ID**: 00-0002-0777-6392, **CVU CONACYT ID**: 46638

1st Co-Author ID: *Laura, Galicia-Luis* / **CVU CONACYT ID**: 120121

2nd Co-Author ID: *Pablo Jesús, Figueroa- Delgado* / **ORD ID**: 0000-0002-7875-8669

DOI: 10.35429/H.2021.6.1.19

M. Lozano, L. Galicia and P. Figueroa.

*Maria.lozano@tesoem.edu.mx

A. Marroquín, J. Olivares, M. Ramírez and L. Cruz (Coord) Engineering and Technology. Handbooks-©ECORFAN-México, Querétaro, 2021.

Abstract

Biogas is a renewable biofuel product of anaerobic digestion, of the decomposition of organic matter (biomass) generating methane (CH_4) with high energy value that represents 50 and 75% gas, it is an excellent ecological alternative in energy production, in order to take advantage of the biogas production from human and animals generated feces in the municipality of Tlalmanalco in the State of Mexico, a theoretical study was carried out in order to verify how feasible it is to implement a system of tubular biodigesters of low cost favoring the community with the lowest resources, as well as reducing the environmental impact of CO_2 emissions.

Tubular biodigester, Fecal matter, Energy Systems, Biogas, Municipality of Tlalmanalco

Resumen

El biogás es un biocombustible renovable producto de la digestión anaerobia, de la descomposición de materia orgánica (biomasa) generando metano (CH_4) con alto valor energético que representa un 50 y un 75%de gas, es una excelente alternativa ecológica en la producción energética, con la finalidad de aprovechar la producción de biogás procedente de las heces fecales generadas por los humanos y animales en el municipio de Tlalmanalco del Estado de México, se realizó un estudio teórico con la finalidad de verificar que tan viable es implementar un sistema de biodigestores tubulares de bajo costo favoreciendo a la comunidad de más bajos recursos, así como a disminuir el impacto ambiental que se tiene por las emisiones de CO_2.

Biodigestor tubular, Materia fecal, Sistemas energéticos, Biogás, Municipio de Tlalmanalco

1. Introduction

Sometimes organic waste does not receive adequate treatment for final disposal, generating various harmful events, such as the spread of diseases that affect human populations or the transmission of pollutants to environmental ecosystems. Often these wastes from human or animal activities are deposited in vacant lots, rivers, ravines, or open-air dumps, where they generate waste. One way to rescind these affectations is using biogas generating systems, with the purpose of treating waste through controlled anaerobic biological processes, where the result is a biogas rich in methane and carbon dioxide, capable of serving as a biofuel to obtain various benefits. Biodigesters are elementary systems to obtain a biogas with the ideal composition to generate energy. There are several models of biodigesters, some have more advanced technological features, but this research proposes the use of low-cost tubular biodigesters as implementation, to the various problems and theoretical solutions, which are suitable to the social, economic and environmental context of the municipality of Tlalmanalco through minimal investment in materials, installation and maintenance, which is focused on sustainability, promoting long-term benefits throughout the community, especially in areas most lacking in economic resources and services, to directly influence sustainable development.

General Objectives

Analyze the characteristics and energy benefits of low-cost tubular systems, for their future implementation in economically vulnerable areas in the municipality of Tlalmanalco.

Specific objectives

- Determine the sustainable potential of Tlalmanalco, to analyze the projection feasibility of biogas generating systems.

- Energy benefits of tubular systems in the population of the municipality of Tlalmanalco.

Methodology

Several scientific articles on biogas generation focused on low-cost tubular systems were analyzed in order to extract relevant information, with the purpose of making known some characteristics about the sustainable energy potential of these systems in order to promote their implementation, acceptance and benefits in the society of Tlalmanalco.

2 Development and method

Anaerobic digestion

Biogas is a gas that is produced under natural conditions, as well as in places designed and established by man, from a series of metabolic processes generating biodegradation reactions of organic matter, by the action of microorganisms (methanogenic bacteria). In anaerobic conditions (without oxygen) where a mixture of compound gases is obtained, which have the capacity to generate biomass energy made up of methane (CH_4), carbon dioxide (CO_2), and a lower proportion of hydrogen (H_2), hydrogen sulfide. During the fermentation process, various bacterial consortia are required that depend on the energy provided by the substrate, which is essential for the degradation of the matter that is transformed into biomass. Thus, the formation of biogas depends on a fundamental process that takes place through the degradation of organic matter; where biodigestion is an intricate system due to the various chemical and biological changes and the various bacterial microorganisms that interact in the process in a synchronized way. (Lorenzo et. al, 2005; Torres, 2021)

Elementary process biology

Bacterial microorganisms require nutrients extracted from organic matter to break down the polymers found in the macromolecules available in the organic material, and enzymes that they use to degrade the cellular structure to obtain acetic acid. (Leon, 1991). This is subsequently transformed into methane (CH_4) and carbon dioxide (CO_2)

Phases of biodigestion

In 1991 Leon considered that the usual anaerobic degradation process consisted of three main stages for both solid waste or sludge (hydrolysis, acidogenesis, methanogenesis) and two for liquid residues (acidogenesis, methanogenesis). Currently, the 4 stages are considered important for obtaining biodigestion, which are defined below

Hydrolysis: The macromolecules (proteins, carbohydrates, and lipids) are hydrolyzed by means of enzymes that require degrading the cellular structure to obtain simpler compounds such as sugars, amino acids or fatty acids. "Proteins are hydrolyzed into peptides and amino acids by the action of proteolytic enzymes called proteases."

Acidogenesis: The product compounds of the hydrolysis are transformed into acid by means of "soluble molecules that can be used directly by methanogenic bacteria in acetic acid and in smaller organic compounds (propanoicobutyric, valeric, lactic and ethanol)".

Acetogenesis: Compound’s products of acidogenesis are transformed by "acetogenic bacteria, where they are transformed into simpler components, such as hydrogen (H_2) and carbon dioxide (CO_2)".

Methanogenesis: The Archeo methanogenic bacteria generate methane gas, through the metabolization of “monocarbon substrates united by the union of acetate covalent bonds, H_2 /CO_2, format, methanol and some methylamines" and the resulting methane is given mostly by means of acetic acid dexcarboxylation (Varnero, 2011).

In Figure 1.1. the diagram of the fundamental phases that describe the anaerobic digestion process is shown.

Figure 1 Phases of anaerobic digestion (Pérez, 2010)

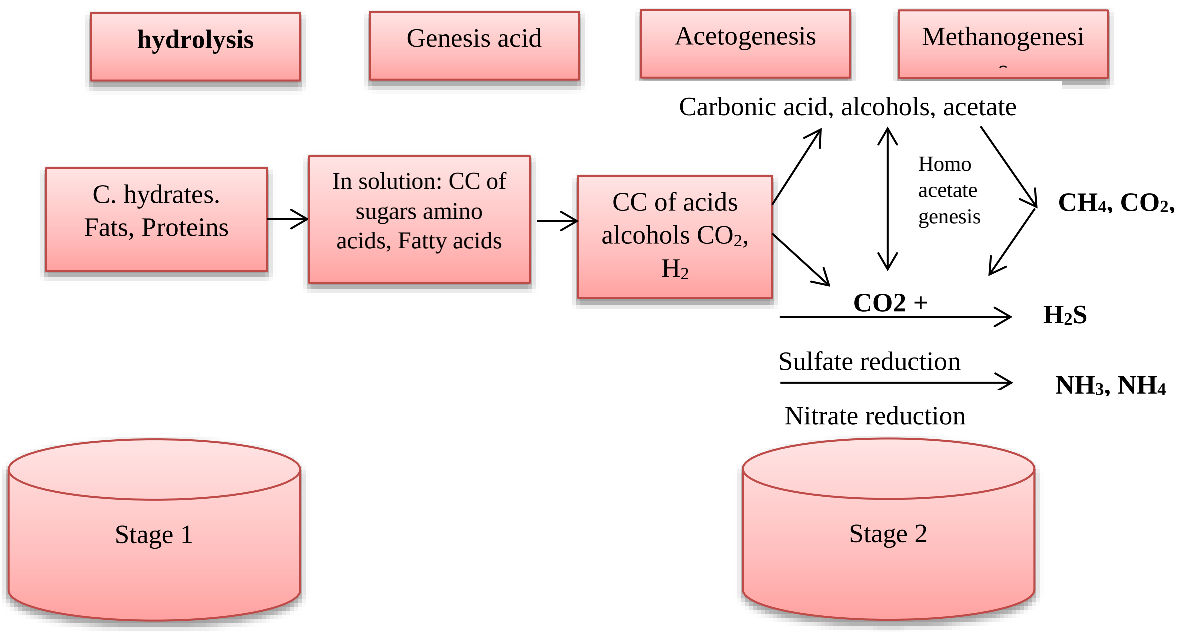

The phases and main characteristics of the most common bacteria generated during the biodigestion process that interfere in the anaerobic phases are shown in Table 1.1.

Table 1.1 Characteristics of common bacteria in the biodigestion process

Phases	Bacteria	Features
Hydrolysis	*Lactobacillus, Propioni- bacterium, Sphingomonas, Sporobacterium, Megasphaera, Bifidobacterium*	Series of bacteria that are responsible for degrading the complex bonds of macromolecules (proteins, cellulose, lignin, and fatty acids).
Acidogenesis	*Clostridium, Paenibacillus and Ruminococcus*	Bacterial consortium that is responsible for metabolizing "sugars, amino acids and lipids into organic acids, alcohols and ketones, acetate, CO_2 and H_2".
Acetogenesis	*Syntrophobacter wolinii, Syntrophomonas wolfei,*	This bacterial group "fatty acids with 4 to 8 carbon atoms, convert propionic, butyric and some alcohols into acetate, hydrogen and carbon dioxide, which is used in methanogenesis"
Methanogenesis	*Methanobacterium, Methanospirillum hungatii, and Methanosarcina.*	Strict methane-forming anaerobic bacteria, their main characteristic is that they are very susceptible to drastic changes in temperature.

Source: :(Varnero, 2011; Constanza, et al., 2015)

Result of biodigestion

Once the biodigestion process is finished, methane gas (CH_4), carbon dioxide (CO_2), and trace compounds such as hydrogen sulfide (H_2S) are obtained as the main product, and as residues of the organic raw material inside the Biodigester is transformed into a semi-liquid fertilizer, which generates sludge or biol, which are used as a mineralizer for crops and plants. It is important to control some parameters (climatic conditions, altitude, composition of the organic substrate, biological conditions) in order to obtain adequate methane, as well as the various resulting compounds; By not correctly stabilizing the parameters inside the biodigester, the process can be inhibited, obtaining biogas with lower capacity to produce biofuel with little efficiency to generate energy.

Biodigestion process conditions

pH*:* This parameter is important to avoid that the substrate during the anaerobic digestion process goes through acidic and/or basic conditions, the optimal pH quantification should be in the range of 6.5 to 7.5, to avoid inhibition during the process since methanogenic microorganisms are more susceptible to pH variations than any other anaerobic microorganism. (Varnero, 2011; Olaya, *et al*, 2009).

Temperature (T): The temperature for anaerobic digestion processes is a very important parameter, due to the fact that, at the beginning of the biodigestion phase, the bacterial microorganisms adapt to the temperature changes that occur inside the biodigester, if this is not the other case bacterial consortium is in charge of surveying the course to avoid affecting the process. The temperature will determine the retention time for obtaining biogas. At higher temperatures the microorganisms work better, this influences the reduction of the time for obtaining biogas. But if the process is carried out at low temperatures, the microorganisms work less and obtaining biogas takes longer, Varnero indicates that there are three temperature ranges in which different bacterial consortia can work,

Holding time: This is when the process begins with the organic substrate available inside the biodigester, until the anaerobic digestion is completed, thus producing biogas. The retention time depends on the ambient temperature and optimal conditions of the process, therefore the characteristics vary according to the climate of each region, the higher the altitude the temperatures drop steadily, while in regions with lower altitude temperatures increase. The countries farther from the equator, located closer to the poles, have lower temperatures in relation to the countries that are closer to the equator, and that have tropical characteristics such as higher temperatures, the retention times vary as shown in table 1.2.

Table 1.2 N Appropriate retention time for each OM in biodigestion

Environment	Holding time
Psychrophile	> 40
Mesophilic	10 - 40
Thermophilic	<10

Source: Olaya et. al., 2009

Carbon / nitrogen ratio (C/N): Affects the determination of biogas rich in methane and carbon dioxide, the appropriate ratio is between 20: 1 and 30: 1, to make this happen, various materials and/or substrates must be incorporated to achieve an adequate balance, carbon and nitrogen they are essential for the essential life of methanogenic microorganisms (Olaya et. al, 2009; Mori, 2021).

Solid / liquid ratio: It is important to maintain adequate humidity inside the biodigester, so that the fecal matter mixes perfectly and anaerobic digestion takes place. Table 1.3 shows the solid-liquid relationship of some fecal materials.

Table 1.3 Ideal solid-liquid mixture of the most common fecal materials

Manure	Solid: Liquid Ratio
Cow	1: 3
Pork	1: 4
Llama / Sheep / Guinea Pig	1.8-9

Source of consultation: Martí, 2019

Inhibition factors: Compounds (volatile acids, ammonia, nitrogen, agrochemicals), of a toxic nature present during the process, which alter the metabolism of the microorganisms and kill the bacteria, interrupting biodigestion. The maximum permissible amount in concentration that the biodigester must contain of the various compounds is shown in Table 1.4.

Table 1.4 Maximum allowable concentration of compound in the biodigester

Inhibitor Compound	Inhibiting Amount
Sulfates	5000 ppm
Sodium chloride	40,000 ppm
Nitrate	0.05 mg /mL
Copper	100 mg/L
Chrome	200 mg/L
nickel	200-500 mg/L
ABS (synthetic detergent)	20-40 mg/L
sodium	3500-5500 mg/L
Potassium	2500-4500 mg/L
Calcium	2500-4500 mg/L
Magnesium	1000-1500 mg/L

Source of consultation: Canales, et. al., 2010

Biogas: It is a gas that is produced in natural conditions, as in places suitable for man, where biodegradation reactions of organic matter originate, by the action of microorganisms (methanogenic bacteria), in anaerobic conditions (without oxygen), where a mixture of compound gases is obtained, which have the ability to generate biomass energy, consisting of methane (CH_4), carbon dioxide (CO_2), and to a lesser extent hydrogen (H_2), hydrogen sulfide. It is understood as an essential process within the organic matter cycle. Table 1.5 shows the composition of biogas as reported by Varnero in 2008.

Table 1.5 Biogas composition

Composition	55 - 70% methane (CH_4) 30 - 45% carbon dioxide (CO_2) Traces of other gases
Energetic content	6.0 - 6.5 kW h m^3
Fuel equivalent	0.60 - 0.65 L oil / m^3 biogas
Explosion limit	6 - 12% biogas in the air
Ignition temperature	650 - 750 ° C (with CH_4 content mentioned)
Critical pressure	74 - 88 atm
Critical temperature	-82.5 ° C
Norm density	1.2 kg m^{-3}
Smell	Rotten egg (the smell of desulfurized biogas is imperceptible
Molar mass	16,043 kg kmol^{-1}

Source of consultation: Varnero, 2011

Chemical compounds CO_2, N_2, O_2, NH_3, H_2S and their effects on biogas

Carbon dioxide (CO_2) is an essential gaseous component for the formation of methane in the biogas generation process, it is necessary to adequately control CO_2 in order not to acidify the course. It is important to homogeneously disperse the substrate inside the biodigester to improve anaerobic degradation.

Nitrogen (N_2) and oxygen (O_2) are found in a 4-1 ratio in the aeration stages and have the function of expelling hydrogen sulfide (H_2SO_4).

Ammonia (NH_3) is regularly found in minimal quantities (<0.1 mg/m^3) when the organic material used comes from bird droppings and some wastes, which increase the amount of the maximum compound by (1.5 mg/m^3). Exceeding these permitted levels can cause damage to combustion engines.

The presence of hydrogen sulfide in the biogas must be controlled and reduced, since this is a very corrosive acid that damages the components of the biodigesters (piping, valves, etc.). It is important to control the filters to avoid damage to the machinery or turbines used in the conversion of biogas into energy (Pérez, 2010).

Biogas and power generation

Biogas has an important potential to produce heat energy, due to the presence of methane gas (CH_4), which is the main component since it is found in concentrations of 40 to 50%. Even though carbon dioxide (CO_2) is the second gaseous compound present during biodigestion, it is produced in large quantities, so it must be controlled to prevent it from reducing the heat capacity of the biogas, to achieve good combustion. There are other trace compounds in small concentrations of 2% in the biogas composition such as hydrogen (H_2) and hydrogen sulfide (H_2S).

The energy generated by biogas has various energy uses.

- It can be used directly to generate lighting or to heat food through special stoves.
- It is used as a heater inside homes or for livestock use to heat animals in the production process.
- It is used as a fuel to power machinery by means of specialized combustion engines or turbines to generate electrical energy, which can be transmitted to the electrical grid.

That is why many researchers have carried out various studies to obtain biogas for energy use, at the Universidad Nacional Agraria la Molina in Peru, (Torres,2021) carried out an investigation on the way to collect feces from different animals existing on campus annually During the period from 2008 to 2018, collecting 7397 kg / day of various livestock waste, thus obtaining 745 Mwh / year, carried out various physicochemical analyzes (pH, electrical conductivity, density, humidity, ash, calorific value, etc.) derived of the quartering method during the obtaining of the sample, relying on the general equation of the gases they were able to calculate the energy potential, to determine the amount of biogas generated, reached the conclusion that manure of equine and bovine origin generate a greater amount of energy than the feces of poultry and other species in table 1.6, the results obtained from the energy capacity in the generation of biogas in the various substrates are shown .

Table 1.6 Energy capacity for the generation of biogas on various substrates

	Methane (m3 /year)	Energy capacity (MWh/year)
Cattle area	111235.2	1104,565
Poultry area	16448.96	163.3382
Equine area	7490.67	74.38244
Minor species	1995.71	19.8174
Sheep and camelids	6030.46	59.88213
Pig area	71758.72	712,564
-	-	2134.59

Reference Source: Torres, 2021

Environmental benefits of biogas

Biogas reduces deforestation in rural areas and avoids dependence on fossil fuels and electricity. In addition to reducing carbon dioxide and greenhouse gas (GHG) emissions, through the generation of biofuels, which are produced from the natural decomposition of biomass (organic waste). This type of energy reduced in polluting gases is known as renewable energy. (Weber, *et al*., 2012).

The promotion and implementation of projects of biogas generating systems is a form of treatment to reduce methane emissions, which generate organic waste, mainly excrement that is emitted into the atmosphere and contributes to part of the greenhouse effect. "Methane contributes 20% to the anthropogenic greenhouse effect. Among the sources of methane of human origin, more than 50% corresponds to livestock and up to 30% comes from rice cultivation " (Varnero, 2011). Biogas, due to its methanogenic characteristics, has the possibility of producing electrical energy through anaerobic digestion, where the final product is a biofuel that can be used to generate various types of energy.

- Heat energy: using a stove
- Electric power: light, some appliances
- steam: generates energy in different types of machinery

Advantage

- It helps to generate sustainable energy, mainly in dispersed rural communities of extreme poverty, where public electricity facilities are often lacking.
- Reduces CO_2 and other types of polluting gases
- Economic cost
- Generation of fiscal stimuli (green bonds)

Biodigesters

They are sealed containers, designed in order to perform anaerobic degradation processes generated by decomposition, different substrates can be used to fill them, such as animal excrement, sewage and vegetable waste, etc. They have the purpose of generating methane-rich biogas (Avila, 2016). The construction materials are usually varied depending on the climatic conditions, the height of the installation site, the type of soil, budgets, usually "concrete, polyethylene and concrete are used. A biodigester is made up by.

Cargo tank: It conducts the organic matter through a tube generally made of materials resistant to high pressure, towards the center line of the tank.

Gas storage tank: Consists of a circular or square brick construction with a polished concrete finish and a sturdy material bag, is used in the globe digesters. These materials serve to retain the gas in a thermal way so that when availability is required, it can be used.

Discharge tank: It is the part of the pipeline where residual sludge is extracted, generally these sludge are used as fertilizer due to its mineralization characteristics in crops or plants.

Driving line: Quantity of gas to be transported, and the distance between the places where the different processes take place in which plastic, copper or metallic piping is used, depending on the characteristics of the project, as well as the environmental conditions to be determined.

Valves: Two valves are required for the gas, the first will be installed at the beginning of the process and the second at the end of the outlet line, must be made of resistant materials such as PVC or stainless steel.

Traps: The gas must be eliminated from impurities such as sulfuric acid, this in order not to damage any part of the system that does not have the resistance to withstand this type of corrosive compound. (Corona, 2007).

Classification of biodigesters

There are various types of biodigesters, the most common being of the "horizontal and vertical type and of the continuous, semi-continuous, discontinuous" type. (Pascual, *et al*, 2011)

Laptops: They are simple biodigesters that are used in domestic activities, they are built of resistant materials but easy to transport.

Continuous flow: It is one that "allows the continuous transport of organic matter, mainly in vertical digesters, they are used in large-scale projects and have high-tech instrumentation such as agitators and heating."

Semi-continuous flow: They are loaded in short periods of approximately 12 hours, 1 time every 24 hours or every 48 hours, the available load of organic raw material is used constantly on a daily basis. The 3 most common digester models that have the semi-continuous flow feature are Indian, Chinese, and Taiwanese. These digesters are used mainly in rural areas.

Discontinuous flow: The organic matter is loaded and unloaded until the end of the process, it is removed when the gas generation stops, only then can the digester be reloaded, the duration of the process depends on the temperature and the "retention time, in usual conditions the process can last between 2 and 4 months " (Avila, 2016). In the table 1.7, conventional biodigesters are shown.

Table 1.7 Main conventional biodigesters

Biodigester	Characteristics	Advantage	Disadvantages
Floating dome (Hindu)	It is buried vertically in what appears to be a well, its structure has resistant materials such as brick or concrete. This digester has a floating hood that regulates the gas pressure and that rises and falls depending on the volume exerted.	Simple systems to understand. Constant gas pressure.	High construction and maintenance costs.
Fixed dome (china)	They are generally cylindrical containers, which are constructed of resistant materials such as concrete, cement or concrete.	Long lasting time. Withstands drastic weather changes.	Fragmentation of the material due to high internal pressures. For its construction it requires skilled labor.
Tubular Biodigester (Taiwanese)	Regularly, the material used for its construction is polyethylene (PE), or geomembrane (PVC), it has a horizontal tubular shape and is half buried in a trench, to adapt the biodigester in a fixed and safe position.	Accesible price. It is portable and can be easily placed in any difficult access place	Short life time. Breakages due to drastic weather changes (solar tent must be used)

Source of Consultation: Avila, 2016

Tlalmanalco municipal context

Tlalmanalco de Velázquez is a municipality located in the eastern part of the State of Mexico, with the following coordinates 19º 80 '48” and 19º 15' 43” of north latitude and 98º 37 '58” and 98º 51' 20” of west longitude. It is adjacent to the municipalities Puebla (West), Chalco (North), Ixtapaluca and Cocotitlán (West), Amecameca, Ayapango and Tenango del Aire (South). The municipality has a current population of 51,804 inhabitants and a territorial extension of 158 km^2, “due to its extensive forest areas, the municipality focuses on the provision of environmental services such as the maintenance of biomass for carbon capture and the provision of oxygen” (Cervantes, 2011). The general aspects of the municipality of Tlalmanalco are shown in table 1.8.

Table 1.8 General aspects of the Municipality of Tlalmanalco

Important aspects (SAE) of Tlalmanalco	General data
Coordinates	19º 80 '48 ”and 19º 15' 43” of north latitude and 98º 37 '58 ”and 98º 51' 20” of west longitude
Total population (2021)	47,390 inhabitants
Area Km^2	158.58 km
HDI (2015)	0.779%
Poverty (2015)	22,833 inhabitants
Altitude	2400m
GDP (2017)	1253.4
Climate	Temperate coniferous forest
Rural population (2010)	7,746 inhabitants

Source of consultation: Municipal Development Plan Tlalmanalco, 2019

In Figure 1.2, the location of the municipality of Tlalmanalco, obtained via satellite with the support of Google Maps, is shown in a red circle, in order to identify the area where it is intended to install biodigesters to supply the most vulnerable community that do not have service of energy, using low-cost and environmentally friendly energy, in addition to minimizing health illnesses experienced by the population due to poor disposal of feces generated in the municipality.

Figure **1.2** Satellite location of the municipality of Tlalmanalco State of Mexico

Reference source: Google maps, 2021

2030 Agenda for the development of renewable energies

The 2030 agenda is a plan with 17 objectives and 169 goals that will be applied over the next 15 years in order to achieve sustainable development, reducing economic, social and environmental deficiencies. (PNUM, 2019)

Social pillar: Is in charge of analyzing the social and economic conditions required by the families of Tlalmanalco to reduce vulnerable characteristics and social inequality, in order to improve human life. This indicator is measured based on the HDI.

Population: Population: In 2015 Tlalmanalco had a population of 47,390 inhabitants. (Planning Unit of the Municipality of Tlalmanalco, 2019). Table 6, shows the statistical data recorded from the population and housing census in the year 2010 and 2015, regarding the number of inhabitants increased by 1,260 in just 5 years as shown in Table 1.9 almost 0.90% which is remarkably little, however, with this increase more public services are required among them the energy supply.

Table 1.9 Population and Housing Census 2010.

Year	2010	%	2015.	%
Men	22,333	51.78%	22,517	47.51%
women	23,797	51.58%	24,873	52.48%
Total	46,130	100%	47,390	100%

Consulted source: Planning Unit of the Municipality of Tlalmanalco,2019

Poverty: In 2015 Tlalmanalco had 22,833 poor inhabitants, 45.6% of the total population. *Planning (Unit of the Municipality of Tlalmanalco,2019),* (see table 1.10). As can be seen in the table, the number of inhabitants with indices of poverty, moderate poverty and extreme poverty represents almost 91.2% of the population reported by IGECEM in 2015, it is a seriously alarming figure since only 8.8% of its population it can lead a moderate life, which is why this project is aimed at designing and placing biodigesters and supplying energy to the community.

Table 1.10 Tlalmanalco Poverty Report

	Year 2012			Year 2015		
Indicators	**Population**	**%**	**Average deficiency**	**Population**	**%**	**Average deficiency**
Poor population	17,903	41.7%	2.4	22,833	45.6%	2.0
Population with moderate poverty	15,484	34.5%	2.1	19,897	39.7%	1.8
Population with extreme poverty	2,420	6.9%	3.7	2,936	5.9%	3.4

Reference source: Planning Unit of the Municipality of Tlalmanalco. (2019)

Public service housing: The home is the main pillar where the family develops and tasks that influence other social factors are carried out. Understanding the conditions in which the population lives and the services that are provided in a private way or through the Government are of great importance to know what percentage of the population such services in table has 1.11, the data reported by INEGI are shown from the years 2010 to 2015.

Table 1.11 Public Housing Services

Availability of public services in Tlalmanalco		Year 2010		Year 2015	
Households	occupants	Households	Occupants	Households	occupants
Total		11,315	45,599	12,047	47,390
Tubing water					
Have		10,918	43,983	11,875	46,716
They do not have		378	1,509	125	490
Not specified		19	67	47	184
Sewer system					
Have		11,064	44,616	11,803	47,115
They do not have		226	856	122	63
Not specified		25	87	122	212
Electric power					
Have		11,263	45,389	11,976	47,115
They do not have		37	122	16	63
Not specified		fifteen	48	55	212

Consulted source: Planning Unit of the Municipality of Tlalmanalco, 2019

HDI: The human development index is an indicator that determines the economic wealth, as well as the quality of life in a country or an established region, where rigorous aspects are determined to complete a high HDI. Tlalmanalco has a high HDI, its range is determined in an approximate of 0.692 to 0917, (Unit of the municipality of Tlalmanalco, 2019).

As can be seen in Table 1.12, in the health system it has 78.6%, in education 73.5%, income 69.8%, although it is not a municipality with a low HDI, it does require to have better human health quality and better economic income

Table 1.12 Huma0n development index (HDI)

	Health	Education	Entry	HDI
Tlalmanalco	0.786	0.735	0.698	0.739

Source consulted: Planning Unit of the Municipality of Tlalmanalco, 2019

Economic pillar: In the municipality of Tlalmanalco, management systems that favor wealth, social values and respect for the environment must be adapted to obtain sustainable development; therefore, when implementing and using biodigesters for the supply of energy, it will favor its economic income.

GDP: The gross domestic product is an indicator of the economic growth of a population, which is acquired through goods and services completed in a set time (see table 1.13). "Tlalmanalco in 2017 had an approximate GDP of 1,254 million pesos". (*Planning Unit of the Municipality of Tlalmanalco, 2019).*

Table 1.13 Gross domestic product of the municipality of Tlalmanalco (GDP)

GDP of Tlalmanalco		
Economic activity sector	**2016**	**2017**
Agriculture, animal husbandry and export, forestry, fishing and home	37.8	48.3
Industry	630.3	637.9
Mining	0.9	1.8
Generation and transmission of electrical energy	35.1	34.4
Manufacturing industry	586.8	595.3
Services	346.5	511.3
Shops	99.5	148.0
Educational services	23.3	34.4
Health and social assistance services	4.8	8.9

Consulted source: Planning Unit of the Municipality of Tlalmanalco, 2019

Tlalmanalco is characterized by being a municipality that is mainly dedicated to the manufacturing industry**,** where the main objective is to reduce poverty in the municipality's labor society.

Environmental pillar: Seeks the care of the environment and the proper use of natural resources, it is essential to supply economic and social needs in a conscious way. Renewable energies are essential to plan a present and a future, which avoids the depletion of non-renewable resources.

Tlalmanalco is a semi-rural municipality that has large extensions of natural areas, as well as diverse flora and fauna, since the municipality locates a large part of its territory in the area of the "Iztaccíhuatl-Popocatépetl snow-capped area". *(Planning Unit of the Municipality of Tlalmanalco, 2019).* Table 1.14 shows the environmental characteristics of the municipality

Table 1.14 Environmental characteristics of the municipality of Tlalmanalco

Indicator	Characteristics	Importance
Climate	Temperate subhumid characterized by having an average annual temperature of 13.2 ° C winter = 10.9 ° C Spring = 15.4 ° C	Climate is essential for optimal growth and development of flora and fauna. Weather disturbances
Flora	Coniferous forest and oaks etc.	Flora and fauna are essential for their incalculable value because they provide balance in ecosystems and are important as natural resources for human survival.
Fauna	Squirrels, gophers, rat's opossum, rabbit, bat, rattlesnake, various types of birds (swallows, crows), and insects.	
Ground	In the Iztaccíhuatl area, the soils are made up of volcanic ash and pumice. Where various soils are constituted, such as andosols, lithosols, cambisols and flurisols	Tlalmanalco has a land area of 15,857 hectares that are mainly provided for the use of forestry, occupying 72. 47%% of the surface, therefore, agricultural use occupying 20.09%.

Hydrography	Sub-basin the company. Micro-basin of San Lorenzo Tlaminilolpa San Rafael micro-basin	Water is a primary resource for the development of activities and survival of the inhabitants of Tlamanalco. For this reason, responsible use is essential, to avoid contamination, damage to bodies of water.
Forest resources	Tlalmanalco has 10,600 hectares of forest occupying more than 50% of the total area.	Forest resources are generally used as raw material to transform cellulose into paper, or as fuel to heat food. Uncontrolled degradation and deforestation are a matter of great concern for the inhabitants of Tlalmanalco

*Consulted source: (*Zamorano, 2009; *INAFED, 2010; Planning Unit of the Municipality of Tlalmanalco, 2019)*

Low cost biodigester

Low-cost biodigesters have been stablished in developing countries since the 1980s. The first model to be implemented was the red mud PVC, later several flexible tubular models were developed, leading to the development of several low cost biodigester models, they lack complex technological systems (stirring and heating systems), and that are adapted to the use of cheap and easy-to-transport materials, to satisfy the demand in rural populations that do not have the necessary sanitary sanitation services, and/or the lack of a comprehensive waste management system (SIGR). They are ideal for domestic use in small farms (agricultural), and/or for the treatment of fecal waste and urine with the use of latrines, In order to obtain biogas that can be used as bioenergetics, they also help prevent the transmission of diseases from the mismanagement of waste spread during the volatilization of pathogenic materials that are transmitted to human beings; That is why these biodigesters help to carry out a comprehensive and controlled treatment of waste, whether of agricultural and/or human origin (Martí, 2019).

Its implementation and use are a good alternative to reduce the consumption of firewood in the kitchen and stop producing high amounts of carbon dioxide (CO_2) that affects the respiratory tract, causes headaches, causes seizures and in extreme cases death, in addition to reducing the physical work of the peasant, thus avoiding long-term diseases caused by poor posture or excessive load. This technology allows the control of the biodigestion process avoiding the transmission of infectious microorganisms from organic waste, since feces of animal and human origin contain various pathogens that cause alterations in human health, which are shown in table 1.15. Providing with this, welfare of the population, having clean energy helps the family economy.

Table 1.15 Pathogens that may be present in stool and associated symptoms

Group	Pathogens	Symptoms
Bacteria	*Aeromas spp*	Enteritis
	Campylobacter jenuni / coli	Camylobacteriosis, diarrhea, colic, abdominal pain, fever, nausea, arthritis, Gullain syndrome, Barre
	Eschererichia coli (EIEC, EPEC, ETEC, EHEC)	Enteritis, with the EHEC variety, there may be even fatal internal bleeding
	Salmonella typhi / paratyphi	Fever, typhoid / paratyphoid, headache, fever, malaise, anorexia, bradycardia, splenomegaly, cough
	Salmonella pp	Salmonellosis, diarrhea, fever, abdominal colic
	Shingella spp	Shingellosis, dysentery (bloody diarrhea), vomiting, colic, fever, Reiter's syndrome
	Vibrio cholera	Cholera, acute diarrhea, fatal if severe and untreated
Virus	*Adenovirus*	Various respiratory problems, some varieties attack the intestines
	Enteric adenovirus, type 40 and 41	Enteritis
	Hepatitis A	Hepatitis, fever, malaise, anorexia, nausea, abdominal pain, jaundice
	Rotavirus	Enteritis
Protozoan parasite	*Cryptosporidium parvum*	Cryptosporidiosis, acute diarrhea, abdominal colic, pain
	Cyclospora histolytica	Diarrhea, abdominal pain
Helminths	*Ascaris lumbricoides*	Usually without symptoms, sometimes wheezing, fever, enteritis, pulmonary eosinophilia
	Taenia solium / saginata	Taeniasis
	Trichuris Trichura	Trichuriasis, without symptoms or general digestive upset, wasting with dry skin and diarrhea

Source consulted: Strande, et al., 2014

The installation of biodigesters represents various social challenges, such as the recycling of organic waste, which allows obtaining biogas, this is not entirely accepted by diverse groups of inhabitants for reasons of religion that does not allow the handling of animal fecal matter and/or stigma**,** they do not share the use of these systems. In order to implement these low-cost structures and educate populations that are not interested in the subject, it is necessary to disseminate and design procedures within communities so that they can see how they work.

Although the design of the project is essentially good, the consumer must be constant in the maintenance of the scheme so that the obtaining of biogas is adequate, if the necessary care is not taken, the project can fail with a great economic loss and if the biodigester is not dismantled It can cause contamination in the area it is located, unfortunately in Mexico projects of this type have been abandoned due to lack of economic resources or of interest on the part of the population or municipalities.

Regarding the governmental and management aspects, should consider planning improvements in obtaining energy and fuels through the implementation of technologies that are friendly to the environment and that are accessible to all the inhabitants of Tlalmanalco. In the case of low-cost tubular biodigesters, the Government and society as a whole will have to adapt to new changes in the management systems, to obtain mutual benefits, giving way to a future that is adapted to the needs of clean energy, to ensure the precepts of the 2030 agenda, achieving the use of biomass in biogas generation supporting sustainable development.

In Figure 1.3, the main aspects that allow promoting the energy generation are shown not only in the municipality of Tlalmanalco, but in the entire Mexican Republic in a gradual and gradual manner. Energy management currently in Mexico is used for the generation of light in areas that do not have lighting in order to obtain heat in cool places, and/or to be able to travel long roads, without any fatigue, with the use of fuels. The use of fuels for the generation of energy represents a great economic investment for society worldwide, another means of obtaining energy is through deforestation from where they obtain the raw material (wood, pulp for paper) caused there is an uncontrolled logging generating degradation forest and soil, as well as the loss of biodiversity; For this reason, viable alternatives are being sought to curb climate change.

Due to the aforementioned, the appropriate use of biogas allows reducing the deforestation of green areas, as well as greenhouse gas emissions (carbon dioxide (CO_2), methane (CH_4), which are found naturally and can be generated during emission and/or volcanic eruption; but for the most part they are emitted into the atmosphere by the various anthropic processes carried out by man, mainly derived from industry or fossil fuels that, when emitted into the environment, cause alterations in temperature worldwide.(Gómez, 2012).

In Mexico, political elements have been implemented to invest less energy resources, such as the Official Mexican Standards on energy efficiency, where reference criteria are established for consumers, support for help, and the reduction of energy consumption in public sectors, good habits, and energy incentives, fundamental in the energy management system, thus promoting responsible energy consumption in the population. It is proposed that Mexico meet various objectives to reduce greenhouse gases (GHG) gradually or definitively, setting the goal of 2050, if it is possible to implement energy management adequately and hierarchically, industries will obtain a considerable reduction in the cost of energy transformation, (Hernández, *et al*., 2014).

Worldwide there is great concern in solving the problem of greenhouse gas emissions, so on December 11, 1997, the international protocol of Kyoto was signed by 84 countries, exhorting companies to emit 1 ton of CO_2 or avoid its total emission, companies that exceed this established limit will be financially sanctioned by the government, while companies that comply with the agreement will receive an intangible bonus for avoiding the emission of said gases (Gómez, 2012).

Figure 1.3 Boost scheme energy management

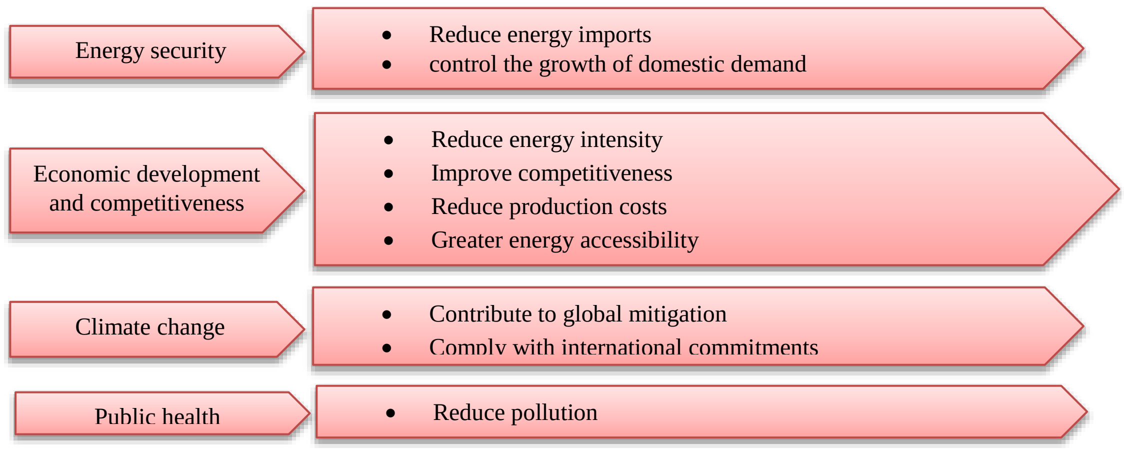

Source consulted: Hernández, et al., 2014

The design and implementation of this type of project must be carried out by people specialized in the area and have the necessary knowledge to obtain favorable results, during planning the first thing to be done is to choose the correct area to make the trench where the pipe will be installed. biodigester for this, the following points must be taken into account:

– The installation should not be carried out in areas close to flammable material, nor removed from the house (do not use unnecessary material)
– Do not place in an area where infants usually carry out their activities, or muddy areas where the earth can cause landslides.
– Delimit the area with bars or obstacles to avoid any accident.
– If its usefulness is predetermined for the use of stoves, it is important to place it with an unevenness with respect to the kitchen, this because the gas flows better from the bottom to the top.

The generation of biogas has taken a great boom in recent years worldwide, among the most recent investigations are those carried out by Chasquibol that has focused on the realization of new procedures in the generation of biofuels focused on the biorefinery and the inputs products of the biomass of algae, carrying out a qualitative analysis of these; as well as investigating informative aspects regarding the transformation of cell extraction and disruption to obtain macromolecules; Sierra and collaborators focused their research to analyze and characterize a multiple tubular biodigester in which six blind treatments were carried out, with different short retention times (5 to 8 days), with a determination of excrement and water (1:4, 1;7,1;10), from swine wastewater from the Agricultural Educational Institution Guacavía in the Municipality of Cumaral in Colombia.

For the subtraction of the organic substrate, various mathematical and statistical calculations were performed, using calculations and software, required to analyze various physicochemical parameters (HRT, excrement: water ratio, BOD sample, COD, TSS, TSS, SSV and temperature), thereby achieving, establishing an efficient procedure in the removal of organic matter for the generation of biogas, the results obtained in their research are shown in table 1.16 (Chasquibol, 202; Sierra, *et al*, 2021).

Table 1.16 Results of organic material subtraction derived from swine wastewater

Parameter (Mg/L)	Subtraction efficiency %
BOD	84.95
COD	88.74
Ssed	84.48
TSS	81.04
SSV	86.50

Source consulted: (Sierra, et al, 2021)

Other researchers focus their research on biogas purification processes theoretically in a physicochemical and biological way using microalgae which have been shown to have great efficiency in the removal of carbon dioxide and hydrogen sulfide in a percentage of 90 to 100% with little environmental impact. In the city of Celedin, Peru, the researcher Mori designed and assembled a tubular sleeve biodigester with a capacity of 7.2 m^2 and 5.7 m in length in order to eradicate a large amount of solids from waste effluents from a slaughterhouse in the same region, thus achieving the removal of materials of meat origin, within his research he carried out physicochemical analyzes, BOD, COD and SST, which allowed him to verify the elimination of residual meat effluent (De la Caridad, et. al., 2021; Mori, 2021).

Table 1.17 Parameters for the eradication of solids generated by residual effluents from a slaughterhouse

	Time in days	% BOD eradication	% total removed
Biological oxygen demand	Four. Five	52.45%	83.17%
	180	99.72%	
	Time in days	% COD eradication	% total removed
Chemical Oxygen Demand	Four. Five	73.00%	86.57%
	180	98.98%	
	Time in days	% BOD eradication	% total removed
Total Suspended Solids	Four. Five	94.73%	95.09%
	180	99.17%	

Source consulted: (Mori, 2021)

The research carried out on the benefits in the use of biodigesters to avoid the emission of GHG, carrying out an adequate comprehensive treatment, in this research the feasibility of installing low-cost biodigesters in the municipality of Tlalmanalco is sought, this being a municipality with a wide environmental importance, since it is considered "a lung for the area of the valley of Mexico" (Cervantes, 2011). In recent yearsthe physical expansion of Mexico City and the State of Mexico has generated a transcendental demographic growth. This growth leads to a greater demand for goods and services that have led to the industrialization of the agricultural sector and various industries.

These processes require electrical energy or fuels in order to carry out the transformation and distribution of the product. Fossil fuels like gasoline, diesel, and natural gas, etc. (From the fossilization of coal for thousands of years). They are considered polluting and inefficient energy generators, not only generalizing the emission of GHG in the atmosphere (CO_2, CH_4, NO_X), but also the extraction and transformation that these fuels require produces great environmental impacts, such as the loss of natural areas and biodiversity, in addition to requiring excessive consumption of the electrical network. “Tlalmanalco has 10,611 hectares of forest that represent more than 50% of the total forest area, a situation that is currently aggravated by poor forest management and profitable activities. Uncontrolled deforestation, pests and diseases, and poor land use have reduced the forest area. (Planning Unit of the Municipality of Tlalmanalco, 2019). Unlike fossil fuels, biogas is a renewable energy that depends on biomass of organic origin, this can be obtained naturally, in a residual way and as an energy crop, so that the available substrate can ferment and degrade from anaerobically in the biodigester and a minimum biogas with "55% methane" is obtained,

Low-cost biodigesters are ideal in the municipality of Tlalmanalco, to transport it to homes in hard-to-reach alpine areas. Low-cost tubular biodigesters are often constructed of lightweight materials that can be easily and compactly transported to avoid unnecessary transportation costs.

This digestor system focuses on the most economically vulnerable populations that lack some good or service, such as the lack of electricity, not having gas for cooking. In Tlalmanalco, poverty is divided into three aspects, which are the following.

Vulnerable with deficiencies refers to the population that, due to some vulnerable situation such as a disease, does not have the means and services to sustain itself adequately. 11,104 people have this condition in Tlalmanalco.

Moderate poverty: has poverty, but still has income. 19,897 people have this condition in Tlalmanalco.

Extreme poverty: population with lower income capacity 2936 people have this condition in Tlalmanalco. (CONEVAL, 2015).

Low-cost tubular system materials are generally sought, which are reused or moderately priced, so that the entire population can have access to these systems and obtain benefits for sustainable development. In graph 1.1, the percentage of energy fuels used in the municipality of Tlalmanalco is shown, among which are gaseous fuels with 28% of use, electricity 23% and liquid with 49%, these data allow to corroborate that it is necessary implement the use of biodigesters to reduce carbon dioxide emissions to the environment.

Graph 1.1 Percentage of energy fuels in the municipality of Tlalmanalco

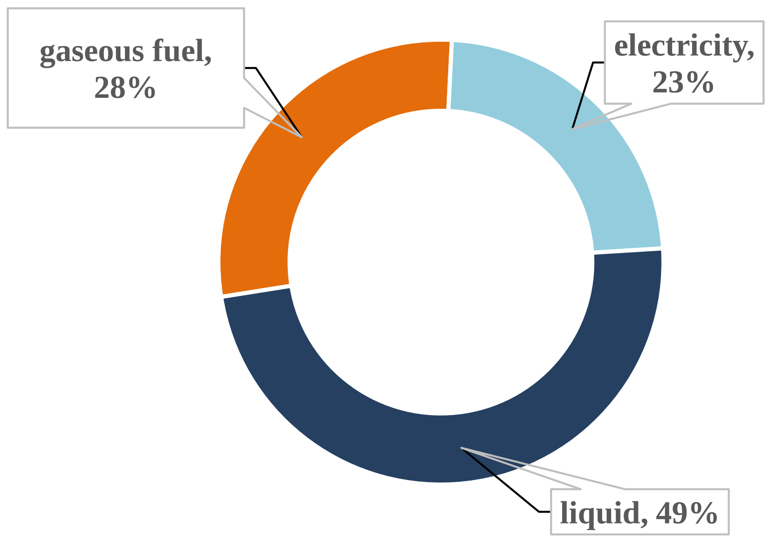

Reference source: Global Covenant of mayors for Climate & Energy, 2019

In graph 1.2, the energy required per inhabitants of the municipality of Tlalmanalco in buildings, transportation and waste generation is shown, having 0.009 TJ per inhabitant that is required in buildings and 0.16 TJ in transportation, as well as 0TJ in the energy used in the waste generated per inhabitant per year.

Graph 1.2 Energy consumption (Buildings and Transportation), and waste generation in 2016 in the municipality of Tlalmanalco

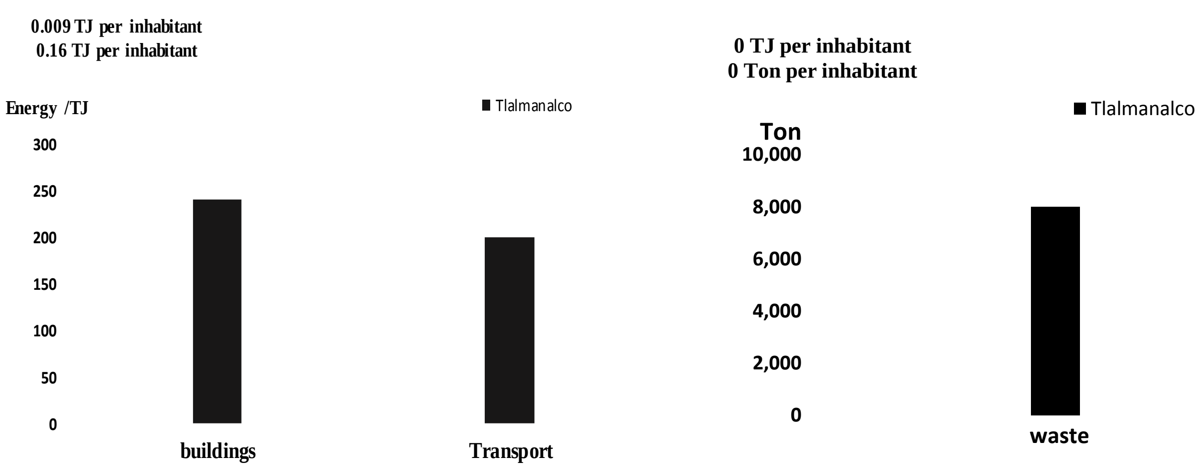

Source consulted: (Global Covenant of mayors for Climate & Energy,2019)

3. Results

By implementing biodigesters in the beginning of Tlalmanalco, it is expected in the short term to have the following aspects as favorable results:

Energy generation: Generates biofuel (biogas), "very similar to butane and propane gas. It can be used for the use of stoves, heating, lighting "

Production: The biol that is produced at the end of the biodigestion process is a fertilizer that has the ability to mineralize through nutrients. This fertilizer can be deposited directly to crops or seeds "improving their yield by 30%"

Family health: Unlike other fuels that emit harmful gases, the biogas used controls harmful gases such as CH_4 and CO_2

Animal hygiene: Bad odors are controlled and diseases generated by vectors (flies and other rodents) are avoided

Environment: "By generating each family their own cooking fuel, deforestation can be gradually reduced." As well as reducing the use of fossil fuels.

Workload and economy: "The time that is invested in obtaining firewood or the expenses in the purchase of fuel " it is replaced by the obtaining of available excrement, which is introduced into the biodigester to begin the biodigestion process and the future obtaining of biogas.

Sustainable technology: Being a technology that avoids the unfavorable use of natural resources, low cost, accessible use and little maintenance, it is considered a sustainable energy

Low cost: The cost of a family biodigester can be variable, depending on the size of the project and the climate. But it is defined that a medium biodigester can cost between 150 and 200 US dollars (Martí, 2021).

4. Acknowledgments

To the Tecnológico de Estudios Superiores del Oriente del Estado de México for providing all the facilities to carry out this research.

5. Conclusions

The theoretical study carried out on the municipality of Tlalmanalco, in terms of geographical area, as well as the most vulnerable areas, the services it has and the energy expenditure it has per inhabitant per year; allows observing that even when there are no statistical data from INEGI, IGECEM for recent years, this municipality has the characteristics and adequate spaces to implement a low-cost tubular biodigester system, greatly favoring the economic energy costs of the community, at the same time, the diseases generated by the various pathogens found in feces that are still exposed to the environment will be reduced, since many houses have latrine systems, there will also be a decrease in carbon dioxide emissions (CO_2)generated favoring the care of the environment.

6. References

Avila, C. (2016). USO DE BIODIGESTORES EN LA INDUSTRIA PECUARIA. 17/07/2021, de UNIVERSIDAD AUTÓNOMA DEL ESTADO DE MÉXICO Sitio web: http://ri.uaemex.mx/bitstream/handle/20.500.11799/66337/TESINA-CAV-1016.pdf?sequence=1

Constanza, L., Antolinez, D, M., Bhórquez, J, A., Corredor, A, M. (2015). Bacterias anaerobias: procesos que realizan y contribuyen a la sostenibilidad de la vida en el planeta. 17/07/2021, de SCIELO Sitio web: http://www.scielo.org.co/pdf/nova/v13n24/v13n24a06.pdf

Canales, M, C., Rivas, L, A., Sorto, R, J. (2010). ESTUDIO DEL PROCESO BIOQUIMICO DE FERMENTACION EN DIGESTORES PARA LA PRODUCCION DE BIOGAS Y BIOFERTILIZANTE A PARTIR DE RESIDUOS ORGANICOS PROVENIENTES DEL CAMPUS DE LA UNIVERSIDAD DE EL SALVADOR. 14/08/2021, de UNIVERSIDAD DE EL SALVADOR Sitio web: http://ri.ues.edu.sv/id/eprint/138/1/10136039.pdf

Corona, I. (2007). Biodigestores. 26/03/2021, de UAEH Sitio web: https://repository.uaeh.edu.mx/bitstream/bitstream/handle/123456789/10722/Biodigestores.pdf?sequence=1

Cervantes, A. (2011). El proceso de urbanización en el municipio de Tlalmanalco. 10/03/2021, de UAM Sitio web: http://hdl.handle.net/11191/626

CONEVAL. (2015). Informe anual sobre la situación de pobreza y rezago social Tlalmanalco. 10/03/2021, de Gobierno de México Sitio web: https://www.gob.mx/cms/uploads/attachment/file/611599/Informe_anual_2021_mun_15103.pdf

Chasquibol Calongos, S. D. (2021). Revisión de las técnicas de producción de biocombustibles a partir de microalgas.

De la Caridad Brunet-Ramos, S., Jiménez-Hernández, J., Pedraza-Gárciga, J., & López-González, L. M. (2021). Consorcios de microalgas-bacterias para la purificación biológica de biogás. Tecnología Química, 41(2), 277-295.

Gómez, S. (2012). DISEÑO, CONSTRUCCIÓN Y PUESTA A PUNTO DE UN BIODIGESTOR TUBULAR. 27/03/2021, de Universidad Carlos lll de Madrid Sitio web: https://e-archivo.uc3m.es/bitstream/handle/10016/17044/PFC_SusanaGomezMunoz.pdf?sequence=1&isAllowed=y

Global Covenant of mayors for Climate & Energy. Data Portal for Cities. (2019). Disponible en línea en: http://www.dataportalforcities.org

Healt. (2016). Hoja informativa de sustancia peligrosa. 28/03/2021, de NJ Healt Sitio web: https://www.nj.gov/health/eoh/rtkweb/documents/fs/0343sp.pdf

Hernández, P., Carmona, G, E., Flores, L., Sosa, R. (2014). MANUAL PARALA IMPLEMENTACIÓN DE UN SITEMA DE GESTÓN DE LA ENERGA. 27/03/21, de Cooperación alemana DEUTSCHE ZUSAMMENARBEIT Sitio web: https://www.gob.mx/cms/uploads/attachment/file/55467/ManualGestionEnergia_V2_1.pdf

INAFED. (2010). 06/04/2021, de Enciclopedia de Los Municipios y Delegaciones de México Sitio web: http://www.inafed.gob.mx/work/enciclopedia/EMM15mexico/municipios/15103a.html

Lorenzo, Y., Abreu, M. (2005). La digestión anaerobia. Aspectos teóricos. ICIDCA, XXXIX, 35-48.

León, R, M. (1991). DISEÑO, CALCULOS Y EVALUACIÓN DE BIODIGESTORES. 10/03/2021, de CORPORACIÓN UNIVERSITARIA AUTONOMA DE OCCIDENTE Sitio web: https://red.uao.edu.co/bitstream/handle/10614/4773/T0002583.pdf?sequence=1&isAllowed=y

Mori Leyva, K. S. (2021). Eficiencia de un biodigestor tubular en la remoción de la carga orgánica y sólidos de un efluente del beneficio cárnico, en Celendín.

Martí Herrero J. (2019). Biodigestores Tubulares: Guía de Diseño y manual de instalación Redbiolac. Ecuador. ISBN:978-9942-36-276-6

Martí, J. (2021). BIODIGESTORES DE BAJO COSTO. 05/04/2021, de IDEASS Sitio web: https://ecotec.unam.mx/wp-content/uploads/Biodigestores-de-bajo-costo.pdf

Olaya, J., Gonzáles, L, O. (2009). FUNDAMENTOS PARA EL DISEÑO DE BIODIGESTORES. 11/03/2021, de UNIVERSIDAD NACIONAL DE COLOMBIA SEDE PALMIRA Sitio web: repositorio.unal.edu.co/bitstream/handle/unal/10762/luisoctaviogonzalezsalcedo.20121.pdf?sequence=1&isAllowed=y

Pascual, A., Ruiz, B., Gómez, P., Flotats, X., Belén, F. (2011). SITACIÓN Y PPOTENCIAL DE GENERACIÓN DE BIOGÁS. 11/07/2021, de IDAE Sitio web: https://www.idae.es/uploads/documentos/documentos_11227_e16_biogas_db43a675.pdf

PNUM. (2019). EL ENFOQUE DE LA AGENDA 2030 EN PLANES Y PROGRAMAS PÚBLICOS EN MÉXICO. 27/03/2021, de Agenda 2030 Sitio web: https://www.undp.org/content/dam/argentina/Publications/Agenda2030/PNUDArgent-DossierODS.pdf

Pérez, J, A. (2010). ESTUDIO Y DISEÑO DE UN BIODIGESTOR PARA APLICACION EN PEQUEÑOS GANADEROS Y LECHEROS. 10/03/2021, de UNIVERSIDAD DE CHILE Sitio web: http://repositorio.uchile.cl/bitstream/handle/2250/103926/cf-perez_jm.pdf?sequence=3

Strande, L., Ronteltap, M., Brdjanovic, D. (2014). Manejo de Lodos Fecales Un enfoque sistémico para su implementación y operación. 05/04/2021, de IWA PUBLISHING Sitio web: https://www.iwapublishing.com/sites/default/files/ebooks/manejo_fsm.pdf

Sierra, D. F. C., Huertas, D. M. H., & León, H. C. (2021). EVALUACIÓN DE LA EFICIENCIA DE REMOCIÓN DE MATERIA ORGÁNICA DE UN BIODIGESTOR TUBULAR ANAEROBIO A ESCALA PILOTO. Ciencia e ingeniería, 5(1), 43-57.

Torres, I., & María, I. A. (2021). Potencial energético de la biomasa residual pecuaria en el Campus de la UNALM.

Unidad de Planeación del Municipio de Tlalmanalco. (2019). PLAN DE DESARROLLO MUNICIPAL 2019-2021. 10/03/2021, de Gobierno Municipal de Tlalmanalco Sitio web: https://www.tlalmanalco.gob.mx/pdf_gacetas/68.pdf

Varnero, M, T. (2011). MANUAL DE BIOGÁS. 10/03/2021, de Gobierno de Chile Ministerio de Energía Sitio web: http://www.fao.org/3/as400s/as400s.pdf

Weber, B., Rojas, M., Torres, M., Pampillón, L. (2012). PRODUCCIÓN DE BIOGÁS EN MÉXICO. 11/03/2021, de Red Mexicana de Bioenergía Sitio web: http://rembio.org.mx/wp-content/uploads/2014/12/CT5.pdf

Zamorano, P. (2009). La flora y fauna silvestre en México. Estudios agrarios, 15, 159-167

Chapter 2 Bifunctional catalysts applied to produce biodiesel from waste cooking oil

Capítulo 2 Catalizadores bifuncionales aplicados a la producción de biodiésel a partir de aceite de cocina usado

CERÓN-FERRUSCA, Montserrat[1]*†, ROMERO-ROMERO, Rubi[1], NATIVIDAD, Reyna[1] and MARTÍNEZ-VARGAS, Sandra Luz[2]

[1]Chemical Engineering Lab., Centro Conjunto de Investigación en Química Sustentable, UAEM-UNAM, Universidad Autónoma del Estado de México, Km 14.5 Toluca-Atlacomulco Road, Toluca, México, 50200
[2]Faculty of Chemistry, Universidad Autónoma del Estado de México, Paseo Colón Esq. Paseo Tollocan, Toluca, México, 50120

ID 1st Author: *Montserrat, Cerón-Ferrusca* / **ORC ID**: 0000-0002-3726-6078, **CVU CONACYT ID**: 1000624

ID 1st Co-author: *Rubi, Romero-Romero* / **ORC ID**: 0000-0001-9163-7936, **CVU CONACYT ID**: 121454

ID 2nd Co-author: *Reyna, Natividad* / **ORC ID**: 0000-0001-8978-1066, **CVU CONACYT ID**: 87755

ID 3rd Co-author: *Sandra Luz, Martínez-Vargas* / **ORC ID**: 0000-0001-5078-7225, **CVU CONACYT ID**: 280129

DOI: 10.35429/H.2021.6.20.36

M. Cerón, R. Romero, R. Natividad and S. Martínez

*mcerfer96@gmail.com

A. Marroquín, J. Olivares, M. Ramírez and L. Cruz (Coord) Engineering and Technology. Handbooks-©ECORFAN-México, Querétaro, 2021.

Abstract

This work aims to present the analysis of the catalytic performance of Fe_2O_3/CaO as a bifunctional catalyst in the production of biodiesel from waste cooking oil. The clamshell was used as a source of calcium oxide by calcination. The catalyst was characterized by Thermogravimetric analysis and Differential scanning calorimetry (TGA-DSC), X-ray diffraction (XRD) and Inductively coupled plasma atomic emission spectroscopy (ICP-AES). The catalytic tests were conducted at 55 °C, the methanol:oil ratio was 12:1, amount of catalyst of 6%wt and reaction time of 5 h. The content of methyl esters in the produced biodiesel was >98% and was found to fulfill the specifications of European Norm UNE-EN 14214.

Biodiesel, Waste cooking oil, Clamshell, Bifunctional, Transesterification

Resumen

El objetivo del presente proyecto fue evaluar el comportamiento catalítico del catalizador bifuncional Fe_2O_3/CaO en la obtención de biodiesel a partir de aceite de cocina usado. La concha de mar se utilizó como fuente alternativa de óxido de calcio por medio de la calcinación de la misma. El catalizador fue caracterizado por medio del análisis termogravimétrico y calorimetría diferencial de barrido (TGA-DSC), difracción de rayos X (DRX) y espectroscopia de emisión atómica de plasma acoplado por inducción (ICP-AES). Las pruebas catalíticas se realizaron a las siguientes condiciones de reacción: 55°C, relación metanol:aceite de 12:1, cantidad de catalizador de 6% en peso y tiempo de reacción de 5h. El biodiesel producido obtuvo un contenido de ésteres metílicos superior al 98%, además de que el mismo cumple con las especificaciones de la Norma Europea UNE-EN 14214.

Biodiesel, Aceite de reúso, Concha de almeja, Bifuncional, Transesterificación

1. Introduction

It is well known that the current energy sector depends mainly on the use of fossil fuels and together with globalization, has led to an increase in greenhouse gas emissions (Hafeez *et al.*, 2020). Also, since it is a non-renewable energy source, the price of fossil fuels has been increasing, while their reserves have been decreasing. This has motivated the search for less polluting alternatives, such as biodiesel.

Biodiesel is currently considered one of the most viable options coming from a renewable and clean energy source, since it can be synthesized from various vegetable and / or animal fats (Borah *et al.*, 2019). In addition, it can be used in diesel engines, because biodiesel has physicochemical properties similar to petroleum diesel (Lv *et al.*, 2020). However, the main challenge to face in the biodiesel synthesis, lies in the decrease of its production cost, as well as looking for alternatives to replace edible oils as a raw lipid source (Khan *et al.*, 2019). Derived from the above, reuse cooking oils have been used as raw material for obtaining biodiesel. However, most of the current heterogeneous catalysts are not capable of handling the high content of free fatty acids (FFA) that this type of lipid raw material has, which makes it necessary to carry out the process of obtaining biodiesel in two separate reactions: esterification and transesterification, thus increasing biodiesel production costs.

Nowadays, studies referring to heterogeneous catalysis have focused on the search for bifunctional catalysts, which can handle lipid raw materials such as used cooking oils, due to the fact that they have two different active sites, one acidic, capable of esterifying free fatty acids and a basic site, which allows the transesterification of triglycerides, in the same stage. For this, the present work proposes the use of a bifunctional catalyst based on clam shell waste from restaurants, impregnated with iron.

The originality of this work lies in the identification of the catalytically active iron crystalline phase for the production of biodiesel, using the reuse cooking oil transesterification reaction, where the calcination temperature of the catalyst is a determining variable for the identification of said complex, within which are those corresponding to the system $Ca_nFe_nO_{2n+1}$ ($1 \leq n \leq 2$) and are directly related to oxygen vacancies. The combination of CaO and Fe salt, at the appropriate calcination temperature, will allow to obtain a bifunctional catalyst.

The foregoing has aroused great interest, because:

1. You can give a second use to a waste such as used cooking oils.

2. Decrease in production costs (approximately 60-70% for raw material only).

3. It involves the principles of "Green Chemistry" (Pájaro & Verbel, 2011) such as:
- The use of processes that use substances with the least possible toxicity.
- Put the use of renewable raw materials first.
- The process must be completed in the minimum number of steps, avoiding extra steps.
- Prioritize the use of catalyzed reactions over non-catalyzed ones.

2. Environmental problem

Nowadays, the energy supply is mainly based on the use of fossil fuels, because at least 60% of the total energy used worldwide is obtained from their use (Mansir *et al*., 2018a). This is mainly attributed to the fact that it was adapted to various sectors such as agriculture, transport and industry (Ogunkunle & Ahmed, 2019).

In recent years, one of the main objectives that various investigations have had is to reduce greenhouse gas emissions such as CO_2, of which approximately 25% correspond to emissions related to the use of fossil fuel for transportation (Hafeez *et al*., 2020; Llanes Cedeño, 2017). In this sense, biodiesel has become one of the most used options to reduce the use of fossil fuels, by having a cleaner combustion, it can help to reduce CO emissions, which is a product of incomplete combustion and that can be transformed in CO_2 in the presence of an atmosphere with a sufficient amount of oxygen (Llanes Cedeño, 2017). However, the commercialization of biodiesel has not spread, because it has a high production cost compared to a diesel of fossil origin (Mansir *et al*., 2018b).

The above problem has led to various investigations that aim to use lower-cost raw materials, such as waste cooking oils, since their use as lipid raw material allows a double benefit by significantly reducing production costs (Mahmood Khan *et al.*, 2020) and by reducing contamination to soils and water bodies, which can be generated by improper disposal (Lee *et al*., 2014).

3. Biodiesel

Biodiesel is defined by the American Society for Testing and Materials (ASTM) as a mixture of long chain fatty acid monoalkyl esters, which can be derived from lipids coming from vegetable or animal fats. In recent decades, biodiesel has become a viable alternative fuel, mainly due to its physicochemical characteristics and its renewable character, since it is possible to obtain it from vegetable oils (refined, inedible or reused), as well as animal fats (Bhavani & Sharma, 2018). Some of the advantages and disadvantages of using biodiesel versus petroleum diesel are summarized in Figure 2.1.

3.1 Lipid raw material

To obtain a biodiesel with the quality to accomplish with different regulations, it is necessary to have a refined lipid raw material, or as clean as possible, because most catalysts cannot handle the presence of free fatty acids (FFA) in percentages greater than 2%.

Currently, there is a great controversy about the use of vegetable oils with nutritional value as lipid raw material for the biodiesel production, due to the enormous demand that exist (Lv *et al*., 2020), for which, various studies have been have oriented to the search for lipid raw materials that do not have a nutritional value, as is the case of used cooking oil, which is a highly polluting waste and available in large quantities (Khodadadi *et al*., 2020). Cooking oil changes its chemical composition when subjected to high temperatures and when it comes into contact with moisture and other substances from food. This results in a large amount of impurities, which greatly affect the performance of the transesterification reaction and the purity of the final product.

The use of used cooking oils allows a double benefit, since by using them as lipid raw material, the costs of manufacturing biodiesel can be significantly reduced, and also it reduces the environmental pollution caused by the discharge of this residue in the water bodies and soils (Lee *et al*., 2014). When a waste cooking oil (WCO) is used as a lipid raw material, this must undergo through a cleaning process. This consists of three main steps: 1) filtration, where the solid contaminants are separated, 2) degumming, to separate the water-soluble phospholipids, and 3) drying, where the water residues are removed.

Figure 2.1. Advantages and disadvantages of using biodiesel

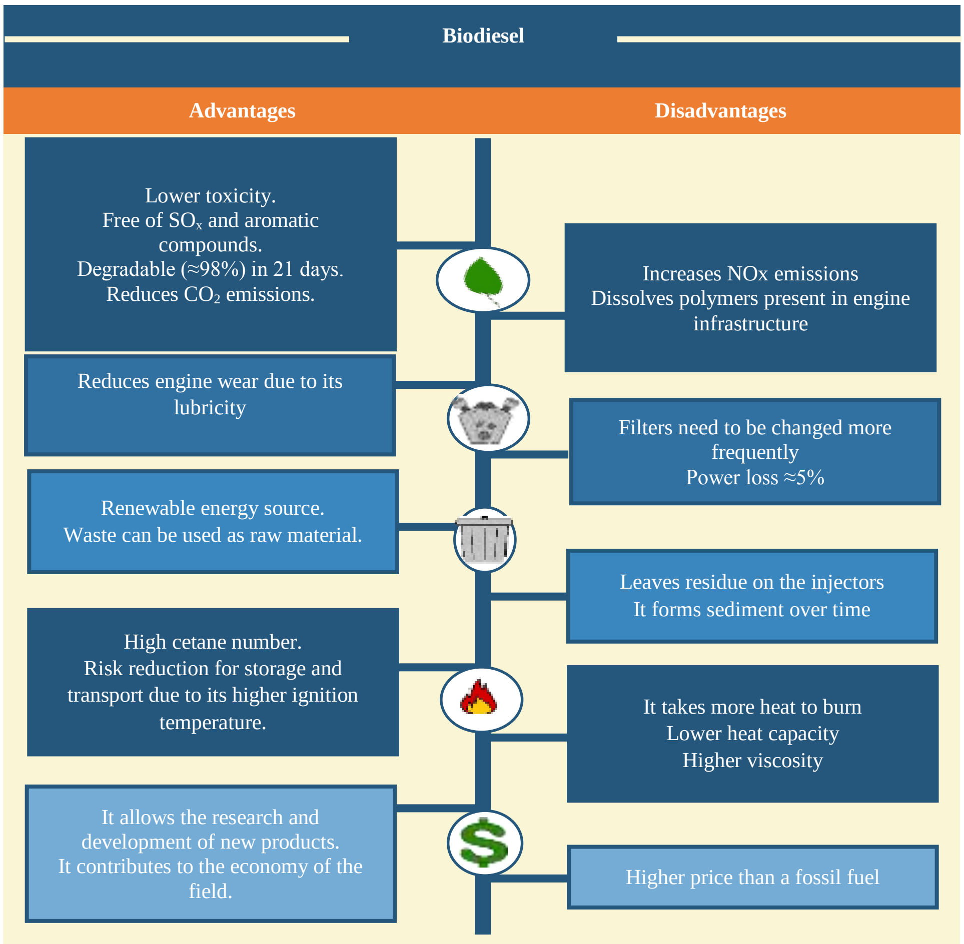

4. Synthesis methods

In this section the main methods to produce biodiesel, are summarized.

4.1 Transesterification

The transesterification reaction is one of the most widely used methods in the synthesis of biodiesel. In this reaction, a triglyceride molecule, from the lipid raw material, and three molecules of an alcohol (mainly methanol) interact, thus obtaining three molecules of methyl esters and one of glycerol. However, this reaction has two main disadvantages, the slow reaction rate and the sensitivity of the reaction to the amount of free fatty acids present in the lipid raw material. In this reaction, it is possible to use both acid catalysts and basic catalysts, in order to improve reaction times and thus increase biodiesel production.

To avoid the environmental and corrosion problems derived from the use of an acid catalyst, this process is commonly catalyzed with a basic catalyst, however, if the lipid raw material has a content greater than 1% by weight of FFA, this reaction will tend to saponify, which leads to a reduction in obtaining biodiesel and hinders the remotion of the catalyst at the end of the reaction (Guo *et al*., 2021). Therefore, it is required to carry out a previous esterification process, or the presence of an appropriate catalyst that can carry out both reactions simultaneously.

4.2 Esterification

In this reaction, a free fatty acid molecule, which can come from a waste cooking oil, interacts with the catalytic surface and with a low molecular weight alcohol molecule, to obtain a monoalkyl ester molecule and a water molecule. This reaction is considered as a previous step in the synthesis of biodiesel from waste cooking oil, since it is capable of converting the FFA contained in the lipid raw material into monoalkyl esters, thus reducing the production of soap and increasing the quality of the biodiesel. However, its main disadvantage lies on the lack of efficient catalysts (Gnanaprakasam *et al*., 2013).

4.3. Pyrolysis

This process consists of a heat treatment in an atmosphere lacking oxygen, because it seeks to decompose large molecules into smaller ones (Hernández N., 2011).

4.4. Blending

This method seeks to reduce the viscosity of an animal fat or vegetable oil by blending it in different proportions with fossil fuels (Gandure *et al*., 2017).

4.5. Microemulsion

This method seeks to reduce the viscosity of a vegetable oil through the use of surfactants such as water or oils (Ramadhas *et al*., 2016). Figure 2.2 summarizes some of the disadvantages of the most widely used synthesis methods for biodiesel.

Figure 2.2 Biodiesel Synthesis Methods

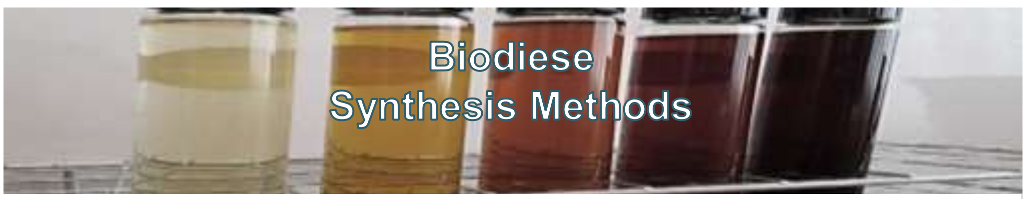

Pyrolysis

Thermal decomposition in an oxygen-deficient atmosphere.
In this method there are unwanted by-products, high production costs, this production method produces polluting gases.

Microemulsion

Formation of a mixture to decrease the viscosity of the vegetable oil.
In this method, incomplete combustion occurs, the biodiesel produced has a low caloric value and there is the possibility of forming carbon deposits in the engine.

Blending

Formation of a stable dispersion to decrease viscosity.
In this method, gas emissions are increased, in addition to favoring the formation of rubber and carbon deposits in the engine.

Esterification

Interaction of free fatty acids in the oil with alcohol.
For this method there are not many efficient catalysts and there is an incomplete combustion of the oils

Transesterification

Interaction of triglycerides present in oils with alcohol.
This method has a low reaction rate and therefore requires a suitable catalyst.

5. Catalysis in the transesterification reaction for the production of biodiesel

As previously mentioned, the transesterification reaction has a low reaction rate, which is why the presence of a catalyst is necessary to help the process be carried out in a faster and more efficient way. The catalysts used in the transesterification reaction can be divided into three main categories: homogeneous, heterogeneous and enzymatic catalysts.

5.1 Homogeneous catalysis

In this type of catalysis, both the reactants and the catalyst are in the same phase, which allows the reactants to mix, forming unstable intermediates that combine with more reagents to obtain the corresponding reaction products (Guo *et al*., 2021). The main disadvantage of this type of catalysis is the loss of the catalyst at the end of the reaction, as well as the need to carry out a cleaning process at the end of the reaction. This cleaning process usually implies the use of large quantities of water and this reduces the process sustainability.

5.1.1 Homogeneous acid catalysis

Within homogeneous catalysis, we can find homogeneous acid catalysts, which are capable of handling unrefined lipid raw materials, since they can catalyze both, the esterification and transesterification reactions. Despite this, these catalysts require longer reaction times and high reaction temperatures (Lam *et al*., 2010). In addition, there is a great risk of environmental damage due to its use, as well as corrosion in the pipes and reactors that handle it. Some of the most commonly used homogeneous acid catalysts are: HCl, CH_2O_2, CH_3COOH, HNO_3, H_2SO_4, $Fe_2(SO_4)_3$, H_2PO_4 (Gebremariam & Marchetti, 2018a).

5.1.2 Basic homogeneous catalysis

Basic homogeneous catalysis is preferred at an industrial level, due to the fact that it is friendly to the environment and has higher reaction rates than acid catalysis, in addition to requiring lower reaction temperatures that can range from room temperature to 70 ° C (Guczi & Erdöhelyi, 2011; Lam *et al*., 2010; Tariq *et al*., 2012). However, this type of catalysis gives low reaction yields with unrefined lipid raw materials, due to the presence of FFA (Guo *et al*., 2021; Lam op. Cit.). Some of the most commonly used basic homogeneous catalyst are: NaOH (Guo op. Cit.), KOH, KOCH (Molina, 2013), $NaOCH_3$ (Guo op. Cit.; Mosali Raj and Bobbili Sharath, 2011; Talha & Sulaiman, 2016)

5.2 Enzyme catalysis

Currently, this type of catalyst has caught attention because this type of catalysis is capable of reducing the number of impurities of the final product and facilitates the work of removing the catalyst at the end of the reaction. However, its main disadvantage is related to the high price of this type of catalyst (Molina, 2013).

Lipases are usually the most used as catalysts, due to their high tolerance to the content of free fatty acids and to obtain yields close to 100%. Some of the most commonly used are: *Pseudomonas cepacia*, *Rhizomucor miehei* , *Rhizopus orizae*, *Candida antárctica*, among others (Guncheva & Zhiryakova, 2011).

5.3 Heterogeneous catalysis

In this type of catalysis, the reagents and the catalyst are in the different phase. These types of catalysts provide a surface on which the reaction will take place. (Aguilar R., 2003).

The main advantages of this type of catalysis are the ease of recovery of the catalyst at the end of the reaction, the possibility of using the catalyst in more than one reaction cycle and also the fact that they can be designed with greater selectivity for the process. However, this type of catalyst also has some important disadvantages, such as the decrease in its catalytic activity due to the deactivation of the catalyst after the reaction cycle.

5.3.1 Heterogeneous acid catalysis

In heterogeneous catalysis, we can find heterogeneous acid catalysis, which is capable of handling unrefined lipid raw materials, since it can esterify and transesterify, as well as not being sensitive to the moisture present in the lipid raw material. However, the most relevant disadvantages of these catalysts lie in the need for longer reaction times and reaction temperatures ranging between 120-200 °C (Faruque *et a*l., 2020; Helwani *et al*., 2009; Lam *et al.*, 2010); in addition to the environmental and corrosion damages mentioned. Among the most commonly used heterogeneous acid catalysts are: sulfonic resins, zeolites, carbon-based catalysts (Lam *et a*l., 2010).

5.3.2 Basic heterogeneous catalysis

On the other hand, basic heterogeneous catalysis has been widely studied due to the high availability of catalysts, as well as the simplicity of recovering such catalysts at the end of the process (Lam *et al*., 2010; Talha & Sulaiman, 2016). However, for this type of catalyst, to obtain good reaction yields, refined lipid raw materials or with low FFA contents (<2%) are required. (Guo *et al*., 2021; Lam *et al*., 2010).

Examples of the most commonly used basic heterogeneous catalysts are: alkaline earth metal oxides (CaO, SnO, MgO), some metal mixtures (Ca / Mg, Mg / Al), zeolites, hydrotalcites, among others (Adepoju *et al*., 2020; Helwani *et al*., 2009; Lam *et al*., 2010; Mansir *et al*., 2018b).

CaO is one of the heterogeneous catalysts most used to obtain biodiesel, due to its low cost, lower toxicity, as well as its great abundance, among other advantages (Borah et al., 2019). This compound is found in many varieties, from quicklime, to the shells of some animals, including mollusks (Borah *et al*., 2019; Mahmood Khan *et al*., 2020; Yuliana *et al*., 2020). Based on this, researchers have tested mollusk waste as a source of CaO.

5.3.3. Bifunctional catalysis

Bifunctional catalysts are those that have two types of active sites, one acidic and one basic, that allow to carry out two processes simultaneously. In the synthesis of biodiesel, these catalysts can work with unrefined lipid raw materials, because they are capable of esterifying the FFAs and transesterifying the triglycerides present (Foldvari, 2011). In recent years, various investigations have been carried out to evaluate various bifunctional catalysts in the transesterification reaction. Table 2.1 shows some of the examples of bifunctional catalysts used, as well as their reaction conditions and yields.

Table 2.1 Bifunctional catalysts for the biodiesel synthesis

Catalyst	Reaction condition				Methyl Esters [%]	References
	T [°C]	Molar ratio methanol:oil	Catalyst weight [%wt]	Reaction time [h]		
TiO_2-MgO	160.0	50:1	10.0	6.0	92.3	(Mohammed & Bandari, 2020)
CaO/MgO	69.4	16.7:1	4.6	7.1	98.4	(Foroutan *et a*l., 2020)
CaO/γ-Fe_2O_3	70.0	15:1	2.0	3.0	98.8	(Shi *et al*., 2017)
K_2O/CaO-ZnO	60.0	15:1	2.0	4.0	81.0	(Mohammed & Bandari, 2020)
CaO-$Ca_3Al_2O_6$	65.0	12:1	10.0	2.0	97.0	(Papargyriou *et al*., 2019)
Mn_2ZnO_4	80.0	12:1	6.0	4.0	72.3	(Sivaprakash *et al*., 2019)
La^{3+}/ZnO-TiO_2	35.0	12:1	4.0	3.0	>87	(Guo *et al*., 2021)
CaO/SnO_2	54.1	10:1	6.0	2.0	89.6	(Solis *et al*., 2016)
$ClSO_3H$	60.0	10:1	2.0	5.0	98.6	(Hamza *et al*., 2021)
Ca/ZM-U	70.0	9:1	5.0	6.0	88.5	(Gaur *et a*l., 2020)
CaO/Al_2O_3	50.0	3.2:10	1.6	2.1	88.9	(Narula *et al*., 2017)

6. Methodology

6.1. Materials

The oil used as lipid raw material for this research was collected in a place dedicated to food preparation, located in Toluca, State of Mexico. In order to be able to use it as a lipid raw material in the transesterification reaction, it was necessary to remove impurities by a previous cleaning treatment.

Anhydrous methanol (99.9%) was supplied by Productos Químicos Monterrey (Fermont). For gas chromatography, methyl heptadecanoate (≥99%) was supplied by Sigma Aldrich, which was used to quantify methyl esters. The clam shells, used as a source of CaO and as a support for the catalyst, were collected from restaurants dedicated to the sale of seafood, located in San Luis Mextepec, State of Mexico.

6.2. Catalyst preparation

The clam shell was subjected to a cleaning process and later, it was ground and sieved (0.42 mm) to homogenize the particle size. In order to obtain CaO, from the CaCO3 present in the shell as the majority component, it was necessary to subject the seashell to a heat treatment (900 ° C) for 6 h.

Once the calcium oxide was obtained, the impregnation of the Fe in the support was carried out, starting from $Fe(NO_3)_3$*9H2O (>99.5%) as precursor salt. In order to verify the effect of the iron load on the transesterification reaction, three different percentages by weight of iron precursor salt were tested (0%, 5% and 7%). Finally, the catalytic sites were activated by means of another thermal treatment at 500 ° C for 6 h.

6.3. Catalyst characterization

The clam shell was analyzed by a simultaneous thermal analysis (SDT Q600 simultaneous TGA / DSC, TA Instruments) under nitrogen flow conditions with a heating rate of 10 ° C / min. The X-ray diffraction analysis technique was used, in order to identify the crystalline species present in the bifunctional catalyst, as well as to determine the crystalline structure of calcium oxide before iron impregnation. These tests were carried out in a Bruker X-ray diffractometer, Advanced 8 model with Cu Kα radiation of 30KV and 35 mA. The data were collected at the scan angle (2θ) from 5° to 80°, with a step time of 56.7s and a step size of 0.029 °.

6.4. Pretreatment of used cooking oil

Due to the fact that the type of oil used in the present work presents impurities derived from the heat treatment to which it was subjected during food preparation, it was necessary to carry out a previous treatment. First, the used cooking oil was filtered with the help of a fine mesh cloth to remove all the larger solid impurities. Subsequently, the oil was centrifuged at 600 rpm for 10 min to separate the smaller impurities. Next, the oil was heated to 80 ° C and was placed in a decanting funnel, it was washed with water (10% of the volume of the oil) at 80 ° C. Finally, the water residues were removed from the oil, placing the organic phase in a glass container under vacuum conditions and heated at 80 ° C for 30 minutes.

6.5. Catalytic evaluation

The catalytic activity of the bifunctional catalyst was evaluated by the waste cooking oil transesterification reaction with methanol, using a 250 mL capacity batch reactor, connected to a reflux system. The experiments were carried out with a constant methanol: oil molar ratio (12: 1). And the amount of catalyst used was 6% by weight of the oil. The reaction temperature (55 ° C) was kept constant with a heating rack throughout the reaction time (5 h). At the end of the reaction, the catalyst was separated from the products (methyl esters and glycerol) by centrifugation. The remaining methanol was separated from the biodiesel by evaporation under vacuum conditions.

6.6. Biodiesel characterization

The determination of the amount of methyl esters was carried out according to the UNE-EN14103 biodiesel test, using a Scion 456-GC gas chromatograph equipped with a flame ionization detector and CPwax capillary column with a length of 30 m, thickness of 0.25 µm film and 0.32 mm internal diameter. The determination of the kinematic viscosity was carried out according to the European standard EN ISO 3104, with the help of a Canon-Fenske capillary viscometer immersed in a bath at constant temperature (40°C). The acid number was determined with the test of the European standard EN 14104, with the help of a potentiometric titrator (877 Titrino Plus-Metrohm) using potassium biphthalate as the primary standard to evaluate the concentration of the titration solution (KOH)

7. Results

7.1. Catalyst characterization

7.1.1 Thermogravimetric analysis and differential scanning calorimetry

During the synthesis of a catalyst, different variables must be taken into account, such as the calcination temperature, the calcination time and the heating ramp, which can affect the formation of the chemical species that will grant the catalytic activity. In the case of clam shell, it is necessary to transform $CaCO_3$ into CaO, otherwise, there is a risk of significantly reducing the activity of the catalyst due to insufficient CaO production, or else, due to the absorption of moisture and CO_2 in the environment.

In order to know and establish an adequate calcination temperature, the clam shell was analyzed, using the TGA and DSC technique; The results obtained by both methods, when analyzing clam shell, are shown in Graphic 2.1.

Graphic 2.1 Results of the TGA-DSC performed on the clam shell

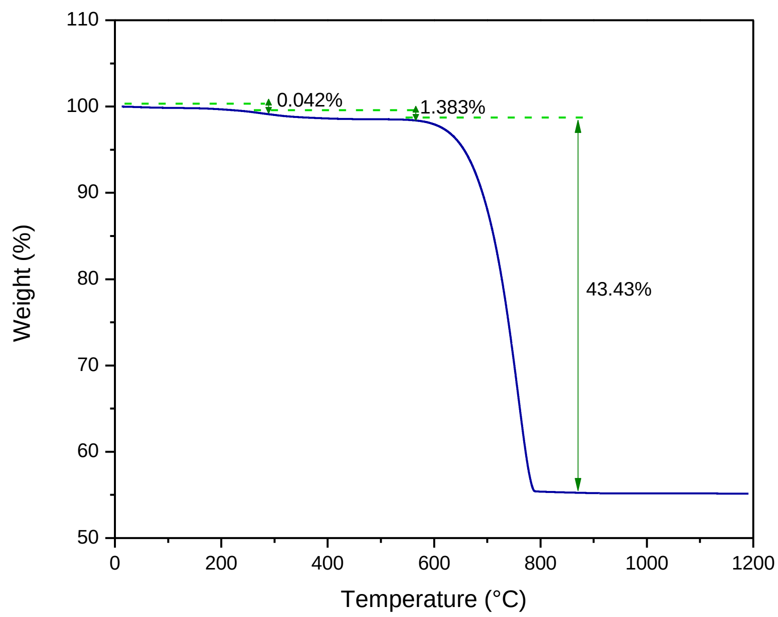

In Graphic 2.2 it is possible to clearly observe three significant weight losses. The first one occurs before 200°C and corresponds to the loss of the physiosorbed water on the surface of the sample.

The second stage, between 250ºC and 550°C, is explained by Yoshioka as the chemical transformation of the aragonite phase to the calcite phase (Yoshioka, 1985). Finally, in the third stage, the most important weight loss is observed, which is associated with the decomposition of $CaCO_3$ into CaO and CO_2, which occurs between 550ºC and 900°C (Foldvari, 2011). As a result of the previous analysis, it was possible to determine that the optimal calcination temperature to fully convert the $CaCO_3$ present into CaO is greater than 800°C, the above is consistent with reports of other investigations (Mansir et al., 2018a).

7.1.2. X-ray diffraction (XRD)

In order to know the crystalline phases in the samples, the X-ray diffraction technique was used. It is well known that the shells of different clams are largely constituted by $CaCO_3$ (Dey *et al.*, 2021; Zhang *et a*l., 2019), (Dey *et al.*, 2021; Zhang *et al.*, 2019), which makes them an ideal raw material for obtaining CaO. To corroborate the presence of $CaCO_3$, an X-ray diffraction analysis was performed on the uncalcined clam shell and on the calcined clam shell at 900 ° C for 6h. The results can be seen in Figures 7.2 and 7.3, respectively. In the case of the uncalcined clam shell (Graphic 2.2), it was possible to identify that the main component of the clam shell is $CaCO_3$, which is also present in the crystalline phases aragonite (JCPDS #760606) and calcite (JCPDS #240027).

Graphic 2.2 Uncalcined clam shell diffractogram

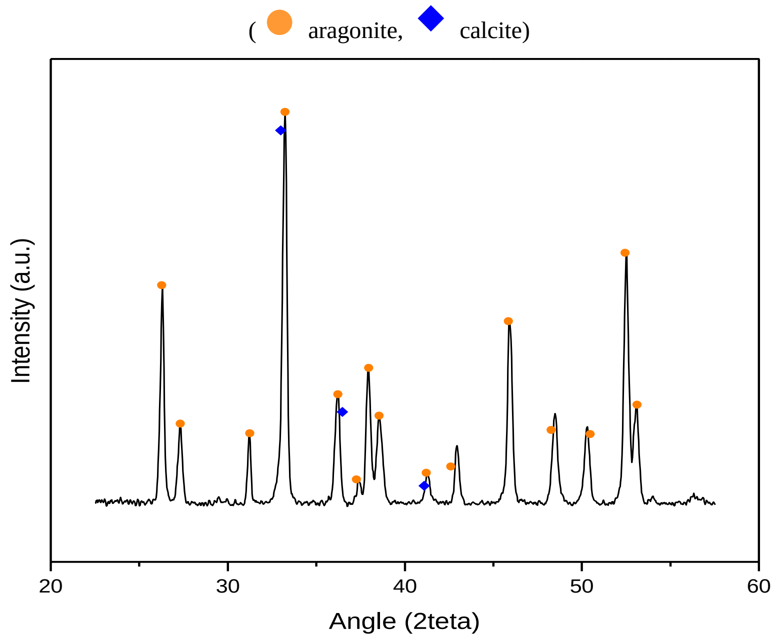

In the shell sample calcined for 6 h at 900ºC (Graphic 2.3) it was possible to identify the complete transformation of $CaCO_3$ into CaO (JCPDS #371497). Similar results were observed in calcium oxide catalysts from natural materials such as eggshell and sea snail shell (Krishnamurthy *et al*., 2020).

Graphic 2.3: Calcined clam shell diffractogram

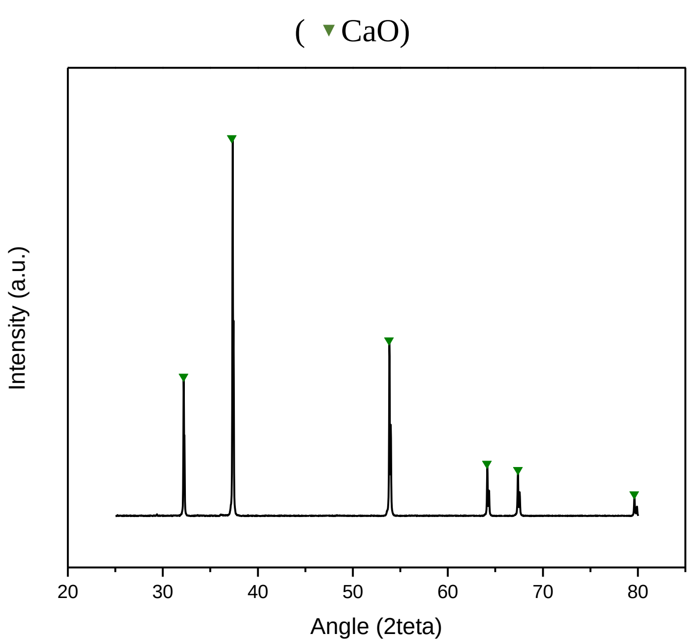

According to the previous diffractograms, all the $CaCO_3$ has been transformed into CaO after subjecting the sample to a calcination of 900ºC, which agrees with the results of the TGA analysis.

On the other hand, for the Fe_2O_3/CaO catalyst (calcined for 6 h at 600ºC), the X-ray diffraction analysis managed to identify the following phases: Fe_2O_3 (JCPDS #330664), Fe_3O_4 (JCPDS #890688), $Ca_2Fe_2O_5$ (JCPDS #712264), $Ca_2Fe_{15.57}O_{25.56}$ (JCPDS #722346) y CaO (JCPDS #371497).

Graphic 2.4 Catalyst diffractogram Fe_2O_3/CaO

(■ Fe_2O_3 ◆ Fe_3O_4 ⬟ $Ca_2Fe_2O_5$ ★ $Ca_2Fe_{15.57}O_{25.56}$ ▼ CaO)

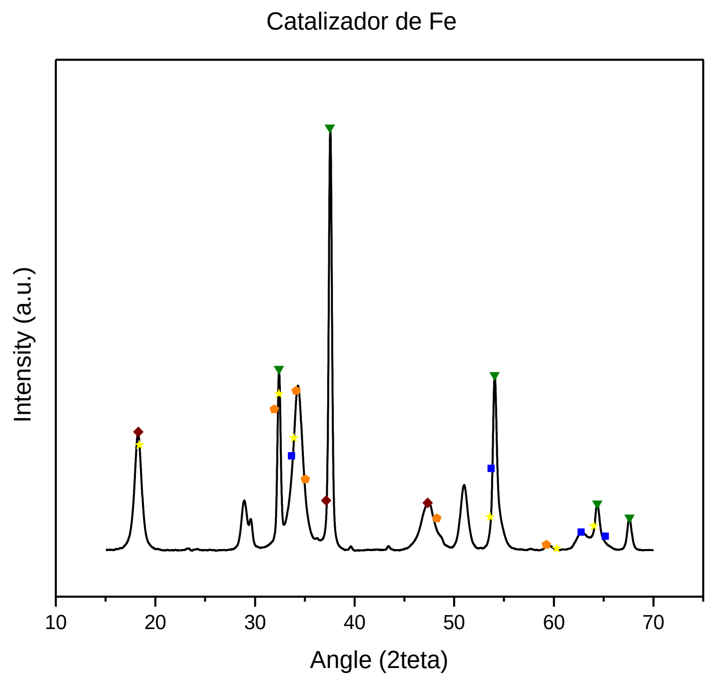

7.1.3 Inductively coupled plasma atomic emission spectroscopy (ICP-AES)

In order to know the composition of the bifunctional catalyst Fe_2O_3/CaO, an induction coupled plasma atomic emission spectrometry (ICP-AES) was performed.

For the synthesized sample, using 7% by weight of the precursor salt, 1.0% by weight corresponding to iron and 57.30% by weight of calcium were obtained.

7.2. Characterization of waste cooking oil

7.2.1. Acid value

To demonstrate the bifunctionality of our catalyst, it is necessary to work with a lipid raw material that has a higher amount of FFA, compared to a refined oil. This is because a conventional basic heterogeneous catalyst would saponify such FFAs.

A comparison was made between the acid value of a refined oil and the waste cooking oil that was used as raw material for the transesterification reaction. This was conducted in order to show that waste cooking oil has more free fatty acids than refined oil.

In this test it was found that the acid value of the refined oil was 0.041 mgKOH/g, in comparison with the 4 mgKOH/g (2%) present in the waste cooking oil.

7.2.2. Viscosity

Viscosity is a parameter that will allow us to know if the transesterification reaction did occur, since there is a decrease in the viscosity of the raw material after the production of methyl esters.

In order to be able to carry out a comparison before and after the transesterification reaction, the measurement of the viscosity of the waste cooking oil was used and, as a reference point, a refined oil.

The kinematic viscosity oil determination was carried out at 40 ° C by triplicate, obtaining an average value of 39.2 mm^2 /s for refining oil and 41.33mm^2/s for waste cooking oil.

7.3. Catalytic evaluation

7.3.1. Influence of the type of catalyst with waste cooking oil

When waste cooking oil is used as lipid raw material, conventional basic catalysts have low reaction yields, which is attributable to the acidic character of the oil, due to the fact that it has a higher presence of FFA (Endalew *et al.*, 2011; Yuliana *et al.*, 2020).

This has been reflected in various investigations that use CaO as a heterogeneous catalyst in the production of biodiesel, obtaining low reaction yields where long reaction times are needed (Endalew *et al.*, 2011; Yuliana *et al.*, 2020). However, the presence of two different active sites in bifunctional catalysts allows them to be able to use lipid raw materials with higher FFA contents, since they can simultaneously carry out their esterification and the transesterification of triglycerides (Zhang *et al.*, 2019).

As a comparison, a reaction was carried out using only CaO as a catalyst (Graphic 2.5a), achieving 67% of methyl esters after 5 hours of reaction. On the other hand, the WCO reaction using a bifunctional iron catalyst (Graph 2.5b), managed to obtain 98.75% of methyl esters in the same reaction time.

Graphic 2.5 a. WCO and CaO reaction and b. WCO and Fe_2O_3/CaO reaction

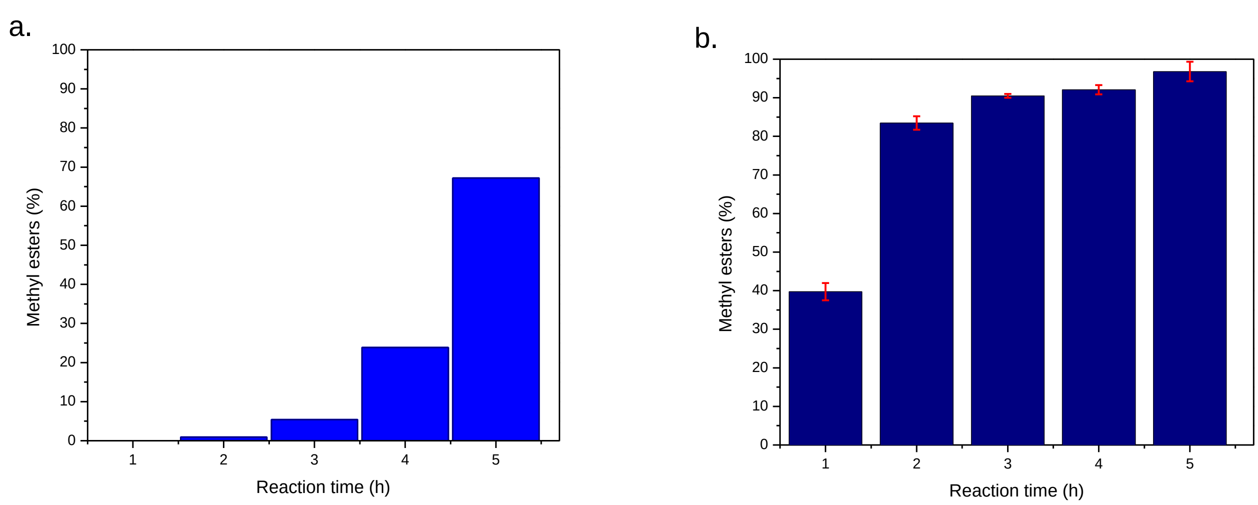

As can be seen in Figure 2.5a and Figure 2.5b, there is a significant difference in the reaction rate, since we can observe how in the fifth hour of reaction with CaO as a catalyst a lower content of methyl esters was reached, compared to the second hour of reaction with a bifunctional catalyst.

7.3.2. Effect of the amount of salt on the bifunctional catalyst (Fe_2O_3/CaO)

Another important variable to study in the use of bifunctional catalysts in the transesterification of waste cooking oil is the precursor salt load.

In order to analyze the effect of the precursor amount of iron, in this project the synthesis of the catalyst was carried out with 5% and 7% by weight of the precursor salt $Fe(NO_3)_3*9H_2O$. The results obtained are shown in Graphic 2.6.

Graphic 2.6 a. Catalyst 5% by weight of $Fe(NO_3)_3$ and b. Catalyst 7% by weight of $Fe(NO_3)_3$.

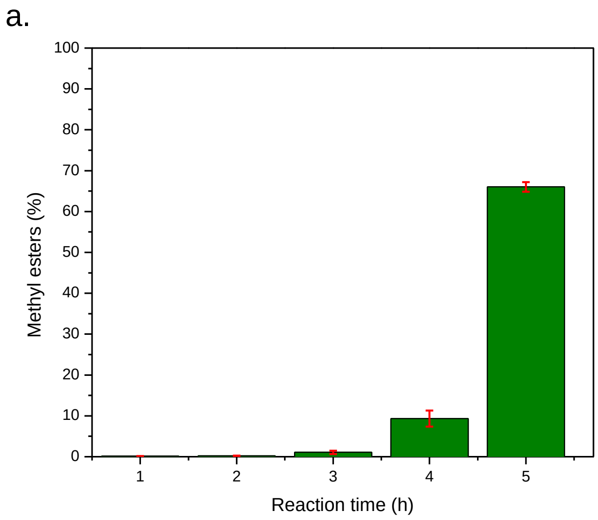

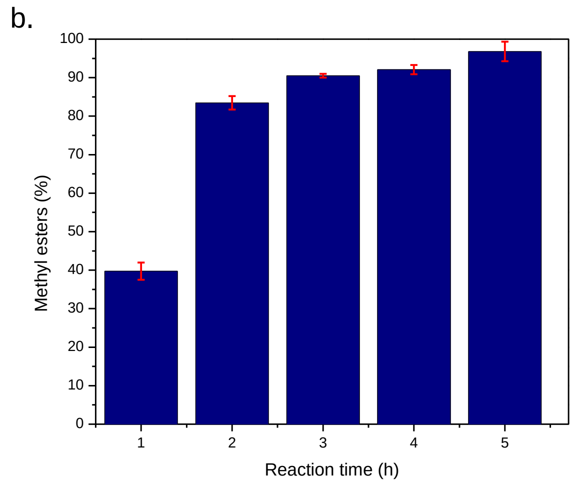

Comparison of the previous results shows that 7% by weight of iron precursor salt is the best amount, due to the fact that 98.8% of methyl esters were obtained after 5 hours of reaction.

The catalyst with 5% by weight managed to obtain 67.7% content of methyl esters, which is similar to the result obtained when using only CaO as a catalyst. This is attributed to the fact that there is no significant impregnation of acidic active sites (from iron), which is why it is not possible for the catalyst to carry out the esterification of the FFA from the waste cooking oil.

7.4. Biodiesel Characterization

To characterize the biodiesel obtained from the previous transesterification reactions, the content of fatty acid methyl esters (FAMEs), viscosity and acid value was determined by means of the standard methods shown in UNE-EN 14103, ISO 3104 and UNE-EN 14104.

To have a point of comparison, the characterization of the biodiesel obtained from the transesterification reaction with refined oil was carried out, using Fe_2O_3/CaO as catalyst, obtaining a 98.8% content of ethyl esters, a viscosity of 4.8mm^2/s and an acid value 0.05mgKOH/g.

On the other hand, for the biodiesel produced from waste cooking oil, an average of 98.8% of FAMEs was obtained, a viscosity of 4.6mm^2/s and an acid value of 0.052mgKOH/g. It is very important to observe the effectiveness of the bifunctional catalyst, because this catalyst allows to obtain contents of methyl esters higher than those required by the EN-14214 standard (96.5%) and a viscosity within the range accepted by the standard (3.5-5.0mm^2/s).

8. Acknowledgements

The authors are grateful for the help given to the characterization of the catalyst to Dr. HERNÁNDEZ-BALDERAS, Uvaldo. PhD, GÓMEZ-ESPINOSA, Rosa María. PhD, HERNÁNDEZ-LÓPEZ, Susana and LÓPEZ-TÉLLEZ, Gustavo, The financial support of the Universidad Autónoma del Estado de México through project 6218/2020CIB. MCF thanks to the Consejo Nacional de Ciencia y Tecnología (CONACYT) for the postgraduate studies scholarship (Number 1000624).

9. Conclusions

A bifunctional catalyst, Fe_2O_3/CaO, was synthesized with basic (provided by CaO) and acid active sites (provided by iron). This bifunctionality allows to process lipid raw materials with higher content of free fatty acids than those present in refined oils.

Biodiesel was obtained through a simultaneous reaction of esterification and transesterification, using 6% by weight of catalyst, a content of 1% by weight of iron, methanol: oil molar ratio of 12: 1, with a reaction time of 5h, obtaining a content of methyl esters higher than 98%.

It was determined that 7% by weight of iron precursor salt in the synthesis of the catalyst is the optimal amount of precursor salt to obtain biodiesel that complies with EN-14214 regulations.

The development of efficient heterogeneous catalysts in the use of lipid raw materials with a higher FFA content represents a significant area of opportunity in reducing the cost of biodiesel production. However, the efficiency of a heterogeneous catalyst depends on several variables, such as the type of raw material, the type of alcohol used, the molar ratio of alcohol: oil, reaction temperature, stirring speed, type of reactor, in addition to the type of catalyst used.

10. References

Adepoju, T. F., Ibeh, M. A., Babatunde, E. O., & Asquo, A. J. (2020). Methanolysis of CaO based catalyst derived from egg shell-snail shell-wood ash mixed for fatty acid methylester (FAME) synthesis from a ternary mixture of Irvingia gabonensis -Pentaclethra macrophylla - Elais guineensis oil blend: An application of simple. *Fuel*, *275*(May), 117997. https://doi.org/10.1016/j.fuel.2020.117997

Adepoju, T. F., Olatunbosun, B. E., Olatunji, O. M., & Ibeh, M. A. (2018). Brette Pearl Spar Mable (BPSM): a potential recoverable catalyst as a renewable source of biodiesel from Thevetia peruviana seed oil for the benefit of sustainable development in West Africa. *Energy, Sustainability and Society*, *8*(1), 1–17. https://doi.org/10.1186/s13705-018-0164-1

Aguilar R., G. y S. B. J. (2003). *Fundamentos de Catálisis. Alfaomega*. México DF, IPN.

Bhavani, A. G., & Sharma, V. K. (2018). Production of Biodiesel from Waste Cooking Oil: A Review. *Journal of Advanced Chemical Sciences*, *4*(1), 549–555. https://doi.org/10.30799/jacs.181.18040105

Borah, M. J., Das, A., Das, V., Bhuyan, N., & Deka, D. (2019). Transesterification of waste cooking oil for biodiesel production catalyzed by Zn substituted waste egg shell derived CaO nanocatalyst. *Fuel*, *242*(January), 345–354. https://doi.org/10.1016/j.fuel.2019.01.060

Dey, S., Reang, N. M., Das, P. K., & Deb, M. (2021). A comprehensive study on prospects of economy, environment, and efficiency of palm oil biodiesel as a renewable fuel. *Journal of Cleaner Production*, *286*, 124981. https://doi.org/10.1016/j.jclepro.2020.124981

Endalew, A. K., Kiros, Y., & Zanzi, R. (2011). Heterogeneous catalysis for biodiesel production from Jatropha curcas oil (JCO). *Energy*, *36*(5), 2693–2700. https://doi.org/10.1016/j.energy.2011.02.010

Ezzah-Mahmudah, S., Lokman, I. M., Saiman, M. I., & Taufiq-Yap, Y. H. (2016). Synthesis and characterization of Fe2O3/CaO derived from Anadara Granosa for methyl ester production. *Energy Conversion and Management*, *126*, 124–131. https://doi.org/10.1016/j.enconman.2016.07.072

Faruque, M. O., Razzak, S. A., & Hossain, M. M. (2020). Application of heterogeneous catalysts for biodiesel production from microalgal oil—a review. *Catalysts*, *10*(9), 1–25. https://doi.org/10.3390/catal10091025

Foldvari, M. (2011). Handbook of thermo-gravimetric system of minerals and its use in geological practice. In *Occasional papers of the geological institute of Hungary* (Vol. 213).

Foroutan, R., Mohammadi, R., Esmaeili, H., Mirzaee Bektashi, F., & Tamjidi, S. (2020). Transesterification of waste edible oils to biodiesel using calcium oxide@magnesium oxide nanocatalyst. *Waste Management*, *105*, 373–383. https://doi.org/10.1016/j.wasman.2020.02.032

Gan, S., Ng, H. K., Chan, P. H., & Leong, F. L. (2012). Heterogeneous free fatty acids esterification in waste cooking oil using ion-exchange resins. *Fuel Processing Technology*, *102*, 67–72. https://doi.org/10.1016/j.fuproc.2012.04.038

Gandure, J., Ketlogetswe, C., & Jonas, M. (2017). Production, Composition and Fuel Properties of Tallow Biodiesel: A Case of Botswana. *Energy and Power Engineering*, *09*(07), 355–365. https://doi.org/10.4236/epe.2017.97024

Gaur, A., Mishra, S., Chowdhury, S., Baredar, P., & Verma, P. (2020). A review on factor affecting biodiesel production from waste cooking oil: An Indian perspective. *Materials Today: Proceedings*, *xxxx*. https://doi.org/10.1016/j.matpr.2020.09.432

Gebremariam, S. N., & Marchetti, J. M. (2018a). *Biodiesel production through sulfuric acid catalyzed transesteri fi cation of acidic oil : Techno economic feasibility of di ff erent process alternatives*. *174*(August), 639–648. https://doi.org/10.1016/j.enconman.2018.08.078

Gebremariam, S. N., & Marchetti, J. M. (2018b). Economics of biodiesel production: Review. In *Energy Conversion and Management* (Vol. 168). https://doi.org/10.1016/j.enconman.2018.05.002

Gnanaprakasam, A., Sivakumar, V. M., Surendhar, A., Thirumarimurugan, M., & Kannadasan, T. (2013). Recent Strategy of Biodiesel Production from Waste Cooking Oil and Process Influencing Parameters: A Review. *Journal of Energy*, *2013*, 1–10. https://doi.org/10.1155/2013/926392

Guczi, L., & Erdöhelyi, A. (2011). Catalysis for alternative energy generation. *Catalysis for Alternative Energy Generation*, *9781461403*, 1–536. https://doi.org/10.1007/978-1-4614-0344-9

Guncheva, M., & Zhiryakova, D. (2011). Catalytic properties and potential applications of Bacillus lipases. *Journal of Molecular Catalysis B: Enzymatic*, *68*(1), 1–21. https://doi.org/10.1016/j.molcatb.2010.09.002

Guo, M., Jiang, W., Chen, C., Qu, S., Lu, J., Yi, W., & Ding, J. (2021). Process optimization of biodiesel production from waste cooking oil by esterification of free fatty acids using La3+/ZnO-TiO2 photocatalyst. *Energy Conversion and Management*, *229*(December 2020), 113745. https://doi.org/10.1016/j.enconman.2020.113745

Hafeez, S., Al-Salem, S. M., Manos, G., & Constantinou, A. (2020). Fuel production using membrane reactors: a review. *Environmental Chemistry Letters*, *18*(5), 1477–1490. https://doi.org/10.1007/s10311-020-01024-7

Hamza, M., Ayoub, M., Shamsuddin, R. Bin, Mukhtar, A., Saqib, S., Zahid, I., Ameen, M., Ullah, S., Al-Sehemi, A. G., & Ibrahim, M. (2021). A review on the waste biomass derived catalysts for biodiesel production. *Environmental Technology and Innovation*, *21*, 101200. https://doi.org/10.1016/j.eti.2020.101200

Helwani, Z., Othman, M. R., Aziz, N., Fernando, W. J. N., & Kim, J. (2009). Technologies for production of biodiesel focusing on green catalytic techniques: A review. *Fuel Processing Technology*, *90*(12), 1502–1514. https://doi.org/10.1016/j.fuproc.2009.07.016

Hernández N. (2011). *Pirólisis de biomasa para producir biocuombustible*. Universidad Autónoma de Nuevo León.

Khan, H. M., Ali, C. H., Iqbal, T., Yasin, S., Sulaiman, M., Mahmood, H., Raashid, M., Pasha, M., & Mu, B. (2019). Current scenario and potential of biodiesel production from waste cooking oil in Pakistan: An overview. *Chinese Journal of Chemical Engineering*, *27*(10), 2238–2250. https://doi.org/10.1016/j.cjche.2018.12.010

Khodadadi, M. R., Malpartida, I., Tsang, C. W., Lin, C. S. K., & Len, C. (2020). Recent advances on the catalytic conversion of waste cooking oil. *Molecular Catalysis*, *494*(July), 111128. https://doi.org/10.1016/j.mcat.2020.111128

Krishnamurthy, K. N., Sridhara, S. N., & Ananda Kumar, C. S. (2020). Optimization and kinetic study of biodiesel production from Hydnocarpus wightiana oil and dairy waste scum using snail shell CaO nano catalyst. *Renewable Energy*, *146*, 280–296. https://doi.org/10.1016/j.renene.2019.06.161

Lam, M. K., Lee, K. T., & Mohamed, A. R. (2010). Homogeneous , heterogeneous and enzymatic catalysis for transesteri fi cation of high free fatty acid oil (waste cooking oil) to biodiesel : A review. *Biotechnology Advances*, *28*(4), 500–518. https://doi.org/10.1016/j.biotechadv.2010.03.002

Lee, A. F., Bennett, J. A., Manayil, J. C., & Wilson, K. (2014). Heterogeneous catalysis for sustainable biodiesel production via esterification and transesterification. *Chemical Society Reviews*, *43*(22), 7887–7916. https://doi.org/10.1039/c4cs00189c

Llanes Cedeño, E. A. (2017). Producción e Impacto del Biodiesel: Una Revisión. *INNOVA Research Journal*, *2*(7), 59–76. https://doi.org/10.33890/innova.v2.n7.2017.229

Lv, E., Dou, T., Ding, S., Lu, J., Li, Z., Yi, W., Li, J., & Ding, J. (2020). Membrane dehydration-enhanced esterification for biodiesel production from a potential feedstock of Firmiana platanifolia L.f. seed oil. *Chemical Engineering Research and Design*, *153*, 1–7. https://doi.org/10.1016/j.cherd.2019.10.020

Mahmood Khan, H., Iqbal, T., Haider Ali, C., Javaid, A., & Iqbal Cheema, I. (2020). Sustainable biodiesel production from waste cooking oil utilizing waste ostrich (Struthio camelus) bones derived heterogeneous catalyst. *Fuel*, *277*(January), 118091. https://doi.org/10.1016/j.fuel.2020.118091

Mansir, N., Teo, S. H., Rashid, U., Saiman, M. I., Tan, Y. P., Alsultan, G. A., & Taufiq-Yap, Y. H. (2018a). Modified waste egg shell derived bifunctional catalyst for biodiesel production from high FFA waste cooking oil. A review. *Renewable and Sustainable Energy Reviews*, *82*(November 2016), 3645–3655. https://doi.org/10.1016/j.rser.2017.10.098

Mansir, N., Teo, S. H., Rashid, U., Saiman, M. I., Tan, Y. P., Alsultan, G. A., & Taufiq-Yap, Y. H. (2018b). Modified waste egg shell derived bifunctional catalyst for biodiesel production from high FFA waste cooking oil. A review. *Renewable and Sustainable Energy Reviews*, *82*(October 2017), 3645–3655. https://doi.org/10.1016/j.rser.2017.10.098

Mohammed, A. R., & Bandari, C. (2020). Lab-scale catalytic production of biodiesel from waste cooking oil – a review. *Biofuels*, *11*(4), 409–419. https://doi.org/10.1080/17597269.2017.1370882

Molina, C. (2013). *Estudio de la composición y estabilidad de biodiesel obtenido a partir de aceites vegetales limpios y procedentes de aceites de fritura.* ftp://h3.bbtk.ull.es/ccppytec/cp439.pdf

Mosali Raj and Bobbili Sharath. (2011). *Biodiesel Magazine - The Latest News and Data About Biodiesel Production*. http://www.biodieselmagazine.com/articles/7793/homogenous-catalyst-and-effects-on-multifeedstock-processing

Narula, V., Khan, M. F., Negi, A., Kalra, S., Thakur, A., & Jain, S. (2017). Low temperature optimization of biodiesel production from algal oil using CaO and CaO/Al2O3 as catalyst by the application of response surface methodology. *Energy*, *140*, 879–884. https://doi.org/10.1016/j.energy.2017.09.028

Nur Syazwani, O., Lokman Ibrahim, M., Wahyudiono, Kanda, H., Goto, M., & Taufiq-Yap, Y. H. (2017). Esterification of high free fatty acids in supercritical methanol using sulfated angel wing shells as catalyst. *Journal of Supercritical Fluids*, *124*, 1–9. https://doi.org/10.1016/j.supflu.2017.01.002

Ogunkunle, O., & Ahmed, N. A. (2019). A review of global current scenario of biodiesel adoption and combustion in vehicular diesel engines. *Energy Reports*, *5*, 1560–1579. https://doi.org/10.1016/j.egyr.2019.10.028

Pájaro, N. P., & Verbel, J. T. (2011). Química verde: un nuevo reto. *Ciencia e Ingeniería Neogranadina*, *21*(2), 169–182.

Papargyriou, D., Broumidis, E., de Vere-Tucker, M., Gavrielides, S., Hilditch, P., Irvine, J. T. S., & Bonaccorso, A. D. (2019). Investigation of solid base catalysts for biodiesel production from fish oil. *Renewable Energy*, *139*, 661–669. https://doi.org/10.1016/j.renene.2019.02.124

Ramadhas, A. S., Jayaraj, S., & Muraleedharan, C. (2016). Biodiesel. In *Alternative Fuels for Transportation* (pp. 41–80). https://doi.org/10.1520/mnl11645m

Shi, M., Zhang, P., Fan, M., Jiang, P., & Dong, Y. (2017). Influence of crystal of Fe2O3 in magnetism and activity of nanoparticle CaO@Fe2O3 for biodiesel production. *Fuel*, *197*, 343–347. https://doi.org/10.1016/j.fuel.2017.02.060

Sivaprakash, G., Mohanrasu, K., Ananthi, V., Jothibasu, M., Nguyen, D. D., Ravindran, B., Chang, S. W., Nguyen-Tri, P., Tran, N. H., Sudhakar, M., Gurunathan, K., Arokiyaraj, S., & Arun, A. (2019). Biodiesel production from Ulva linza, Ulva tubulosa, Ulva fasciata, Ulva rigida, Ulva reticulate by using Mn2ZnO4 heterogenous nanocatalysts. *Fuel*, *255*(February), 115744. https://doi.org/10.1016/j.fuel.2019.115744

Solis, J. L., Alejo, L., & Kiros, Y. (2016). Calcium and tin oxides for heterogeneous transesterification of Babasssu oil (Attalea speciosa). *Journal of Environmental Chemical Engineering*, *4*(4), 4870–4877. https://doi.org/10.1016/j.jece.2016.04.006

Talha, N. S., & Sulaiman, S. (2016). Overview of catalysts in biodiesel production. *ARPN Journal of Engineering and Applied Sciences*, *11*(1), 439–442.

Tariq, M., Ali, S., & Khalid, N. (2012). Activity of homogeneous and heterogeneous catalysts, spectroscopic and chromatographic characterization of biodiesel: A review. *Renewable and Sustainable Energy Reviews*, *16*(8), 6303–6316. https://doi.org/10.1016/j.rser.2012.07.005
Yoshioka, S. (1985). *A-i*. *19*, 245–249.

Yuliana, M., Santoso, S. P., Soetaredjo, F. E., Ismadji, S., Angkawijaya, A. E., Irawaty, W., Ju, Y. H., Tran-Nguyen, P. L., & Hartono, S. B. (2020). Utilization of waste capiz shell - Based catalyst for the conversion of leather tanning waste into biodiesel. *Journal of Environmental Chemical Engineering*, *8*(4), 104012. https://doi.org/10.1016/j.jece.2020.104012

Zhang, H., Li, H., Hu, Y., Venkateswara Rao, K. T., Xu, C. (Charles), & Yang, S. (2019). Advances in production of bio-based ester fuels with heterogeneous bifunctional catalysts. *Renewable and Sustainable Energy Reviews*, *114*(February). https://doi.org/10.1016/j.rser.2019.109296

Chapter 3 Biodiesel production as an alternative to reduce the environmental impact of University food courts

Capítulo 3 Producción de biodiesel como escenario alternativo para mejorar el desempeño ambiental de cafeterías universitarias

ALANIS-RAMÍREZ, Claudia Ivett†*, ÁVILA-CORDOBA, Liliana[2], ROMERO-ROMERO, Rubi[1] and NATIVIDAD, Reyna[1]

[1]*Chemical Eng. Lab., Centro Conjunto de Investigación en Química Sustentable UAEM-UNAM, Universidad Autónoma del Estado de México, Toluca, Mexico, CP 50200*
[2]*Universidad Autónoma del Estado de México, Centro Conjunto en Química Sustentable.*

ID 1st Author: *Claudia Ivett, Alanis-Ramírez* / **ORC ID**: 0000-0001-6935-1798, **CVU CONACYT ID:** 360631

ID 1st Co-author: *Liliana, Ávila-Cordoba* / **ORC ID**: 0000-0002-1073-5196, **CVU CONACYT ID:** 323060

ID 2nd Co-author: *Rubi, Romero-Romero* / **ORC ID**: 0000-0001-9163-7936, **CVU CONACYT ID:** 121454

ID 3rd Co-author: *Reyna, Natividad* / **ORC ID**: 0000-0001-8978-1066, **CVU CONACYT ID:** 87755

DOI: 10.35429/H.2021.6.37.50

C. Alanis, L. Ávila, R. Rubi and R. Natividad

*claudia.alanis.iq@gmail.com

A. Marroquín, J. Olivares, M. Ramírez and L. Cruz (Coord). Engineering and Technology. Handbooks-©ECORFAN-México, Querétaro, 2021.

Abstract

The objective of this work was to assess the environmental impacts of producing biodiesel by heterogeneous and homogeneous catalysis. The raw material for the process was the waste cooking oil (WCO) generated at 27 food courts of Autonomous University of the State of Mexico. The study was conducted by applying Life Cycle Assessment methodology and the environmental impacts were calculated with the SimaPro 9.1.0.11 PhD software with the Ecoinvent database. The method was CML-IA base line C3.06/EU25. The assessed impact categories were: Abiotic Depletion Potential (ADP, elements), Abiotic Depletion Potential (ADP, fossil fuels), Global Warming Potential (100 years) (GWP), Ozone Layer Depletion (ODP), Human Toxicity (HT), Freshwater Aquatic Ecotoxicity (FWAE), Marine Aquatic Ecotoxicity (MAE), Terrestrial Ecotoxicity (TE), Photochemical Oxidation (PO), Acidification (A) and Eutrophication (E). In addition, end point environmental indicators were also calculated (Ecosystems Quality, Human Health Damage and Resources Availability) by the method ReCiPe 2016 Endpoint (H) V1.04 / World (2010) H/A. The system boundary enclosed three main stages, WCO collection, pre-treatment and reaction (to produce biodiesel). It was concluded that the reaction stage is the one with the highest environmental impact. In this sense, the highest impact categories were ADP (fossil fuels) (105.56 MJ), GWP (8.91 kg $CO_{2\ eq}$) and MAE (2387.89 kg 1, 4-DB $_{eq}$). Nevertheless, it was also found that the GWP for the heterogeneous process is 82.52 % lower than that calculated for the homogeneous process. In addition, the human health damage of the homogeneous process is 1.77 points and is higher than the observed with the heterogeneous process.

Waste cooking oil, Life cycle analysis, Heterogeneous process, Homogeneous process, Bifuntional catalyst

Resumen

El objetivo de este trabajo fue evaluar los impactos ambientales de la producción de biodiésel mediante catálisis heterogénea y homogénenea. La materia prima para el proceso fue el aceite de cocina residual (ACR) generado en 27 cafeterías de la Universidad Autónoma del Estado de México. El estudio se realizó aplicando la metodología de Análisis de Ciclo de Vida y los impactos ambientales se calcularon con el software SimaPro 9.1.0.11 y la base de datos Ecoinvent. El método fue CML-IA C3.06/EU25. Las categorías de impacto evaluadas fueron: Agotamiento Abiótico Potencial (AAP, elementos), Agotamiento Abiótico Potential (AAP, combustibles fósiles), Potencial de Calentamiento Global (100 años) (PCG), Agotamiento Capa de Ozono (ACO), Toxicidad Humana (TH), Ecotoxicidad de Agua Dulce (EAD), Ecotoxicidad de Agua Marina (EAM), Ecotoxicidad Terrestre (ET), Oxidación Fotoquímica (OF), Acidificación (A) y Eutrofización (E). También se calcularon indicadores ambientales de punto final (Calidad de los Ecosistemas, Daño a la Salud Humana y Disponibilidad de Recursos) por el método ReCiPe 2016 Endpoint (H) V1.04 / World (2010) H/A. El sistema analizado consistió en tres etapas principales: colecta, pretratamiento y reacción del ACR para producir biodiésel. Se concluyó que la etapa de reacción es la que tiene el mayor impacto ambiental. En este sentido, las categorías de mayor impacto fueron: ACF (105.56 MJ), PCG (8.91 kg de $CO_{2\ eq}$) y EAM (2387.89 kg 1,4-DB eq). No obstante, también se constató que el PCG para el proceso heterogéneo es 82.52 % inferior al reportado proceso homogéneneo. Además, el daño a la salud humana del proceso homogéneo es 1.77 puntos mayor que en el proceso heterogéneo estudiado.

Aceite residual de cocina, Análisis de ciclo de vida, Proceso heterogéneo, Proceso homogéneo, Catalizador bifuncional

1. Introduction

The Ministry of the Environmental and Natural Resources (SEMARNAT in spanish) in its Sectoral Program 2020-2024 (SEMARNAT, 2020), suggests that for the sustainable management of organic waste, it is necessary to strengthen its comprehensive management under a circular economy approach, integrating this vision into educational processes to promote environmental management in national and international academic institutions (green schools) (SEMARNAT, 2019). For this, it is necessary to identify the stages with the greatest environmental impact and this can be achieved by applying a life cycle assessment (LCA) (Chung *et al.*, 2019). This is an approved international methodology for the evaluation of bioenergy systems using residual biomass streams from food (Antoniadou *et al.*, 2020).

Recently, Universities from the United Kingdom (Gu *et al*., 2018), India (Sangwan *et al*., 2018), China (Tsai *et al*., 2020), the United States (Clabeaux *et al*., 2020) and Mexico (Güereca *et al*., 2013), have been carried out analysis from a life cycle perspective, to reduce and avoid the waste of food, promoting pilot programs aimed at the sustainable management of its waste in University campus with the aim of reducing its environmental footprint, taking advantage of the technical and scientific capabilities of their human resources and infrastructure.

Yañez *et al*., (2020), carried out, for example, a study on carbon footprint in tonnes of carbon dioxide equivalent (tCO_{2eq}), units per student for various Latin American universities with the aim of facilitating institutional decision-making. In Mexico, studies have been reported in two universities, the Autonomous Metropolitan University (UAM) (Mendoza *et al*., 2019) and the National Autonomous University of Mexico (UNAM) (Güereca *et al*., 2013). These studies focus mainly on solid waste management.

The studies above-mentioned show that waste from coffee shops or restaurants is an environmental problem that can be remediated through proper use and management. For this, an assessment of the environmental performance of waste disposal scenarios, both solid and liquid, is essential. Among the liquid waste, one that has attracted special interest is the waste cooking oil (WCO) because one liter of WCO represents five thousand times more polluting load than that of the sewage and can contaminate up to 40 thousand liters of water, which is equivalent to the annual consumption of a person's sanitary water (EPA, 2000), (Rincón *et al*., 2019) and (González & González, 2015).

An alternative that has been the subject of numerous investigations is the use of WCO as a second-generation raw material to produce biodiesel. Its use has been demonstrated to reduce the negative environmental impact inherent to the process, as it is a raw material that does not require a stage of cultivation or extraction (Foteinis *et al*., 2020), (Amaya *et al*., 2020) and (Viornery *et al*., 2020). Recycling cooking oil for biodiesel production is an example of a sustainable action that, well organized, could satisfy the criteria for green circular economic activity in the context of promoting a continuous reduction of the environmental impacts using low CO_2 emissions energy. Simultaneously, achieving the goal of employment creation, helping to benefit human health and increasing social inclusion (Sheinbaum *et al*., 2013), (Orjuela & Clark, 2020). In the European Union, 32% of biodiesel is produced exclusively from recovered WCO (Flach *et al*., 2019).

Within the sustainable processing routes of the WCO to biodiesel, there is the physico-chemical conversion (Rincón & Silva, 2015), by an esterification and transesterification treatment for the conversion of free fatty acids (FFA) and triglycerides into biodiesel (fatty acid methyl esters, FAME's). Esterification and transesterification are the chemical reactions of an oil or fat with an alcohol, which are catalyzed by an acid catalyst or base to form esters and glycerol. The most relevant variables to carry out the reaction with an efficient conversion of WCO with high FFA content, are: temperature, alcohol and oil molar ratio, catalyst quantity and reuse, stirring speed, the type of homogeneous or heterogeneous catalyst (acid or base), and the type of WCO (source of raw material), (Narasimhan *et al*., 2021). A product of this process is glycerol and this must be separated from biodiesel. This separation is typically conducted by decantation. There are also residues of the process that can be reused and recycled, such is the case of the catalyst and methanol (Marinković *et al*., 2016).

In the context of biodiesel production from WCO, it has been reported that the heterogeneous over homogeneous catalysis has great advantages due to its lower cost, lower corrosion, reuse, and easy separation (Gaur *et al*., 2020). The generation of residues in the reaction is a variable to consider for the determination of the environmental impacts in a LCA. Carlos and Diaz (2018), report that a heterogeneous process has an emission of pollutants below 65%. Furthermore, there are bifunctional catalysts that contain both, acid and basic sites, on the same catalytic surface that allow carrying out simultaneously the esterification of free fatty acids and the transesterification of triglycerides (Enguilo *et al*., 2021) and (Al-Muhtaseb *et al*., 2021).

As described above, the production of biodiesel is an alternative scenario for the use of WCO, which improves the environmental performance of the generating sites. This improvement should be established in order to contribute to the decision making of institutions and the consequent implementation of waste management programs to promote environmental management.

In this chapter it is presented as a subject of study, the University food courts (UFC) of the Autonomous University of the State of Mexico (UAEMéx). This institution has a guide for the management of solid urban waste, which classifies the WCO as a waste of special management, coming mainly from the UFC. However, the destination remains unknown even though collection campaigns have been conducted to facilitate and ensure final disposal.

The least favorable route is one that negatively impacts the sewage system, wastewater treatment and increases the risk of contaminating the soil and water bodies (ecotoxicity) (Hartini *et al*., 2020), directly affecting biodiversity; for the UFC, is the landfill located in San Luis Mextepec, in the municipality of Zinacantepec, State of Mexico, approximately 50 kilometers from the central area, managed by the private company of Environmental Services and Maintenance S.A de C.V (MASERA). It is worth mentioning that the standard (NADF-012-AMBT-2015) was published in Mexico City, which *"envisages establishing separation as a basic strategy of environmental policy, with the aim of implementing the management and adequate disposal of waste animal and/or plant fats and oils, seeking to consider the adoption of management measures, to prevent and reduce environmental impacts and harmful health effects"* (Gaceta oficial de la Ciudad de México, 2018). Based on the above, the main objective of this work was to establish alternative scenarios to valorize the WCO generated in the UFC of the Autonomous University of the State of Mexico to biodiesel, through a heterogeneous catalyzed process and compare it with a homogeneous one.

The objective described in the previous paragraph was achieved through applying the LCA methodology under ISO 14044 (Environmental management, life cycle analysis, requirements, and guidelines), which is described in detail in Section 2. In defining the scope, the following aspects were considered: intended application, reasons for carrying out the study, benefited sector of society, comparative and individual description of the process under study, functional unit definition, reference flow and system boundaries. In addition, an inventory was integrated from the data collection, with the application of surveys to the UFC managers, defining the general characteristics of the WCO generated in the UFC in the current waste management system. In the analysis of the inventory, inputs and outputs in the production of biodiesel were quantified, with the experimental information generated in the Chemical Engineering Laboratory of the Joint Research Center on Sustainable Chemistry UAEM-UNAM (CCIQS) triglycerides (Enguilo *et a*l., 2021).

For the homogeneous process, theoretical data were obtained from documentary information (Talens *et al*., 2010). The results are reported in Section 3, where data for the assessment of mid-point environmental impacts for the WCO are analyzed, as well as weighting and grouping of those directly related to life cycle impacts (characterization and classification) for the heterogeneous process. In addition, the mid-point and end-point environmental impacts for alternative esterification and transesterification scenarios are compared using homogeneous and heterogeneous catalysis. Finally, the conclusions section establishes the magnitude of the environmental impacts of the current management of WCO in the UFC and the feasibility of its reduction, through the production and use of biodiesel in mobile transport.

The aforementioned opens a window of opportunity, to reduce the environmental footprint of the University through the implementation of sustainable actions aimed at evaluating environmental performance indicators such as the reduction of the volume of organic waste for special management discharged to landfills, extending the lifetime of universities towards a circular economy and promoting sustainable consumption patterns, and waste management among the University community and subsequently in other social sectors, within the local level.

2. Methodology

The methodology was developed under the Mexican Standard of Life Cycle Assessment, Requirements and Guidelines (ISO 14044, 2006) and (UNEP/SETAC Life cycle Initiative, 2005), as shown in Figure 3.1.

Figure 3.1 Stages of a LCA according to the ISO 14040 series of standards

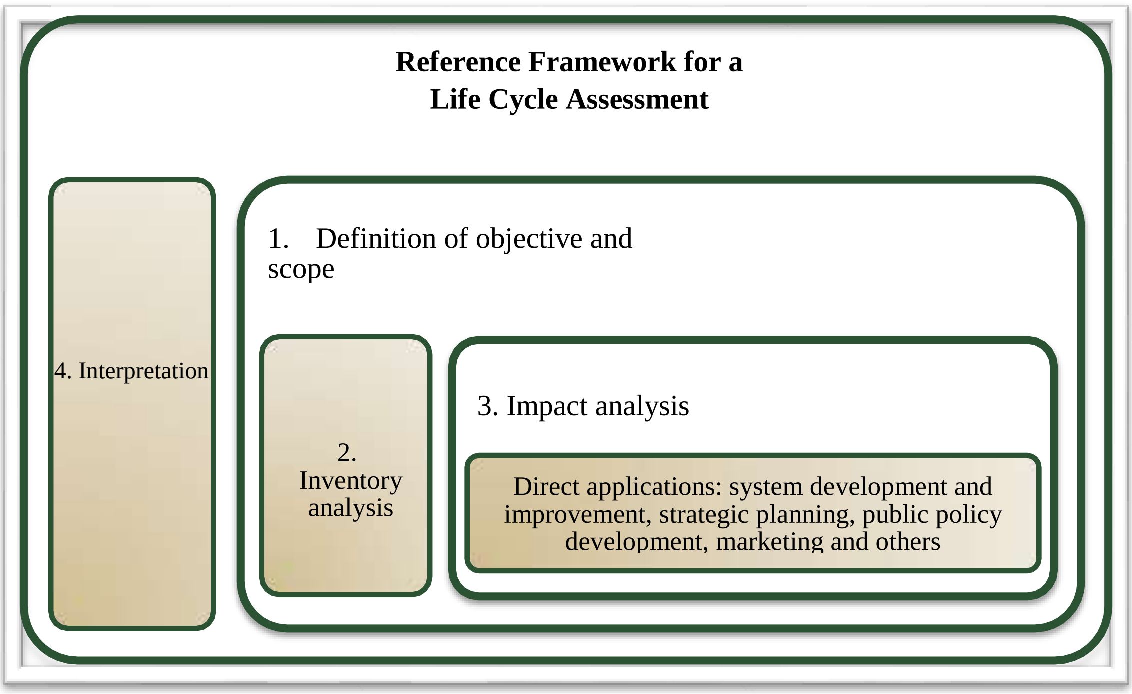

Source: (ISO 14044, 2006)

This study was conducted in the municipality of Toluca, State of Mexico, considering 27 UFC, which are classified into four collection routes (Colón-Espacios Deportivos "R1", Centro-Cerrillo "R2", Ciudad Universitaria "R3" and Remolques "R4") by the Department of Services of the UAEMéx, see Table 3.1. The data collection was carried out by means of a survey that was answered by the UFC managers as well as identifying the alternative scenarios of the WCO, see Figure 3.2, with information by route, management capacity from the institution, mobile infrastructure and management options with a scientific approach that is developed within the same University spaces.

Table 3.1 WCO collection routes generated in the University food courts of the UAEMéx

Collection route	University in academic spaces
R1	Faculty of Medicine Faculty of Urban Planning Faculty of Nursing Faculty of Chemistry Faculty of Anthropology Faculty of Languages Faculty of Dentistry
R2	San Cayetano Faculty of Gastronomy and Tourism Administrative Building Faculty of Agricultural Sciences Cerrillo piedras blancas El Rosedal
R3	International Centre for Language and Culture (CILC) Faculty of Tourism and Gastronomy University Town Faculty of Performing Arts Faculty of Economics Faculty of Geography Faculty of Engineering
R4	Campus No. 2 of the Preparatory School "Nezahualcóyotl" Faculty of Accounting and Administration UAEM "Unidad Los Uribe" Santa Cruz Azcapotzaltongo Central Library Faculty of Psychology Preparatory 3 "Cuauhtémoc" Center of Sustainable Chemistry UNAM-UAEM Campus no. 4 of the Preparatory School "Lic. Ignacio Ramírez Calzada" Campus no. 1 of the "Lic. Adolfo López Mateos" Campus No. 5 of the Preparatory School "Dr. Angel Ma. Garibay Kintana "

Source: Author´s Own Creation

To carry out the inventory analysis indicated by the LCA methodology, the unit processes in the production of biodiesel were determined, see Figure 3.3, establishing the system boundary for the management of WCO, from the WCO collection in the UFC, transport to the CCIQS for pretreatment was subsequently considered. In the laboratory, once the oil has been purified, esterification and transesterification reaction are carried out with a heterogeneous process, to finally produce biodiesel; it should be mentioned that glycerol is part of the coproducts. Methanol is reused as a reagent in the heterogeneous process stage, as well as a bifunctional catalyst. The functional unit of the experimental process is 1L of biodiesel produced, the reference flow is 150L per week of biodiesel, with a mass allocation of 100 % for its production.

The evaluation was performed using SimaPro 9.1.0.11 PhD software and the Ecoinvent database. The method was CML-IA baseline C3.06/EU25 with impact categories: Abiotic Depletion Potencial (ADP, elements), Abiotic Depletion Potential (ADP, fossil fuels), Global Warming Potential (100 years) (GWP), Ozone Layer Depletion (ODP), Human Toxicity (HT), Freshwater Aquatic Ecotoxicity (FWAE), Marine Aquatic Ecotoxicity (MAE), Terrestrial Ecotoxicity (TE), Photochemical Oxidation (PO), Acidification (A) and Eutrophication (E). In the interpretation, a heterogeneous process (scenario 1) was compared with a homogeneous process (scenario 2), the results are shown in Figure 3.3. Data reported by (Talens *et al;* 2010), were used for the homogeneous process. The assessment of end-point environmental indicators (Ecosystem Quality, Human Health Damage and Resource Availability) was carried out using the ReCiPe 2016 Endpoint (H) V1.04 / World (2010) H/A.

Figure 3.2. Integral Management System of Organic Waste of the UAEMéx, with alternative scenarios

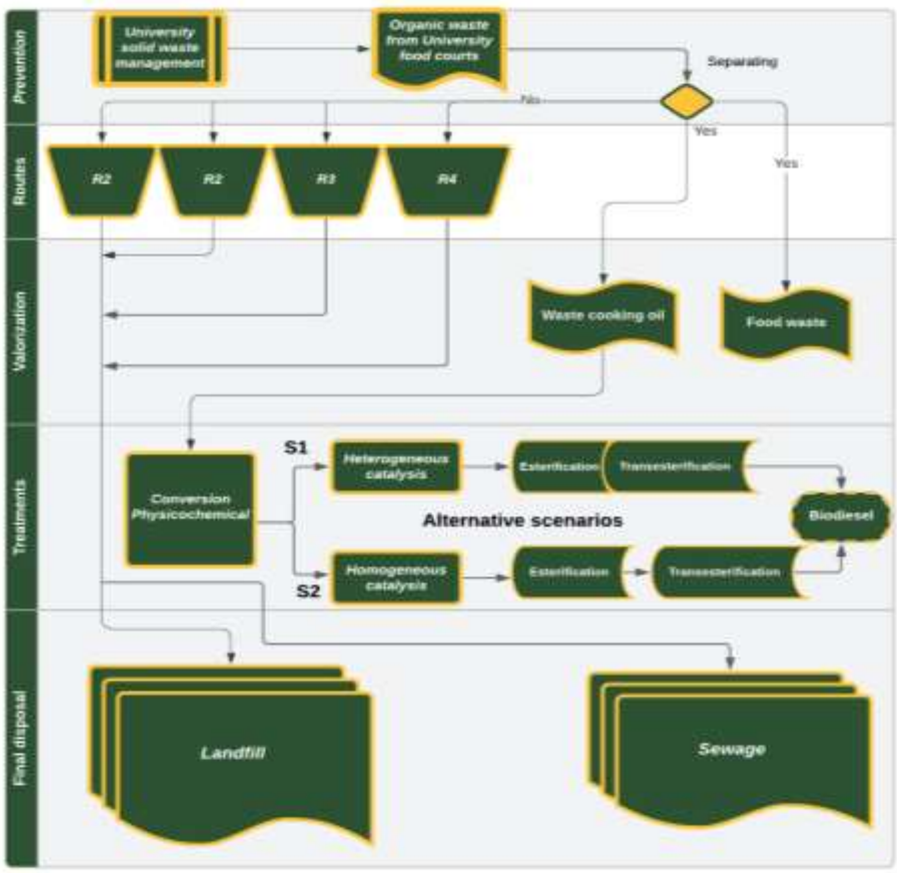

Source: Author´s Own Creation
Diagramming software: Ludichart Web 2.0

Figure 3.3 System boundary for the management of WCO in the University food courts of the UAEMéx, through a heterogeneous process (scenario 1) or homogeneous process (scenario 2)

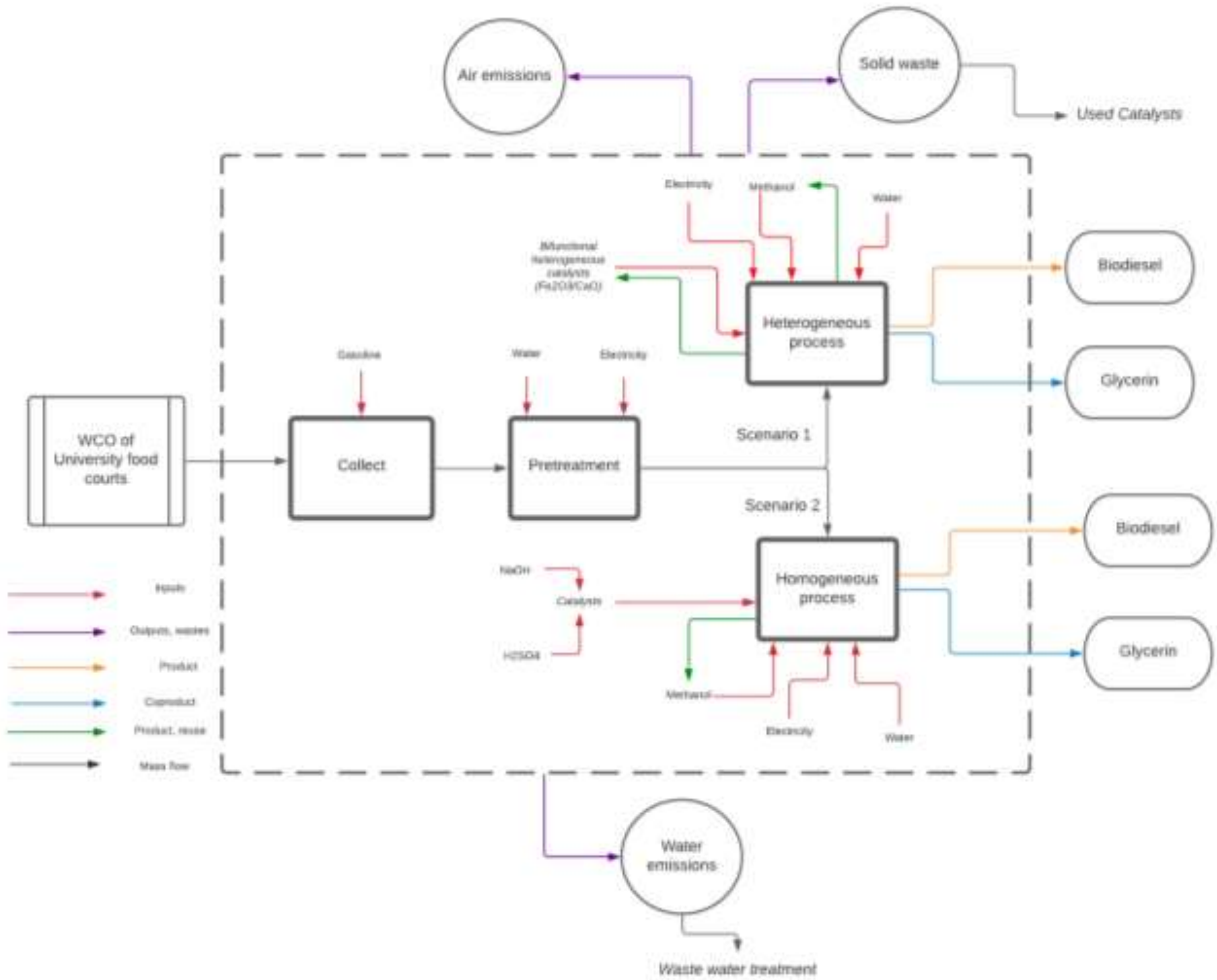

Source: Author´s Own Creation
Diagramming software: Ludichart Web 2.0

3. Results

From the survey of UFC managers, it appears that from the type of oil used for food preparation and/or cooking, see Graph 3.1, the responses showed that 34% is sunflower oil, 31% corn, 16% soy, 13% olive and 3% palm oil. It was also concluded that 85% of the UFC surveyed use a fryer and the consumption of oil varies in a range of 0 to 5 L and from 12 to 20 L in 30% of the total spaces under study, 10 to 15 L and 5 to 10 L in 19% and 4% reported that none. The 27 UFC managers were also questioned whether or not the oil was reused, a *negative* response was obtained in 74% of the answers, *affirmative* in 11% and *perhaps* reached a percentage of 15%. Regarding the use and disposal of labelled containers, 93 per cent answered that WCO is placed in labelled containers. The arrangement of these containers varies according to the UFC as follows: monthly (37%), weekly (33%), daily (19%) and not collected (7%). Only 4% is reused. This allows us to identify the lack of a well-established policy for the management of the WCO in the UFC of the UAEMéx, a behavior that has now occurred in households in other countries (Hartini *et al*., 2020).

Graph 3.1 Percentage of consumption by type of oil in the University food courts of the UAEMéx

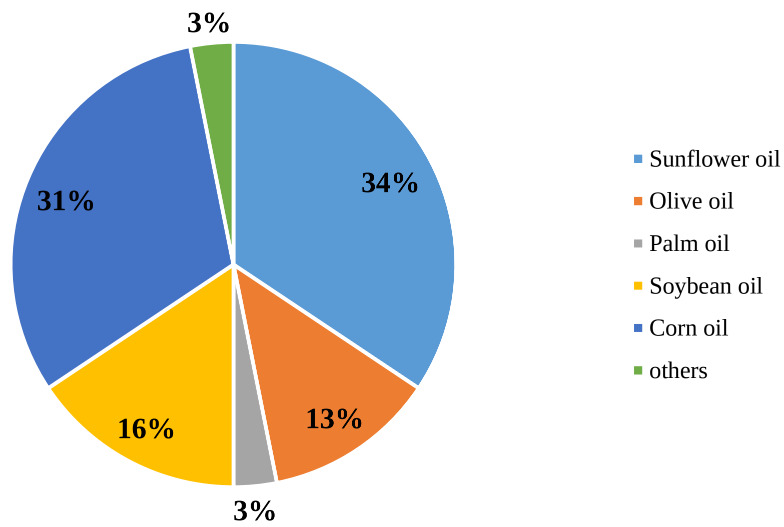

Source: Author´s Own Creation

Regarding the information on the generation of WCO (L/week), it was classified by collection route to the landfill and the distance traveled by the four units of transport with gasoline engine. The route that collects the most WCO is the R4 (80 L/week), the UFC of the Preparatory 5 "Dr. Angel Ma. Garibay Kintana" has a participation of 50% regarding the academic spaces included in the route. In second place, there is the RI (44 L/week) with 7 UFC, like the R3, generating 31 L/week and finally the R2 with 10 L/week. It is important to note that this route is the one that travels the longest towards the filling, 65 km and only includes 4 UFC.

Based on the results described above, for the analysis of the LCA inventory, see Table 3.2, we considered the total WCO reported as generated (165 L/week) and the total distance traveled per week (138.1 km), in a 1.5-ton van with an approximate yield of 2.5 L/km. The functional unit to produce biodiesel in the heterogeneous process was 1L. For the homogeneous process, the inputs, and outputs of (Talens *et al*., 2010) were considered in the same calculation base, it should be noted that in their inventory analysis they do not specify the stages and only one electricity consumption was reported.

Table 3.2 Inventory analysis according to the functional unit (1 L) in biodiesel production with a heterogeneous process

Stage	**Input**				**Output**			
	Flow	**Parameter**	**Amount**	**Unit**	**Flow**	**Parameter**	**Amount**	**Unit**
Collect	Energy	Gasoline	0.128	tkm	Middle flow	WCO	1.100	L
	Raw material	WCO	1.100	L				
Pre treatment	Energy	Electricity consumption	0.722	kWh	Middle flow	WCO	1.100	L
	Raw material	Potable water	0.745	L	Residue	Waste water	0.745	L
		WCO	1.100	L				
Reaction	Energy	Electricity consumption	11.20	kWh	Product	Biodiesel	1.000	L
	Raw material	WCO	1.100	L				
		Pig iron (Fe_2O_3)	0.005	kg	Co-product	Glycero	0.100	L
		Hydraulic lime (CaO)	0.079	kg	Residue	Waste water	0.819	L
					Recyclable product	Methanol	0.209	L
		Water, deionized	0.819	L	Reusable product	Bifuntional catalysts (Fe_2O_3/CaO)	0.084	kg
		Methanol	0.232	L				

Source: Author´s Own Creation

The assessment of the environmental impacts of each stage, using the CML-IA baseline method C3.06/EU25, includes 11 impact categories, see Table 3.3.

In the LCA of biodiesel production, the WCO has a zero initial environmental charge at the collection stage. This is because it is a waste that becomes a raw material and its environmental impact has a lower ecological burden compared to first and third generation biodiesel (Foteinis *et al*., 2020), as it does not require a stage of cultivation or extraction. Accordingly, it is reported that emissions avoided in these stages are 88% (Flach *et al*., 2019). From the above, the use of used oils reduces the deforestation that arises from continuous and extensive cultivation, as well as the loss of biodiversity (Ayoola *et al*., 2015; Viornery *et al*., 2020)

The consumption of sunflower oil in UFC has an environmental impact benchmark that has been studied from the cultivation of seed to the production of biodiesel, the latter considering WCO as waste biomass producing energy from a renewable source, through the reuse and recycling of waste. At the cultivation stage, the most affected impact category is that of land use on agricultural land due to the use of fertilizers, as well as electricity consumption during drying and extraction; the greatest amount of CO_2 emissions from the waste generated are presented during refining (Sanz R. *et al*., 2011), the above has been compared with seeds such as rapeseed and soybean. It should be noted that, in this research, they mention that there is a positive contribution to the climate change category, given that there is a net balance between CO_2 uptake by plants of sunflower seeds and emissions of greenhouse gases and compounds in the production process. This represents an area of opportunity, as several oils (soy, sunflower, and canola) studied by Belkhanchi *et al*., (2021) the one employed in the present study (sunflower), is reported as the best yield for conversion to biodiesel by 99.3%, by homogeneous catalysis (NaOH and KOH). For the heterogeneous process with a bifunctional catalyst, WCO from UFC had a conversion to FAME of 91% triglycerides (Enguilo *et al*., 2021).

The bifunctional catalyst (Fe_2O_3/CaO) used in the heterogeneous reaction replaces H_2SO_4 and NaOH in the homogeneous reaction, performing in a single step the esterification and transesterification reactions, although for simulation purposes it was assigned separately in the SimaPro. Calcium oxide is a potential catalyst for biodiesel production through transesterification that can be derived from biomass and waste resources due to its availability, low cost, and non-corrosive nature, as well as a low environmental impact thanks to its very low solubility in methanol (De Mora *et al*., 2015) and (Marinković *et al*., 2016).

In the reaction stage for the heterogeneous process, the impacts that had the greatest contribution of damage due to the high electrical and thermal consumption are summarized in Table 3.3 and were ADP (fossil fuels) (105.56 MJ), GWP (8.91 kg $CO_{2\,eq}$) and MAE (2568.40 kg 1.4-DB eq). These damages are attributed to fossil fuel consumption in the following equipment used during the reaction and separation stage of the biofuel: rotary evaporator, stirring system, recirculation system, vacuum pump and centrifuge. Studies conducted by Chung and collaborators (2019) indicate that the transesterification process is the stage that has the most impact categories due to its high electricity consumption, compared to the other stages of the process. The carbon footprint of the entire process has an emission of 9.61 kg CO_{2eq} per liter of biodiesel produced weekly, the reaction stage represents 93%.

Table 3.3 Environmental impacts in the collection, pretreatment and heterogeneous reaction stages using the CML-IA baseline method V3.06/EU25 for 1 L biodiesel

Impact category	Unit	Collect	Pretreatment	Heterogeneous reaction	Total
ADP (elements)	kg Sb $_{eq}$	5.34E-06	1.72E-06	2.94E-05	3.64E-05
ADP (fossil fuels)	MJ	3.39	5.98	105.56	114.93
GWP	kg $CO_{2\,eq}$	0.24	0.46	8.91	9.61
ODP	kg CFC-11 $_{eq}$	3.87E-08	3.46E-08	6.10E-07	6.83E-07
HT	kg 1,4-DB $_{eq}$	0.06	6.99E-02	1.23	1.36
FWAE	kg 1,4-DB $_{eq}$	2.12E-03	8.18E-03	0.14	0.15
MAE	kg 1,4-DB $_{eq}$	44.50	136.01	2387.89	2568.40
TE	kg 1,4-DB $_{eq}$	4.11E-04	2.47E-03	0.04	0.05
PO	kg $C_2H_{4\,eq}$	9.02E-05	7.91E-05	1.55E-03	1.72E-03
A	kg $SO_{2\,eq}$	1.07E-03	1.96E-03	0.03	3.76E-02
E	kg $PO_{4\,eq}$	1.67E-04	1.96E-04	3.45E-03	3.81E-03

Source: Author´s Own Creation

To interpret the above results, the mid-point environmental impacts were compared with the CML-IA baseline method V3.06/EU25 for alternative scenarios of heterogeneous catalysis esterification and transesterification (scenario 1) and homogeneous catalysis (scenario 2), see Graph 3.2, which reports the largest contribution in all environmental impacts due to its high energy consumption. Talens Peiró and collaborators, (2010), mention that approximately 68% of the electricity production in the homogeneous process is due to the burning of coal, causing the release of toxic materials that affect different species in an ecosystem. Therefore, environmental impacts can be reduced through using alternative energy sources such as solar. The impact category TE of scenario 1 has a contribution of 71.43% with respect to scenario 2, which is interpreted by the final management of waste as methanol, catalyst and glycerol.

Graph 3.2 Percentage contribution of the mid-point impact categories for the heterogeneous process (scenario 1) and the homogeneous process (scenario 2) using the CML-IA baseline method V3.06/EU25

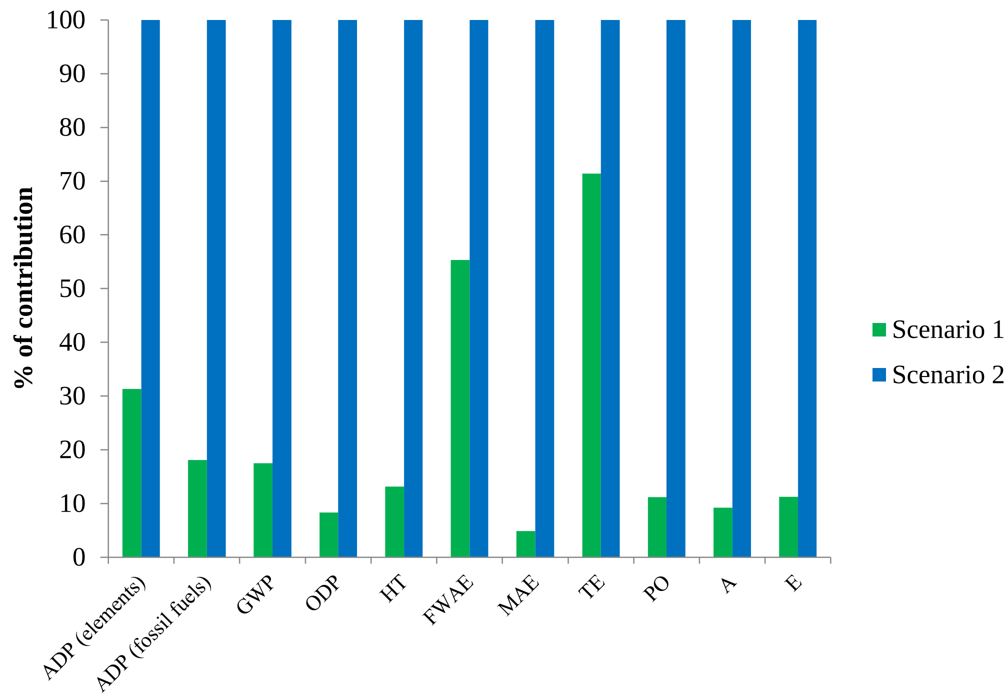

Source: Author´s Own Creation

The environmental endpoint indicators using the ReCiPe 2016 Endpoint (H) V1.04 method, to produce biodiesel in a heterogeneous process (scenario 1) with homogeneous process (scenario 2), are shown in Graph 3.3; the category of human health damage was the most affected in both processes, followed by the category concerning ecosystems and the category with the lowest natural resource score. Electrical energy consumption generates emissions such as sulphur oxides (SOx), nitrogen oxides (NOx), carbon monoxide (CO), particles below 10 micrometres (PM_{10}) and particles below 2.5 micrometres ($PM_{2.5}$) and volatile organic compounds (VOCs) affecting air quality by causing respiratory diseases.

Specifically, the category human health damage in scenario 1 is smaller with 1.77 points than that of scenario 2, because the heterogeneous process consumes less electricity and reuses the bifunctional catalyst (Fe_2O_3/CaO) at least three times triglycerides (Enguilo *et al*., 2021). This is an important characteristic to consider for a LCA with circular economy approach (Al-Muhtaseb *et al*., 2021), which secure sustainability in biodiesel production, compensating for the depletion of natural resources. It has been reported that homogeneous catalysts such as NaOH require the addition of chemicals, in addition to processes such as purification and neutralization, compared to the heterogeneous one, where there is only one purification process, avoiding the discharge of wastewater (Atadashi *et al*., 2013).

Graph 3.3 Endpoint impacts for alternative scenarios using ReCiPe 2016.: heterogeneous process (scenario 1) and homogeneous process (scenario 2)

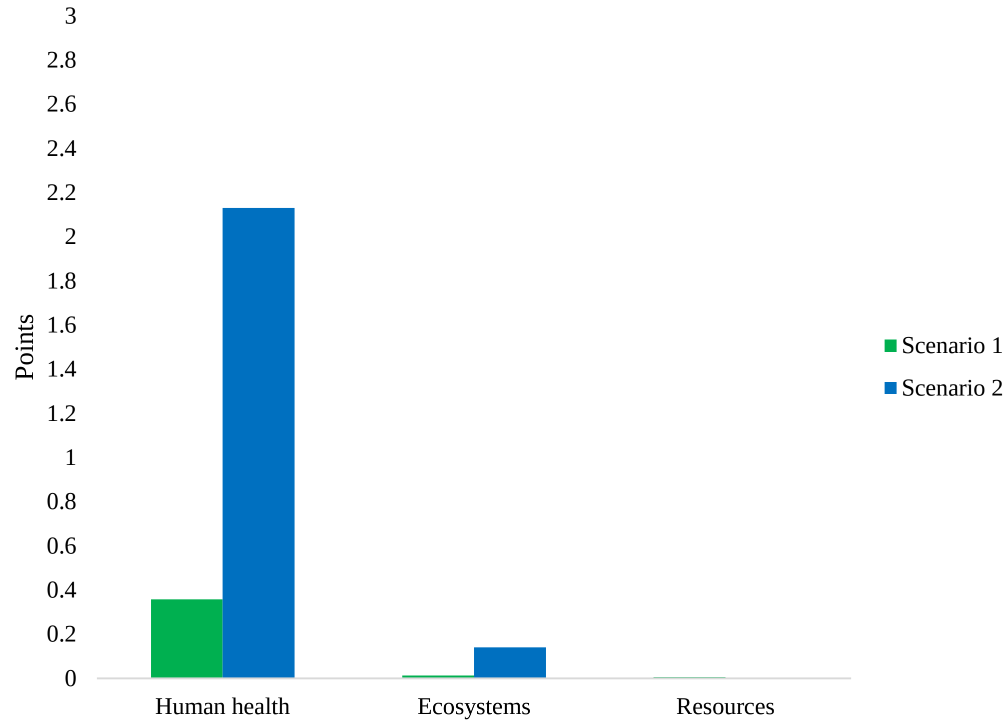

Source: Author´s Own

In the context of environmental sustainability, the production of biodiesel through a large scale heterogeneous process, has been reported technically efficient and economically viable in the industrial sector (Liu *et al*., 2021). For the development of public policies of the impact categories in a report of LCA, one of the most relevant and comparable impacts is 100-year global warming (GWP) or carbon footprint (Sala *et al*., 2021). In this case, the GWP or carbon footprint for the heterogeneous process is 82.52% lower than the homogeneous process (see Graph 3.2). This impact can still be further reduced with the use of renewable energies such as solar photovoltaic to power the reactor and separation equipment.

Acknowledgements

C. Alanis is grateful to the National Council of Science and Technology for the scholarship (CVU 360631) to obtain her doctorate degree. To Sustainable University Network for the Integral Management of Organic Waste of the Autonomous University of the State of Mexico with registration number 5083/REDP202 and to UAEMéx for financial support through project 6219/2020CIB. The technical support of Citlalit Martínez Soto is also acknowledged.

Conclusions

The type of oil consumed in the University food courts of the UAEMéx is mainly of sunflower and is converted into waste oil when subjected to cooking under high temperature; this was the raw material to produce biodiesel under a heterogeneous process. In this regard, the initial environmental load is zero because it is a residue, it should be noted that the impact was not quantified from the stage of cultivation or extraction of the oil, which makes the process studied sustainable.

Within the system boundary, it was established that the collection of waste cooking oil had the least contribution in the impacts studied, then the pretreatment stage. In the reaction stage for the heterogeneous process, the energy consumption due to electrical and thermal demands resulted in the greatest environmental impacts in the following categories: abiotic depletion potential (fossil fuels) (105.56MJ), 100-year global warming (8.91 kg $CO_{2\ eq}$) and marine water ecotoxicity (2387.89 kg 1.4-DB eq).

In the heterogeneous reaction step, the bifunctional catalyst (Fe_2O_3/CaO) replaces H_2SO_4 and NaOH, performing in a single step the esterification and transesterification, consuming less electricity at the activation of the catalyst that is at least three times reused and does not require any further thermal treatment; methanol is recovered for recycling during the reaction; as for glycerol, it is purified, which gives the process a circular economy approach that ensures the sustainability of biodiesel production.

With respect to the end-point environmental impacts, the homogeneous process has greater to human health damage with 1.77 points more than the heterogeneous process. This process is mainly affected by emissions from waste disposal and electricity consumption.

The carbon footprint for the heterogeneous process is lower by 82.52% compared to the homogeneous process. This contributes to the mitigation of greenhouse gases and compounds, as it replaces fossil fuels, maintains carbon sinks and prevents deforestation.

The identified areas of opportunity were the reduction of electricity consumption using renewable energies such as solar photovoltaics; the environmental sustainability of the process from the energy generated by the production of biodiesel and the energy consumed; the economic and environmental valorization of glycerol. In the University food courts, it is suggested to conduct environmental education campaigns in the collection sites to efficiently perform this stage with a pretreatment (purification of impurities), as well as standardizing a process that allows sampling to verify the initial quality of waste cooking oil and a collection route that guarantees the recycling of waste cooking oil. Finally, it was also concluded that a program of management of waste cooking oil in the UAEMéx should be implemented in order to reduce the carbon footprint of the University food courts.

References

Al-Muhtaseb, A. H., Osman, A. I., Murphin Kumar, P. S., Jamil, F., Al-Haj, L., Al Nabhani, A., Kyaw, H. H., Myint, M. T. Z., Mehta, N., & Rooney, D. W. (2021). Circular economy approach of enhanced bifunctional catalytic system of CaO/CeO2 for biodiesel production from waste loquat seed oil with life cycle assessment study. *Energy Conversion and Management*, *236*, 114040. https://doi.org/10.1016/j.enconman.2021.114040

Amaya, J., Coello, S., Crespo, T., Hidalgo, J., Jervis, F., Moreira, C., & Soto, M. (2020). Waste to Energy Potential of Domestic Waste Cooking Oil in Guayaquil: A review. *18th LACCEI International Multi-Conference for Engineering, Education, and Technology:*, 1–7. https://doi.org/10.18687/laccei2020.1.1.485

Antoniadou, M., Tsarouhas, P., & Varzakas, T. (2020). *GSC Advanced Research and Reviews Life cycle assessment and circular economy in conjunction with treatment methodologies : Presentation and critical comparison between different food industry waste*. *03*(03).

Atadashi, I. M., Aroua, M. K., Abdul Aziz, A. R., & Sulaiman, N. M. N. (2013). The effects of catalysts in biodiesel production: A review. *Journal of Industrial and Engineering Chemistry*, *19*(1), 14–26. https://doi.org/10.1016/j.jiec.2012.07.009

Ayoola, B., Ayodele, A., Submitted, T., Engineering, C., & Engineering, C. (2015). *Production and Life Cycle Assessment of Biodiesel from Three Waste Oils By A Thesis Submitted in the Department of Chemical Engineering to the School of Post Graduate Studies (Ph . D .) in Chemical Engineering , College of Science and Technology , Covena*.

Belkhanchi, H., Rouan, M., Hammi, M., & Ziat, Y. (2021). *Synthesis of Biodiesel by Transesterification of Used Frying Oils (UFO) through Basic Homogeneous Catalysts (NaOH and KOH)*. *11*(5), 12858–12868.

Carlos, S., & Díaz, M. D. L. V. (2018). Evaluación De Un Proceso Industrial De Producción De Biodiésel Mediante Análisis De Ciclo De Vida. *Revista Internacional de Contaminacion Ambiental*, *34*(3), 453–465. https://doi.org/10.20937/RICA.2018.34.03.08

Chung, Z. L., Tan, Y. H., Chan, Y. S., Kansedo, J., Mubarak, N. M., Ghasemi, M., & Abdullah, M. O. (2019). Life cycle assessment of waste cooking oil for biodiesel production using waste chicken eggshell derived CaO as catalyst via transesterification. *Biocatalysis and Agricultural Biotechnology*. https://doi.org/10.1016/j.bcab.2019.101317

Clabeaux, R., Carbajales-dale, M., Ladner, D., & Walker, T. (2020). Assessing the carbon footprint of a university campus using a life cycle assessment approach. *Journal of Cleaner Production*, 122600. https://doi.org/10.1016/j.jclepro.2020.122600

De Mora, E. F., Torres, C., & Valero, A. (2015). Thermoeconomic analysis of biodiesel production from used cooking oils. *Sustainability (Switzerland)*, *7*(5), 6321–6335. https://doi.org/10.3390/su7056321

Enguilo, V., Romero, R., Gómez-Espinosa, R. M., Romero, A., Martínez, S. L., & Natividad, R. (2021). Biodiesel Production from Waste Cooking Oil Catalyzed by a Bifunctional Catalyst. *ACS Omega*. 24092−24105. https://doi.org/10.1021/acsomega.1c03586

EPA. (2000). Recycled cooking oils: Assessment of risks for public health. *Working document for Scientific and Technological Options Assessment (STOA). European Union*, *September*, 373–385. http://dx.doi.org/10.1016/B978-1-893997-92-9.50027-X

Flach, B., Lieberz, S., & Bolla, S. (2019). GAIN Report - EU Biofuels Annual 2019. *Global Agricultural Information Network*, 52. https://apps.fas.usda.gov/newgainapi/api/report/downloadreportbyfilename?filename=Biofuels Annual_The Hague_EU-28_7-15-2019.pdf

Foteinis, S., Chatzisymeon, E., Litinas, A., & Tsoutsos, T. (2020). Used-cooking-oil biodiesel: Life cycle assessment and comparison with first- and third-generation biofuel. *Renewable Energy*, *153*, 588–600. https://doi.org/10.1016/j.renene.2020.02.022

Gaceta oficial de la Ciudad de México. (2018). NADF- 012-AMBT-2015. En *Diario Oficial de la Federación*. https://doi.org/10.1017/CBO9781107415324.004

Gaur, A., Mishra, S., Chowdhury, S., Baredar, P., & Verma, P. (2020). Materials Today : Proceedings A review on factor affecting biodiesel production from waste cooking oil : An Indian perspective. *Materials Today: Proceedings*, 7. https://doi.org/10.1016/j.matpr.2020.09.432

González, I., & González, J. (2015). Aceites usados de cocina. problemática ambiental, incidencias en redes de saneamiento y coste del tratamiento en depuradoras. *Consorcio de Aguas Bilbao Bizkaia*, 1–8. http://www.aguasresiduales.info/revista/articulos/problematica-ambiental-incidencias-en-redes-de-saneamiento-y-coste-del-tratamiento-en-depuradoras-de-los-aceites-usados-en-cocina

Gu, Y., Wang, H., Robinson, Z. P., Wang, X., Wu, J., Li, X., Xu, J., & Li, F. (2018). Environmental footprint assessment of green campus from a food-water-energy nexus perspective. *Energy Procedia*. https://doi.org/10.1016/j.egypro.2018.09.109

Güereca, L. P., Torres, N., & Noyola, A. (2013). Carbon Footprint as a basis for a cleaner research institute in Mexico. *Journal of Cleaner Production*, *47*, 396–403. https://doi.org/10.1016/j.jclepro.2013.01.030

Hartini, S., Puspitasari, D., Aisy, N. R., & Widharto, Y. (2020). Eco-efficiency Level of Production Process of Waste Cooking Oil to be Biodiesel with Life Cycle Assessment. *ICENIS*, *10004*, 1–9.

ISO 14044. (2006). Environmental management — Life cycle assessment — Requirements and guidelines. En *International Organization for Standardization*. http://www.springerlink.com/index/10.1007/s11367-011-0297-3

Liu, Y., Yang, X., & Zhu, Z. (2021). Economic evaluation and production process simulation of biodiesel production from waste cooking oil. *Current Research in Green and Sustainable Chemistry*, 100091. https://doi.org/10.1016/j.crgsc.2021.100091

Marinković, D. M., Stanković, M. V., Veličković, A. V., Avramović, J. M., Miladinović, M. R., Stamenković, O. O., Veljković, V. B., & Jovanović, D. M. (2016). Calcium oxide as a promising heterogeneous catalyst for biodiesel production: Current state and perspectives. *Renewable and Sustainable Energy Reviews*, *56*, 1387–1408. https://doi.org/10.1016/j.rser.2015.12.007

Mendoza, R., Quintero, R., & Ortiz, I. (2019). The carbon footprint of a public university campus in Mexico City. *Carbon Management*, *10*(5), 501–511. https://doi.org/10.1080/17583004.2019.1642042

Narasimhan, M., Chandrasekaran, M., Govindasamy, S., & Aravamudhan, A. (2021). Heterogeneous nanocatalysts for sustainable biodiesel production: A review. *Journal of Environmental Chemical Engineering*, *9*(1), 104876. https://doi.org/10.1016/j.jece.2020.104876

Orjuela, A., & Clark, J. (2020). Green Chemicals from Used Cooking Oils: Trends, Challenges and Opportunities. *Current Opinion in Green and Sustainable Chemistry*, 100369. https://doi.org/10.1016/j.cogsc.2020.100369

Rincón, J., & Silva, E. (2015). *Bioenergía: Fuentes, conversión y sustentabilidad* (CYTED). https://books.google.com/books?id=YpnxCAAAQBAJ&pgis=1

Rincón, L., Cadavid, J., & Orjuela, A. (2019). Used cooking oils as potential oleochemical feedstock for urban biorefineries – Study case in Bogota, Colombia. *Waste Management*, *88*, 200–210. https://doi.org/10.1016/j.wasman.2019.03.042

Sala, S., Martino, A., Antoine, A., & Fulvio, B. (2021). The evolution of life cycle assessment in European policies over three decades. *The International Journal of Life Cycle Assessment*, *0123456789*. https://doi.org/10.1007/s11367-021-01893-2

Sangwan, K. S., Bhakar, V., Arora, V., & Solanki, P. (2018). Measuring Carbon Footprint of an Indian University Using Life Cycle Assessment. *Procedia CIRP*, *69*(May), 475–480. https://doi.org/10.1016/j.procir.2017.11.111

Sanz R., J. F., Guimaraes, A. C., Quirós Alpera, S., Relea Gangas, E., Hernandez-Navarro, S., Navas Gracia, L. M., Martin-Gil, J., & Fresneda Cuesta, H. (2011). Life Cycle Assessment (LCA) of the biofuel production process from sunflower oil, rapeseed oil and soybean oil. *Fuel Processing Technology*, *92*(2), 190–199. https://doi.org/10.1016/j.fuproc.2010.03.004

SEMARNAT. (2019). *Visión Nacional hacia una gestión Sustentable: Cero Residuos*.

SEMARNAT. (2020). *Programa Sectorial de Medio Ambiente y Recursos Naturales 2020-2024.*

Sheinbaum, C., Caldero, A., & Ramı, M. (2013). Potential of biodiesel from waste cooking oil in Mexico. *Biomass and Bioenergy*, *6*(55). https://doi.org/10.1016/j.biombioe.2013.05.008

Talens, L., Lombardi, L., Villalba Méndez, G., & Gabarrell i Durany, X. (2010). Life cycle assessment (LCA) and exergetic life cycle assessment (ELCA) of the production of biodiesel from used cooking oil (UCO). *Energy*, *35*(2), 889–893. https://doi.org/10.1016/j.energy.2009.07.013

Tsai, W.-C., Chen, X., & Yang, C. (2020). Consumer Food Waste Behavior among Emerging Adults: Evidence from China. *Foods*, *9*(7), 961. https://doi.org/10.3390/foods9070961

UNEP/SETAC Life cycle Initiative. (2005). Life Cycle approaches : The road from analysis to practice. En *Assessment*.

Viornery, E. A., Bravo, B., & Mena, V. Y. (2020). Life cycle assessment and emission analysis of waste cooking oil biodiesel blend and fossil diesel used in a power generator. *Fuel*, *281*(March), 118739. https://doi.org/10.1016/j.fuel.2020.118739

Yañez, P., Sinha, A., & Vásquez, M. (2020). Carbon footprint estimation in a university campus: Evaluation and insights. *Sustainability (Switzerland)*, *12*(1), 1–15. https://doi.org/10.3390/SU12010181

Chapter 4 Absorption and reaction of CO_2 in capillaries

Capítulo 4 Absorción y reacción de CO_2 en capilares

PEÑA, Rosaura†[1], HURTADO, Lourdes[2], ROMERO, Rubi[1] and NATIVIDAD, Reyna*[1]

[1]Chemical Engineering Lab / Centro Conjunto de Investigación en Química Sustentable UAEM-UNAM, Universidad Autónoma del Estado de México
[2]Unidad Académica Profesional Acolman, Universidad Autónoma del Estado de México

ID 1st Author: *Rosaura, Peña* / **ORC ID**: 0000-0001-9184-8477, **CVU CONACYT ID**: 239954

ID 1st Co-author: *Lourdes, Hurtado* / **ORC ID**: 0000-0001-9892-9528, **CVU CONACYT ID**: 368065

ID 2nd Co-author: *Rubi, Romero* / **ORC ID**: 0000-0001-9163-7936, **CVU CONACYT ID**: 121454

ID 3rd Co-author: *Reyna, Natividad* / **ORC ID**: 0000-0001-8978-1066, **CVU CONACYT ID**: 87755

DOI: 10.35429/H.2021.6.51.74

R. Peña, L. Hurtado, R. Romero, and R. Natividad

*rnatividadr@uaemex.mx

A. Marroquín, J. Olivares, M. Ramírez and L. Cruz (Coord) Engineering and Technology. Handbooks-©ECORFAN-México, Querétaro, 2021.

Abstract

The process of carbon dioxide (CO_2) reduction to value-added chemicals is being extensively studied worldwide. The main purpose is to decrease emissions to the environment that are associated with global warming, as well as the creation of renewable and sustainable energy sources. In the aforementioned process, the absorption of CO_2 is of paramount importance as well as the reactor where the CO_2 conversion takes place. In this context, the objective of this chapter is to present and analyze the results of the CO_2 absorption in alkaline solutions in capillary reactors. A hydrodynamic study is included in order to establish the operational window of liquid and gas velocities in order to achieve the Taylor flow regime. All experiments were conducted in a capillary reactor (d_c = 3 mm). The studied variables were temperature, NaOH concentration (0-0.75 M) and capillary length (300 and 100 mm). It was found that the volumetric mass transfer coefficient of the absorption of CO_2 in water increases when the temperature decreases, while the CO_2 absorption in NaOH solutions increases directly with temperature. By means of the Ha number, it was concluded that the mass transfer controlled the absorption process when using alkaline solutions.

CO_2 absorption, capillary reactor, mass transfer, pH, reactive absorption

Resumen

El proceso de reducción de dióxido de carbono (CO_2) a productos químicos de valor agregado se está estudiando ampliamente a nivel mundial. La finalidad principal es disminuir emisiones al medio ambiente, las cuales se asocian al calentamiento global, así como la creación de fuentes de energías renovables y sustentables. En el proceso antes mencionado, la absorción de CO_2 es de suma importancia, así como el reactor donde se realiza la conversión del CO_2. En este contexto, el objetivo de este capítulo es presentar los resultados de la absorción de CO_2 en soluciones alcalinas llevada a cabo en un reactor capilar. Se incluye un estudio hidrodinámico para establecer la ventana de operación de velocidades de líquido y gas para obtener el régimen tipo Taylor. Todos los experimentos se realizaron en un reactor capilar (d_c = 3 mm). Las variables estudiadas fueron temperatura, concentración de NaOH (0-0.75M) y la longitud del capilar (300 y 100 mm). Se encontró que el valor del coeficiente de transferencia de masa si la absorción de CO_2 se realiza en agua incrementa cuando la temperatura disminuye mientras que la absorción en soluciones de NaOH incrementa directamente con la temperatura. Mediante el número de Hatta (Ha) se concluye que la transferencia de masa controla el proceso de absorción cuando se emplean soluciones alcalinas.

Absorción de CO_2, reactor capilar, transferencia de masa, pH, absorción reactiva

1. Introduction

Currently, the conservation of terrestrial ecosystems has attracted the attention of the scientific community due to the fact that damage to these ecosystems because of global warming has been observed. In this context, various research groups have focused on proposing strategies aimed at reducing pollutants in the environment. Global warming is caused by the greenhouse effect, a natural mechanism in which the Earth's atmosphere heats up, and it occurs thanks to the presence of certain gases, including carbon dioxide and other gases present in the air -such as water vapor (H_2O), methane (CH_4), nitrogen oxides (NO, N_2O, NO_2) and ozone (O_3), which are known as greenhouse gases. These gases can absorb solar radiation favoring the increase in temperature in the atmosphere. One of the most important is carbon dioxide since its concentration in the atmosphere is constantly increasing. The exponential increase in anthropogenic activities such as agriculture, industry, indiscriminate felling of trees, destruction of vegetation, the burning of fossil fuels along with the intensive destruction of ecosystems, have caused carbon dioxide emissions to the atmosphere to be greater than the amount required to carry out photosynthesis or the amount of gas that dissolves in ocean waters.

In addition to this, the development of alternative energy sources to replace fossil fuels has focused mainly on the development of clean energy sources, without carbon emissions, such as turbines powered by water and wind and solar energy; however, the drawback with renewable energy sources is the intermittent nature of the energy produced (Mebrahtu et al., 2019).

While the development of alternative sources of energy is in process and in progress, there is also an urgent need to find a solution to mitigate, store or convert the CO_2 produced or emitted to the environment, in order to contribute to CO_2 atmospheric level remains constant or even decreases. Even though this greenhouse gas has several applications, the amount used is minimal. Some of the compounds produced from CO_2 are: urea (for nitrogen fertilizers and plastics), salicylic acid (a pharmaceutical ingredient), polycarbonates (for plastics), ethylene, propylene, carbonates (Centi & Perathoner, 2009). It is also used as a refrigerant, carbonating agent, supercritical solvent, inert medium, pressurizing and neutralizing agent (Ganesh, 2016).

In general, two strategic routes have been proposed to avoid an increase in the concentration of CO_2 in the atmosphere: 1) mitigation and 2) capture and use of CO_2. Regarding the first route, it seeks to minimize CO_2 emissions that come from large facilities such as the cement, metal, bioethanol, oil and petrochemical refining industries, from power plants for the production of electricity, from medium sources such as industrial and commercial buildings and from small sources such as transportation; through different approaches, including the establishment of environmental regulations and the limitation of vehicular traffic. However, these actions are insufficient, because they require improvements in energy efficiency and a shift from fossil fuels to less carbon-intensive energy sources.

The second strategy, capture and use (CCU) to generate value-added chemicals, is particularly interesting as it can alleviate dependence on fossil fuels for energy, while promoting new technical sinks in the cycle biogeochemistry of carbon. In recent years, the use of CO_2 to produce value-added fuels and chemicals has become very important and challenging, mainly because the molecule is chemically stable due to its carbon-oxygen bonds (with a bond enthalpy of C=O +805 kJ/mol) and therefore its conversion to carbon-based fuels requires a large amount of energy to break the bond.

The transformation of CO_2 to chemicals of commercial interest (short chain) such as carbon monoxide (CO), methanol (CH_3OH), formaldehyde (HCHO) and acetic acid (CH_3COOH) and even formic acid (HCOOH) and the formation of fuels such as ethanol (CH_3CH_2OH), methane (CH_4) or hydrogen (H_2), can be carried out by different processes, including biological reduction, electrochemical reduction, photo-catalytic reduction, thermo-catalysis, among others (Ola & Maroto-Valer, 2015). Recent research results also indicate that CO_2 can be used to produce methanol, using it instead of carbon monoxide in the synthesis gas mixture (mixture of carbon monoxide and hydrogen CO + H_2) *(Yang et al.*, 2017).

The generation of fuels from CO_2 through the photo-reduction process seems to be the most economical and ecological approach for sustainable development because an economic reducing agent such as water can be used, solar energy is available in abundance, there is no generation of toxic products or waste, and little or no carbon emission (Shehzad, Tahir, Johari, & Murugesan, 2018). In this sense, Lourdes Hurtado, Natividad, & García, 2016 demonstrated that the use of capillary reactors, instead of the typical stirred tank reactors, lead to a different distribution of products when the photo-reduction of CO_2 is carried out. Therefore, it is important to study the absorption of this gas in this type of reactors.

Capillary reactors are tubes with internal diameters of 1 to 4 mm. They are distinguished from microreactors because the internal diameter of these latter is less than 1 mm. The option of using a capillary reactor in multiphase reaction processes is supported by the statement that the mass transfer between the phases is intensified, mainly due to the reduction of the contact length between the phases and because it also has the advantage of being able to immobilize the catalyst onto the reactor wall (Natividad *et al.*, 2004).

In the capillary reactor ($d_c < 4$ mm), the flow regime is dictated by the flow rates and the properties of the liquid and gas, as well as the diameter of the capillary. The existence of four main flow regimes in a vertical capillary is well known and they are: bubble type, Taylor type (plug), aerated and annular flow (Figure 4.1).

Figure 4.1 Main flow regimes in a capillary a) bubble, b) aerated c) annular, d) Taylor (plug)

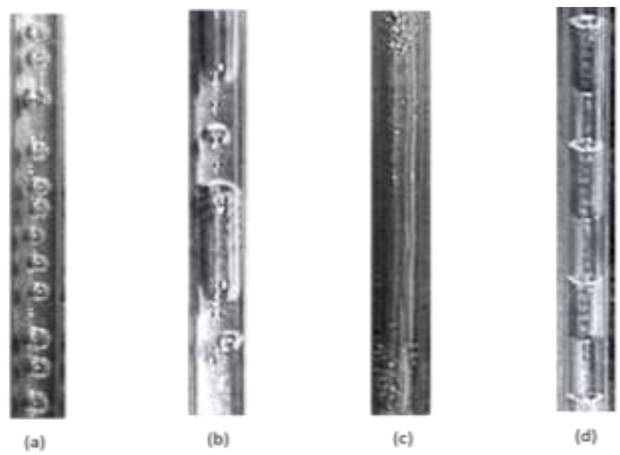

Source: Natividad, PhD thesis, 2004

The Taylor (or plug) flow consists of gas bubbles with a length greater than the diameter of the capillary that move along the tube separated between them by the elongated parts of the liquid. Due to their size, the bubbles leave only a thin film of liquid between the bubble and the wall. One characteristic that makes Taylor flow unique is the micro-mixing pattern found in the liquid segments, this pattern enhances mixing within the liquid phase and eliminates any possible radial concentration gradients. This determines the high efficiency of mass transfer in a capillary reactor (Heiszwolf, Kreutzer, Eijnden, Kapteijn, & Moulijn, 2001; Natividad *et al*., 2004).

In this context, this chapter aims to present the results of the hydrodynamic study of a capillary reactor (d_c = 3 mm) in order to establish the operating window in which the Taylor flow is obtained. Under this operating regime, results of carbon dioxide absorption (CO_2) in aqueous solutions of sodium hydroxide (NaOH) (reactive absorption) are presented. The mass transfer coefficients and the species involved in the reactive absorption process were also calculated.

It is important to mention that reactive absorption has two main advantages: 1) the absorbed solute reduces the partial pressure at equilibrium, improving the driving force between the gas and the interface, 2) the mass transfer coefficient in the liquid phase increases. The theoretical framework for the absorption of CO_2 in aqueous solutions is presented below.

1.1 CO_2 absorption in aqueous solutions

The absorption of CO_2 in water (pH less than 8) is considered purely physical absorption, because when equilibrium is reached, only a small fraction (0.2% - 1%) of the dissolved CO_2 (see Equation 1) is found as carbonic acid: $H_2CO_{3(ac)}$ (Ganesh, 2016), a product of the reaction between molecules (Equation 2). In other words, the equilibrium position prefers carbon dioxide and water ($k_{-1} \gg k_1$) (Holum, 1990; Palmer & Van Eldik, 1983) as it is shown in Figure 4.2, and therefore the CO_2 in the solution remains as molecularly solvated or freely hydrated (Cotton, 1999).

Figure 4.2 $CO_{2\,(ac)}$ + $H_2CO_{3\,(ac)}$ balance

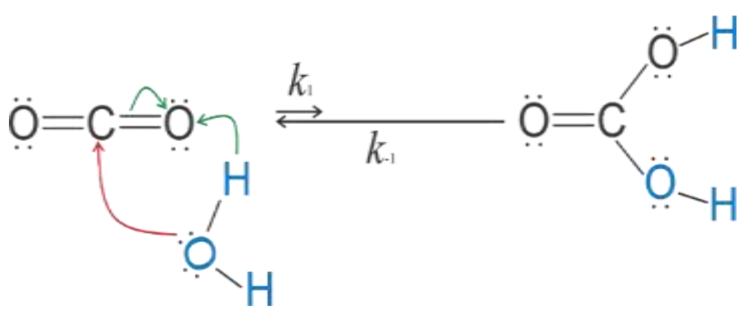

Source: Salgado, Bachelor thesis, 2020

Equilibrium is reached when carbonic acid, which is a weak acid, dissociates twice due to its two protons attached to its oxygen atoms. In the first dissociation (Equation 3) a proton (H^+) and a bicarbonate ion (HCO_3^-) are released, in the second dissociation (Equation 4) the carbonate ion (CO_3^{2-}) is generated and the second H^+ proton is released. If the conjugated bases are not found with another species with a positive charge different from the protons, carbonic acid is formed again. Therefore, it can be asserted that, if the absorption medium is only water, the only species found in solution is dissolved CO_2, for practical purposes $H_2CO_3^*$, without omitting the small amount of carbonic acid formed (Equation 5) (Ganesh, 2016).

$$CO_{2(g)} \leftrightarrow CO_{2(aq)} \tag{1}$$

$$CO_{2\,(aq)} + H_2O \leftrightarrow H_2CO_3^* \tag{2}$$

$$H_2CO_3 \leftrightarrow H^+ + HCO_3^- \tag{3}$$

$$HCO_3^- \leftrightarrow H^+ + CO_3^{2-} \tag{4}$$

$$H_2CO_3^* = H_2CO_{3\,(aq)} + CO_{2\,(aq)} \tag{5}$$

During the reactive absorption of CO_2, the dissolution is carried out in solutions at a pH higher than 8, which is reached when alkaline solutions are used. The presence of cations (Na^+, K^+, Mg^{2+}, Ca^{2+}) and anions (OH^-) in aqueous solution causes that the equilibrium in the reaction $H_2CO_3^*$ is not reached until the reactions between the dissolved ions and the resulting ions of the dissociation reactions of $H_2CO_3^*$ take place (Savage, Astarita, & Joshi, 1980; Shim, Lee, Lee, & Kwak, 2016; Skoog, 2014).

$$H_2CO_3 + OH^- \leftrightarrow HCO_3^- + H_2O \tag{6}$$

$$HCO_3^- + OH^- \leftrightarrow CO_3^{2-} + H_2O \tag{7}$$

The absorption of CO_2 in alkaline aqueous solutions involves fairly rapid homogeneous reactions (Skoog, 2014). The global reactions are presented in Equations 8 and 9,

$$CO_{2(aq)} + 2OH^- \rightarrow CO_3^{2-} + H_2O \tag{8}$$

$$CO_{2\,(aq)} + H_2O + CO_3^{2-} \rightarrow 2HCO_3^- \tag{9}$$

2. Methodology

2.1 Set up of the CO_2 absorption and reaction system

The system used to absorb CO_2 in the capillary reactor was set up according to that described in the patent application MX/Aa/2017/003883 and is described below (see Figure 4.3). At the top of the capillary reactor, a "T" shaped connection was installed to simultaneously feed the liquid and gas phases. In one of the “T” outlets, the quartz capillary with an internal diameter of 3 mm and a length of 300 mm was placed and this was submerged in a 100 mL 3 neck ball flask, the temperature was monitored inside the flask and it was controlled with a thermal bath.

The gas phase was supplied through a stainless-steel pipe and the gas flow was controlled by an AALBORG mass flow controller (model GFC17). A Masterflex peristaltic pump (model 7557-12) with a Masterflex flow controller (model 07557-14) was used to recirculate the liquid phase.

Figure 4.3 Experimental set-up for the absorption of CO_2 (Original image)

Source: "Obtained by the author"

2.2 Hydrodynamic study

The experiment set-up depicted in Figure 4.3 was used to carry out a hydrodynamic study, which consisted in obtaining the velocity operating window for both phases, in order to develop a Taylor flow regime. The experiments were carried out using two different reducing agents: water and a 0.5 M solution of sodium hydroxide. The surface velocity of CO_2 was varied between 0.01 m/s and 0.53 m/s, while the interval of variation of the surface velocity for the liquid phase was set between 0.01 m/s and 0.26 m/s.

Next steps were followed to carry out this study: after the installation of the system, a previous washing was carried out using 60 mL of deionized water and recirculating it through the pipes, connections and the capillary reactor through the peristaltic pump. The temperature was kept constant at each assessed value by using a thermal bath, 60 mL of either water or NaOH solution were added and the flow rate was regulated by adjusting the liquid flow rate in the pump. The reactor CO_2 supply valve was opened, and the speed was adjusted using the mass flow meter. The gas and liquid flow rates were independently changed, and the hydrodynamic regime observed in the capillary reactor was recorded.

2.2.1 Effect of temperature on the hydrodynamics of the system

The experiments were performed at 10 and 25 °C, to determine the effect of this variable on the hydrodynamics of the system, as the section 2.2 indicates, by modifying the temperature under study.

2.3 CO_2 absorption

The effect of three operational variables (temperature, NaOH concentration and reactor length) on CO_2 absorption has been elucidated. This study was carried out with a superficial gas velocity of 0.05 m/s and liquid of 0.08 m/s, these velocities showed a Taylor-type regime, in a capillary with an internal diameter of 3 mm. To determine the effect of temperature on the amount of absorbed CO_2, experiments were carried out at 10, 15, 25, 35 and 40 °C, the concentration of the NaOH solution was 0.5 M. The effect of NaOH concentration on the CO_2 absorption was established by performing experiments with solutions of different initial concentration (0.25, 0.5 and 0.75 M), in this case the temperature was kept constant at 25 °C.

For the study of both variables, temperature and NaOH concentration, a 300 mm length quartz capillary was used. An additional experiment was carried out at a temperature of 25 °C and a solution with a molar concentration of NaOH of 0.5M, using a 100 mm capillary in order to establish the effect of the length of the capillary reactor. In all cases, the response variable was the amount of CO_2 absorbed in the solutions, which, in turn, was used to estimate the mass transfer coefficients between the different phases.

CO_2 quantification was carried out by means of a volumetric analysis with a standardized acid solution. This technique is known as the Warder method (Grzelka, Sobieszuk, Pohorecki, & Cygan, 2011). This method is very useful to differentiate and quantify the species that participate in the reactive absorption process and in this way to study the behavior of the species involved in the capillary reactor (CO_2, H_2CO_3, CO_3^{2-} and HCO_3^-). Methyl orange and phenolphthalein were used as indicators (with pH ranges of 3.1-4.4 and 8.3 -10, respectively), the titration was carried out with a 0.1M sulfuric acid solution standardized with Na_2CO_3 solutions.

3. Results

3.1 Hydrodinamic study in the capillary reactor

The study of the hydrodynamics of the system was limited to establish the surface velocity of the fluids to obtain the operating window in which each of the possible flow regimes illustrated in Figure 4.1 (annular, bubble, aerated or Taylor flow) is obtained. The Taylor or plug type flow is presented in Figure 4.4.

Figure 4.4 Taylor flow in a capillary reactor (d_C= 3mm) (Original image)

Source: "Obtained by the author"

The flow of the gas phase and the liquid phase was gradually varied, keeping one of the two flows constant. Its conversion to surface velocity allowed establishing a map of hydrodynamic regimes for a capillary with an internal diameter of 3 mm and a length of 300 mm, handling a liquid temperature of 10 and 25 °C. In the study, several two-phase flow patterns were observed; the resulting flow patterns are shown in Graphic 4.1.

In general, for all conditions, at a relatively low gas velocity (u_G) a Taylor flow was noticed, which is described by an alternating arrangement of liquid plugs and elongated bubbles with a length greater than the diameter of the capillary and separated from the wall of the capillary tube by a very thin film of liquid. The occurrence of periodic instabilities led to a phenomenon that periodically broke the elongated bubble and created an unstable slug zone (Graphic 4.1a and 4.1b).

This effect occurs with an increase in u_G, which led to a greater amplitude of the velocity of recirculation of gas bubbles, but on the contrary, increasing liquid velocity (u_L) led to a rapid flow of liquid creating a fast plug zone (Graphic 4.1a and 4.1b). The annular flow was the only regime observed in all the conditions studied (Graphic 4.1a, 4.1b, 4.1c and 4.1c) at a relatively higher u_G, for this type of flow the liquid phase does not collide with the gas phase and instead has a continuous flow. A gas core surrounded by a liquid film or even with periodic interfacial waves were observed (annular-wavy). These interfacial waves become less dominant at higher gas concentrations but less liquid flow, becoming an aerated type (Graphic 4.1c).

Moreover, in Graphic 1, we can observe that operating at low temperature (10 °C) and low gas velocity (0.01 m/s), there is a larger operating window to obtain the plug type flow than operating at 25 °C. This behavior is observed when using both water and 0.5M NaOH. This hydrodynamic regime is the one of greatest interest in this work, for which an operating window for both phases was determined and Table 4.1 summarizes the operating conditions to operate in a Taylor-type regime.

Graphic 4.1 Flow regimes map in the 300 mm length and 3 mm internal diameter quartz capillary, using a) water at 10 °C, b) water at 25 °C, c) NaOH 0.5M at 10 °C and d) 0.5M NaOH at 25 °C

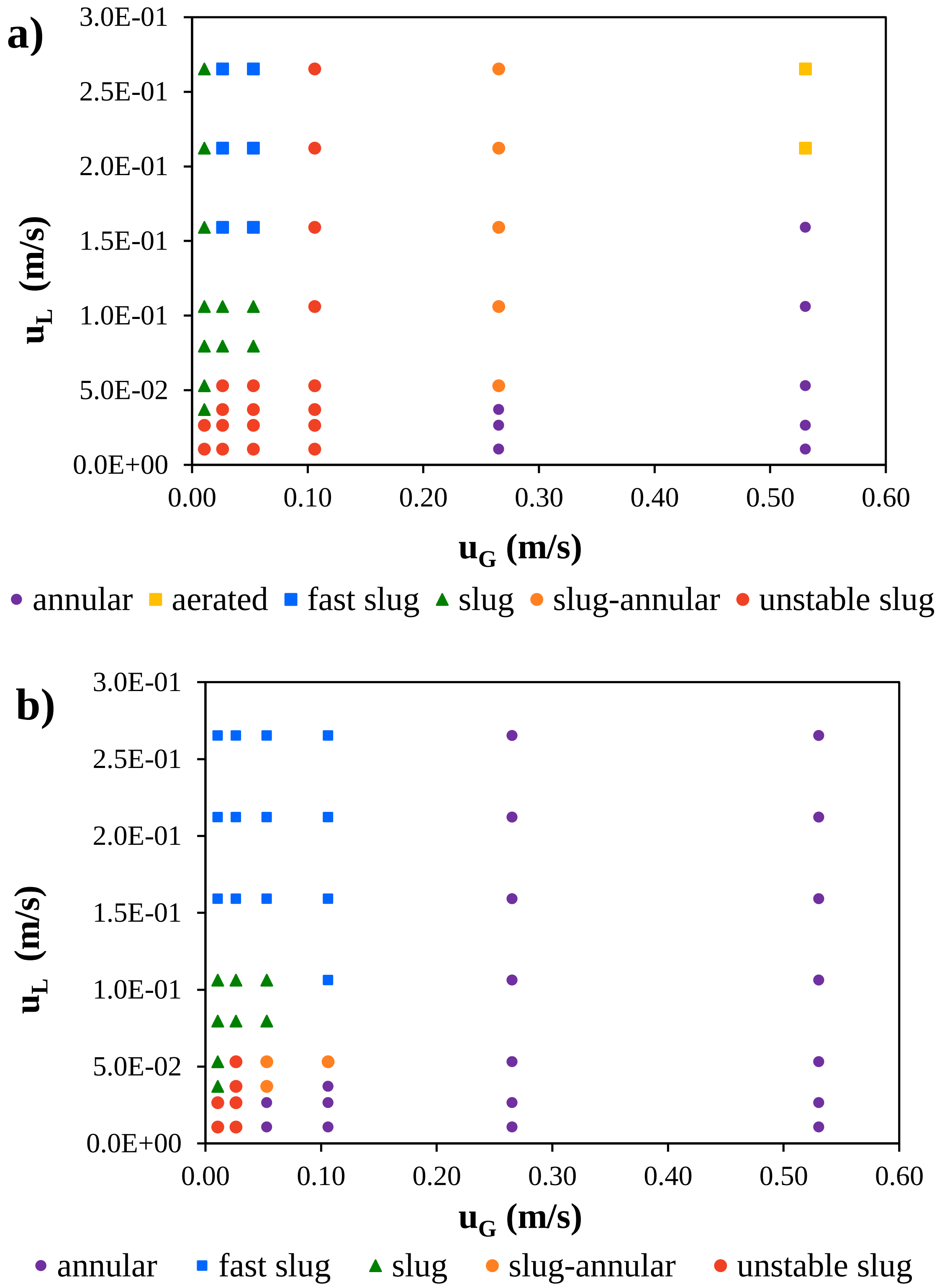

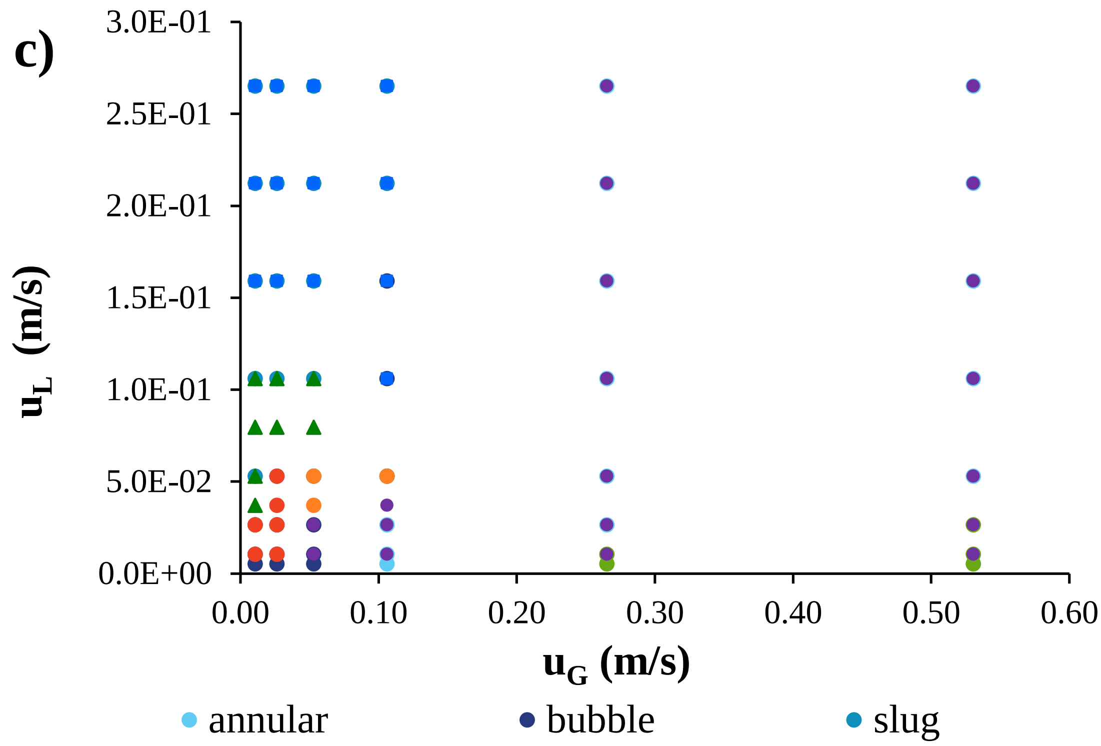

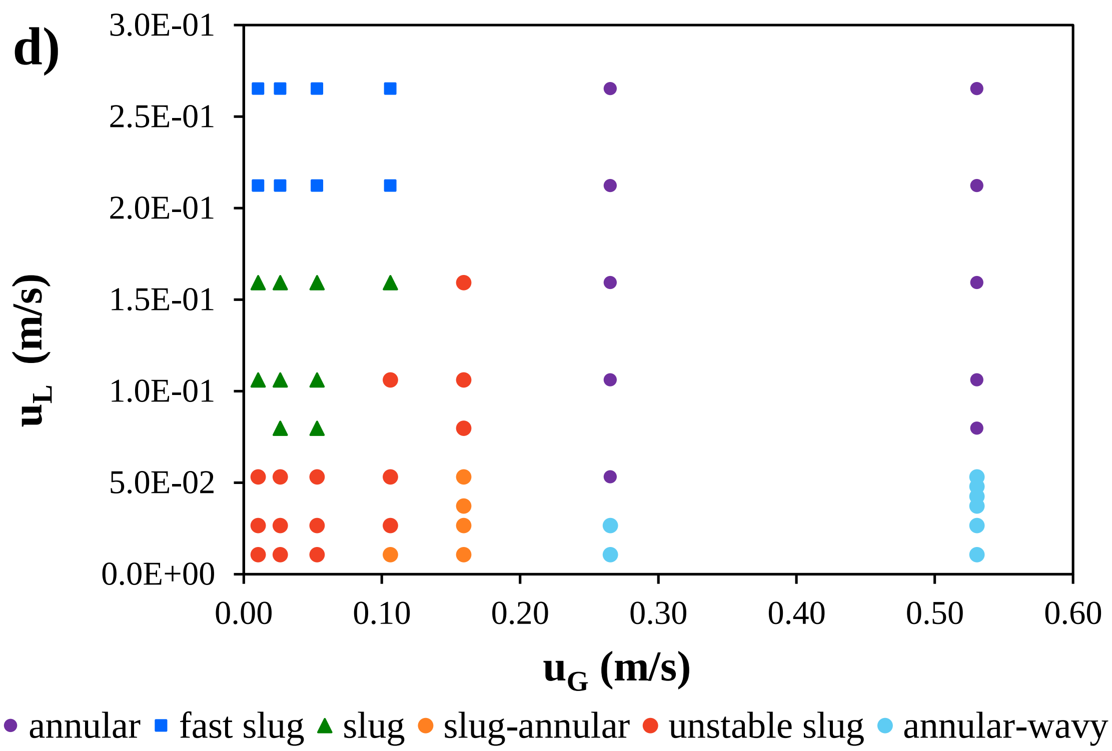

Source: "Elaborated by the author"

Table 4.1 Gas and liquid surface velocity operating window in the 300 mm length, 3 mm internal diameter capillary

Temperature, °C	Liquid phase	Operation window, m/s
10/ 25	Water	$1x10^{-2}<u_G<5x10^{-2}$, $7.9x10^{-2}<u_L<1.1x10^{-1}$
10	NaOH 0.5M	$1x10^{-2} <u_G<1x10^{-1}$, $5.3x10^{-2}<u_L<2.6x10^{-1}$
25	NaOH 0.5M	$1x10^{-2} <u_G<1x10^{-1}$, $7.9x10^{-2}<u_L<1.6x10^{-1}$

Source: "Elaborated by the author"

The established operational windows are very similar to those reported by Hurtado Alva, 2016; Hurtado, Solís-Casados, Escobar-Alarcón, Romero, & Natividad, 2016. In these studies the same type of capillaries was used and the established operating window was $1x10^{-2}<u_G<7x10^{-2}$ y $4x10^{-2}<u_L<5x10^{-1}$ m/s.

3.1.1 Effect of temperature on the hydrodinamics in the capillary reactor

According to Graphic 4.1, the temperature has a significant influence on the development of the type of regime in the capillaries. Using a temperature of 10 °C, there is a wider operating window to obtain the Taylor-type flow in both fluids (Graphic 4.1a and 4.1c) than operating at 25 °C (Graphic 4.1b and 4.1d) (values reported in Table 4.1) This is due to the fact that the formation of the Taylor-type regime is dominated by the forces of surface tension and viscosity, and therefore by temperature, since both physicochemical properties are dependent on it, as well as on the nature of the chemical solution. The lower the temperature, the higher the viscosity of the liquid and the greater the resistance of the liquid to flow in the capillary wall. The values of the different dimensionless numbers that affect the process are presented in Table 4.2.

Table 4.2 Reynolds, Schmidt and capillary numbers in the system CO_2-H_2O

Temperature, °C	Re_L	Re_G	Sc_L	Ca
10	182.4	21.3	1031.9	0.00139
25	267.1	19.5	455.9	0.00097
35	329.6	18.7	288.9	0.00081

Source: "Elaborated by the author"

The Reynolds numbers of liquid and gas indicate that both flows are under a laminar regime, that is, in a direction perpendicular to the gas-liquid interface, which confirms the consideration that the species only move in one direction, when applying the equation of continuity in the cap and the film. Finally, the capillary number validates that the surface tension forces have a greater contribution to the Taylor-type flow pattern than the viscous forces, which indicates that as the capillary number increases, the liquid film formed between the capillary wall and the bubble increases in thickness.

3.2 CO_2 absorption in the capillary reactor

3.2.1 Effect of the temperature on the CO_2 chemical absorption

According to the absorption profile shown in Graphic 4.2, in the absorption process with reaction, the modification of the operation temperature does not present any effect, since, for the five temperatures, the absorption behavior of CO_2 in 0.5M NaOH is similar in terms of saturation concentration and time to reach equilibrium. The equilibrium concentration was approximately 470 mol/m^3 and the time to reach equilibrium was approximately 2 hours.

The explanation for this phenomenon lies in the fact that temperature affects both the rate of diffusion of gases in a liquid and the rate constant of reaction but in opposite ways. As the temperature increases, the collision of the gas molecules increases, decreasing their diffusion speed in the liquid phase and also increases the number of molecules with an energy equal to or greater than the activation energy, thereby increasing the number of effective collisions, increasing the reaction rate constant. For this reason, there is a compensation between reaction kinetics and mass transfer, and therefore there is no difference in chemical absorption profiles when changing temperature.

At the same time, it should be noted that the quantity of CO_2 at equilibrium increased indisputably in the process with chemical reaction (NaOH as reducing agent) with respect to the physical absorption process, in a ratio of 40:1 compared to the maximum absorption achieved at 10 °C in the physical process. Definitely, the use of 0.5M NaOH in chemical absorption shows better results than the use of water in physical absorption.

Graphic 4.2 Comparison of the CO_2 absorption profile in a) water and b) in 0.5M NaOH, using a quartz capillary (300 mm length and 3 mm internal diameter)

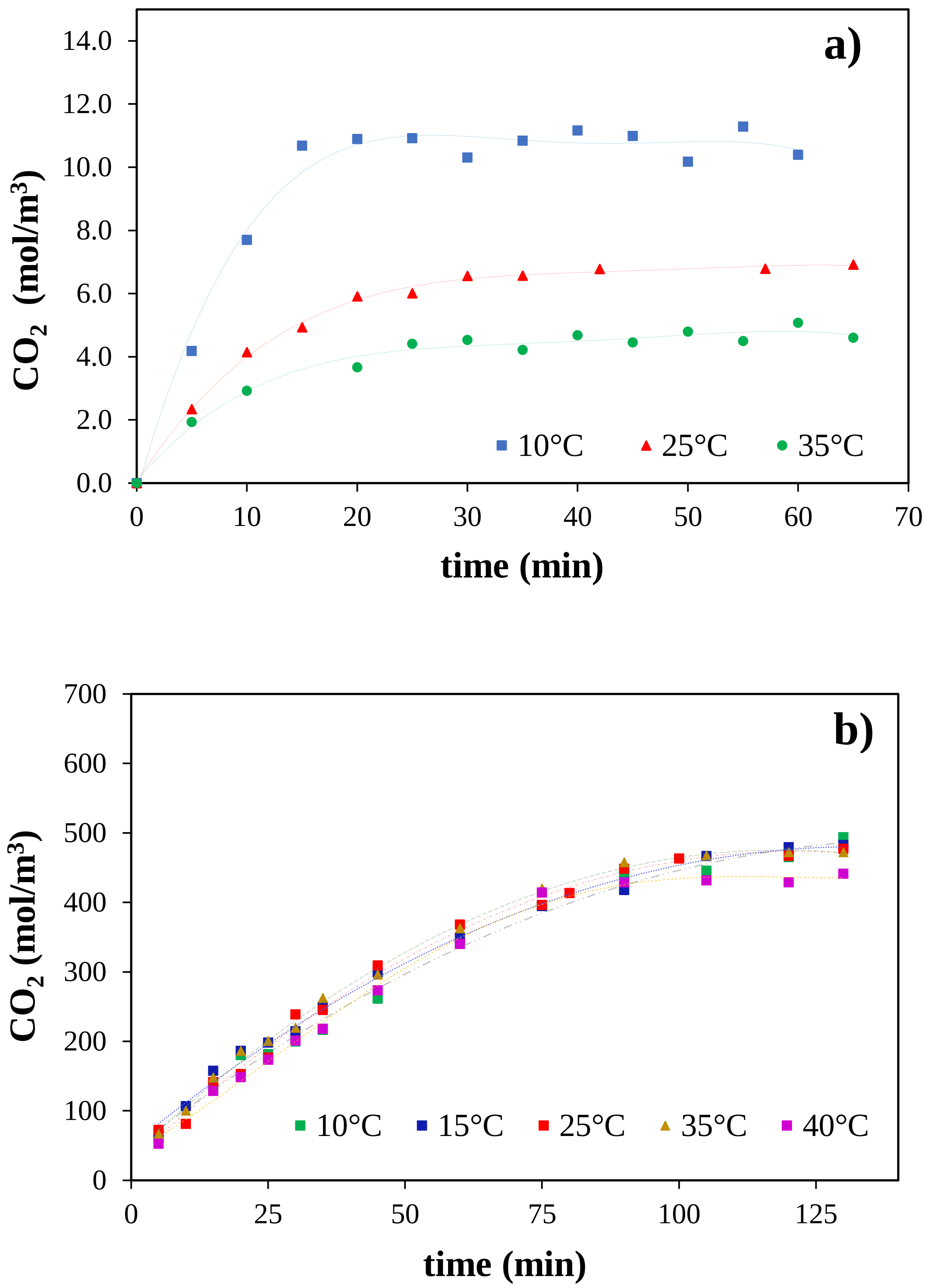

Source: "Elaborated by the author"

The pH of the liquid phase was measured during the absorption process. The profile obtained is shown in Graphic 4.3.

Graphic 4.3 Evolution of pH during CO_2 absorption in 0.5 M NaOH using a 3 x 300mm quartz capillary

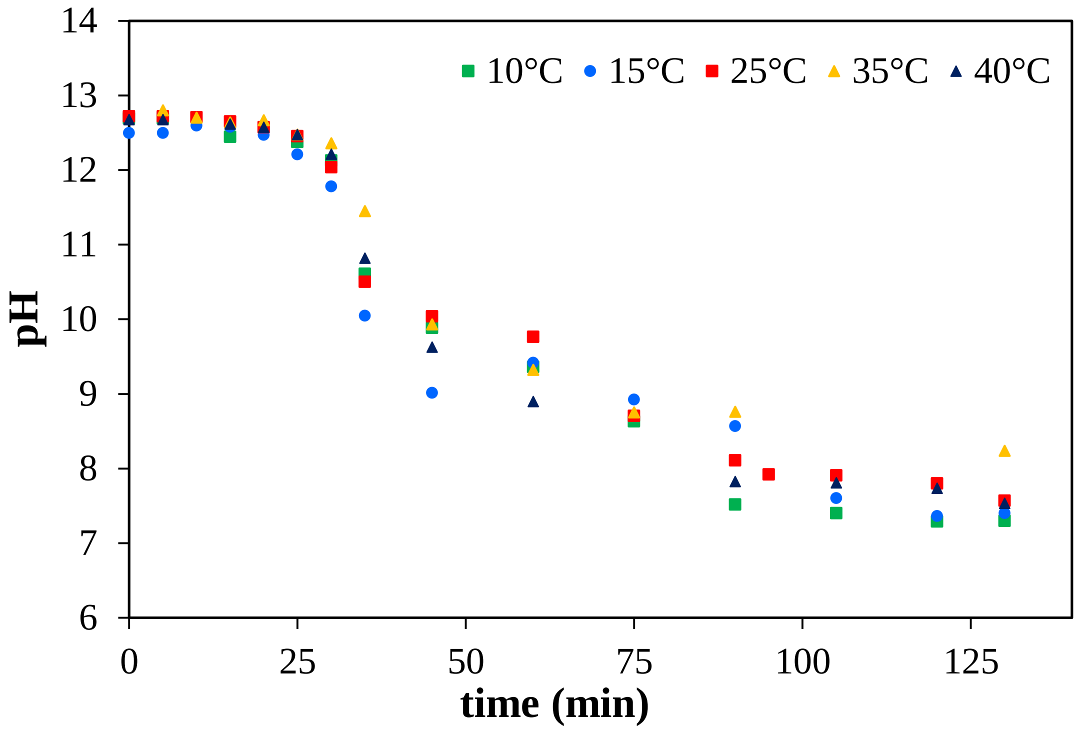

Source: "Elaborated by the author"

In Graphic 4.3, it can be observed that the pH follows the same trend in all cases. During the first two hours the pH decreases until it stabilizes at a pH around 7.5, regardless of the temperature tested. From the species distribution diagrams found in the literature (Ganesh, 2016), it can be inferred that the main chemical specie at the steady state is the bicarbonate ion. It can also be observed that at minute 35 a sudden drop in pH begins and it starts to stabilize at minute 65. After one hour and a half, a greater stability is observed in the curve, which is an indicative of the equilibrium condition.

This behavior coincides with the absorption profiles shown in Graphic 4.2b, so carrying out the pH monitoring to establish the time in which the steady state is achieved in the process is essential in addition to establish the concentration of species that participate in the reaction.

On the other hand, the abrupt drop in pH is a suggestion that the concentration of OH^- ions is rapidly reduced. Since the OH^- ions initially available in the medium are in excess, the reaction with CO_2 is fast during the first minutes causing the reduction of the OH^- ions and the formation of the carbonate ions (CO_3^{2-}). Once the available OH^- are consumed, the formation of bicarbonate ions begins at around a pH of 10.0. This trend is in concordance with the species distribution diagram reported by Ganesh, 2016.

3.2.2 Effect of NaOH concentration on the CO_2 absorption

Since the chemical absorption of CO_2 is influenced by the presence of the amount of OH^- ions available, experiments were carried out modifying the concentration of NaOH. Three concentrations were tested: 0.25M, 0.5M and 0.75M and the results obtained are shown in Graphic 4.4.

Graphic 4.4 CO_2 absorption profile in NaOH 0.25M, 0.5M and 0.75M

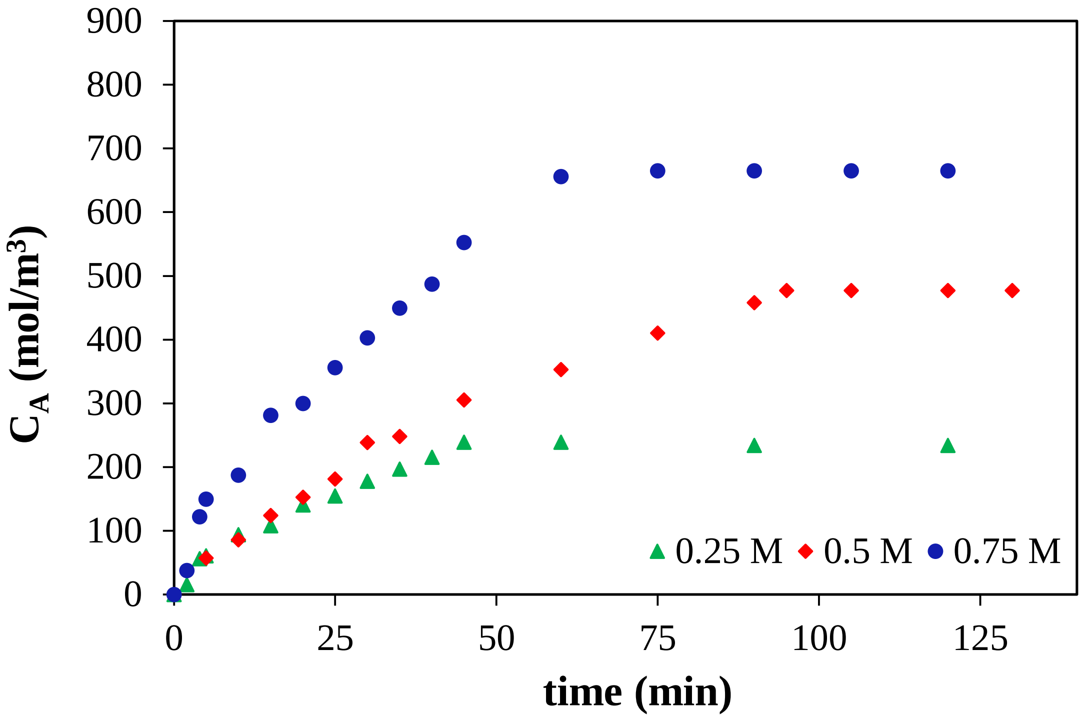

Source: "Elaborated by the author"

The greater availability of OH^- ions with a NaOH concentration of 0.75M, contributes to extend the stage where the chemical reaction of CO_2 with the OH^- ions takes place (initial slope of the curve) and a concentration of saturation greater than when using a NaOH concentration of 0.5M is also reached. A CO_2 concentration equal to 665 mol/m^3 was achieved, representing a greater amount of reactant available for its transformation to organic chemical species. It is also inferred that once the steady state is accomplished, in any of the cases, the only phenomenon is the mass transfer because there are not more OH^- ions to react with and this favors the formation of bicarbonate ions (via Equation 9) with the carbonate ions that were formed in Equation 8.

The pH profile of the solution during two hours of the experiment with different concentrations of NaOH is shown in Graphic 4.5. There is variation in the pH measured at the end of the experiment and this is related to the species that have been formed in the chemical absorption at the steady state. As indicated in section 3.4, the bicarbonate formed either by the dissociation of carbonic acid or by reaction with the hydroxyl ion (Equation 3 and Equation 6) is quickly consumed once it is formed, to generate carbonates until the ions OH^- are completely consumed (Equation 7); then bicarbonates are produced (Equation 9) until reaching the steady state.

Therefore, a final pH of 8.7, 7.6 and 7.0 was obtained in the solutions from higher to lower concentration of NaOH, respectively, and this value keeps a direct relationship with the bicarbonate ions concentration at the end of the process.

Graphic 4.5 Effect of NaOH concentration on the pH temporary profile during CO_2 absorption

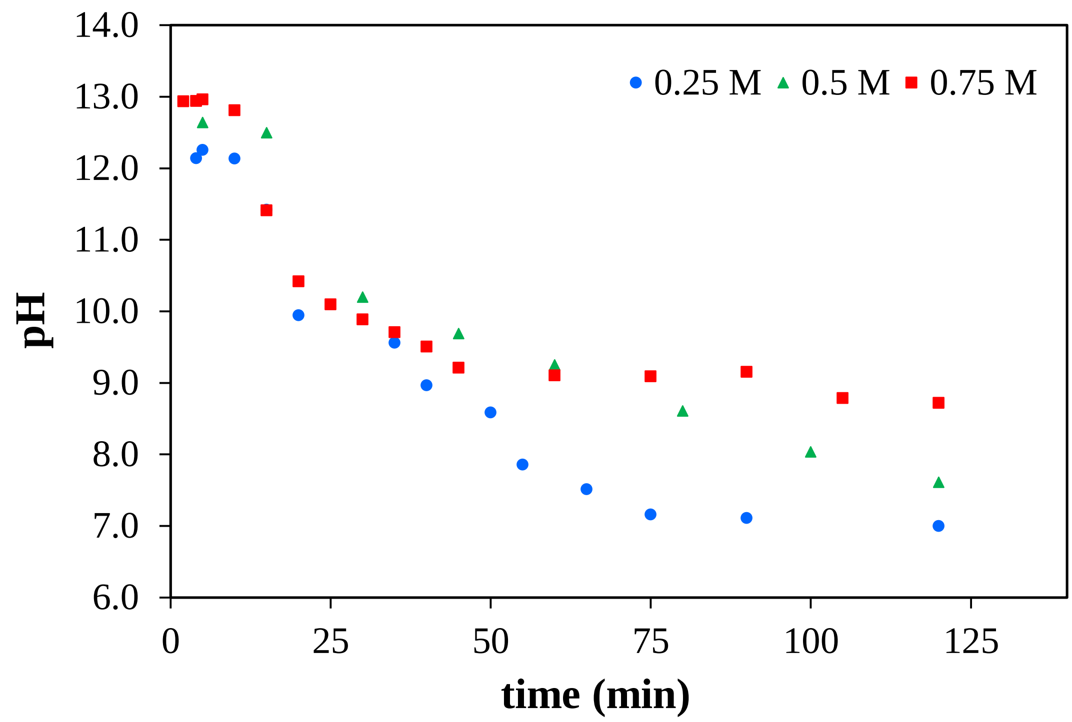

Source: "Elaborated by the author"

3.2.3 Effect of the length of the capillary reactor on the absorption of CO_2

Another important factor to study was the length of the capillary reactor (quartz capillary), assuming that modifying the residence time of the reactants within the capillary would have an effect on the absorbed amount of CO_2. An experiment was carried out using a 100 mm capillary instead of 300 mm, keeping the internal diameter of 3mm, the results are shown in Graphic 4.6.

Graphic 4.6 Effect of the capillary length on CO_2 absorption in NaOH 0.5 M at 25°C

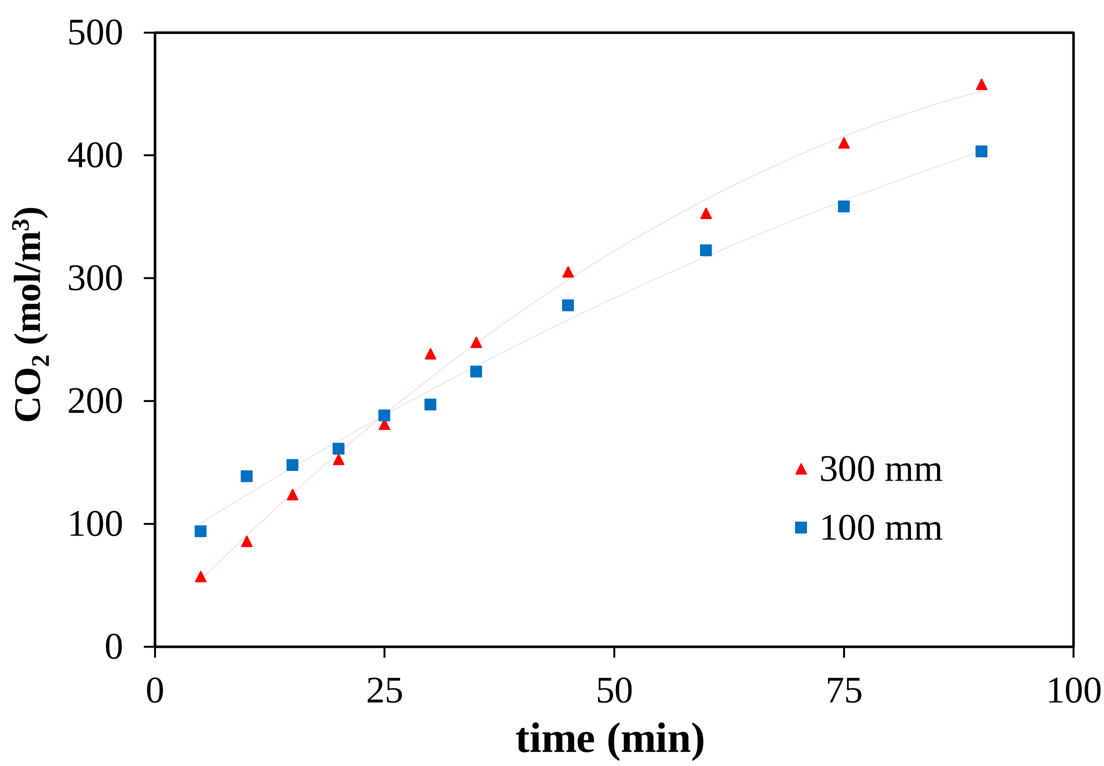

Source: "Elaborated by the author"

The concentration of saturation in the capillary of 100 mm reached 403 mol/m^3, in 90 minutes, which implies a decrease of 14% for the concentration obtained with the capillary of 300 mm, in the same period. This difference is considered as significant since the determined error is 0.47%. This result suggests that the residence time of the reactants is an important variable influencing the amount of CO_2 absorbed.

3.3 Determination of mass transfer coefficients

Physical absorption

For the determination of the mass transfer coefficient in the absorption with water, some considerations were made. Performing the molar flow balance in the system, we arrive at the continuity equation for a component in a binary mixture (Equation 10), which describes the variation of the concentration of a component with respect to time for a given point in space (Fogler, 2008),

$$\mathrm{D_{AB}}\left[\frac{\partial^2 \mathrm{C_A}}{\partial \mathrm{x}^2}+\frac{\partial^2 \mathrm{C_A}}{\partial \mathrm{y}^2}+\frac{\partial^2 \mathrm{C_A}}{\partial \mathrm{z}^2}\right]-\mathrm{U_x}\frac{\partial \mathrm{C_A}}{\partial \mathrm{x}}-\mathrm{U_y}\frac{\partial \mathrm{C_A}}{\partial \mathrm{y}}-\mathrm{U_z}\frac{\partial \mathrm{C_A}}{\partial \mathrm{z}}+\mathrm{r_A}=\frac{\partial \mathrm{C_A}}{\partial \mathrm{t}} \quad (10)$$

This equation has been simplified, according to film theory, by assuming that the mass transfer occurs only in one direction by diffusion, in a gas-liquid system with two films, one for each phase, and stationary state; that is, the concentration of CO_2 in the liquid phase does not vary during the contact time between the gas phase of the bubble and the liquid phase, since the CO_2 is absorbed relatively slowly in water. The volumetric movement is too small to influence the diffusion of gases has also been considered (Beltrán, 2003). The equation has been reduced to a single term (Equation 11), with the boundary conditions indicated below,

$$D_{AB}\frac{d^2C_A}{dx^2}=0 \quad (11)$$

$x=0;\ C_A=C_A^*$
$x=\delta;\ C_A=C_{Ab}$

and it was related to Fick's first law, obtaining the following equation:

$$A_sN_i=\frac{d}{dt}V_cC_A=A_sk_L^0(C_e-C_{Ab}) \quad (12)$$

$$k_L^0=\frac{D_{AB}}{\delta} \quad (13)$$

Where:
A_s = Contact area between phases
N_i = Molar flux
V_c = Microreactor volume (capillary)
C_A = CO_2 concentration (variable)
k_L^0 = Mass transfer coefficient for physical absorption (in water)
C_e = Equilibrium concentration in liquid phase
C_{Ab} = CO_2 concentration at equilibrium (saturation)
D_{AB} = Diffusion coefficient of CO_2 – water system
δ = film thickness

Since the volume of the capillary reactor, V_c, is considered constant, the Equation 14 is obtained,

$$\frac{dC_A}{dt}=k_L^0a(C_e-C_{Ab}) \quad (14)$$

Chemical absorption

In the Taylor-type regime, the mass transfer from the bubble to the gas-liquid interface can be neglected if the gas phase is pure CO_2, so the contribution is due only to the processes that occur within the liquid phase.

Furthermore, it is considered that the speed with which CO_2 diffuses into the liquid is the same which OH^- ions diffuse to the area where they are consumed. Applying the continuity equation to both CO_2 (species A) and OH^- ions (species B) and considering that they move in the x direction, the chemical absorption of CO_2 is described with Equations 15 and 16 (Nijsing, 1959; Beltrán, 2004)

$$\frac{\partial C_A}{\partial t} = \mathcal{D}_A \frac{\partial^2 C_A}{dx^2} - k_B C_B C_A \tag{15}$$

$$\frac{\partial C_B}{\partial t} = \mathcal{D}_B \frac{\partial^2 C_B}{dx^2} - k_B C_B C_A \tag{16}$$

This system of differential equations has an infinite number of solutions, the initial and boundary conditions were established,

$$t = 0,\ x \geq 0,\ C_A = 0\ ,\quad C_B = C_{B,0}$$

$$x = 0,\ t > 0,\ C_A = C_A^i\ ,\quad \frac{\partial C_B}{\partial x} = 0$$

$$x = \infty,\ t \geq 0,\quad C_A = 0,\quad C_B = C_{B,0}$$

A general solution makes use of the term improvement factor (Φ), which is based on the relationship between the mass transfer coefficient for chemical absorption (k_L) and that of physical absorption (k_L^0) (Perry, Green, & Maloney, 1992). The solution is a function of the Hatta number (Ha), the relationship between the initial OH^- concentration and the CO_2 concentration at the interface, and the relationship between the diffusivities of OH^- and CO_2 ions in water. Hatta is a dimensionless number that relates the rate of reaction in a liquid film to the rate of diffusion through the film (Beltrán, 2003) and is calculated as follows,

$$Ha = \frac{\sqrt{k_B C_{B,0} \mathcal{D}_{AB}}}{k_L^0} \tag{17}$$

On the other hand, it is necessary to know the reaction rate constant to determine the mass transfer coefficient. Regarding the order of reaction, two cases have been proposed, among several:

a. Pseudo-first order reaction, when C_B is too large compared to C^i_A and its diffusion rate to the reaction zone is very fast compared to the rate at which it is consumed in the reaction.
b. Second order reaction (extremely fast), when C_B is not so large compared to C^i_A and both species diffuse towards areas where their concentrations are lower.

With regard to reaction kinetics, it has been widely reported that the kinetic constant depends on the reaction temperature, the ionic strength of the solution, and the nature of the cation (Danckwerts & Kennedy, 1958; Harish Ganapathy, Al-hajri, & Ohadi, 2013; Grzelka *et al*., 2011; Pohorecki & Moniuk, 1988). Therefore, the equation proposed by Pohorecki & Moniuk, 1988 (Equation 18) was used to estimate the value of the kinetic constant in the chemical absorption of CO_2 in aqueous electrolyte solutions, in this equation, the kinetic constant depends on the temperature (T) and the ionic strength (I),

$$log_{10}(k_B) = 11.916 - \frac{2382}{T} + 0.221I - 0.016I^2 \tag{18}$$

The ionic strength is calculated with the molar concentration of the ions (C_i) present and their respective valence (z_i), characteristic of each ion, as indicates Equation 19.

$$I = 0.5 \sum_i C_i z_i^2 \tag{19}$$

In this study, during physical absorption (k_L^0), Equation 14 was used to estimate the mass transfer coefficient, using the slope of the straight line of the absorption profiles when using water as absorbent (data from Graphic 4.2a). Graphic 4.7 shows the trend lines for each temperature and Table 4.3 shows the results of the volumetric mass transfer coefficient for each temperature as well as the coefficients of determination (R^2) for each trend line.

It is worth commenting that when carrying out the experiments, the concentration of initial CO_2 in the liquid solution (blank) was disregarded from each value, so the initial conditions are $t = 0,\ C_A = 0$, the coefficient of determination in Table 4.3 tells the data fit well to the lineal model and is higher when temperature increases (with $p<0.05$) for the three temperatures.

Graphic 4.7 Graph for the calculation of the volumetric mass transfer coefficient in the CO_2-H_2O system

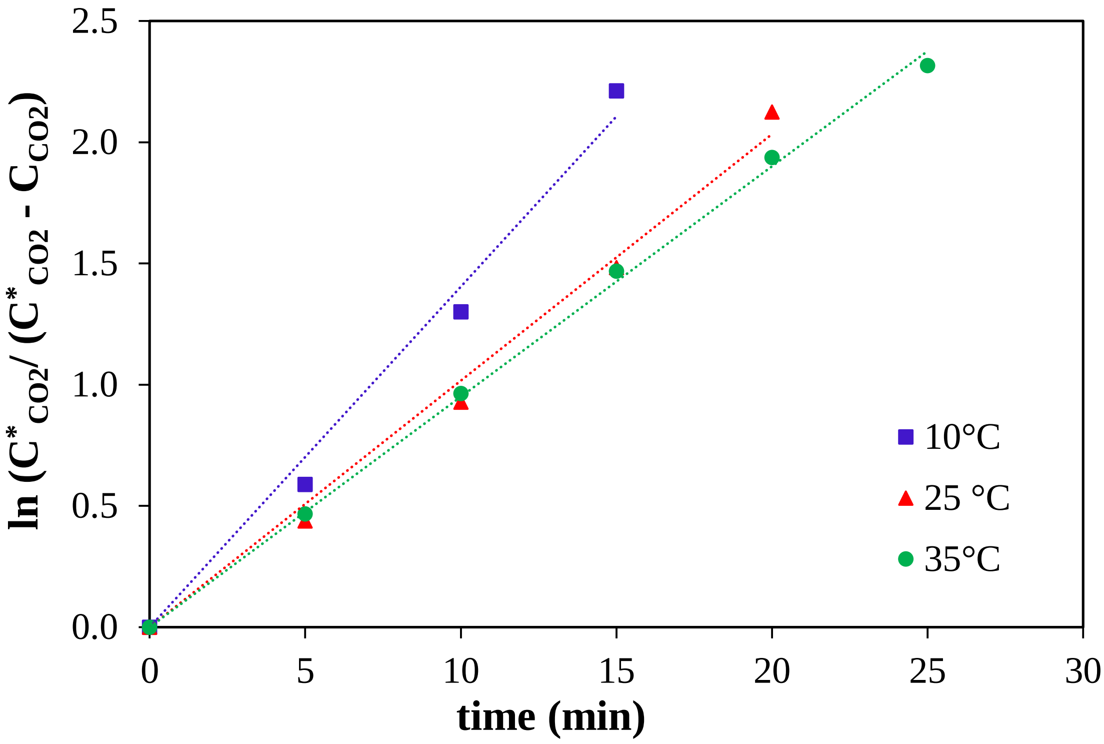

Source: "Elaborated by the author"

Table 4.3 Determination coefficient and slope of the linear equations plotted in Graphic 7

Temperature, °C	Time to reach equilibrium, minutes	Slope = $k_L{}^0a$, s^{-1}	Determination coefficient, R^2	p-value
10	15	0.00234	0.987	<0.005
25	20	0.00169	0.992	<0.0002
35	25	0.00158	0.998	<0.0002

Source: "Elaborated by the author"

In Table 4.3, it can be seen that the value of the volumetric mass transfer coefficient ($k_L{}^0a$) increases when the temperature decreases, and this behavior is in concordance with the fact that the solubility of CO_2 increases when the temperature decreases (Henry's Law). Empirical correlations reported in the literature were used to compare the volumetric mass transfer coefficients with those determined in this study during the absorption of CO_2 in water. Table 4.4 presents a comparison of the results. It can be seen that the experimental data obtained fit very well with the correlation of H. Ganapathy, Shooshtari, Dessiatoun, Ohadi, & Alshehhi, 2015. It is important to specify that in all the cases, in the literature reported in Table 4, the flow channels had a smaller diameter than that used in this study by at least one order of magnitude, also the length.

Table 4.4 Determination of mass transfer coefficients using correlations reported in the literature

Temperature, °C	k_La, experimental	Yue, 2007	Kuhn and Jensen, 2012	Yao, 2015	Ganapathy, 2015
10	0.00234	0.14378	0.000145	0.044193	0.00227
25	0.00169	0.20725	0.000128	0.019798	0.00111
35	0.00158	0.25464	0.000123	0.012934	0.00075

Source: "Elaborated by the author"

The results of the reaction rate constant and the mass transfer coefficient when performing chemical absorption are shown in Table 4.5. The Hatta number relates the rate of reaction in a liquid film to the rate of diffusion through the film and indicates whether or not the reaction occurs faster than the mass transfer, identifying the controlling step of the absorption process.

Table 4.5 Kinetic and mass transfer coefficients obtained in the chemical absorption process of CO_2 in 0.5M NaOH

Temperature	10°C	25°C	35°C
Ha	47.0	72.7	127.1
k_B (m^3/mol s)	0.0372	0.0551	0.0716
k_L x 10^5 (m/s)	3.381	2.831	2.296
k^0_L x 10^6 (m/s)	1.657	1.272	9.939
k_L/k^0_L	20	22	23

Source: "Elaborated by the author"

The Ha values shown in Table 4.5, indicate that the chemical reaction is much faster than diffusion, and therefore, the absorption process is controlled by mass transfer. The behavior observed in the CO_2 absorption profiles obtained by modifying the NaOH concentration in the solution (Graphic 4.4) is consistent with the previous statement: on the initial slope of the absorption profile curve, the OH^- ions are found in excess and all absorbed CO_2 reacts immediately, in contrast, later the concentration of OH^- ions decreases and this chemical species is no longer available to react with the CO_2 molecules at the interface.

As for the kinetic constant, k_B, it is observed that it increases proportionally with temperature, since the increase in temperature affects the activation energy of the molecules. The value of the mass transfer coefficient, k_L, decreases with increasing temperature and this behavior is consistent with that reported in the literature. These results confirm that there is a compensation between the chemical reaction and the mass transfer in the process of chemical absorption of CO_2 in the 0.5 M NaOH solution when carried out at different temperatures. As the temperature increases, the OH^- ions and CO_2 in the reaction are activated more quickly, however, the increase in temperature represents a lower availability of OH^- ions due to the low solubility and molecular diffusion.

In this way, there is a compensation in both phenomena (while one grows the other decreases due to the effect of temperature) obtaining similar absorption profiles (Graphic 4.2). Another important point to conclude besides that the use of a NaOH solution improves the absorption process of CO_2 in water, is the relationship between the mass transfer coefficient with chemical absorption and that of physical absorption, which is approximately 20 times higher.

From the results of Table 4.6, when modifying the concentration of NaOH in the solution, no significant effect is observed in the reaction rate constant (k_B), since the kinetic constants for the three concentrations are similar. This indicates that the rate at which the OH^- ions is consumed is similar, regardless of whether there is a greater quantity of them as their concentration increases. However, there is a very slight increase in the mass transfer constant (k_L) when the concentration of the ions increases, which indicates that having more ions leads to a better mass transfer.

Table 4.6 Kinetic and mass transfer coefficients obtained at 25 ° C in the process of chemical absorption of CO_2 in NaOH solutions with concentrations of 0.25, 0.5 and 0.75M

NaOH concentration	0.25M	0.5M	0.75M
Ha	40.5	72.7	103.1
k_B (m^3/mol s)	0.0537	0.0551	0.0573
k_L x 10^5 (m/s)	2.466	2.83	2.924
k^0_L x 10^6 (m/s)	1.272	1.272	1.272
k_L/k^0_L	19	22	23

Source: "Elaborated by the author"

3.4 Variation of involved species

During the absorption process with chemical reaction, in addition to the CO_2 dissolved in the liquid phase, other ions are also present, such as bicarbonate and carbonate (HCO_3^- and CO_3^{2-}). Graphic 4.8 shows the evolution of the concentration of the species involved in the process over time for NaOH concentrations 0.25, 0.5 and 0.75M at 25 °C as well as the evolution of pH. In Graphic 4.8, we can see that, when consuming NaOH, due to the reaction with CO_2, carbonate ions begin to be generated until reaching a maximum concentration. The experimental relationship between the concentration of hydroxide and carbonate is 2:1 as shown in Graphic 4.8 a, c and d, which coincides with the stoichiometry of the reaction (Equation 8), obtaining molar yields of almost 100%. Once the hydroxyl ion has been used up, the formed carbonate begins to react with CO_2 to produce the bicarbonate ion, which is the final product of the general reaction (Equation 9). Once the carbonate is depleted in reactive absorption to produce bicarbonate, then the physical absorption of CO_2 begins. This, considering that the absorption of CO_2 implies, on the one hand, the reaction rate and, on the other, the diffusion of the OH^- ions; consequently, only the mass transfer prevails once the concentration of OH^- ions is minimum.

In Graphic 4.8b, d and e, it is identified that the predominance of the reaction to form bicarbonate (Equation 6) occurs when the pH is greater than 10 in the hydroxide/carbonate mixture, due to the instantaneous reaction to form carbonate (Equation 7). The carbonate is formed instantly once a bicarbonate ion is generated; thus, the generation of bicarbonate is appreciated until the production of carbonate ends due to the depletion of the OH^- ions, most of the carbonate/bicarbonate mixtures occur between a pH from 8-10.5. Likewise, it can be observed that the pH tends to stabilize when all the carbonate has reacted and has become bicarbonate (pH approximately 8). This indicates that the final solution is a saturated solution where is no longer possible to continue chemically absorbing CO_2 given the carbonic acid/bicarbonate balance in physical absorption (Equation 3). Recapitulating, the bicarbonate ion generated by the dissociation of carbonic acid and also by the presence of the hydroxyl ion (Equation 3 and Equation 6) is consumed immediately once it is formed, as they are quite fast reactions, for the generation of carbonate until all are exhausted. The OH^- ions (Equation 7), from that moment on, bicarbonates will be produced (Equation 6), until equilibrium is reached. The time in which the OH^- is depleted depends on its concentration: the higher the concentration, the longer the period of time during which the reaction between CO_2 and OH^- occurs. Finally, it only remains to point out the importance of constant monitoring of pH in this type of process, since from the slopes in its temporal profile, the beginning and end of each of the reactions in which CO_2 participates in solutions can be inferred until it reaches equilibrium.

Graphic 4.8 Chemical Species Concentration and pH temporary profiles in the CO_2 absorption process at 25 °C

a) C*i* in NaOH 0.25M

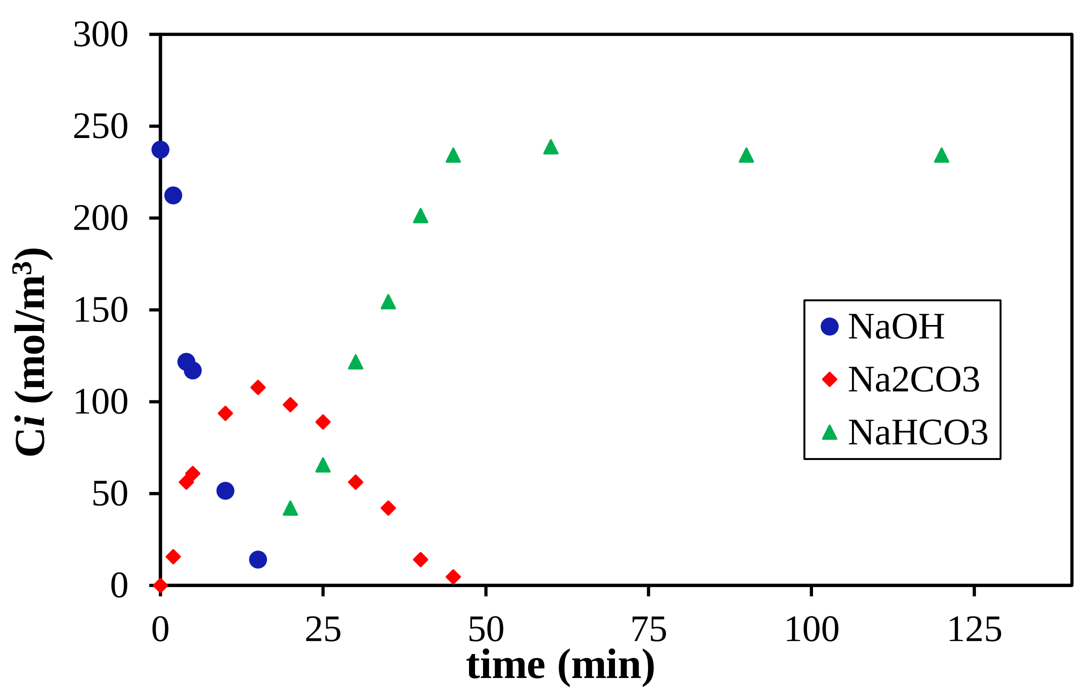

b) pH in NaOH 0.25M

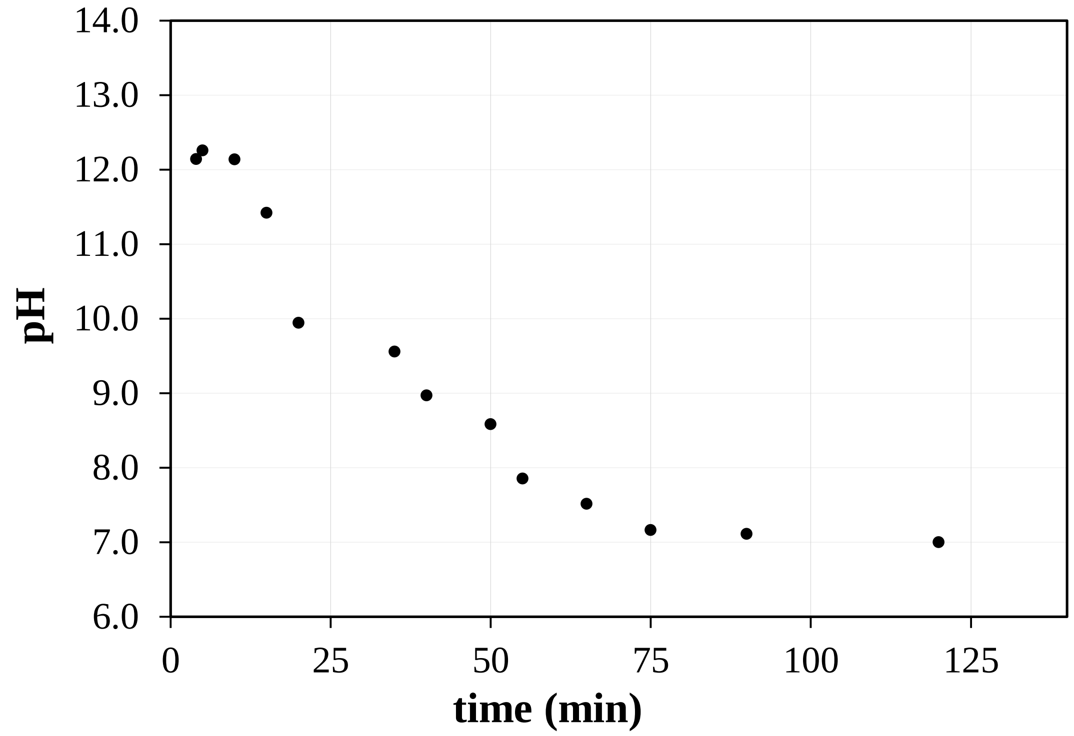

c) C*i* in NaOH 0.5M

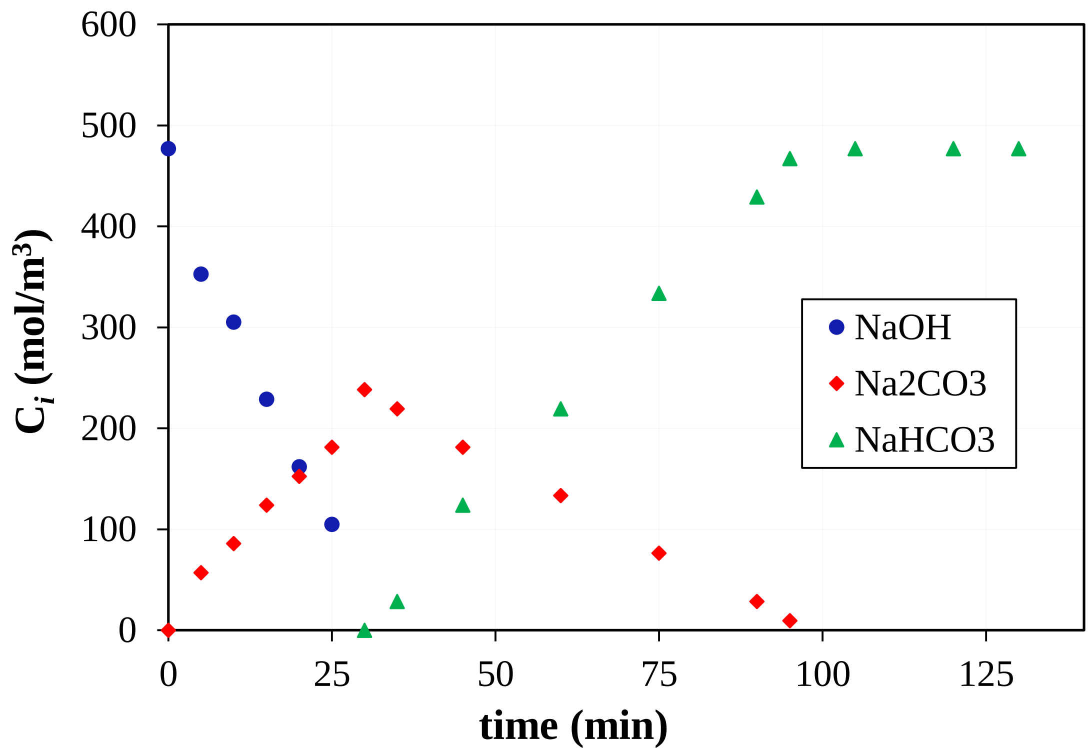

d) pH in NaOH 0.5M

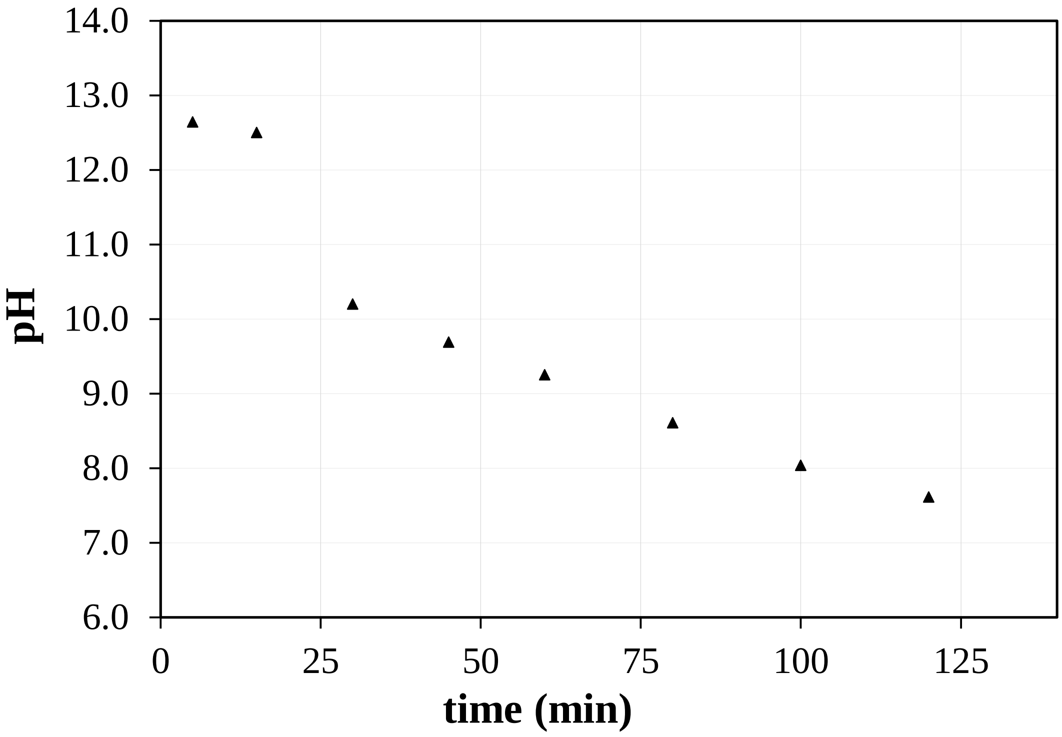

e) C*i* in NaOH 0.75M

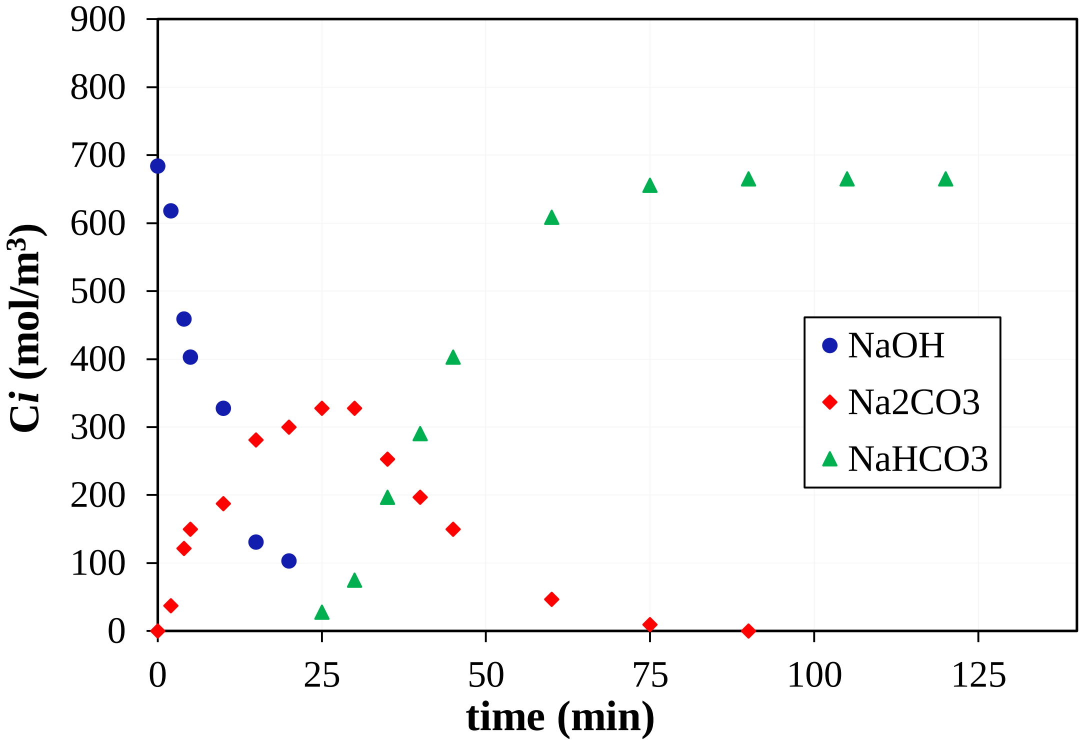

f) pH in NaOH 0.75M

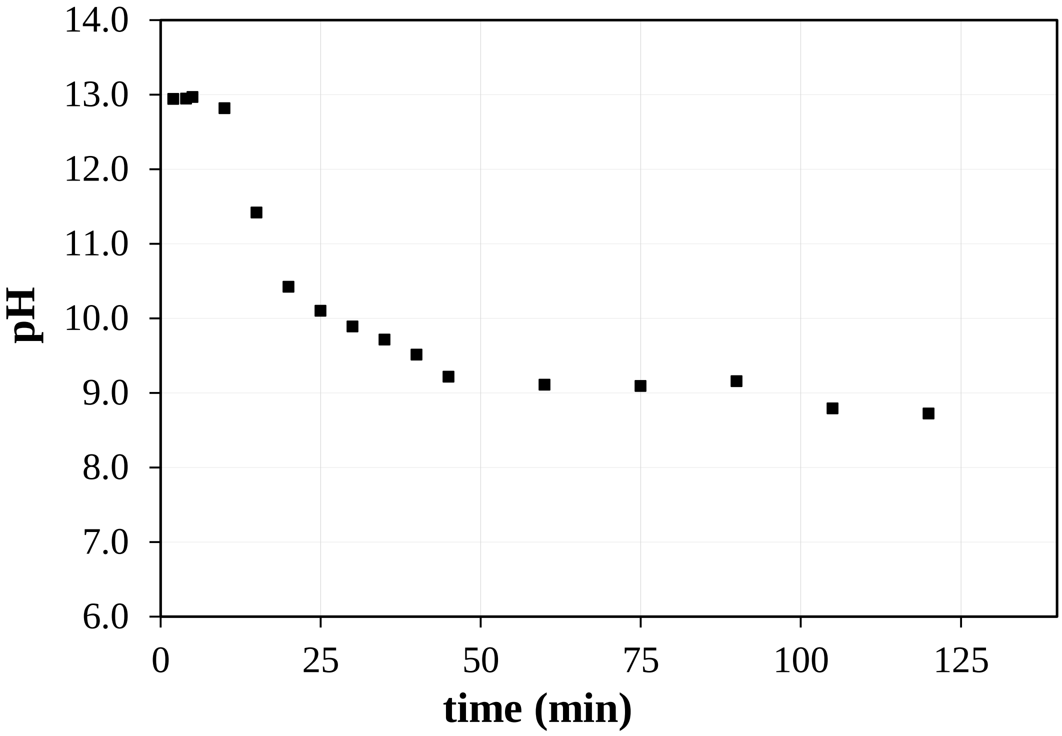

Source: "Elaborated by the author"

4. Acknowledgments

Rosaura Peña thanks the National Council of Science and Technology (CONACyT) for the financial support through scholarship No. 239954 to conduct doctoral studies. Authors also thank CONACyT for the project No. 269093 and Universidad Autónoma del Estado de México for project 6235/2020CIB. Authors also would like to thank Citlalit Martínez Soto for technical support.

5. Conclusions

– The operating window of the gas and liquid surface velocity to obtain the Taylor-type regime, at 10 ° C in a capillary with 3mm internal diameter is $1x10^{-2} < u_G < 5x10^{-2}$ and $7.9x10^{-2} < u_L < 1.1x10^{-1}$ m/s, using water and 0.5M NaOH, respectively.

– The operating window of the gas and liquid surface velocity to obtain the Taylor-type regime, at 25 ° C in a capillary with 3mm internal diameter is $1x10^{-2} < u_G < 5x10^{-2}$ and $8x10^{-2} < u_L < 1.6x\ 10^{-1}$ m/s, using water and 0.5M NaOH, respectively.

– There is a greater absorption of CO_2 using alkaline solutions than using only water.

– The value of the volumetric mass transfer coefficient in the absorption of CO_2 with water, increases with decreasing temperature

– The mass transfer coefficient in the absorption of CO_2 with NaOH in solution increases directly with temperature.

– The combined method of titration and pH measurement allows monitoring the behavior of the different ionic species that can be generated during the absorption of CO_2 in alkaline solutions.

6. References

Beltrán, F. J. (2003). *Ozone reaction kinetics for water and wastewater systems*. Lewis Publishers.

Centi, G., & Perathoner, S. (2009). Opportunities and prospects in the chemical recycling of carbon dioxide to fuels. *Catalysis Today, 148*(3–4), 191–205. https://doi.org/10.1016/j.cattod.2009.07.075

Cotton, F. A. et al. (1999). *Advanced inorganic chemistry* (6a ed.). Wiley.

Danckwerts, P. V., & Kennedy, A. M. (1958). The kinetics of absorption of carbon dioxide into neutral and alkaline solutions. *Chemical Engineering Science*, *8*(3–4), 201–215. https://doi.org/10.1016/0009-2509(58)85027-7

Fogler, H. S. (2008). *Elementos de ingeniería de las reacciones químicas* (4a ed.). México: PEARSON EDUCACIÓN.

Ganapathy, H, Shooshtari, A., Dessiatoun, S., Ohadi, M. M., & Alshehhi, M. (2015). Hydrodynamics and mass transfer performance of a microreactor for enhanced gas separation processes. *Chemical Engineering Journal*, *266*, 258–270.

Ganapathy, Harish, Al-hajri, E., & Ohadi, M. (2013). Mass transfer characteristics of gas – liquid absorption during Taylor fl ow in mini / microchannel reactors. *Chemical Engineering Science*, *101*, 69–80. https://doi.org/10.1016/j.ces.2013.06.005

Ganesh, I. (2016). Electrochemical conversion of carbon dioxide into renewable fuel chemicals – The role of nanomaterials and the commercialization. *Renewable and Sustainable Energy Reviews*, *59*, 1269–1297. https://doi.org/10.1016/j.rser.2016.01.026

Grzelka, J., Sobieszuk, P., Pohorecki, R., & Cygan, P. (2011). Determination of the interfacial area and mass transfer coefficients in the Taylor gas – liquid flow in a microchannel, *66*, 6048–6056. https://doi.org/10.1016/j.ces.2011.08.029

Heiszwolf, J. J., Kreutzer, M. T., Eijnden, M. G. Van Den, Kapteijn, F., & Moulijn, J. A. (2001). Gas – liquid mass transfer of aqueous Taylor flow in monoliths, *69*, 51–55.

Holum, J. R. (1990). *Principios de fisicoquímica, química orgánica y química*. México: Limusa.

Hurtado Alva, L. (2016). *Reactores capilares para fotosíntesis artificial*. Universidad Autónoma del Estado de México.

Hurtado, L., Solís-Casados, D., Escobar-Alarcón, L., Romero, R., & Natividad, R. (2016). Multiphase photo-capillary reactors coated with TiO_2 films: Preparation, characterization and photocatalytic performance. *Chemical Engineering Journal*, *304*, 39–47. https://doi.org/10.1016/j.cej.2016.06.003

Hurtado, Lourdes, Natividad, R., & García, H. (2016). Photocatalytic activity of Cu_2O supported on multi layers graphene for CO_2 reduction by water under batch and continuous flow. *Catalysis Communications*, *84*, 30–35.

Mebrahtu, C., Krebs, F., Abate, S., Perathoner, S., Centi, G., & Palkovits, R. (2019). and Challenges, *178*, 85–103.

Natividad, R., Kulkarni, R., Nuithitikul, K., Raymahasay, S., Wood, J., & Winterbottom, J. M. (2004). Analysis of the performance of single capillary and multiple capillary (monolith) reactors for the multiphase Pd-catalyzed hydrogenation of 2-butyne-1,4-diol. *Chemical Engineering Science*, *59*(22–23), 5431–5438. https://doi.org/10.1016/j.ces.2004.09.011

Ola, O., & Maroto-Valer, M. M. (2015). Review of material design and reactor engineering on TiO_2 photocatalysis for CO_2 reduction. *Journal of Photochemistry and Photobiology C: Photochemistry Reviews*, *24*, 16–42. https://doi.org/10.1016/j.jphotochemrev.2015.06.001

Palmer, D. A., & Van Eldik, R. (1983). The chemistry of metal carbonato and carbon dioxide complexes. *American Chemical Society*, *83*, 651–731.

Perry, R. H., Green, D. W., & Maloney, J. O. (1992). *Manual del ingeniero químico* (6a ed.). McGraw-Hill.

Pohorecki, R., & Moniuk, W. (1988). Kinetics of reaction between carbon dioxide and ions in aqueous electrolyte solutions. *Chemical Engineering Science*, *43*(7), 1677–1684.

Savage, D. W., Astarita, G., & Joshi, S. (1980). Chemical absorption and desorption of carbon dioxide from hot carbonate solutions. *Chemical Enginering Science*, *35*, 1513–1522.

Shehzad, N., Tahir, M., Johari, K., & Murugesan, T. (2018). A critical review on TiO_2 based photocatalytic CO_2 reduction system : Strategies to improve efficiency, *26*(May), 98–122. https://doi.org/10.1016/j.jcou.2018.04.026

Shim, J.-G., Lee, D. W., Lee, J. H., & Kwak, N.-S. (2016). Experimental study on capture of carbon dioxide and production of sodium bicarbonate from sodium hydroxide. *Environmental Engineering Research*, *21*, 297–303.

Skoog, D. R. (2014). *Fundamentals of analytical chemistry* (9th ed.). CENGAGE Learning.

Yang, H., Zhang, C., Gao, P., Wang, H., Li, X., Zhong, L., Sun, Y. (2017). A review of the catalytic hydrogenation of carbon dioxide into value-added hydrocarbons. *Catalysis Science and Technology*, *7*(20), 4580–4598. https://doi.org/10.1039/c7cy01403a

Chapter 5 Mechanical characterization of the L4 and L5 lumbar vertebrae

Capítulo 5 Caracterización mecánica de las vértebras lumbares L4 y L5

VILLAGRÁN-VILLEGAS, Luz Yazmin[1]†*, SIORDIA-VÁSQUEZ, Xóchitl[2], CUÉLLAR-OROZCO, Maricela[2] and PATIÑO-ORTIZ, Miguel[1]

[1]Instituto Politécnico Nacional. Unidad Profesional "Adolfo López Mateos"- Zacatenco, Gustavo A. Madero, Mexico D.F.
[2]Universidad Veracruzana. Faculty of Engineering and Chemical Sciences"Campus Poza Rica-Tuxpan"- Av. Venustiano Carranza s/n Col. Revolución, Poza Rica, Ver. Ph: +52 782 8238143

ID 1[er] Author: *Luz Yazmin, Villagrán-Villegas* / **ORC ID**: 0000-0003-3860-2923, **CVU CONACYT ID:** 96365

ID 1[er] Co-author: *Xóchitl, Siordia-Vásquez* / **ORC ID**: 0002-8472-8001, **CVU CONACYT ID**: 1036998

ID 2[do] Co-author: *Maricela, Cuéllar-Orozco* / **ORC ID**: 0000-0002-6558-4938, **CVU CONACYT ID**: 662076

ID 3[er] Co-author: *Miguel, Patiño-Ortiz* / **ORC ID**: 0000-0002-5630-8077, **CVU CONACYT ID**: 167388

DOI: 10.35429/H.2021.6.75.85

L. Villagrán, X. Siordia, M. Cuéllar and M. Patiño

*yvillagran@uv.mx

A. Marroquín, J. Olivares, M. Ramírez and L. Cruz (Coord) Engineering and Technology. Handbooks-©ECORFAN-México, Querétaro, 2021.

Abstract (Mechanical characterization of the lumbar vertebrae)

Compression fractures in the lumbar region are usually caused by excessive pressure at the level of the vertebral body. The fracture occurs when the vertebral body is crushed, causing the anterior part of the vertebral body to acquire a wedge shape. Bone tissue inside the vertebral body is crushed or compressed. Compression fractures due to trauma may be due to a fall, a strong jump, a car accident, or any other event that emphasizes the spine beyond its breaking point [1]. In a simulation of the fracture in recent studies, loads are applied to real vertebral samples (destructive tests), where both compression loads are fixed on the upper and lower faces of the vertebral body. The literature mentions tests with loads of approximately 8000N emulating a daily accident, so this research aims to obtain a precise model with the use of an optical scanner, which will allow the obtaining of points (meshing) of the piece in real time with an individual measurement of up to 16 million independent measurement points captured from 1 to 2 seconds. The measurement data is characterized by a very detailed reproduction and therefore also allows the measurement of sample components up to 38mm. The following study will begin with the acquisition of plaster and aluminum models, for the different types of samples mentioned below:

- Swine lumbar vertebral simple.
- Human lumbar vertebral simple 4.
- Human lumbar vertebral simple 5.

With the help of the ATOS&GOM® optical scanner, point clouds were acquired from each of the samples that were used to acquire 3D printing models and obtain 3D solid digital models to perform the Von-Mises stress analysis. As a result of the Von-Mises stress analysis process, when applying compressive loads of 960 N and shear of 8000 N distributed in each lumbar vertebra, a maximum Von Mises effort of 134.82 MPa Max and 6.203e-10 MPa Min was obtained for lumbar vertebra 4, 189.6 MPa Max and 2.0437e-9 for lumbar vertebra 5 and 101.2 MPa Max and 0 Min for porcine lumbar vertebra. Critical points are above 100 MPa for all three cases. The maximum values of effort in the vertebral body and the minimum in the spinous process were presented.

Lumbar, Compression fracture, Point cloud, Model acquisition, Von-Mises analysis

Resumen

Las fracturas por compresión en la región lumbar, por lo general, se producen por la presión excesiva a nivel del cuerpo vertebral. La fractura se produce cuando se aplasta el cuerpo vertebral, causando que la parte anterior del cuerpo vertebral adquiera forma de cuña. El tejido óseo en el interior del cuerpo vertebral es aplastado, o se comprime. Las fracturas por compresión debido a un traumatismo pueden deberse a una caída, un salto, un accidente de coche, o cualquier otro evento que produce un impacto en la columna vertebral más allá de su punto de ruptura [1]. En una simulación de la fractura en estudios recientes se aplican cargas a muestra vertebrales reales (pruebas destructivas), en donde ambas cargas a compresión se fijan en las caras superior e inferior del cuerpo vertebral. La literatura menciona ensayos con cargas de aproximadamente 8000N emulando un accidente cotidiano, por lo que esta investigación pretende obtener un modelo preciso con el empleo de un scanner óptico; el cual permitirá la obtención de puntos (mallado) de la pieza en tiempo real con una medición individual de hasta 16 millones de puntos de medición independientes capturados de 1 a 2 segundos. Los datos de medición se caracterizan por una reproducción muy detallada y por lo tanto también permiten la medición de componentes muestras de hasta de 38mm. El estudio inicia con la adquisición de modelos en yeso y aluminio de vertebras con similitudes geométricas:

- Muestra vertebral lumbar porcina
- Muestra vertebral lumbar humana 4.
- Muestra vertebral lumbar humana 5.

El escáner óptico ATOS&GOM® adquirió nubes de puntos de cada de una de las muestras mencionadas para el diseño de modelos con impresión 3D y la obtención de modelos digitales sólidos 3D, con la finalidad de realizar el análisis de esfuerzos de Von-Mises; como resultado del proceso de análisis de esfuerzos de Von-Mises, al aplicar cargas a compresión de 960 N y cortante de 8000 N distribuidas en cada vértebra lumbar.

El esfuerzo máximo de Von Mises obtenido fue de 134.82 MPa Max y 6.203e-10 MPa Min para la vértebra lumbar 4, 189.6 MPa Max y 2.0437e-9 para la vértebra lumbar 5 y 101.2 MPa Max y 0 Min para la vértebra lumbar porcina. Los puntos críticos son arriba de los 100 MPa para los tres casos. La simulación presenta los valores máximos de esfuerzo en el cuerpo vertebral y los mínimos en la apófisis espinosa.

Lumbar, Fractura por compresión, Nube de puntos, adquisición de modelos, Análisis de Von-Mises

1. Introduction

The present research work intends to make a mechanical characterization of the L4 and L5 lumbar vertebrae, by means of the use of the ATOS&GOM® optical scanner, since at present 3D models have not been worked with high resolution as the one provided by the mentioned scanner. The selection of the L4 and L5 lumbar vertebrae is due to the fact that the lumbar region is prone to suffer some type of injury, as shown in Figure 5.1, since this region is the one that supports the weight of all the body elements added to them.

Figure 5.1 Compression fracture

For a better understanding of the clinical problems of the spine and its function, the application of the mechanical theory is indispensable. In this sense, this work focuses on the lumbar region of the human being. The main objective of this research is to perform a Von-Mises stress analysis in ANSYS® Release 18.0 software on vertebral specimens, simulating the stress caused in a vertebral compression fracture.

2. Development

The methodology used to carry out this study can be described as follows:

Figure 5.2 Methodology for stress analysis in lumbar L4 and L5

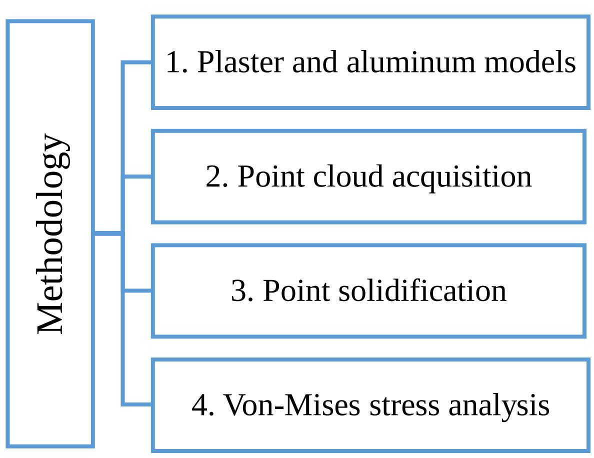

2.1 Plaster and aluminum models

The acquisition of the plaster and aluminum models was for the samples of human lumbar vertebrae 4 and 5. Initially, bipartite molds were obtained with the help of dental alginate, which is a gelling agent that allows obtaining impressions; two impressions were made in each vertebral sample, the first one on the upper faces and the second one on the lower faces. (Figure 5.3).

Figure 5.3 Bipartite mold

When the bipartite molds were obtained, Type IV high resistance dental plaster with a compressive strength of 510 kg/cm2 was poured into them to obtain the plaster models. With the help of a micromotor and a pink stone bur, special for polishing and conical cutting, the excess material generated during the casting was removed (Figure 5.4).

Figure 5.4 Plaster model of L4 vertebra

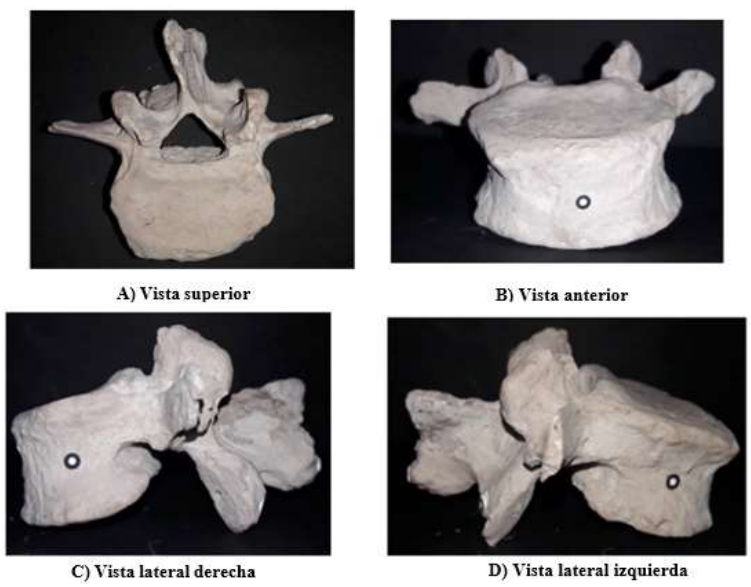

Taking advantage of the bipartite molds in alginate, kerosene wax was poured in them to obtain replicas of the vertebrae shown in Figure 5.5, which allowed acquiring new plaster molds, with the technique known as "lost wax", which were used to receive the molten aluminum. (Figure 5.5)

Figure 5.5 Wax replicas of the vertebrae.

Figure 5.6 Plaster model with the lost wax technique.

Subsequently, with the help of a smelting furnace, using LP gas and charcoal as fuel and adding a preheated air source, the furnace heating process was carried out, reaching temperatures over 660.3 °C, which allowed the aluminum to be melted. When the aluminum was in a liquid state, it was poured by gravity into the plaster molds; after cooling, and with a manipulable temperature, they were demolded, sacrificing the plaster models and removing the excess generated by the casting with the help of a bench grinder and the micromotor with a metal milling cutter (Figure 5.7).

Figure 5.7 Aluminum model of the L4 vertebrae

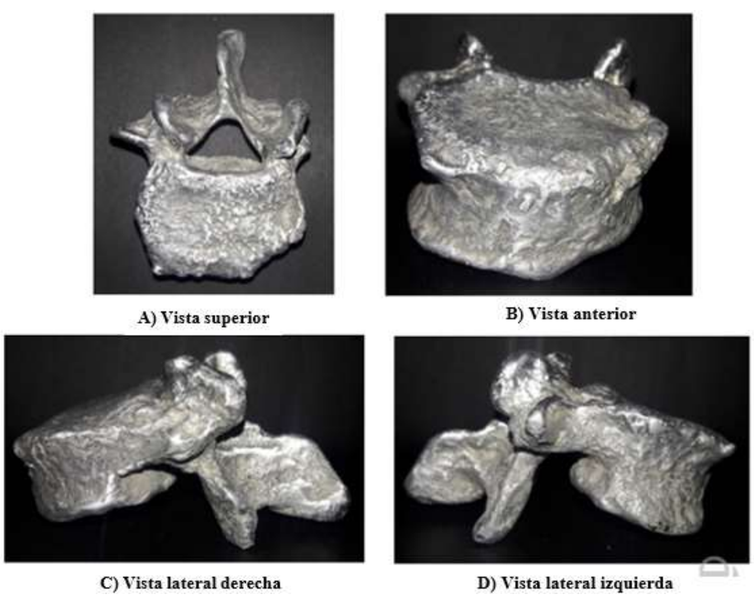

2.2 Point cloud acquisition

Comparing the plaster and aluminum models of the human lumbar vertebrae, it was decided to use the plaster models for scanning, since they were the ones that had the greatest similarity with the original samples. For the scanning process, it is required that the samples be of a white and opaque color, so that they can be detected by the ATOS&GOM® optical scanner. It was not possible to scan the original samples due to the characteristics they showed and it was not possible to apply any type of coating on them in order not to damage them, since they were on loan. Particularly the plaster models were detected by the optical scanner without the need to apply any coating.

On the other hand, to scan the porcine lumbar vertebra, since it was an own acquisition, it went through a dissection process and a coating of zinc oxide diluted in alcohol was applied with the help of an airbrush so that the optical scanner could detect the sample.

Once the samples to be used were defined and prepared, they were scanned, having an advanced calibration for the scanner, in order to have greater precision. Different shots of the samples were acquired: lateral and frontal, taking as reference the stickers previously placed on them; this allowed the scanner to have references, since for each of the samples scans were made to the top and bottom, with the mentioned points, allowing the software to join both scans to convert them into a single piece. (Figure 5.8)

Figure 5.8 Scanning process

As a result, the point clouds of the vertebral specimens were obtained in STL format, as shown in Table 5.1.

Table 5.1 Number of points in vertebral specimens

Sample	No. of points
Porcine lumbar vertebrae	372 498
Human lumbar vertebrae 4	531 324
Human lumbar vertebrae 5	399 298

2.3 Point cloud solidification

In order to carry out the numerical analysis, the lumbar vertebral samples in 3D must be solidified, so with the help of the CREO PARAMETRIC 5.0® software the point cloud in STL format was converted into a solid 3D drawing in SAT format.

The quality used for the solid drawings of the vertebral specimens required by the software can vary from Level 1 to 10; for the vertebral specimens it was Level 10, since this level is the highest in drawing definition, which helped the numerical analysis to be closer and more accurate to the geometries of the original specimens. (Figure 5.9)

Figure 5.9 Solidified human vertebral specimen

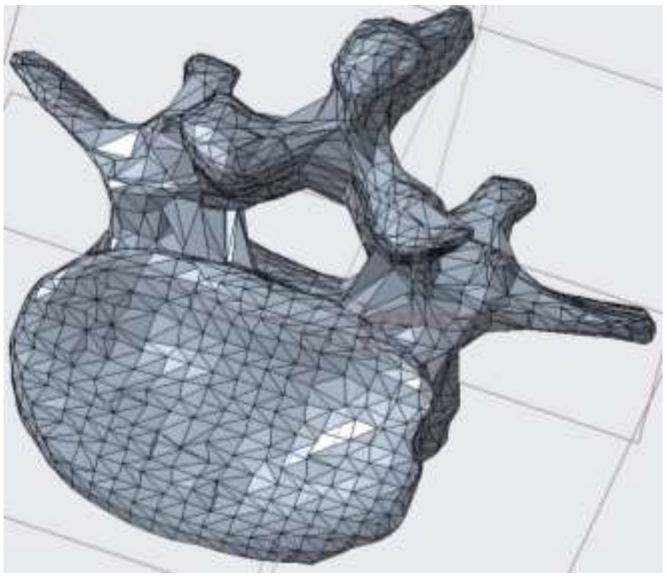

4.4 Von-Mises stress analysis

ANSYS® Workbench™ Release 18.0 software was used to perform the stress analysis, the solidified specimens were imported into CREO PARAMETRIC 5.0® to work on them. The following data were used to establish the properties of human and porcine lumbar bone.

Table 5.2 Material properties

Material	**Elastic modulus (mpa)**	**Poisson's coefficient**	**Apparent density (g/cm^3)**	**References**
Porcine lumbar bone	229	0.3	0.14 [3]	[2] J. Teo, 2006 [3] T. Keavy, 1997
Human lumbar bone	100	0.2	0.14 [3]	[4] J. Wang, 2000 [3] T. Keavy, 1997

To perform the meshing process of the vertebral samples, all the small faces that by default had the solid samples obtained from CREO PARAMETRIC 5.0® were converted by sections into the faces with the largest surface area, so that the software could detect them and perform the meshing. (Figure 5.10)

Figure 5.10 Sectioning of faces with larger surface area

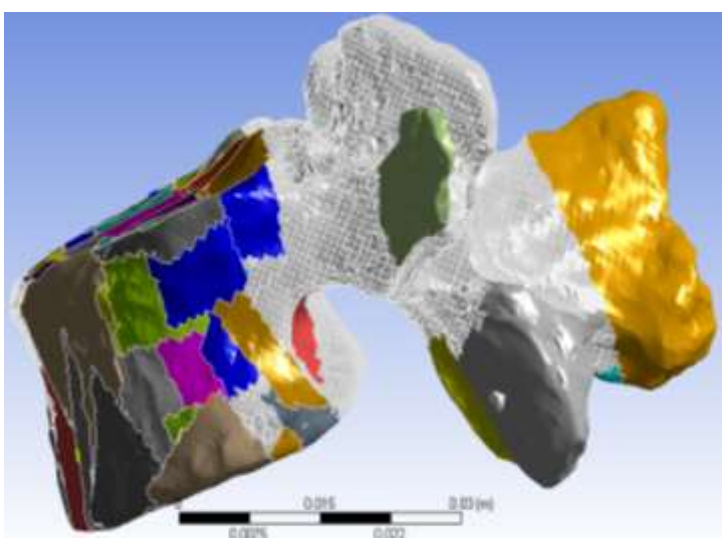

After finishing joining the faces, the parameters that were modified to perform a fine meshing were established, in order to match the geometries of the lumbar vertebrae for greater accuracy in the results. Tables 5.3 and 5.4 show only the parameters that were modified in the software, leaving the others by default for the human vertebral samples and the porcine sample.

Table 5.3 Meshing parameters for human vertebral samples

Human vertebral samples	
Defaults	
Relevance	100
Sizing	
Relevance center	Fine
Element size	5.e-004 m
Span angle center	Fine
Defeature size	5.e-004 m
Quality	
Target quality	5.e-004 m
Smoothing	High

Table 5.4 Meshing parameters for porcine vertebral specimen

Porcine vertebral specimen	
Defaults	
Relevance	50
Sizing	
Relevance center	Medium
Transition	Slow
Span angle center	Fine
Defeature size	5.e-004 m
Quality	
Smoothing	High

After finishing the meshing of the vertebral samples, the statistics in Table 5.5 were obtained. Figure 5.11 presents a meshed vertebral sample.

Table 5.5 Meshing statistics

Muestra	Nodes	Elements
Porcine lumbar vertebrae	260 796	176 696
Human lumbar vertebra 4	180 294	113 346
Human lumbar vertebra 5	175 373	109 781

Figure 5.11 Meshed vertebral specimen

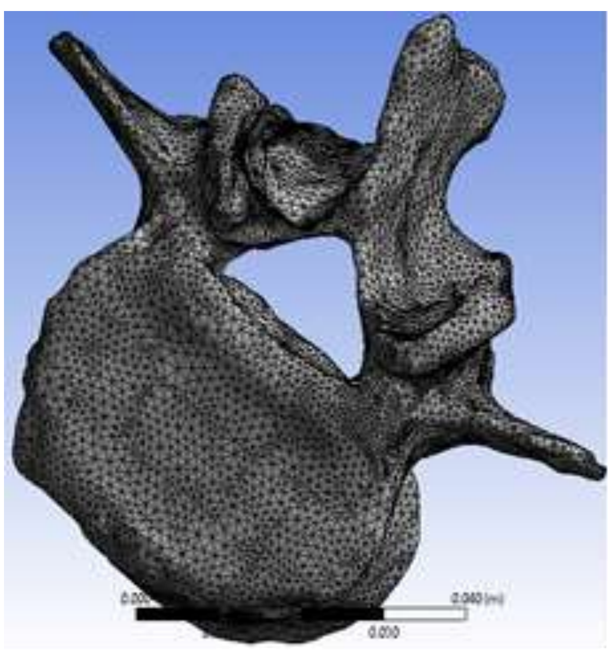

To simulate the compression fracture, the boundary conditions were established with the following data: three loads were applied to each vertebral specimen, two of them according to studies carried out by Nachemson in 1976 [5]; a subject who paradoxically when sitting (sedentary) without dorsal support increases the pressure to 140% of his body weight. For this case the subject has 70 kg, so a load of 960 N was used. In which both compression loads are fixed on the upper and lower faces of the vertebral body.

The third load was 8000 N, maximum load at which the lumbar bone fails, taken from the literature "Clinical Biomechanics of the Spine" of 1990 [6], considering that it can be produced by an accident in daily life. This shear load was fixed in the anterior area of the vertebral body.

Figure 5.12 shows in red the areas in which the three loads mentioned above were fixed and in purple the areas that supported these loads. [7]

Figure 5.12 Boundary conditions

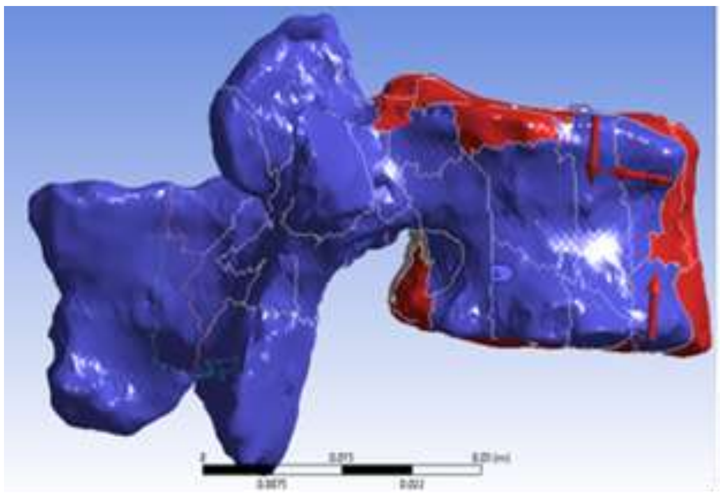

5 Results

The results obtained for the porcine vertebral specimen are the maximum and minimum values of stress concentration in the lateral zones, upper and lower faces and anterior zone of the vertebral body, as well as in the vertebral arch zone and in the upper notch. Particularly, the maximum stresses were found in the lateral zone and vertebral arch and the minimum stresses in the spinous process zone. (Figure 12)For the human vertebral specimens, the maximum and minimum values of stress concentration were found in the lateral zones, upper and lower faces and anterior zone of the vertebral body, as well as in the vertebral arch zone and in the upper notch. In particular, maximum stresses were found in the lower face and lateral zone and minimum stresses in the area of the spinous process. (Figures 5.13 and 5.14) The results also show the Von-Mises stress concentration values shown in Table 5.6.

Figure 5.13 Results in porcine lumbar vertebra

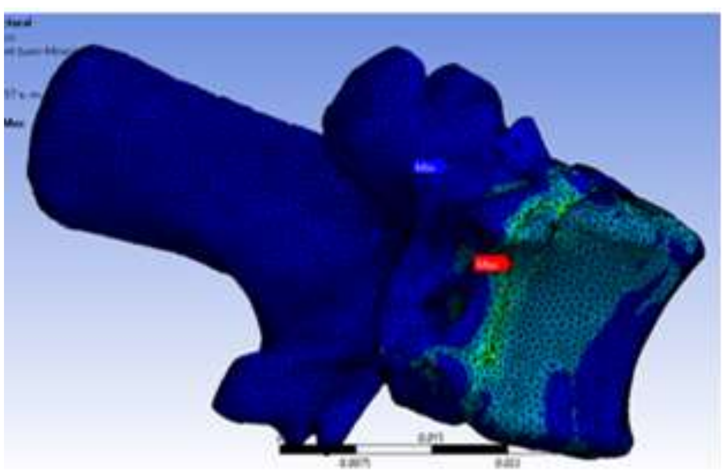

Figure 5.14 Results in human lumbar vertebra 4

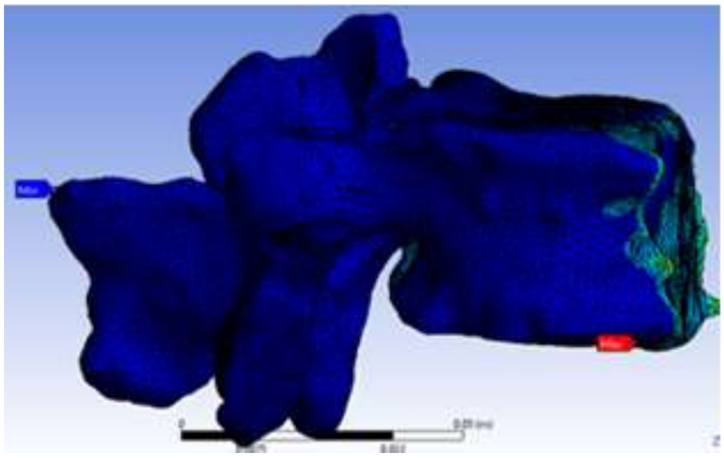

Figure 5.15 Results in human lumbar vertebra 5

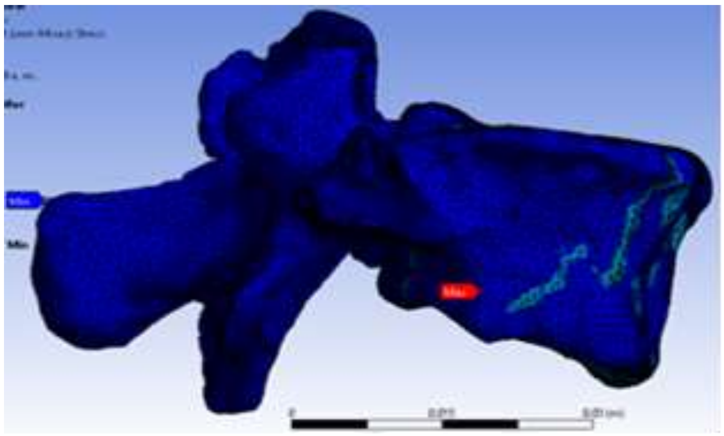

Table 5.6 Von-Mises stress analysis values

Muestra	Nodes	Elements
Porcine lumbar vertebrae	101.2	0
Human lumbar vertebra 4	134.82	6.203e-10
Human lumbar vertebra 5	189.6	2.0437e-9

It should be pointed out that in spite of the porcine lumbar vertebra being geometrically smaller compared to the human lumbar vertebrae, a lower value was obtained in the maximum stress and even remained at zero in the minimum stress.

6 Conclusions

In the simulation process, when applying compressive loads of 960 N and shear loads of 8000 N distributed in each lumbar vertebra, a maximum Von Mises stress of 134.82 MPa Max and 6.203e-10 MPa Min was obtained for lumbar vertebra 4, 189.6 MPa Max and 2.0437e-9 for lumbar vertebra 5 and 101.2 MPa Max and 0 Min for the porcine lumbar vertebra. The critical points are above 100 MPa for all three cases. The maximum values of stress in the vertebral body and the minimum values in the spinous process were presented.

In the present work it was possible to obtain a numerical model of the porcine lumbar and human lumbar spine L4 and L5. It is suggested to replicate different situations and mechanical conditions to the obtained models for future studies.

3D models of real porcine and human samples (L4 and L5) were obtained with a scanning accuracy of 16 million points in a 1-2 second capture. It is important to have a computer with the capacity to carry out the simulation process. In this case, a computer with an Intel Core i7 processor, 64 GB of internal memory and a storage capacity of 1 TB was used.

Acknowledgements

The authors would like to thank the Unidad ESIME Zacatenco of the Instituto Politécnico Nacional for their kindness and the Unidad de Ciencias de la Salud of the Universidad Veracruzana Campus Poza Rica - Tuxpan for their support.

7 References

[1] Vanaclocha, V. (2016). *Clínica Neuros*. Obtenido de Clínica Neuros: http://neuros.net/es/fractura-aplastamiento_vertebral/

[2] J. Teo, K. S.-H. (2006). "Reationship between CT intensity, micro-architecture and mechanical properties of porcine vertebral cancellous bone". En *Clinical Biomechanics* (Vol. 21, págs. 235-244).

[3] T. Keavy, T. p. (1997). "Systematic and random errors in compression testing of trabecular bone". En *Orthopaedic Research* (Vol. 15, págs. 101-110).

[4] J. Wang, M. P.-A. (2000). "Viscoelastic finite-element analysis of a lumbar motion segment in combined compression and sagital flexion". En *Spine* (Vol. 25, págs. 310-318).

[5] Nachemson A.L (1976). *The lumbar spine*. An orthopedic challenge. Spine.

[6] A. White III, M. Panjabi (1990). *Clinical Biomechanics of the Spine*. 2da Ed. Lippincott Williams & Wilkins. Philadelphia, USA. pp. 2-56.

[7] Blanco Ortiz, K. A. A. (2021). Propuesta de protocolo de ejercicios para fortalecimiento del CORE como medida preventiva en lesiones músculo esqueléticas del raquis lumbar en trabajadores que se encuentran en sedestación con edades comprendidas entre 25 y 30 años por medio de un análisis (Doctoral dissertation).

Chapter 6 Applied study of training projects as a learning strategy

Capítulo 6 Estudio aplicado de proyectos formativos como estrategia de aprendizaje

HERNÁNDEZ-CRUZ, Luz María †*, MEX-ALVAREZ, Diana Concepción, ORTIZ-CUEVAS, Nancy Georgina and CASTILLO-TÉLLEZ, Margarita

Universidad Autónoma de Campeche. Faculty of Engineering

ID 1st Author: *Luz María, Hernández-Cruz* / **ORC ID:** 0000-0002-0469-5298, **Researcher ID Thomson:** H-3153-2018, **CVU CONACYT ID:** 662220

ID 1st Co-author: *Diana Concepción, Mex-Álvarez* / **ORC ID:** 0000-0001-9419-7868, **Researcher ID Thomson:** I-4164-2018, **CVU CONACYT ID:** 842039

ID 2nd Co-author: *Nancy Georgina, Ortiz-Cuevas* / **ORC ID**: 0000-0003-4191-9630, **CVU CONACYT ID:** 964285

ID 3rd Co-author: *Margarita, Castillo-Téllez* / **ORC ID:** 0000-0001-9639-1736, **Researcher ID Thomson:** S-2283-2018, **CVU CONACYT ID:** 210428

DOI: 10.35429/H.2021.6.86.98

L. Hernández, D. Mex, N. Ortiz and M. Castillo

*lmhernan@uacam.mx

A. Marroquín, J. Olivares, M. Ramírez and L. Cruz (Coord) Engineering and Technology. Handbooks-©ECORFAN-México, Querétaro, 2021.

Abstract

This article analyzes the use of Training Projects as a learning strategy, a two-step methodology is carried out: the first corresponds to an applied research, in which the phases of the Training Project are implemented during the course of a learning unit (Software Project Management). The second, once the case study has been put into practice, a field investigation is applied, for the self-evaluation of the applied strategy. The data collection instrument is a survey designed with the Google Forms tool and shared via institutional email. The results of the study are promising, the use of Formative Projects in learning, they are fully aligned to the learning unit and the achievement of its competence was very satisfactory, showing that 96.1% of the students agree or fully agree that they successfully completed their projects and clearly identify the disciplinary competence achieved in the process. There is no doubt that this study opens the gap to design methodologies and/or action plans where Training Projects can contribute to the achievement of the skills of knowledge, know-how and know-how in the disciplinary field of any area.

Training projects, Competencies, Learning

Resumen

Este artículo analiza el uso de los Proyectos Formativos como una estrategia de aprendizaje; se lleva a cabo una metodología de dos pasos: el primero corresponde a una investigación aplicada, en la que las fases del Proyecto Formativo se implementan durante el transcurso de una unidad de aprendizaje (Proyecto de Software Gestión). En el segundo paso, una vez puesto en práctica el estudio de caso, se aplica una investigación de campo, para la autoevaluación de la estrategia propuesta. El instrumento de recolección de datos es una encuesta diseñada con la herramienta Google Forms y compartida a través de correo electrónico institucional. Los resultados del estudio son prometedores, el uso de Proyectos Formativos en el aprendizaje, están totalmente alineados a la unidad de aprendizaje y el logro de su competencia fue muy satisfactorio, mostrando que el 96,1% de los estudiantes están de acuerdo o totalmente de acuerdo en haber culminado con éxito sus proyectos e identificar claramente la competencia disciplinaria lograda en el proceso. No cabe duda, de que este estudio abre la brecha para diseñar metodologías y/o planes de acción donde los Proyectos Formativos puedan contribuir al logro de las competencias de conocimiento, saber y saber hacer en el ámbito disciplinar de cualquier área.

Proyectos formativos, Competencias, Aprendizaje

1 Introduction

A project is an operation of remarkable complexity, singular, with defined start and finish dates. It is a non-repetitive job that must be planned and executed according to predetermined technical specifications, with a preset budget and temporal organization, with the participation of various departments of a company later dismantled at the end of the project, and maybe the collaboration of third parties.

At some point of our academic education, we must work on certain projects, which contribute important lessons when we reach the labour market. Nevertheless, we must consider that for a project's management and execution to have a guarantee of success, it is important to know what a project is, as well as its peculiarities in both its approach and management.

Formative projects' goal is the realisation of certain activities that help to the resolution of a problem, during the course of the project, the competences determined in an educational program will be developed, in this type of project the final product is important because, based on it, the capability and the learning advances developed will be determined, as well as the realization of the acquired competences.

2 Project

Nowadays, "project" is one of the most daily used terms, everybody, either consciously or unconsciously, is involved in one. Neverthless, defining the concept of "project" is not easy at all, so it's best to understand its meaning. The word "project" comes from the latin "projectus" (projected), plant and disposition formed for the realisation of an agreement, or execution of something important.

“A project is a unique mission with clearly defined objectives and results, perfectly determined start and finish dates, and most of the times, a budget” (Biafore, 2018).

The Formative Projects

“A project is an operation of remarkable complexity, singular, with defined start and finish dates. It is a non-repetitive job that must be planned and executed according to predetermined technical specifications, with a preset budget and temporal organization, with the participation of various departments of a company later dismantled at the end of the project, and maybe the collaboration of third parties” (Aceves, 2018).

The term project refers to that activity conducted to give an answer to an idea, problem or non-identified opportunity, with a unique and concrete product or service.

According to the PMI (Project Management Institute) (PMI, 2020):

A project is a temporary entrepreneurship conducted to create a product or service. It is a process, with a defined duration and a concrete finish, composed of different tasks and activities, that can be elaborated gradually. Every project must be directed or managed by a project director. The projects direction would be the application of knowledge, skills, tools and techniques to the activities that make a project, with the goal of satisfying the requirements of the project. According to this Institute, the direction of projects is accomplished through the execution of processes, using knowledge, skills, tools and direction techniques.

A project is performing various articulated activities in order to solve a context problem. The problems can be needs, difficulties or improvement actions, creation and innovation of services, processes or products.

Figure 6.1 A project

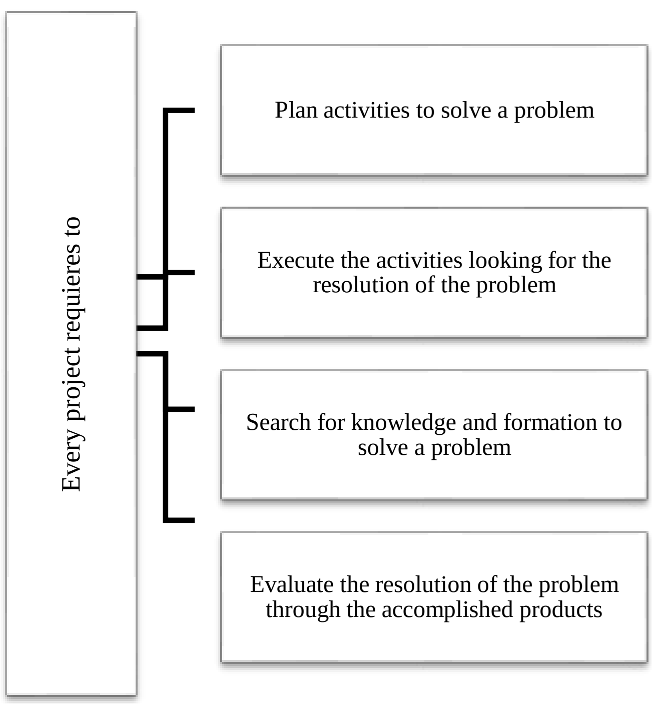

Source: (Tobón, 2014)

Formative Projects

In education, it’s been proposed that students form by making projects. This way, there would be a bigger impact in the formation of entrepreneurial people. The methodology of formative projects consists in the students performing articulated activities to solve contextual problems and that way they develop the competences of the profile of graduation of a particular educational program, being very important the need to demonstrate them with evidence (products).

Its essential characteristics according to Tobón (2013) are:

- Working in the context.
- Co-create knowledge.
- Know how to be, live, know, do.
- Solve context problems.
- Consider the ethical part.

Figure 6.2 A formative project

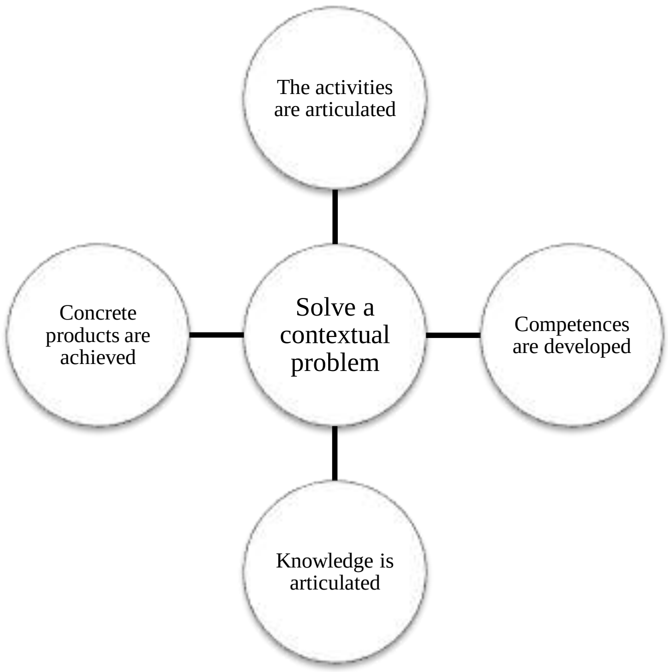

Source: (Tobón, 2014)

A formative project is structured through phases in which both professor and student participate. These phases are the scenarios where requiered learning activities are stablished for students to accomplish the defined competences. The phases of a formative project are: addressing, planning, execution and socialization (Tobón, 2010).

- Addressing is the phase in which it's defined between proffesors and students, the purpouse of the project, the expected competences and the evaluation process.
- In planning the students present to the instructor the project's activities to do, according to the defined purpouse in the addressing phase.
- In the execution phase the students execute the designed project with the instructor's mediation, looking for the programmed competences' achievement.
- Finally, in the socialization phase, the students present the formative project's results to the academic community. (Eva)

Formative projects have multiple benefits. The most important benefit is they make the development of competences possible in all its essence, articulating theory and practice in a meaningful context for the student, through activities that address diferent wisdoms (wisdom of being, wisdom of doing and wisdom of knowing). Also, it says that:

- It is learned how to apply the wisdoms in meaningful contexts
- The creativity and innovation is developed
- Benefits to the person, community and environmental setting are offered
- It is learned how to work in a colaborative manner

3. Methodology to develop

The methodology recognizes two main steps:

- Study and implementation of the strategy “Formative projects” in the learning unit “Software Development Project Management” from the Educational Program “Computer Systems Engineering” of the Engineering Faculty in the Autonomous University of Campeche (applied research).
- Self-evaluation from the students in regards of the results obtained in the development of the generic and professional competences in the learning unit “Management of Software Projects” (field research).

Figure 6.3 Study Methodology

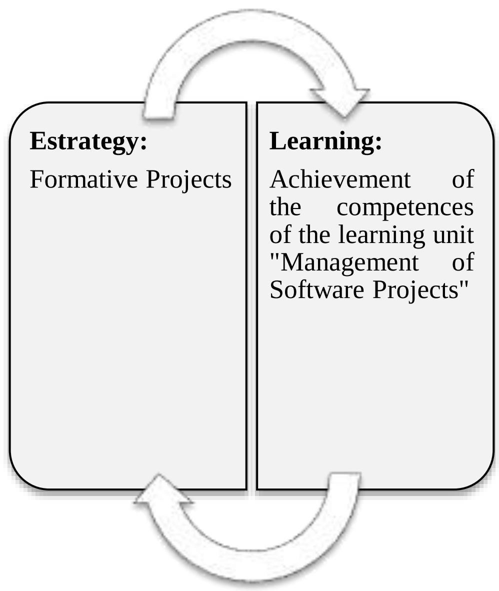

Source: Own Authorship

Study and implementation of the strategy “Formative Projects”

The context to conduct the investigation is the learning unit “Unidad de Aprendizaje” (UA) named “Management of Software Projects” taught in the eighth semester of the educational program Computer Systems Engineering in the Engineering Faculty of the Autonomous University of Campeche (Universidad Autónoma de Campeche), Campeche, Mexico. The UA of the nucleus: integrative, type: mandatory, area: applied engineering, credits: 4 and a total of 4 weekly hours (2 theorical and 2 practical) (Universidad Autónoma de Campeche).

The competence in the UA:

“To manage software projects for the development of custom computational systems, based on the standard PMBOK Guide”

A Guide to the Project Management Body of Knowledge (PMBOK® Guide) is PMI’s flagship publication and is a fundamental resource for effective project management in any industry. Over the years, business has changed considerably, but projects remain critical drivers of business success. The book includes The Standard for Project Management. The standard is the foundation upon which the vast body of knowledge builds, and the guide serves to capture and summarize that knowledge.

Over the past few years, emerging technology, new approaches and rapid market changes have changed the world of work, driving the profession to evolve. A Guide to the Project Management Body of Knowledge (PMBOK® Guide) – Seventh Edition has been updated to meet these challenges, better align to how people work today and help you be more proactive, innovative and nimble.
This edition of the PMBOK® Guide:

– Reflects the full range of development approaches (predictive, traditional, adaptive, agile, hybrid, etc.)
– Provides an entire section devoted to tailoring the development approach and processes
– Expands the list of tools and techniques in a new section, “Models, Methods, and Artifacts”
– Focuses on project outcomes in addition to deliverables
– Integrates with PMIstandards+™ for access to content that helps the user apply the PMBOK® Guide on the job

Including both The Standard for Project Management and the PMBOK® Guide, this modern edition presents 12 principles of project management and eight project performance domains critical for the effective delivery of project outcomes. The study poses the application of the Formative Projects as a learning strategy in the aforementioned UA, that allows to guarantee the accomplishment of its competence at the end of the course. Initially, the evidence for each one of the Formative Projects’ development phases are defined.

Table 6.1 Evaluation Process

Phase of Formative Proyect	Description	Evidence
Addressing	The instructor exhibits to the students the competences to accomplish, the formative project’s own characteristics and the methodology to follow for the development of the project.	Evidence 1: register/capture of the formative project’s approach
Planning	The students make the project’s certificate of incorporation, definition of the extent and the project plan based on the PMBOK Guide.	Evidence 2: documents of planning (project’s certificate of incorporation, definition of the extent and plan for the direction of the project)
Execution	The students develop the project according to the designed plan, following the thematic content of the UA and the PMBOK Guide. In this phase, an information system is created, fulfilling the specifications described in the previous phase.	Evidence 3: Software product (Information system) with flawless operable functionalities alined with the characterisctics and specifications described in the definition of its extent.
Socialization	The students display their formative project to the group	Evidence 4: Multimedia presenation and/or auxiliary material for the project’s final product (information system) presentation

Source: Own Authorship

Due to the characteristics of the PUA (Learning Unit Program), the weighing of the evaluation is far greater in the Second Term, because of the delivery and presentation of the finished Formative Project.

Table 6.2 Phases of the Formative Project and its percentage in the weighing of the UA

Phase	Evaluation Report	Weighing
Addressing	First term	30%
Planning	Second term	70%
Execution	Second term	
Socialization	Second term	

Source: Own Authorship

According to Formative Projects is very important to define the kind of evaluation to conduct and the tool used for it.

Table 6.3 Types of evaluation

Phase	Type of evaluation	Evaluation tool
Addressing	None	None
Planning	Heteroevaluation	Rubric
Execution	Heteroevaluation	Checklist
Socialization	Heteroevaluation/Self-evaluation	Rubric

Source: Own Authorship

Immediately, each phase of the Formative Project strategy is described for the raised case study.

Phase 1: Addressing

The experimentation with the students was conducted on the january-july 2021 school cycle. In the first session the instructor conducts the addressing phase. Students have one week to clarify doubts, and once work-teams are assembled, they capture in an *ad-hoc* Quiz the formative project to implement.

The addressing phase does not have a weighing in the student's evaluation process, so, there is no evaluation tool assigned. Evidence is not assessable, it's required. It is worth mentioning that the technological tool used in this study is Google Workspace (formerly G Suite). This way, the virtual learning platform of the UA is Classroom.

Google Classroom enables teachers to create an online classroom area in which they can manage all the documents that their students need. Documents are stored on Google Drive and can be edited in Drive's apps, such as Google Docs, Sheets, and so on. But what separates Google Classroom from the regular Google Drive experience is the teacher/student interface, which Google designed for the way teachers and students think and work. Google Classroom sits between you and Google Drive and provides a teacher/student-friendly way of managing classroom documents.

Here's what you can do with Google Classroom:

– Make assignments: The main thing you, as the teacher, will do with Google Classroom is making homework assignments for your students. When you create an assignment, you can upload the necessary documents for the students to read or work on. Students receive e-mail notification of new assignment. The students "turn in" the assignments when finished, and you can then grade the assignments.
– Make announcements: If you have a quick announcement for the entire class, you can quickly type in the announcement, which is e-mailed to all your students in the class.
– Store classroom materials: The materials you add to an assignment aren't the only documents you can store. You can store any other necessary documents for students on Google Drive.
– Allow students to interact: Students have the ability to comment on assignments and announcements, as well as e-mail each other through the Classroom interface.

Phase 2. Planning

The planning phase is directly related to the group of processes Management of Integration of the Project from the PMBOK Guide.

1. *Develop the project's certificate of incorporation:* Is the process of developing a document that formally authorizes the existence of the project and gives the director of the project the authority to apply the organization's resources to the project's activities. The key benefits of this process are that it provides a direct link between the project and the organization's strategic objectives, creates a formal register of the project and shows the organization's commitment to the project.
2. *Develop the plan for the addressing of the project:* Is the process of defining, preparing and coordinating all of the plan's components and consolidate them in an integrative plan for the addressing of the project.

The Project's Certificate of Incorporation is a document issued by the project's initiator or sponsor, who formally authorizes the existence of a project and gives the director of the project the authority to apply the organization's resources to the project's activities. It documents the high-level information about the project and product, service or result that the project pretends to satisfy, such as:

– The project's purpose
– The measurable objectives of the project and the associated success criteria
– The high-level requirements
– The high-level description of the project, the limits and the key deliverables
– The project's general risk

- The accomplishment schedule's summary
- The pre-approved finantial resources
- The key investors list
- The project approval requirements (what does the project consist of who decides if the project is successful and who signs the project's approval)
- The project's release criteria (what conditions must be accomplished in order to close or cancel the project of phase)
- The assigned project director, its responsibility and authority level
- The name and level of authority of the sponsor or whoever authorizes the project's certificate of incorporation.

At a high level, the project's certificate of incorporation secures a common understanding by the stakeholders of the key deliverables, the accomplishments, the roles and the responsibilities of everybody involved in the project (PMBOK, 2017). The project's certificate of incorporation was evaluated with a rubric. On its behalf, according to the PMBOK Guide, the plan for the direction of the project defines the way the project is executed, monitored, controlled and closed. The plan's content for the direction of the project varies in function of the area of application and the project's complexity. The plan for the project's direction can be presented either summarized or detailed. Each plan component is described to the level required for the specific project. The plan for the addressing of the project should be robust enough to respond to the project's always changing environment.

This agility can give place to more precise information as the project advances. The base lines of the plan should be defined for the project's addressing, meaning, it is necessary to define at least the project's reference in terms of extent, time and cost, that way the execution of the project can be measured and compared with those references and the performance can be managed. Before defining the base lines, the plan for the addressing of the project can be updated as many times as necessary. Any formal process of any kind is not required in that moment. Nevertheless, once the base lines have been defined, the plan for the addressing of the project can only be modified through the process "Realizar el Control Integrado de Cambios". Therefore, every time a change is requested, change forms will be generated and decided. This results in a plan for the addressing of the project that is progressively elaborated through controlled and approved updates that extent to the project's closure.

Phase 3. Execution

In this phase the next processes are considered (PMBOK, 2017):

1. *Monitor and control the project's work:* This is the process of following, revise and inform the general advance in order to accomplish the pre-stablished performance objectives in the addressing of the project.
2. *Make the Integrated Change Control:* It is the process of revising all the change requests, approve and manage the changes for deliverables, actives of the organization's processes, project documents and the plan for the addressing of the project, as well as communicating the choices.

Phase 4. Socialization

In addition to considering the end of the Formative Project, this phase wraps the final evaluation, meaning, the competences accomplishment for the learning unit. The only process in this phase, according to the PMBOK Guide is:

1. *Close the project or phase:* Is the process of finishing all the activities for the project, phase or contract.

4 Results

The results of the investigation were oriented towards:

- Analyzing the results of the self-evaluation of the students according to the accomplishment of the learning unit's competences.

By the nature of its objectives, the research was both field and applied, due to the use of theoretical fundamentals in order to know the nature of formative projects, the students being the source of data used for the development of disciplinary academic competences. The design of the research is exploratory descriptive, using qualitative methods for measuring frequencies, elements and categories. The universe is the eighth semester students studying the learning unit “Software Projects Management” (Facultad de Ingeniería, UAC) with a total of 38 students.

The investigation was conducted in an environment controlled by the researchers, in which a standardized survey was made using the Likert Scale from 1 to 5 (Strongly agree, Agree, neither agree or disagree, Disagree and Strongly disagree) for their answers. The instrument items’ validity was made with the technique “Juicio de expertos” (Expert judgement), considering 4 university instructors, experts in the knowledge area of software engineering, particularly in Project Management and Systems Development. The instructor evaluates under two criteria: form and content. Table 6.4 shows the criteria defined with the Delphi Technique by the group of experts to evaluate the form and content criteria.

Table 6.4 Validity of the tool’s content

Form	Content
Clarity	Coherence
Relevance	Purpose
Scale	Relevance
Orthography	Identify the variables
Presentation	Leads to the design of the methodology
Extent	Relevance of the information
Size and fond	Correlation
Order	Redundancy

Source: Own Authorship

The student participation in the experiment was requested in a voluntary manner and through informed consent. It was emphasized that the registered information and the data analysis would only be used for means of investigative nature, respecting the confidential nature of personal data, in lined with the Federal Law of Personal Data Protection in Possession of Private Individuals, or Law of Data Protection. The research was conducted with 26 students that answered the survey in the respective reception time. The sex distribution is 80.8% women and 19.2% men. A 92.3% of the students are between 20 and 25 years old. The 57.7% of the students Agree and 30.8% Strongly Agree that the addressing phase let known the competences to accomplish through the Formative Project. As well as the criteria, types, moments and tools of evaluation. Letting it be clear that first phase of the Formative Projects strategy has had an acceptable result in the self-evaluation from the students.

Graphic 6.1 Surveyed by gender

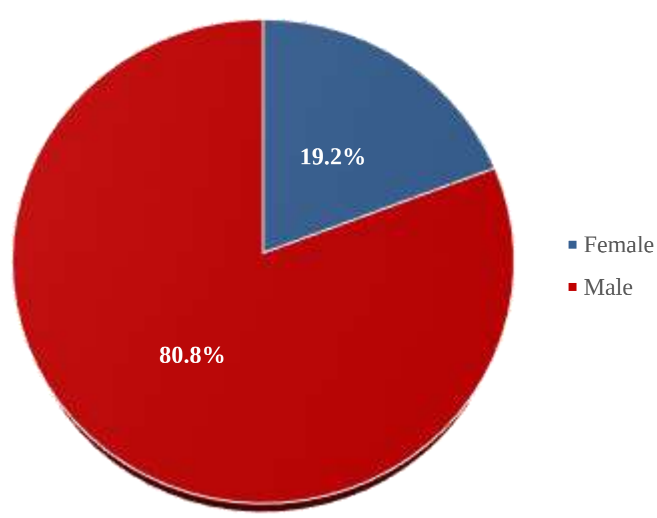

Source: Own Authorship

Graphic 6.2 Surveyed by age

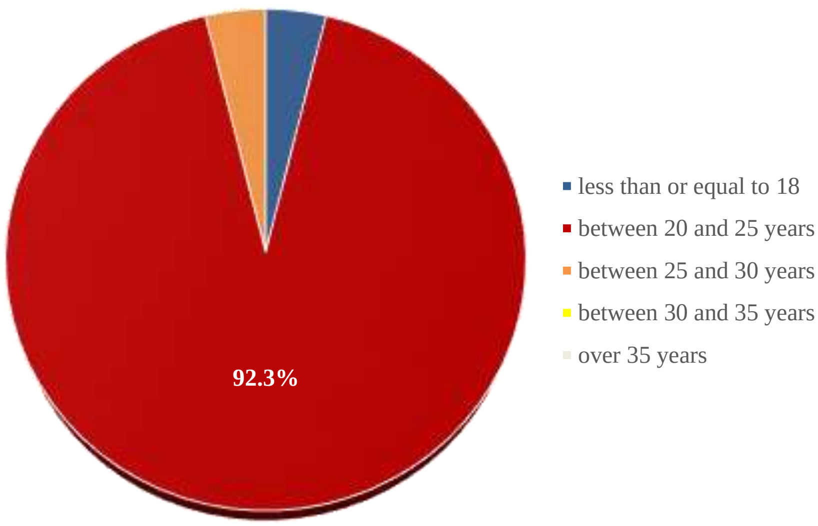

Source: Own Authorship

Despite the fact the survey was applied to students studying a learning unit correspondent to the eighth semester, with the flexibility of the educational model plus the freedom of academic load students' possess, not all of the surveyed study the last semester of the educational program. The results show that only 57.5% of the students are studying the eighth semester.

Graphic 6.3 Semester in attendance

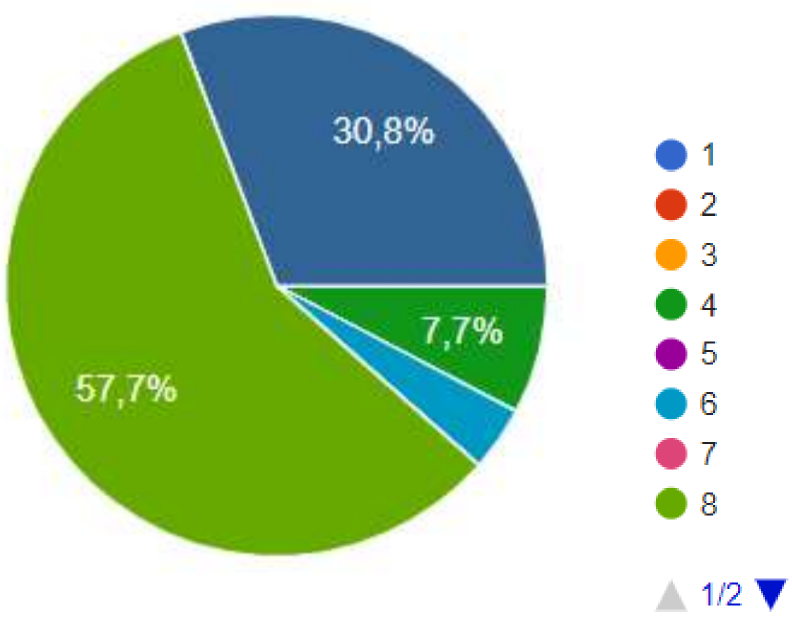

Source: Own Authorship

In the phase of addressing, it has an acceptable result, considering a 57.7% of answers were "Agree", adding a 30.8% "Strongly agree". This phase defines an 88.5% of good understanding of the learning strategy (Formative Project) from the students. Graphic 6.4 displays the results accomplished for the addressing phase.

Graphic 6.4 The addressing phase makes known the competences to accomplish through the Formative Project. As well as the criteria, types, moments and tools of evaluation

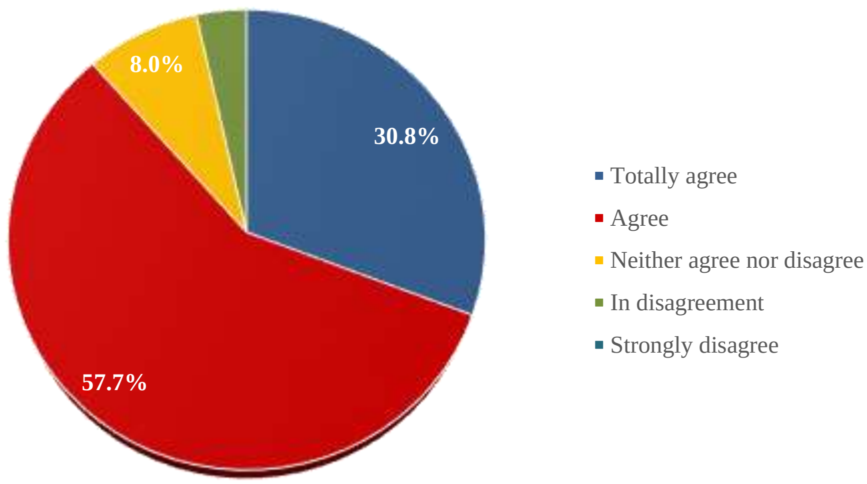

Source: Own Authorship

The planning phase obtained a 65.4% of answers on "Agree" and a 19.2% on "Strongly Agree", that way adding to a total 84.6% of positive answers to the phase. It is to be noted that the additional 15.4% answered "Neither agree nor disagree", opening to the possibility of increasing the percentage of positive appreciation. Graphic 6.5 shows the results of the planning phase.

Graphic 6.5 The planning phase allows to properly specify the requirements of the formative project.

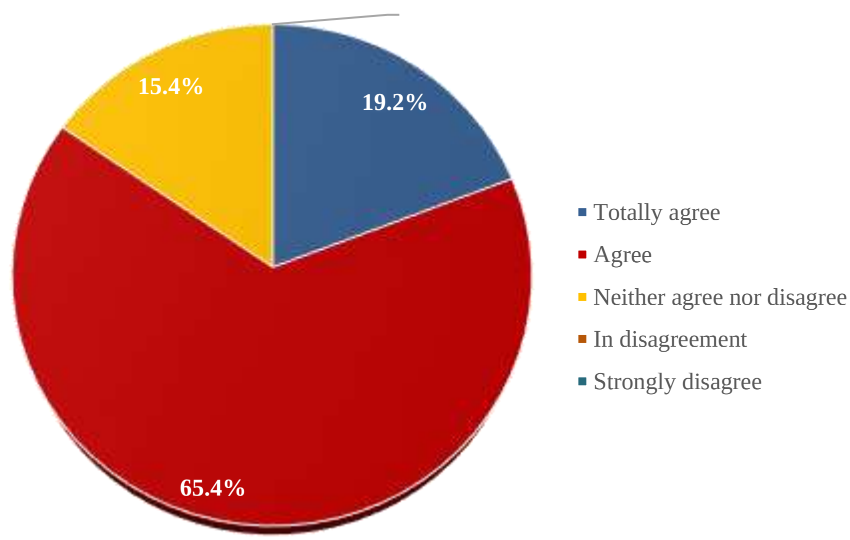

Source: Own authorship

The execution phase concerns to the development of the Formative Project including the following and control phases. The document specifically designed for that matter is the Project Plan, and the software tool of specific use is Microsoft Project 2019. The students' opinion in the self-evaluation shows that 65.4% "agree" with the obtained results managed with the so-called tool, and the other 26.9% percent "strongly agree". This adds to a total of 92.3% of surveyed in accordance with this questioning. Graphic 6.6 shows the results of the Execution phases.

Graphic 6.6 The execution phase concerns to the development of the Formative Project including the following and control phases, whose base tool is the Project Plan, allowing to the accomplishment of the objectives

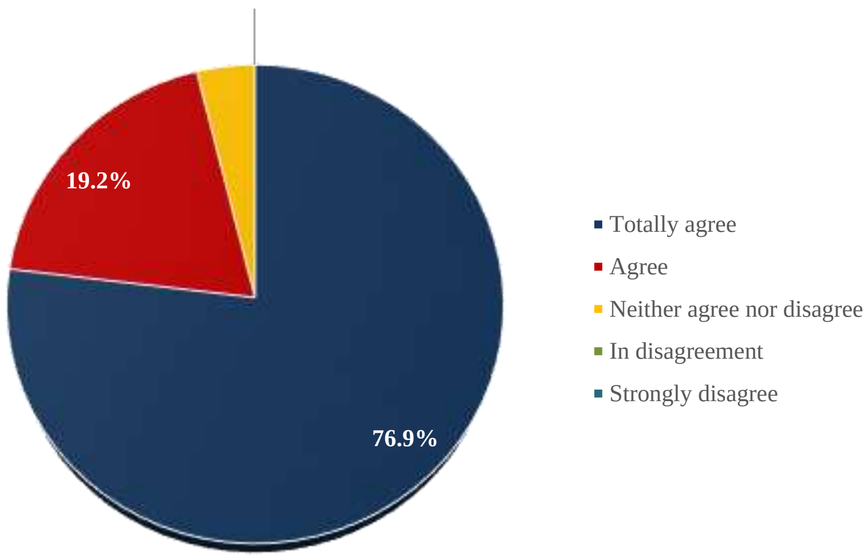

Source: Own Authorship

At last, in the closure phase the formative project finalizes with the presentation of the product (Information System), and the rating accomplished shows the goal of the competence of the learning unit. Graphic 6.7 shows the results obtained from the self-evaluation made by the students. Obtaining a 76.9% of "Strongly agree" answers and a 19.2% "agree" answers. Having a total of 96.1% of survey respondents that successfully finished their Formative Projects and are capable of distinguishing the competences they developed in the learning unit.

Graphic 6.7 The closure phase concludes with the presentation of the promised results complying with all the stablished requirements, and at the same time, showing the accomplishment of the competence of the learning unit

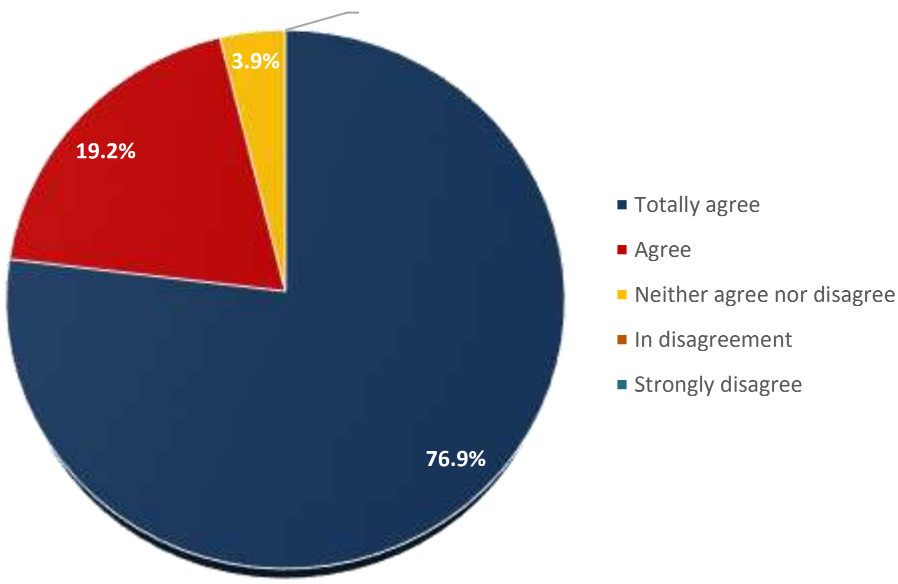

Source: Own Authorship

Acknowledgements

Broad gratitude is extended to Prof. José Román Ruiz Carrillo, rector of the Unanimous University of Campeche for the disposition and support given for the publication of this article. Likewise, the recognition to the MAC Francisco Javier Barrera Lao, director of the Faculty of Engineering and to the Prof. Nancy Georgina Ortiz Cuevas, coordinator of the Engineering in Computer Systems Educational Program for the empathy to boost the research studies in the Computer Sciences' area.

Conclusions

The Formative Projects are a didactic method for the purpose of students to learn, construct and develop the competences of the expected profile, for the case study, to reach the competence of the learning unit. It is important not only to define the project, but to have an organized teaching-learning process composed of a group of pedagogical and communication methodologies, content management and use of tools of Technologies of Information and Communication (TICS).

About the process, it is recommended to take more emphasis to the evaluation process, defining criteria, types and tools that allow to correctly prove the knowledge and skills that students develop during the whole Formative Project process.

Certainly, the four phases of the Formative Project (addressing, planning, execution and socialization) are crucial and indispensable to successfully achieve the development of thereof. On its behalf, each learning unit from each Educational Program must initially have to make an analysis of correspondence to accurately frame the phases and be able to successfully implement the Formative Projects strategy.

Finally, the importance of the Formative Projects as a significant learning strategy, in addition to the accomplishment of the general and disciplinary competences. Another crucial factor is the collaborative work, and of course, the experience.

References

(s.f.). Obtenido de Evaluacion_de_competencias_con_apoyo_de_un_sistema.pdf

Aceves, P. (2018). *Administracion de Proyectos. Enfoque por Competencias.* México: Grupo Editorial.

Biafore, B. y. (2018). *Gestión de Proyectos en el Mundo Real.* Anaya Multimedia.

Española, R. A. (2018). *Real Acedemia Española.* Real Academia Española.

Ollé, C. y. (2018). *Gestión de Proyectos Paso a Paso.* Barcelona: UOC.

Patria. (s.f.). S.A de C.v.

PMBOK. (2017). *PMBOK.* PMI.

PMI. (2020).

Tobón, S. (2014). *Proyectos Formativos: Teoría y Metodología*. Obtenido de Person Educación: https://elibro.net/es/ereader/uacam/37979?page=26

Universidad Autónoma de Campeche. (enero de 2021). *Facultad de Ingeniería*. Obtenido de https://fi.uacam.mx/view/paginas/82

Chapter 7 Remediation of soils contaminated by hydrocarbons using a polymeric material (carboxymethylcellulose gel)

Capítulo 7 Remediación de suelos contaminados por hidrocarburos mediante un material polimérico (gel de carboximetilcelulosa)

ANTONIO-CRUZ, Rocío†*, PURATA-PÉREZ, Nora Alicia, VÁZQUEZ-GONZÁLEZ, María Berzabé and TREJO-VALENCIA, Radamés

Tecnológico Nacional de México campus Villahermosa, Chemical, Biochemical and Environmental Engineering Department. Carr. Villahermosa-Frontera km 3.5 Cd Industrial, Villahermosa, Tabasco, México. C.P. 86010.
Tecnológico Nacional de México campus Minatitlán, Department of Chemical and Environmental Engineering. Blvd. Institutos Tecnológicos S/N Col. Buena Vista Norte, Minatitlán, Veracruz, México. C.P. 96848

ID 1st Author: *Rocío, Antonio-Cruz* / **ORC ID**: 0000-0003-3638-5152, **CVU CONACYT**: 25705

ID 1st Co-author: *Nora Alicia, Purata-Pérez* / **ORC ID**: 0000-0002-6823-6912, **CVU CONACYT ID**: 328771

ID 2nd Co-author: *María Berzabé, Vázquez-González* / **ORC ID**: 0000-003-2814-8819, **CVU CONACYT ID**: 774648

ID 3rd Co-author: *Radamés, Trejo-Valencia* / **ORC ID**: 0000-0002-3046-4872, **CVU CONACYT ID**: 721964

DOI: 10.35429/H.2021.6.99.111

R. Antonio, N. Purata, M. Vázquez and R. Trejo

*rocio.antonio.cruz@gmail.com

A. Marroquín, J. Olivares, M. Ramírez and L. Cruz (Coord) Engineering and Technology. Handbooks-©ECORFAN-México, Querétaro, 2021.

Abstract

In recent years, the pollution caused by hydrocarbon spills has increased, and this leads to research to mitigate the deterioration caused to the environment, therefore, this work has the purpose of remedying a contaminated soil due to the explosion of the Well Terra 123 of Mexican Oil (PEMEX) occurred in October 2013, which left in its wake contamination, death of animals and diseases in the population, causing both environmental and health effects on the inhabitants of the region such as vitiligo, problems vision, throat, cough and flu (Reporte Indigo, 2019). The studies carried out by Duran in 2015 on "Environmental impact on the indigenous communities of Nacajuca, Tabasco, due to the explosion of the Well Terra 123", gathered evidence of the impact that this oil accident had on the health of those close to it to the facilities and the environment. This chapter will deal with the remediation of soil contaminated by hydrocarbons due to the explosion of the Terra 123 Well, using a polymeric material (carboxymethylcellulose gel), which was synthesized at the laboratory level using carboxymethylcellulose (CMC), glutaraldehyde (GA) as agent of crosslinking and hydrochloric acid (HCl) as a catalyst for synthesis. The CMC gel was incorporated into the contaminated soil for the absorption of the hydrocarbon for a period of three months. The samples were collected from the soil contaminated with hydrocarbon from Terra 123 well, located in Oxiacaque, Nacajuca, Tabasco, and the effectiveness was studied in two stages: (1) The soil particle was decreased by sieving and (2) Pre and post soil analyzes were carried out (moisture percentage and fat content). In addition, the CMC gels were analyzed using infrared spectroscopy (FTIR) and scanning electron microscopy (SEM) techniques before and after being incorporated into the contaminated soil. The amount of hydrocarbon initially contained in the soil was made using the Soxhlet method, obtaining 0.99 mg of hydrocarbon / kg of soil.

Remediation, Gel, Carboxymethylcellulose, Hydrocarbons, Polymers

Resumen

En los últimos años se ha incrementado la contaminación provocado por derrames de hidrocarburos, y esto conlleva a realizar investigaciones que permitan mitigar el deterioro provocado al medio ambiente, por lo tanto, este trabajo tiene la finalidad de remediar un suelo contaminado debido a la explosión del Pozo Terra 123 de Petróleos Mexicanos (PEMEX) ocurrido en el mes de octubre del año 2013, lo cual dejó a su paso contaminación, muerte de animales y enfermedades en la población, provocando afectaciones tanto ambientales como de salud en los pobladores de la región como vitíligo, problemas de visión, de garganta, tos y gripa (Reporte Indigo, 2019). Los estudios realizados por Duran en el 2015 de "Impacto ambiental en las comunidades indígenas de Nacajuca, Tabasco, a causa de la explosión del Pozo Terra 123", acudieron a recoger evidencias del impacto que tuvo este accidente petrolero en la salud de las personas cercanas a las instalaciones y en el medio ambiente. El presente capítulo tratará sobre la remediación del suelo contaminado por hidrocarburos debido a la explosión del Pozo Terra 123, empleando un material polimérico (gel de carboximetilcelulosa), el cual se sintetizó a nivel laboratorio utilizando carboximetilcelulosa (CMC), glutaraldehído (GA) como agente de entrecruzamiento y ácido clorhídrico (HCl) como catalizador de la síntesis. El gel de CMC se incorporó al suelo contaminado para la absorción del hidrocarburo por un periodo de tres meses. Las muestras fueron recolectadas del suelo contaminado con hidrocarburo proveniente del pozo Terra 123, ubicado en el ejido Oxiacaque, municipio de Nacajuca, Tabasco y, se estudió la efectividad en dos etapas: (1) Se disminuyó la partícula de suelo mediante tamizado y (2) Se realizaron análisis previos y posteriores al suelo (porcentaje de humedad y contenido de grasa). Además, los geles de CMC se analizaron mediante las técnicas de espectroscopia de infrarrojo (FTIR) y microscopia electrónica de barrido (SEM) antes y después de ser incorporados al suelo contaminado. La cantidad de hidrocarburo que contenía inicialmente el suelo se realizó mediante el método Soxhlet, obteniendo 0.99 mg de hidrocarburo/kg de suelo.

Remediación, Gel, Carboximetilcelulosa, Hidrocarburos, Polímeros

1 Introduction

The petrochemical industry in Mexico has developed rapidly, generating diverse economic benefits. However, its expansion and development has also given rise to serious environmental problems, resulting in environmental emergencies, with serious repercussions on the health of the population and the ecological balance of ecosystems (Quadri 1994).

Among the causes that have generated this environmental deterioration due to the contamination of water bodies and soils throughout the country are the following: (i) improper handling and abandonment of hazardous materials and waste; (ii) inadequate maintenance or lack thereof in oil facilities; (iii) explosions in high-risk facilities; (iv) leaks in pipelines; and (v) hydrocarbon spills (CENAPRED 2001, PROFEPA 2002).

In PEMEX's final inventory of hazardous waste, with a total of 19.6 thousand tons at the end of 2020 (SISPA, 2021), the inventory increased 16% over 2019. During 2020, 56 thousand tons were generated and 53.2 thousand tons were disposed of, resulting in a disposal to generation ratio of 0.95. Pemex Transformación Industrial's activities account for 76% of the hazardous waste inventory, where 45% corresponds to oily sludge, 14% to solid waste impregnated with hydrocarbons, 13% to spent soda and the rest to others (laboratory, sewage treatment sludge, etc.).

On the other hand, the total number of leaks and spills in Pemex in 2020 was 931 events (not including those due to clandestine outlets), with respect to 2019, showing a 15% decrease, mainly due to a reduction in the number of events presented in Pemex Logística and Pemex Exploración y Producción (PEP). Of these events, 77% correspond to PEP, 13% to Pemex Logística, 8% to Pemex TRI (Transformación Industrial) and 2% to PMI (Comercio Internacional, S.A. de C.V.).

Among the most serious environmental disasters that threaten biodiversity are oil spills, and it is estimated that 3,800 million liters enter the oceans each year as a result of human activities. Of these, only 8 percent are due to natural sources; at least 22 percent to intentional operational discharges from ships, 12 percent to spills from ships, and another 36 percent to sewage discharges (Suchanek, 1993).

In a biodiversity report in 2006, it published that in 2002, Mexico spilled 160 barrels of hydrocarbons, thus increasing the area of contaminated soil. On the other hand, the Procuraduría de Protección al Ambiente (PROFEPA, 2016), published that, in the state of Tabasco, only in the last 11 years, a total of 385 oil spills have been registered.

Garcia *et al*. in 2010, conducted a study on the removal of polycyclic aromatic hydrocarbons (PAH) and total petroleum hydrocarbons (TPH) in a soil contaminated with crude oil, using two types of agro-industrial residues, cachaza and sugarcane bagasse as amendments and texturizers, where cachaza was highly effective for the removal of PAH and TPH hydrocarbons, obtaining similar results with sugarcane bagasse. On the other hand, the cachaza, besides obtaining good results in the repair, has as an additional advantage the contribution of microorganisms to the soil, which have the capacity to bio-transform the toxics and provide nutrients in higher concentration.

At the Instituto Tecnológico de Durango in 2011, the evaluation of the aerobic bioremediation process of a soil contaminated with petroleum hydrocarbons using residual sludge (biosolids) from a domestic wastewater treatment plant (WWTP) as an alternative source of macro and micronutrients was carried out, which resulted in the conclusion that sewage sludge is a viable alternative for the removal of petroleum hydrocarbons, in addition to being an alternative source of nutrients, also mentioning that the mineralization or maturity of the sludge influenced the rate of hydrocarbon removal (Martínez *et al*. 2011).

Ordaz *et al*. in 2011 conducted bioremediation tests at the microcosm level on a clay soil contaminated with crude oil, with different concentrations of total petroleum hydrocarbons (TPH) and used sugarcane bagasse as a texturizer and amendment, being sugarcane bagasse a profitable alternative for the development of microcosms, in addition to being effective in the removal of TPH.

By obtaining favorable results with these types of techniques, in Peru in 2013, the Soil Fertility Laboratory of the National Agrarian University La Molina, conducted a bioassay experiment where manure and sawdust were used, having as substrate the "corn" indicator plant (*Zea mays L.*), for the elimination of total petroleum hydrocarbons, obtaining as a result that the greatest reduction in the concentration of petroleum hydrocarbons was obtained with the use of manure; however, with the use of sawdust there is also a reduction in the concentration, but in smaller quantities (Buendía, 2013).

On the other hand, the Institute of Biotechnology and Applied Ecology of the University of Veracruz, conducted a research, in which they used endogeous earthworms (*Pontoscolex corethururs*) for the removal of the polyaromatic hydrocarbon Benzo(a)Pyrene, affirming that the endogeous species *P. corethururs* can be used in the remediation of soils contaminated with polyaromatic hydrocarbons in tropical areas (Hernández, 2013).

Quijano in 2015 conducted a study to evaluate the degradation of total petroleum hydrocarbons (TPH) in contaminated soil under nursery conditions. In which two tree species Swietenia macrophylla (mahogany) and Tabebuia rosea (macuilis) were planted in combination with bat guano vermi-compost, and cachaza and sheep manure composts in different doses, being the species S. macrophylla and T. rosea, those that improve the chemical parameters of the soil, helping to restore the contaminated soil.

Hydrocarbons are the most demanded petroleum products in the world, as they are the main energy generators for human beings and constitute the essential elements of petroleum; their molecules contain only carbon and hydrogen and are divided into several chemical families according to their structure. All these structures are based on the tetravalency of carbon (Wauquier, 2004).

Garcia *et al*. in 2010 studied the removal efficiency of polycyclic aromatic hydrocarbons (PAH) and total petroleum hydrocarbons (TPH) from a soil contaminated with crude oil, using two types of agroindustrial wastes, cachaza and sugarcane bagasse as amendments and texturizer. They conducted tests in solid culture microcosms for the bioremediation of a soil contaminated with 14,300 mg/kg of TPH and 23.14 mg/kg of PAH. The soil:residue ratios used in the tests were as follows (%): 100:0, 98:2, 96:4 and 94:6, and the addition of macro-nutrients based on a carbon/nitrogen/phosphorus ratio of 100:10:1. TPH removal was 60.1 % for bagasse and 51.4 % for cachaza. The cachaza turns out to be an alternative for bioremediation processes of soils contaminated with hydrocarbons.

Buendía in 2012 conducted a study in which he used manure and sawdust as substrate for the indicator plant "corn" (*Zea mays L.*), planted and controlled for a period of two months. Taking as a reference sample 36 pots in which 12 treatments were evaluated with three replicates each, obtaining as results an average decrease of 22.5% of the hydrocarbon content in the soil, using only manure decreased 16.5% and using only sawdust decreased 9.6%.

Arrieta *et al*. conducted a study in 2010 in which they isolated and characterized biochemically and molecularly a bacterial consortium capable of degrading the different hydrocarbons present in diesel, made up of the following genera: Enterobacter sp, Bacillus sp, Staphylococcus aureus, Sanguibacter soli, Arthrobacter sp, and Flavobacterium sp, using soil contaminated with diesel at laboratory scale, using two bioremediation technologies: natural attenuation and biostimulation. They defined as a control parameter the concentration of total hydrocarbons (TPH), concluding with a reduction in concentration over a period of 4 months of 36.86% for natural attenuation and 50.99% for biostimulation.

Anza *et al*, in 2016 conducted a research where they used biopiles as a method of bioremediation of soil contaminated with used oils from automotive service workshops, using four soil samples and analyzed moisture, organic matter, texture, pH, temperature, total nitrogen and phosphorus, they built four biopiles, developing three treatments with three replicates and a control, and were contaminated in concentrations for control 30,000 ppm, first treatment 10,000 ppm, second 30,000 ppm and third 50,000 ppm of total petroleum hydrocarbons (TPH). The strains used were: Acinetobacter Sp, Sphingobacterium Sp and Stenotrophomona Sp and they concluded that the treatment obtained high percentages of removal of the aliphatic fractions from 93.7 to 87.1% in 90 days.

Martinez *et al*., in 2011, conducted a study in which they evaluated the aerobic bioremediation process of a soil contaminated with petroleum hydrocarbons using residual sludge (biosolids) from a domestic wastewater treatment plant (WWTP) as an alternative source of macro and micronutrients. The results showed that the residual sludge stimulated the stimulation of native soil microorganisms, which in turn were responsible for degrading the hydrocarbons. The soil subjected to aerobic remediation reached the maximum permissible limit (MPL) established in current Mexican regulations (NOM-138-SEMARNAT/SS-2003).

Cartaya *et al*. in 2011 conducted trials to study the uptake and distribution of heavy metals (Cu) in tomato seedlings treated with natural polymers (oligo¬galacturonides, Ogal) grown in a medium with toxic levels of copper. They analyzed the assimilable metals in the soil in order to determine the residual effect and mobility of these elements and concluded that the use of the oligogalacturonide mixture counteracts the effect of heavy metal toxicity and produced changes in the pattern of metal accumulation in plants treated with natural polymers, even though the low mobility and bioavailability of heavy metals are mainly due to soil characteristics. Manzano *et al*. in 2011, analyzed the use of cattle manure in the decontamination of diesel contaminated soil (1.4% by weight). Applying an ex-situ methodology of diesel contaminated soils and the characterization of hydrocarbon contamination, and the diesel fraction in particular can determine the doses of manure and wastewater to be contributed initially. The decontamination behavior of a diesel contaminated soil using biopiles with the addition of cattle manure can be modeled using a logistic curve type, and thus it is estimated that at 183 days 99.8% of diesel was removed from the soil.

Carboxymethyl cellulose (CMC)

Figure 7.1 shows the structure of carboxymethylcellulose (CMC), an organic compound derived from cellulose, consisting of carboxymethyl groups linked to some hydroxyl groups, which is present in the polymer. CMC is similar to cellulose, but unlike cellulose, it is soluble in water and appears as a white or almost white granular powder, hygroscopic after drying.

Figure 7.1 Structure of carboxymethylcellulose

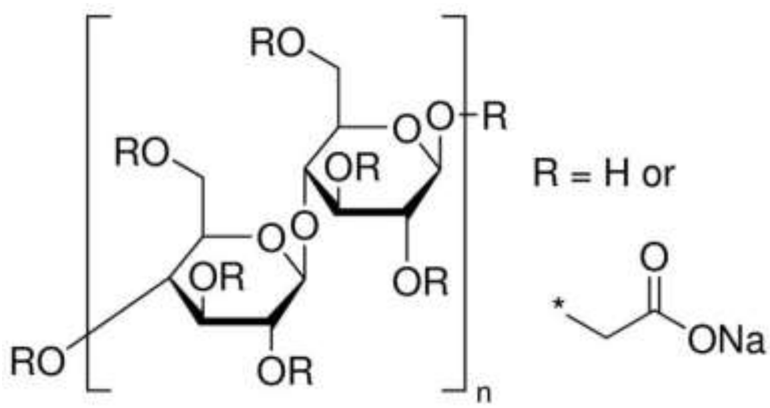

Source: (Guise & et al., 2014)

Among its most important physical properties are its hydrophilic nature of action, its high viscosity in diluted solutions, being practically insoluble in acetone, ethanol and toluene, it also has similar uses to methylcellulose, has the ability to form gels with good consistency, but without great transparency and caramel brown color with high adhesiveness, which makes them very useful as semi-solid oral excipients. Table 7.1 shows the various industrial areas where CMC is used.

Table 7.1 Industrial uses of Carboxymethylcellulose

Application	Dispersant	Protective Colloid	Water Retainer	Thickener	Film Forming
Water-based paints	X	X	X	X	X
Construction products	X		X	X	
Adhesives for wallpapering				X	X
Paper coatings	X	X		X	X
Detergents		X		X	
Emulsions		X		X	
Ceramics	X	X	X	X	X
Tobacco					X
Cosmetics and Pharmaceuticals	X	X	X	X	
Food products	X	X	X	X	X
Oil sludge		X	X	X	

Source: https://www.quiminet.com/articulos/las-diversas-aplicaciones-de-la-carboximetilcelulosa-cmc-16089.htm

Hydrocarbons

A hydrocarbon is an organic compound that arises by combining hydrogen atoms with carbon atoms. These chains of carbon atoms can be open or closed and linear or branched. The great majority of hydrocarbons come from petroleum and because it is the result of the decomposition of organic matter, it offers a great quantity and concentration of carbon and hydrogen. Being these parts of a very important industry for the economy since from them fossil fuels are obtained, used in the industry to produce lubricants, plastics and other products.

Among the main characteristics it is worth mentioning that their boiling point increases as the size of the molecule increases, their density also increases when the molecule is larger, they are insoluble in water because they are polar substances, i.e. the electrical charges of each molecule are separated, they are mostly used as fuels, they are highly polluting and toxic.

They are also one of the main sources of soil and water pollution in the world, due to accidents during transportation, usually by pipeline, but a substantial volume of the oil that reaches the markets is transported by tanker or road.

Oil spills

An oil spill also known as an oil slick is caused by an oil spill that occurs due to an accident or improper practice that pollutes the environment.

These spills affect the entire ecosystem where the spill occurs, seriously damaging the fauna and flora with effects that can be very persistent over time. Hydrocarbon contamination is caused by spills in transportation, loading and unloading operations, leaks from pipelines or industrial facilities, and accidents.

The oil spill affects the soil structure, increasing its water retention capacity, in the surface layer the hydrocarbons decrease the soil pH, increase the available manganese, iron and phosphorus, making it acidic and therefore less suitable for cultivation or the growth of wild plants. Due to the drastic changes that occur after the spill, various forms of recovery have been implemented in order to restore the affected territory.

Soil remediation

Remediation is the treatment or set of operations carried out with the objective of recovering the quality of the contaminated subsoil as shown in Figure 7.2, there are different techniques that allow the recovery of the soil for its use and guarantee the health of people and ecosystems.

Figure 7.2 Soil remediation

Source: (Burnett, 2014)

Remediation techniques are applied depending on the type of pollutant. Treatment systems can be classified into three main areas.

1. Non-recovery, for which the properties of the soil must be modified and the affected space must be perfectly delimited, in addition to monitoring to ensure the impossibility of affecting third parties.
2. Isolation of contamination, consists of establishing correct safety measures to prevent the progression of contamination and mitigating the adverse effects related to the dispersion of contaminating substances.
3. Remediation, remediation measures are divided into in situ treatment, which involves the removal of contaminants without removing the soil, and ex situ where the material to be treated is taken to a confined space or treated in appropriate facilities.

Gels

A gel is a material made from cross-linked polymers in the form of a network, hydrophilic in nature, i.e. it has the capacity to absorb liquids. They can be classified into two types, depending on the nature of the junctions of the three-dimensional network that constitute them.

1. Chemical gels: These are those in which the network is formed through covalent bonds. This type of bond is very strong and its rupture leads to the degradation of the gel.
2. Physical gels: They present a three-dimensional network formed by bonds that are not completely stable. Generally, the bonds are of the Van der Waals type, much weaker than covalent bonds.

The objective of this chapter is to calculate the maximum amount of hydrocarbon absorption by means of a polymeric material (carboxymethylcellulose gel) for the remediation of a contaminated soil due to the explosion of PEMEX's Terra 123 well, performing several analyses (maximum swelling percentage, amount of hydrocarbon removed, pH, conductivity, etc.), where the results will constitute a basis for the remediation of hydrocarbon-contaminated soils.

In addition, it will contribute to and, if necessary, solve different national problems identified by the National Council of Science and Technology (CONACYT), among the areas related to PRONACES that affect the social welfare, sustainability and economic and cultural development of Mexico, among which the following stand out:

1. Social-ecological systems and sustainability.
2. Toxic agents and polluting processes.
3. Risk and disaster prevention
4. Sustainable cities
5. Sustainable, safe, culturally and environmentally relevant housing

2 Methodology

Sampling área

The sampling area was in the town of Oxiacaque in the municipality of Nacajuca, Tabasco in the facilities of the Terra 123 well of Petróleos Mexicanos (PEMEX), where an explosion occurred in one of the pipelines, affecting 120 by 160 m^2 of industrial land, as well as surrounding areas (agricultural land) as a result of the spill of crude oil (PROFEPA, 2015).

Soil sampling

Samples were taken in accordance with the guidelines of the NOM-021-SEMARNAT-2000 standard "Establishing specifications for fertility, salinity and soil classification, study, sampling and analysis", selecting two points. Samples were taken with a shovel at a depth of 50 cm and placed in transparent plastic bags for transport to the laboratory. The samples were dried in the sun for 12 hours, after which time they were crushed using a mortar with a pestle to reduce the particle diameter of the sample and then sieved to obtain uniform particles of approximately 2 mm in diameter, in order to carry out the pertinent analyses.

Moisture determination

For moisture content determination, 2 g of sieved soil was placed in an aluminum container and placed in the Labrem Thermobalaza for 10 minutes for analysis.

Determination of the amount of hydrocarbons

Two g of dry and sieved contaminated soil were weighed and placed in a 100 ml volumetric flask, this was done in triplicate and the flasks were placed inside an extraction hood, then 25 ml of ethylene tetrachloride was added and the flasks were volumetrized with distilled water, finally they were left to stand for a period of 48 hours. After this time, the substrates were filtered using a cone-shaped Whatman filter over a beaker to obtain the samples and were analyzed five times to obtain absorbance records and calculate the hydrocarbon content present in the contaminated soil with the INFRACAL equipment using the EPA method (Infrared Spectrometry).

Determination of the amount of fats (Soxhlet)

This analysis was carried out according to the standard, using a 250 ml flat bottom flask and 90 ml of hexane was added. A homogeneous mixture of 10 g of sieved contaminated soil sample and 10 g of sodium sulfate was introduced into the cellulose capsule and placed in the cornet of the Soxhlet equipment. Subsequently, the Soxhlet equipment was correctly installed and a temperature of 75°C was set for a period of 8 hours, until the sample performed 6 cycles. At the end of the process, the flask was removed and placed in an oven at 60°C for 45 min to remove the remaining steam, after which time it was placed in a desiccator until a constant weight was obtained.

Synthesis of carboxymethyl cellulose (CMC) gel:

In a glass batch reactor with a capacity of 500 ml, 10 g of CMC and distilled water were added until obtaining a 5% solution in weight and it was stirred for a period of 1 hour with constant agitation at 80°C in an electric grill with agitation and controlled temperature, once the solution was diluted, 4 ml of glutaraldehyde was added as crosslinking agent and 4 ml of hydrochloric acid as catalyst, and it was maintained in constant agitation at 80°C during a reaction time of 2 h. After that time, the mixture was placed in molds and dried in an oven maintaining a slow drying at a temperature of 60°C for 48 h, to obtain the CMC gel film. Finally, the films were removed from the molds for use in the remediation treatment of hydrocarbon-contaminated soils.

Fourier Transform Infrared Spectroscopy (FTIR)

Infrared spectroscopy is a technique that works with a small sample that is placed in an infrared cell, where it is subjected to an infrared light source,which scans from wavelengths of 4000 cm^{-1} to 600 $cm^{-1.}$

The intensity of the light transmitted through the sample is measured at each wavenumber, which allows the amount of light absorbed by the sample to be calculated by the difference between the intensity of the light before and after passing through the sample cell.

This analysis was performed on the carboxymethyl cellulose gel film to determine the characteristic functional groups of the polymer before and after exposure to the contaminated soil, in order to observe if there are significant changes in the structure of the polymeric material.

Scanning electron microscopy (SEM)

Scanning electron microscopy is a technique based on the principle of optical microscopy in which the light beam is replaced by an electron beam used for the visualization and analysis of the characteristics of high-resolution solid samples. It works by scanning a beam of electrons over the sample, the sample is coated with a very thin layer of gold or carbon, which gives it conductive properties.

This analysis was performed on the carboxymethyl cellulose gel film to determine the morphological surface of the polymer before and after being exposed to the contaminated soil, in order to observe if there are significant changes in the morphology of the polymeric material.

3 Results

Moisture determination

Two sampling points (samples 1 and 2) of the hydrocarbon contaminated soil were selected and the percent moisture content was determined with the data provided by the Labrem thermobalance. Table 7.2 presents the results before and after drying, according to ASTM D-2216, moisture content determination shall be performed as soon as possible after sampling, especially if corrodible containers (such as thin-walled steel tubes, paint cans, etc.) or plastic bags are used.

Table 7.2 Moisture content of oil-contaminated soil

Sample	Maximum particle size	Initial weight (g)	Final weight (g)	% humidity
1	2 mm	350	20	5.7
2	2 mm	350	21	6.0

Source: Own Elaboration

Determination of hydrocarbons

A soil analysis was performed prior to treatment in order to determine the amount of hydrocarbons contained in samples 1 and 2, as shown in Table 7.3 To obtain a valid result, the samples were run in the INFRACAL equipment five times, and an average was obtained, this being the actual amount of hydrocarbons in mg/l.

Table 7.3 Hydrocarbon content of contaminated soil

Sample	Test 1	Test 2	Test 3	Test 4	Test 5	Average	Co (mg/l)	MCo (mg/kg)
1	0.1	0.1	0	0	0	0.04	0.0792	0.99
2	8.1	8.1	8.5	8.2	8.2	8.22	16.498	206.225

Source: Own Elaboration

In this analysis, two standard equations were used, equation 1 refers to the conversion of the milliliters of Tetrachloroethylene obtained by running the samples in units of mg/l of hydrocarbons, and equation 2 is the conversion of mg/l to mg/kg of soil.

$$Co = \frac{(1.9807\ x\ abs)}{[1-(0.0016\ x\ abs)]} \tag{1}$$

Where:
Co = level of concentration in mg/l
1.9807 = value given by the standard
abs = absorbance obtained from the equipment INFRACAL

$$MCo = \left(1/_{1000}\right)\left(25/_{g\ de\ suelo}\right)(1000) \tag{2}$$

Where:
MCo = level of concentration in mg/kg

Fat extraction

The determination of fats was performed by the Soxhlet method and consisted of the differences in weights between the flask before and after analysis by bringing them to constant weight using equation 3 provided by the standard.

$$MED = \left[\frac{(Pf-Pi)}{kg\ base\ húmeda}\right] x\ 100 \tag{3}$$

Where:
MED = amount of fat in percent (%)
Pf = peso final
Pi = Peso inicial
kg wet basis = amount of sample analyzed

The results of the analysis are shown in Table 7.3 for the initial and final weights of samples 1 and 2.

Table 7.3 Amount of grease in soil contaminated with oil

Sample	Initial weight (g)	Final weight (g)	Amount of fat (%)
1	103.51	106.20	26.9
2	104.18	112.22	80.4

Source: Own Elaboration

Once the hydrocarbon contaminated soil was analyzed, the CMC gel was incorporated for a period of three months, after which the film was removed and the soil was analyzed again using the INFRACAL equipment in order to determine the amount of hydrocarbons absorbed by the CMC gel, the fat content was also determined using the Soxhlet method and the percentage of moisture. The results obtained after removing the CMC gel film in the soil contaminated with hydrocarbon from Terra 123 well did not show a decrease in the readings obtained, due to the fact that the exposure time was not adequate to decrease the amount of hydrocarbon present in the soil. Therefore, a study would have to be done extending the exposure time to 4, 6 and 9 months to determine the adequate time for the decrease of hydrocarbon in a contaminated soil.

Figure 7.3 shows the CMC gel film before being incorporated into the soil contaminated with hydrocarbon showing a clear tone, with smooth surface and little flexibility to the touch and also shows the SEM analysis of the CMC gel film after being removed from the contaminated soil presenting a homogeneous, smooth surface and without significant change in its pores, so we can deduce that the exposure time was not adequate.

Figure 7.3 CMC gel film (a) before exposure and (b) after exposure to hydrocarbon contaminated soil

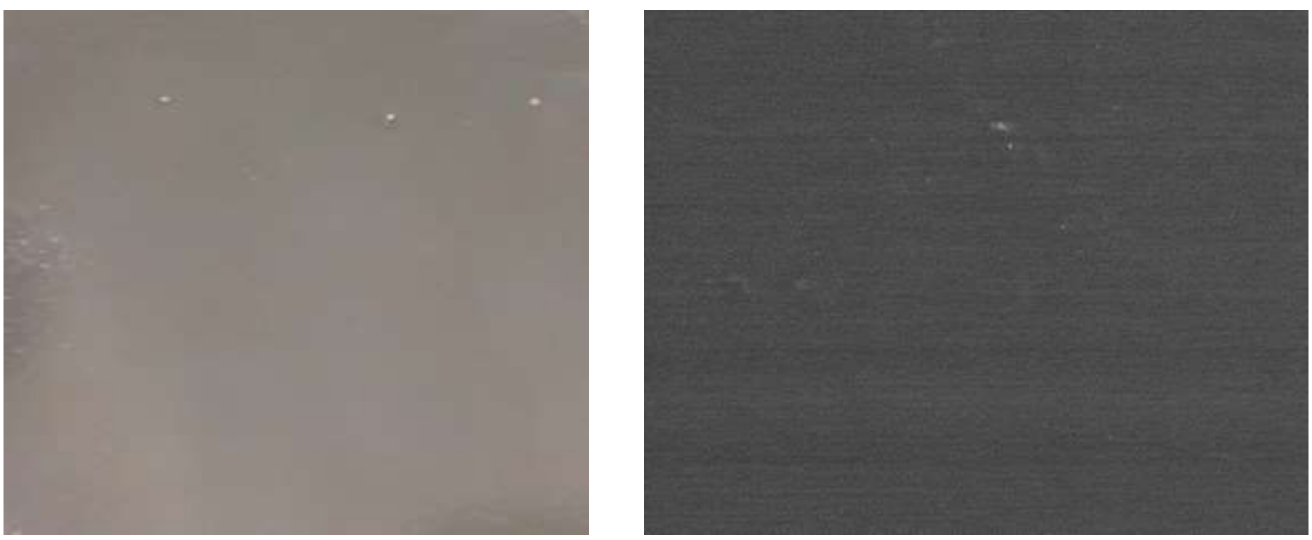

(a) (b)

Source: Own Elaboration

Figure 7.4 the FTIR spectrum of the synthesized carboxymethyl cellulose gel is observed, where the characteristic functional groups of the material can be appreciated and at the wavelength of 3276 cm-1 a wide and pronounced band is observed due to the -OH group characteristic in the CMC structure, at 2362 cm^{-1} a signal appears characteristic of the CO_2 present in the environment at the moment of the equipment calibration, at 1591 cm^{-1} a stretching of the carbonyl group is shown and in the band of 1417 cm^{-1} it is attributed to the carboxyl group.

On the other hand, at 1323 cm^{-1} a bending of the -CH_2- group is observed and in the 1038 cm^{-1} region it is due to the C-C bond. The results agree with those reported by Antonio *et al*. in 2008, where the identification of the different functional groups characteristic of hydrogels was carried out and the wavelengths of the FTIR spectrum of the gel synthesized in this research work are very similar. It is worth mentioning that after 600 cm^{-1} wavelength there is a decrease in the spectrum, due to noise interference in the equipment, which often happens in some cases to voltage variation. However, it does not affect the analysis of the main groups of the CMC gel.

Figure 7.4 FTIR spectrum of the carboxymethylcellulose gel

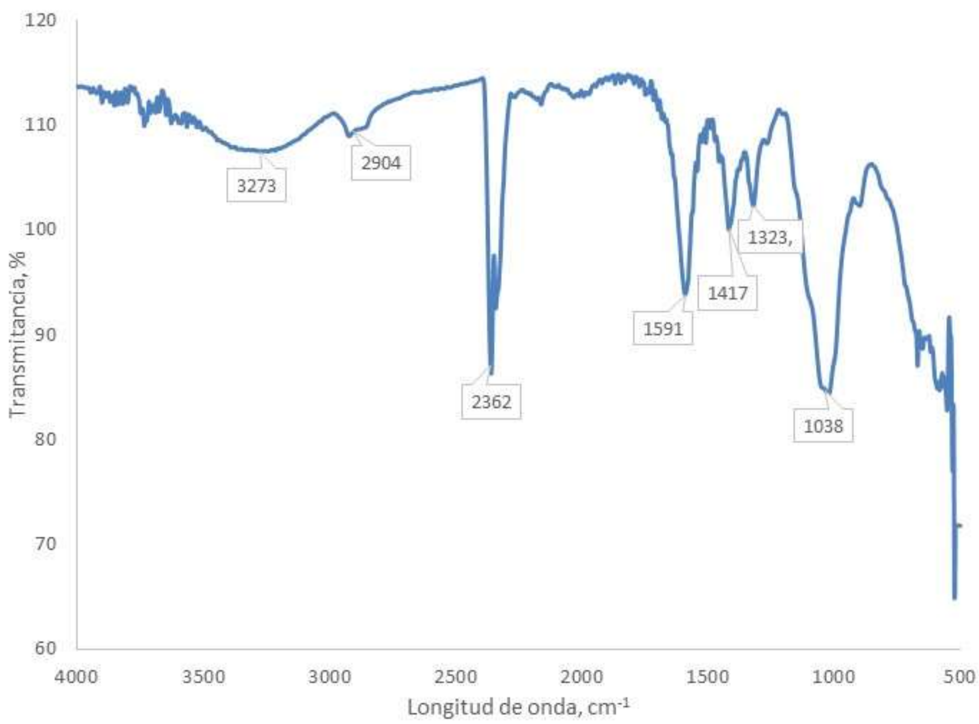

Source: Own Elaboration

Conclusions

The purpose of this chapter was to prove that a carboxymethyl cellulose gel can be employed as a remediation method in a hydrocarbon contaminated soil and that it allows the recovery of the soil for further use. According to the results, it can be concluded that the synthesized CMC gel did not reduce the amount of hydrocarbon found in the contaminated soil during the exposure period, because the moisture analysis, fat determination and hydrocarbon content did not decrease during the exposure period. Therefore, it is recommended to increase the exposure period of the CMC gel in the hydrocarbon contaminated soil.

References

Alonso Riesco, Raquel. (2012). Proyecto de recuperación de suelos contaminados por hidrocarburos *(Ingeniería Técnica Industrial, Especialidad Química Industrial)*. Recuperado de https://ddd.uab.cat/pub/trerecpro/2012/hdl_2072_206396/PFC_RaquelAlonsoRiesco.pdf

Antonio-Cruz, Rocío; Purata-Pérez, Nora Alicia; Urrieta-Saltijeral, Juan Manuel; Sosa-Domínguez, Noé. (2017). Liberación de ketoprofeno en un gel de carboximetilcelulosa. *Revista de Análisis Cuantitativo y Estadísitico, 4*(11), 36-47.

Burnett Pérez, Carol Sthephanie. (2019). Síntesis del gel de carboximetilcelulosa para absorción de hidrocarburo en suelo contaminado. [Tesis de Maestría, Tecnológico Nacional de México, campus Villahermosa]. Repositorio Académico del Tecnológico Nacional de México, campus Villahermosa. http://villahermosa.tecnm.mx/docs/departamentos/tesis/repositorio_de_tesis_2014-2020/Tesis_Carol.pdf

CARTAYA, Omar E.; REYNALDO, Inés; PENICHE, Carlos; y GARRIDO, María. L. (2011). Empleo de polímeros naturales como alternativa para la remediación de suelos contaminados por metales pesados. *Revista Internacional de Contaminación Ambiental, 27*(1), 41-46.

Centro Nacional de Prevención de Desastres (CENAPRED) 2001. Diagnóstico de peligros e identificación de riesgos de desastres en México: *Atlas Nacional de Riesgos de la República Mexicana*. Secretaría de Gobernación, México.

Daniel Coria Ignacio. (2007). Remediación de suelos contaminados con hidrocarburos. 17/Mayo/2021, de *Universidad Abierta Interamericana (UAIS),* Sitio web: http://sustentabilidad.uai.edu.ar/pdf/ing/UAIS-IGA-600-001%20-%20Remediacion.pdf

Duran-Carmona, Verónica. (2015). Impacto ambiental en las comunidades indígenas de Nacajuca, Tabasco a causa de la explosión del pozo Terra 123. *Actas Educación Ambiental desde la Innovación, la Transdisciplinariedad e Interculturalidad T-I,* 1, 54-68.

García-Torres, Reyna; Rios-Leal, Elvira; Martínez-Toledo, Ángeles; Ramos-Morales, Fernando Rafael; Cruz-Sanchez, Jesús Samuel y Cuevas-Díaz, María del Carmen. (2011). Uso de cachaza y bagazo de caña de azúcar en la remoción de hidrocarburos en suelo contaminado. *Revista Internacional de Contaminación Ambiental, 27*(1), 31-39.

Guise, R., Filipe-Ribeiro, L., Nascimento, D., Bessa, O., Nunes, F. M., Cosme, F. (2014). Comparison between different types of carboxylmethylcellulose and other oenological additives used for white wine tartaric stabilization. *Food Chemistry, 25,* 150-157

Hildebrando Buendía R. (2012). Biorremediación de suelos contaminados por hidrocarburos mediante el compost de aserrín y estiércol. *Revista del Instituto de Investigación (RIIGEO), 15*(30), 123-130.

Mejía Sandoval, Gregory. (2006). Aproximación teórica a la biosorción de metales pesados por medio de microorganismos. *Revista CES Medicina Veterinaria y Zootecnia, 1*(1), 77-99.

Nahle, N., & Romero O. (2020). Informa Anual 2020. México: Petróleos Mexicanos.

Nápoles, J.; Marañón, A.; Cumbá, F.; Anllo, Y.; Abalos, A. (2005). Tratabilidad de suelos contaminados con petróleo aplicando microcosmos. *Revista Cubana de Química, 17*(1), 179-188.

NORMA OFICIAL MEXICANA NOM-138-SEMARNAT/SSA1-2012, límites máximos permisibles de hidrocarburos en suelos y lineamientos para el muestreo en la caracterización y especificaciones para la remediación.

NORMA OFICIAL MEXICANA NOM-021-RETNAT-2000, que establece las especificaciones de fertilidad, sanidad y clasificación de suelos.

Ortínez Brito, Oscar; Ize Lema, Irina; Gavilán García, Arturo. (2003). La restauración de suelos contaminados con hidrocarburos en México. *Gaceta ecológica, Secretaría de Medio Ambiente y Recursos Naturales,* (69), 83-92.

Ortiz Bernad, Irene; Sanz García, Juana; Dorado Valiño, Miriam; Villar Fernández, Susana. (2011), Técnicas de recuperación de suelos contaminados: Estrategia de biorrecuperación para la precipitación e inmovilización de Uranio y otros metales tóxicos en suelos contaminados de la desembocadura de Río Tinto (Huelva, España)". *Nanomedicina Informe de vigilancia tecnológica,* 1-109.

Petróleos Mexicanos (PEMEX) 2001. Informe 2001: Seguridad, salud y medio ambiente. *Dirección Corporativa de Seguridad Industrial y Protección Ambiental,* PEMEX, México.

Pérez Casimiro, Guillermina; Iturbe Argüelles, Rosario; Flores Serrano, Rosa María (2006). Cambio en las propiedades físicas de un suelo contaminado con hidrocarburos debido a la aplicación de una tecnología de remediación. *Revista AIDIS de Ingeniería y Ciencias Ambientales: Investigación, desarrollo y práctica, 1*(1), 1-10.

Procuraduría Federal de Protección al Ambiente (PROFEPA) 2002. *Dirección General de Inspección de Fuentes de Contaminación,* México. http://www.profepa.gob.mx/

Procuraduría Federal de Protección al Ambiente PROFEPA (2015), *Inspección preliminar en Pozo Terra 123 en Tabasco,* https://www.profepa.gob.mx/innovaportal/v/5681/1/mx.wap/realiza_profepa_inspeccion_preliminar_en_pozo_terra_123_en_tabasco.html

Quadri, G. 1994. Industria y política ambiental. *El Nacional, sábado 18 de junio,* México.

Reporte Indigo (2019), https://www.reporteindigo.com/reporte/la-maldicion-petroleraproyectos-pemex-tabasco-riesgos-poblacion-dos-bocas/

Rodríguez, Héctor; Donado, Rafael; Lozada, Jefferson. (2013). Espectroscopia Infrarroja por Transformada de Fourier. *17/Mayo/2021, de IDOCPUB* Sitio web: https://idoc.pub/documents/espectroscopia-infrarroja-con-transformada-de-fourier-klzzp093d7lg

Suchanek, Thomas H. (1993). Oil Impacts on Marine Invertebrate Populations and Communities. *American Zoologist*, *33*(6), 510-523.

Wauquier, Jean-Pierre. (2004). *El Refino del Petróleo.* Madrid: Díaz de Santos.

Chapter 8 A review on electrospinning technologies and their potential use in the Biomedical Industry

Capítulo 8 Una revisión sobre las tecnologías de electrohilado y su uso potencial en la Industria Biomédica

CUAHUIZO-HUITZIL, Guadalupe†*, SANTACRUZ-VÁZQUEZ, Claudia and SANTACRUZ-VÁZQUEZ, Verónica

Benemérita Universidad Autónoma de Puebla, Faculty of Engineering

ID 1st Author: *Guadalupe, Cuahuizo-Huitzil* / **ORC ID**: 0000-0003-1541-1454, **CVU CONACYT ID**: 781460

ID 1st Co-author: *Claudia, Santacruz-Vázquez* / **ORC ID**: 0000-0001-6660-469X, **CVU CONACYT ID**: 70094

ID 2nd Co-author: *Verónica, Santacruz-Vázquez* / **ORC ID**: 0000-0003-0527-5815, **CVU CONACYT ID**: 70091

DOI: 10.35429/H.2021.6.112.124

G. Cuahuizo, V. Santacruz, and C.Santacruz

*guadalupe.cuahuizo@alumno.buap.mx

A. Marroquín, J. Olivares, M. Ramírez and L. Cruz (Coord) Engineering and Technology. Handbooks-©ECORFAN-México, Querétaro, 2021.

Abstract

Electrospinning is a technique to obtain new fibrous structures from synthetic or natural polymers for the development of materials used in pharmaceutical and biomedical industries, among others. However, the low production rate of electrospinning has limited industrial application. This review comments on the various electrospinning technologies to increase productivity based on specific examples from the literature.

Review, Nanofibers, Electrospinning

Resumen

El electrospinning es una técnica para obtener nuevas estructuras fibrosas a partir de polímeros sintéticos o naturales para el desarrollo de materiales utilizados en la industria farmacéutica y biomédica, entre otros. Sin embargo, la baja tasa de producción del electrospinning ha limitado su aplicación industrial. En esta revisión se comentan las distintas tecnologías de electrospinning para aumentar la productividad a partir de ejemplos concretos de la literatura.

Revisión, Nanofibras, Electrospinning

1 Introduction

Electrospinning is a versatile manufacturing technique used to produce continuous fibers from natural or synthetic polymers with diameters ranging from nanometers to microns. This technique allows one to manipulate the different variables of the process and properties of the solution to obtain fibers with specific physical characteristics such as composition, porosity and contact surface per unit volume, alignment and morphology (Erickson *et al*., 2015, Haider *et al*., 2018, Patil *et al*., 2017) among others.
At present, electrospinning is seeing increased interest because the resulting nanofibers are finding applications in biomedicine (Ibrahim & Klingner, 2020), as well as in the textile industry (Mirjalili & Zohoori, 2016), environment (García-Zamora *et al*., 2019), and food and packaging industry (Kumar *et al*. 2019). In this chapter, the different electrospinning techniques are described, classified according to their operating principle: nozzle and free surface methods. The basic configuration of electrospinning, the different injectors, the variables that affect electrospinning and their microstructure, as well as the biomedical applications of coaxial and free-surface injectors, are also described.

1.1. Electrospinning basic configuration

Electrospinning is the increasingly lauded technique for the manufacture of continuous, thin fibers and consists of a high voltage power supply, a needle connected to a syringe, and a metal collector, with the large electrical potential difference applied between the needle and metal collector. In Figure 8.1, the key components of an electrospinning machine are presented.

Figure 8.1 Schematic diagram of the electrospinning process

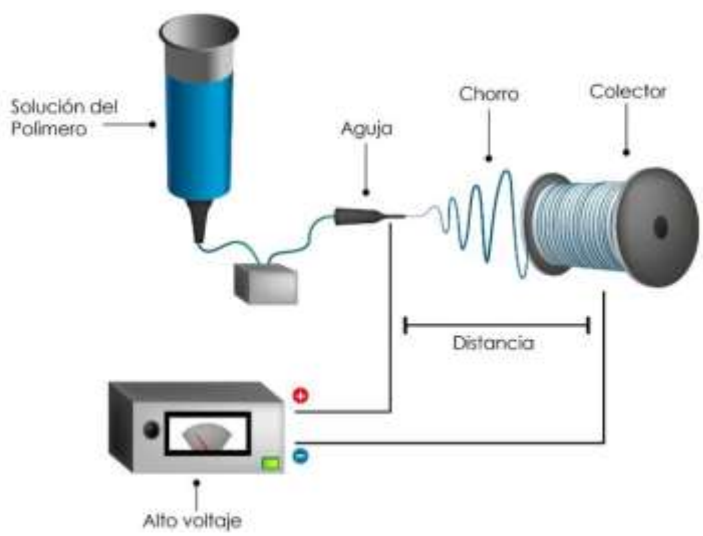

(Adapted from Jiang, Carbone, & Lo, 2015)

Initially, the polymer solution is held at the tip of the needle due to surface tension. When the electrical potential is applied, the hemispherical surface of the polymer drop at the tip of the needle elongates to form a conical shape known as the Taylor cone (Figure 8.2). The formation of the cone immediately precedes the formation of the fibers (Cano *et al*., 2010; Jiang, Carbone & Lo, 2015).

Figure 8.2 Formation of a Taylor cone in capillary

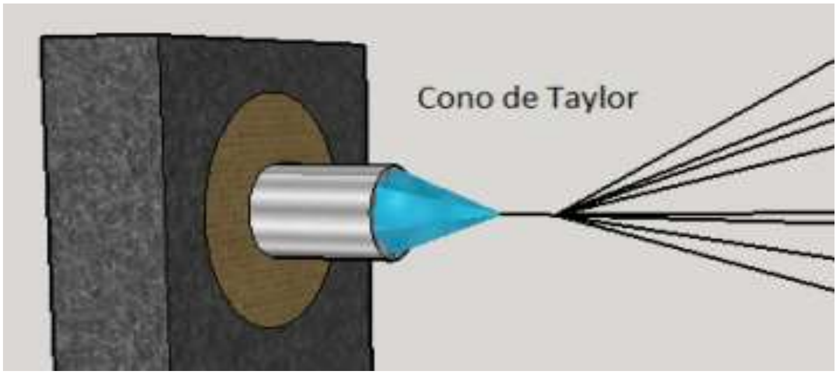

(Taken from Olguin, Fuentes, 2016)

Subsequently, the nanofibers are deposited randomly on the collector forming veils or films and can be manufactured using a stationary collector or a rotating dynamic collector. There are two configurations in electrospinning equipment, horizontal (Figure 8.3a) and vertical (Figure 8.3b). The first one is called a horizontal electrospinner since the injector and the collector are in the same plane, unlike the vertical electrospinner, in which the collector is located in the normal direction just below the injector. Most electrospinners have the horizontal configuration, since this configuration presents fibers with fewer defects such as drops or beadings.

Figure 8.3 Installation diagram for a) horizontal electrospinner b) vertical electrospinner

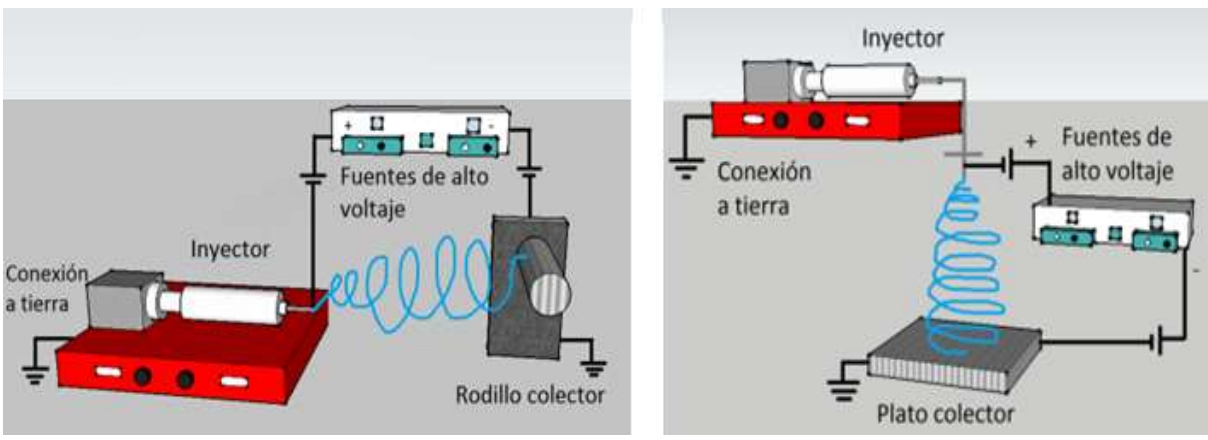

(Taken from Santacruz Vázquez, V. et al., (2017)

It is essential to consider the physics of the electric field that occurs between the injector and the collector of the electrospinner. Because the electrostatic force is the phenomenon that dominates the process, the electric field that acts on the drop of polymeric solution drags the fibers in an axial or tangential direction depending on the configuration of the equipment.

In Figure 8.4, a diagram of the trajectory of the charged particles in the electric field for the two types of collector is shown. If the system is needle-roller, the electric field will simulate an ellipsoid under which the polymer solution from the injector will travel to the collector. If the system changes to that of a plate collector, the electric field can be described as a truncated ellipsoid (Sahay, Thavasi, & Ramakrishna, 2011).

Figure 8.4 Configuration of the electric field in electrospinning equipment

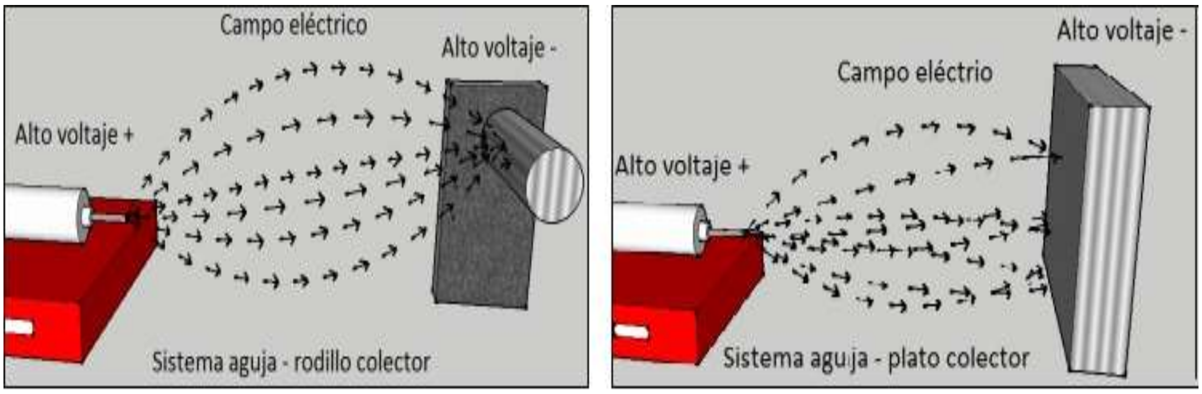

(Taken from Olguin, Fuentes, 2016)

In the same way, the injectors have different configurations, among them the simple needle injector also called a capillary injector, coaxial injector and multi-injector (Yao, Chang, Ahmad, & Li, 2016).

1.2 Technologies used in the electrospinning process

The needle injector is the most widely used configuration according to the reported literature and was the first injector designed for the electrospinning process (Huang, Zhang, Kotaki, & Ramakrishna, 2003). It consists of a plunger or syringe that has an electrically charged capillary attached and that serves as a duct for the supply of the fluid to be electrospun. This injector has disadvantages such as: low feed flow rate, impossibility of obtaining fibers from immiscible mixtures (Tang *et al*., 2016; Vyslouzilova *et al*., 2017), and low productivity (<1 g/h). This last problem has been resolved with modified injectors classified into nozzle and free surface methods (Vass *et al*., 2019). The first method refers to injectors in which the solution is fed directly to multiple needle arrays, while the free surface injectors refer to those in which a greater number of Taylor cones can be formed, and the jets of liquid can freely leave the surface of the solution. Table 8.1 presents a diagram and the different characteristics of several types of multiple injectors used in the electrospinning process.

Table 8.1 Productivity data and diagrams of the different multiple injectors used in the electrospinning process

Author	Productivity	Setting
Theron *et al.,* (2005) used a 9-needle configuration	Productivity 0.1-1 g / h. Voltage 10 kV.	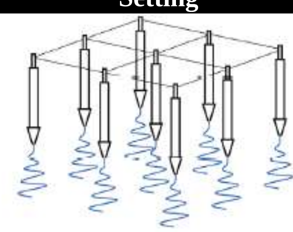 Taken from Theron *et al.* (2005)
Tomaszewski & Szadkowski, (2005) compared three different arrangements of 10 nozzles arranged in linear, concentric, and elliptical forms: The concentric configuration presented higher process stability and fiber quality. They used PVA solutions.	Productivity 60 mg / h Voltage 20 kV.	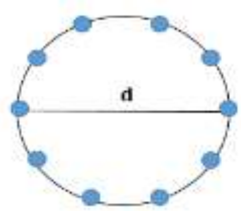 Taken from Tomaszewski & Szadkowski, (2005)

Jiang *et al.*, (2013) used a stepped pyramid configuration, where the formation of several jets was observed, for PVA solutions.	Productivity 2.3- 5.7 g / h Voltages 55-70 kV.	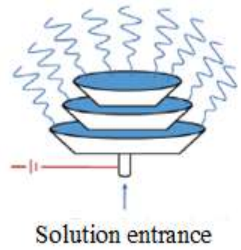 Taken from Jiang *et al.*, (2013)
Varabhas *et al.*, (2008) used a porous tube configuration of 13 cm long with 20 holes, with a solution of polyvinylpyrrolidone.	Productivity 0.3- 0.5 g / h Voltage 40-60 kV.	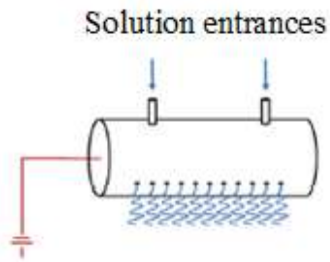 Taken from Varabhas *et al.*, (2008)
Zhou *et al.*, (2009) employed a flat electrode configuration with 4 holes. A polyethylene oxide solution was used.	Productivity 1.68 g / h Voltage 19.8 - 21.0 kV.	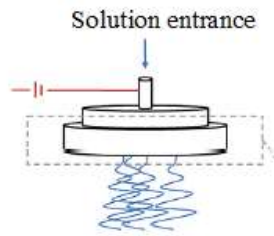 Taken from Zhou *et al.*, (2009)
Niu *et al.*, (2009) employed cylindrical and disc nozzles for use in polyvinyl alcohol solutions. Bhattacharyya *et al.*, (2016) used the free surface electrospinning method from a star-shaped wire electrode, using polyvinyl alcohol solutions.	Cylindrical nozzles Productivity 6 g/h Voltage greater than 57 kV. Disc nozzle Productivity 6.5g/h Voltage 62kV	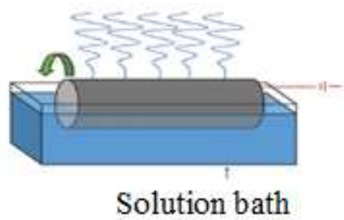 Taken form Niu *et al.*, (2009)
Yoon *et al.*, (2018) conclude that coaxial electrospinning allows functional macromolecules, such as proteins and drugs, to be encapsulated in a single step.		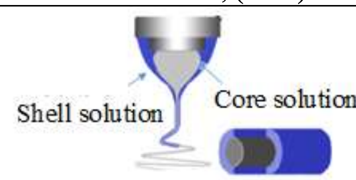 Taken from Yoon *et al.*, (2018)

Free surface electrospinning presents high productivity although is limited to non-volatile solutions. This method is suitable for large-scale nanofiber production. Despite multiple nozzle methods resulting in a lower productivity, it is possible to better control the distribution of the fibers (Noyan *et al.* (2018). Table 8.2 presents the advantages and disadvantages of these methods.

Table 8.2 Advantages and Disadvantages of Multiple Nozzle and Free Surface Electrospinning

Electrospun method	Advantage	Disadvantages
Multiple electrospinning: nozzles	Lower potential difference requirement. Adequate control of the fibers. Ability to form specific fiber structures such as core-shell, porous and multicomponent fiber.	Possibility of the solution clogging the outlet at the tips of the nozzles. Interaction between jets that cause repulsion and deflection of the jet.
Free surface electrospinning	Higher production rate. No problems associated with the nozzles, such as clogging with the solution.	Reduced control of the jets. Difficulty obtaining multi-component fibers. Higher potential difference requirement.

1.3 Coaxial injector

The coaxial injector (Figure 8.5) is a modification of the conventional electrospinning process that involves the provision of multiple feed systems for simultaneous electrospinning. Generally, a matrix arrangement of needle injectors is used, allowing the injection of an internal solution into an external one, to produce continuous coated or hollow nanofibers (Rojas *et al*., 2020). The coaxial electrospinning configuration implies a core-shell nozzle that is coupled to the material deposits respectively (Gualandi *et al.*, 2015; Yarin, 2011). When applying the voltage to the injector, the formation of the Taylor cone occurs, and the internal fluid remains inside as the core of the fiber, while the external fluid encapsulates the internal fluid, while allowing the evaporation of the solvent. It has been reported that the fibers obtained from a coaxial injector present a greater encapsulation efficiency of active compounds compared to the fibers obtained in a simple injector (Cuvellier *et al*., 2018; Chen *et al*., 2020).

Figure 8.5 Diagram of a coaxial injector

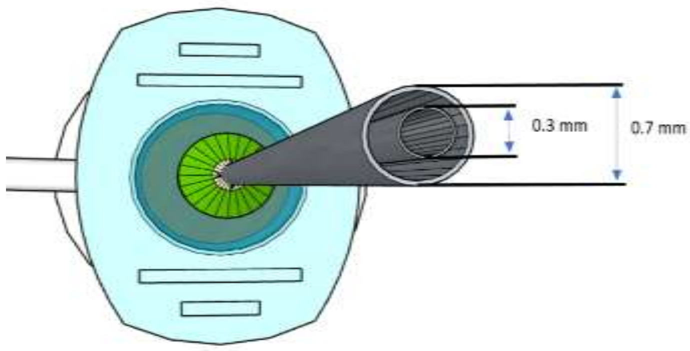

The importance of the coaxial injector lies in the possibility of producing polymer / organic compound and polymer / inorganic compound biphasic fibers, whose properties include high surface-volume ratio, porosity, pore size and adjustable diameter from fluids with different physical and chemical (Yao, Chang, Ahmad, & Li, 2016; Ahmed & Ikram, 2016; Quin *et al*., 2018). The use of the coaxial injector in electrospinning equipment permits the obtention of sophisticated fibers with innovative nanoscale architecture (branched, tube yarn, multichannel, porous, etc.) for drug administration, engineering fabrics, nanoelectronics, energy storage devices and sensors (Pant, Park & Park, 2019; Zhang *et al*., 2015; Huang *et al*., 2018). Table 8.3 shows the results of recent investigations that report on creating electrospun fibers using a coaxial injector and the operating conditions used. From this information, it can be concluded that this injector represents an opportunity for the development of new materials.

Table 8.3 Operating conditions for obtaining electrospun fibers with a coaxial injector

Feed flow rate (mL/h) Core /Shell		Distance Needle-Collector (cm)	Voltage (kV)	Fiber Diameter (nm)	Polymer	Authors
0.094 0.189	1.5	12	18.5	70	PEG PA6	Babapoor, Karimi, Golestaneh, & Mezjin (2017)
0.1	0.2	15	19	200	PLA PVA	Alharbi *et al.* (2018[a])
0.02-0.05	0.01-0.040	15	7-8	590-1170	PAN PEGME	Noyan *et al.* (2018)
0.2	1.3 1.5 1.7	20	20	420	Epoxi-amine Pullulan	Cuvellier *et al.* (2018)
0.1	0.4	10	25	-	SSC GELATIN	Isik, Altay, & Capanoglu (2018)
0.8	0.8	25	25	516-403	PAN ZnO	Methaapanon *et al.* (2019)
0.2	0.4	15	12	100	OIL PMoA/PAN	Zhang *et al. (*2019)
0.06	0.06	10	26	500	SSI-GO SPEEK	Wu *et al.* (2019)
0.4	1.3	13	25	671	PLA/CS	Afshar *et al.* (2019)
0.6	0.12	15	14	112	PAN/SDBS	Peng *et al.* (2019)
0.6	0.3	-	18	573-624	PCL GAS	Chen *et al.* (2020)

1.4 Variables that affect electrospinning process

The process of elecrtrospinning is governed by three aspects: the characteristics of the solution, the process variables, and variables corresponding to the surrounding environment all of which interact to determine the characteristics of the resultant fiber. Table 8.4 summarizes the effects of the variables corresponding to each of these aspects (Nagihan, Pinar, & Filiz, 2014).

Table 8.4 The effects of various **v**ariables and parameters on the electrospinning process

Aspect	Dependent variable	Effect	Effect on fiber feature
Solution	Concentration	An increase in the solute concentration increases the solution's viscosity and consequently the fiber diameter. Conversely, if the solution is of insufficient concentration, it breaks into drops generating instability in the Taylor cone, preventing electrospinning.	Fiber Size and fiber morphology.
	Surface tension	The value of the tension surface depends on the polymer and the solvent, since a decrease in this parameter will reduce the possibility of the formation of drops and favors the formation of the Taylor cone.	Veil Uniformity.
	Conductivity	Experimentally it has been shown that an increase in conductivity brings with it a decrease in the fiber diameter.	Fiber Diameter
	Dielectric constant of the solvent	A solution with a high dielectric constant result in fibers with a reduced diameter and reduces the probability of defects, drops, or beading.	Fiber formation
Process	Voltage	A critically important parameter. A higher voltage favors the formation of thinner fibers and prevents the formation of drops.	Fiber Diameter
	Feed flow rate	A low supply flow rate generates a more stable Taylor cone, evaporating the solution in a gradual way avoiding defect formation in the fiber. An increased flow results in a corresponding increase in fiber diameter.	Veil Uniformity.
	Injector distance to manifold	This parameter is related to the properties of the solution; an ideal distance must be determined that allows obtaining suitable fibers and evaporation of the solvent.	Fiber Morphology
Environmental	Humidity	An increased ambient moisture level favors the existence of circular pores on the surface of the fibers.	Veil Uniformity.
	Temperature	A critical parameter due temperature affects the solution viscosity, thermal conductivity, vapor pressure etc.	

(Adapted from Duque Sánchez, Rodríguez & López, 2013)

1.5 Types of microstructures obtained by the electrospinning process

Different types of structures in the electrospun fibers can be obtained, according to the application (Wang *et al.*, 2011). These structures are classified into porous, flat, hollow, and branched fibers (Table 8.5).

Table 8.5 Classification of the structure of micro and nanofibers obtained by electrospinning

Name	Source	Shape
Porous	Pores are generated when the solvent used to dissolve the polymer is thermodynamically unstable and when subjected to an electric field the solvent coexists in two phases, liquid and gaseous. (Li & Hsieh, 2006)	
Flat	Flattened nanofibers occur when high molecular weight polymers electrospun fibers impact against the collector (Yu *et al*., 2014).	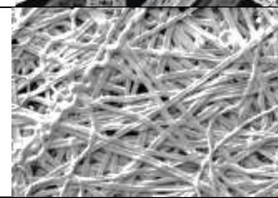
Hollow	Hollow structures are achieved by using a coaxial electrospinning head of the tube-shell type. The polymer is injected through the shell and through the internal tube a compound that is immiscible with the external polymer is passed (Li, McCann, & Xia, 2005).	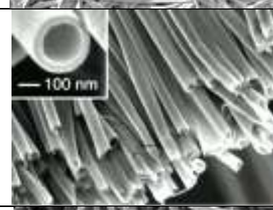
Branched	Branched structure is obtained when electrospun primary jets form branches prior to arriving at the collector. due a balance between electrostatic forces and surface tension of the polymeric solution (Huang, Zhang, Kotaki & Ramakrishna, 2003).	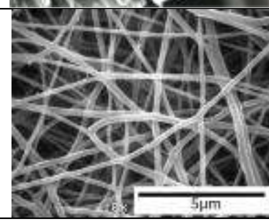

1.6 Most commonly used polymers electrospinning process

Electrospinning technique is restricted to polymeric substances that allow the formation of fibers, and for the selection of electrospinning polymers, specific physical and chemical properties such as density, electrical conductivity, viscosity, molecular weight of the polymer must be considered, as well as polymer-solvent interactions (Frenot & Chronakis, 2003). A wide variety of electrospinning polymers have been reported; however, polymers of natural origin have the advantage of being biocompatible and immunogenic in comparison with synthetic ones (Liao *et al*., 2018). Among them are collagen, elastin, silk, gelatin, chitosan etc. (Horng Lin, Kuang Chen, Lin Huang, & Chieh Huang, 2015). Table 8.6 lists some of investigations carried out with electrospun biopolymers.

Table 8.6 Biopolymers most frequently used for electrospinning

Polymers	Fibers uses	Operation conditions	Reference
Gelatin and poly-caprolactone	Pharmaceutical industry	Solution 10% w/v. Feed flow rate 1 mL/h. Applied voltage 0.5, 0.8, and 0.3 kV.	Zhang, Ouyang, Lim, Ramakrishna, & Huang, (2004)
Jelly	Nutritional products	Solution in a range of 7 to 20% w/v. Feed flow rate 0.1 and 1 mL/h. Applied voltage 28 and 35 kV.	Nagihan, Pinar, & Filiz, (2014)
Gelatin and polyvinyl alcohol	Packing industry	Solutions 10% w/v. Feed flow rate 0.5 mL/h. Applied voltage 15, 20 and 25 kV.	Horng Lin, Kuang Chen, Lin Huang, & Chieh Huang, (2015)
Jelly	Biomedical industry	Solutions 2.5 to 15% w/v. Feed flow rate 0.8mL/h. Applied voltage 10 to 16 kV.	Huang, Zhang, Kotaki, & Ramakrishna, (2003)
Chitosan and PVA	Management Drugs	Feed flow rate 0.6 mL/h. Applied voltaje 22 kV.	Roya *et al.*, (2016)
Chitosan and PVA	Biomedical industry	Solution of QS/PVA 30/70 Feed flow rate 0.5 mL/h. Applied voltage 20 kV.	Koosha, & Mirzadeh, (2015)

1.7. Biomedical Applications of Coaxial and Free Surface Injectors

Coaxial and free-surface electrospinning have potential applications in the biomedical industry; such fibers are used as tissue engineering scaffolds, wound dressings, and drug delivery devices (Table 8.7). The controlled release of incorporated drugs is a very important feature, especially for toxic drugs such as doxorubicin. Electrospun nanofibers allow controlled drug release in order to minimize negative side effects for patients. In most cases, drug molecules are incorporated into coaxial fibers, in which the drug is introduced into the core of the fiber and are protected by biopolymeric materials in the shell, allowing sustained release.

Table 8.7 Uses of coaxial and free surface injectors and their biomedical applications

Injector type	Application	Author
Coaxial	Controlled release of hygroscopic drug poly (DL-lactic acid) and dimethyloxalylglycine fed into the core and poly (3-hydroxy butyrate) fed into the fiber shell.	Wang *et al.* (2010)
Coaxial	Chemotherapy against ovary cancer. The doxorubicin is dispersed in the solution of PVA solution into the core and PVA and chitosan solution located in the shell.	Yan *et al.* (2014)
Coaxial	Controlled release for wounds dressings. Sodium hyaluronate located in the core and cellulose acetate in the shell.	Li *et al*. (2014)
Coaxial	Proliferation of Schwann cells. Laminin localized in the nucleus and poly (L-lactide) -co-poly (ε - caprolactone) in the shell.	Kijeńska *et al.* (2014)
Coaxial	Tissue regeneration. The antibiotic metronidazole is incorporated into the core of poly (ε - caprolactone) providing good mechanical properties, while the shell of zein provides good biocompatibility and a hydrophobic barrier for the prolonged release of the drug from the core.	He *et al*. (2017)
Coaxial	Antibacterial material as dressing for wounds and filtration against *Escherichia coli*. Polylactic acid was located in the nucleus and chitosan solution in the shell.	Nguyen *et al.* (2011)
Free sueface	Antibacterial properties against *Escherichia coli* gram - negative and *Staphylococcus aureus* gram - positive. Chitosan / PVA / $AgNO_3$ or Chitosan / PVA / TiO_2 nanofibers.	Wang *et al.* (2016)
Free surface	Anti-inflammatory activity and analgesic effect. Niflumic acid and polyvinylpyrrolidone nanofibers.	Radacsi *et al.* (2019)
Free surface	Microbicide. PVA fibers with Tenofovir.	Krogstad & Woodrow (2014)

Conclusions

In this review, research articles on electrospinning and its applications in materials for the medical and pharmaceutical industries have been evaluated. Electrospun nanofiber structures have great potential to be applied in processes that use membranes due to their high porosity of up to 90% and a large specific surface area. Therefore, the authors comment on the need to develop injectors that allow higher efficiency of the electrospinning technique and thereby increase the feasibility for large-scale production of these nanostructures.

Acknowledgements

The first author appreciates the support of the National Council of Science and Technology (CONACYT) for the scholarship granted to pursue a doctorate in Chemical Engineering at the Meritorious Autonomous University of Puebla, included in the register of Postgraduates of Excellence.

References

Ahmed, S., & Ikram, S. (2016). Achievements in the Life Sciences Chitosan Based Scaffolds and Their Applications in Wound Healing. *Achievements in the Life Sciences*, *10*(1), 27–37.

Afshar, S., Rashedi, S., Nazozkdast, H., Ghazalian, M. (2019). Preparation and characterization of electrospun poly(lactic acid)- chitosan core-shell nanofibers with a new solvent system. *International Journal of Biological Macromolecules*. 138, 1130-1137.

Alharbi, H., Luqman, M., Fouad, H., Khalil, K.A., Alharthi, N.H. (2018). Viscoelastic behavior of core-shell structured nanofibers of PLA and PVA produced by coaxial electrospinning. *Polymer Testing*. 67, 136-143.

Alharbi, H., Luqman, M., Khalil, K.A., Elnakady, Y.A., Abb-Elkader, H.O., Rady, A.M., Alharthi, N.H., Karim, M.R. (2018). Fabrication of core-shell structured nanofibers of poly (lactic acid) and poly(vinyl alcohol) by coaxial electrospinning for tissue engineering. *European Polymer Journal*. 98, 483-491.

Babapoor, A., Karimi, g., Golestaneh, S.I., & Mezjin, M.A. (2017). Coaxial electro-spun PEG/PA6 composite fibers: Fabrication and characterization. *Applied Termal Engineering*. 118 (25), 398-407.

Bhattacharyya, I., Molaro, C.M., Braatz, D.R., Rutledge, C.G. (2016). Free surface electrospinning of aqueous polymer solutions from a wire electrod. *Chemical Engineering Journal*, 203-311.

Cano, F., Tornero., A., & Naik, A. (2010). Produccion de nanofibras a partir de un diseño innovador de maqinaria protopito de electrospinning. Boletin Intexter (UPC), 5-11.

Chen, W., Wang, C., Gao, Y., Wu, Y., Wu, G., Shi, X., Du, Y., Deng, H. (2020). Incorporating chitin derived glucosamine sulfate into nanofibers via coaxial electrospinning for cartilage regeneration. *Carbohydrate Polymers*. 229.

Cuvellier, A., Torre-Muruzabal, A., Kizildag, N., Daelemans, L., Ba, Y., Clerck, D.K., Rahier, H. (2018). Coaxial electrospinning of epoxy and amine monomers in a pullulan shell for self-healing nanovascular systems. *Polymer Testing*, 69, 146.156.

Duque Sánchez, L. M., Rodríguez, L., & López, M. (2013). Electrospinning: La era de las nanofibras. *Iberoamericana de Polímeros*, 10 - 27.

Erickson, A. E., Edmondson, D., Chang, F., Wood, D., Gong, A., Levengood, S. L., & Zhang, M. (2015). High-throughput and high-yield fabrication of uniaxially-aligned chitosan- based nanofibers by centrifugal electrospinning. *Carbohydrate Polymers*, *134*, 467–474.

Frenot, A., & Chronakis, I. S. (2003). Polymer nanofibers assembled by electrospinning. *Current Opinion in Colloid and Interface Science*, 8, 64 - 75.

García-Zamora, J.L. Santacruz-Vázquez, V., Valera-Pérez, M.A., Moreira, M.T., Cardenas-Chavez, D.L., Tapia-Salazar, M., Torres, E. (2019). Oxidation of Flame Retardant Tetrabromobisphenol A by a Biocatalytic Nanofiber of Chloroperoxidase. *Int. J. Environ. Res. Public Health*, 16, 4917.

Gualandi, C., Celli, A., Zucchelli, A., Focarete, M.L., (2015). Nanohybrid materials by electrospinning. Organic–Inorganic Hybrid Nanomaterials. Springer, Berlin.

Haider, A., Haider, S., Kang, I-K. (2018). A comprehensive review summarizing the effect of electrospinning parameters and potential applications of nanofibers in biomedical and biotechnology, *Arabian Journal of Chemistry*, 11, 1165-1188.

He, M., Jiang, H., Wang, R., Xie, Y.X., Zhao, C. (2017). Fabrication of metronidazole loaded poly (e-caprolactone)/zein core/ shell nanofiber membranes via coaxial electrospinning for guided tissue regeneration. *Journal of Colloid and Interface Science*, 490, 270-278.

Horng Lin, J., Kuang Chen, C., Lin Huang, C., & Chieh Huang, S. (2015). Manufacturing techniques and property evaluations of PVA/Gelatin electrospinning nanofiber membranes. *Applied Mechanics and Materials*, 749, 178 - 181.

Huang, Z.-M., Zhang, Y., Kotaki, M., & Ramakrishna, S. (2003). A review on polymer nanofibers by electrospinning and their applications in nanocomposites. *Composites science and technology*, 6, 2223-2253.

Huang, B., Zhang, Z., Zhao, C., Cairang, L., Bai, J., Zhang, Y., Mu, X., Du, J., Wang, H., Pan, X., Zhou, J., Xie, E. (2018). Enhanced gas-sensing performance of ZnO@In_2O_3 core@shell nanofibers prepared by coaxial electrospinning. *Sensors and Actuators B: Chemical*, 255(2), 2248-2257.

Ibrahim, M.H & Klingner, A. (2020). A review on electrospun polymeric nanofibers: Production parameters and potential applications. *Polymer Testing*, 90, 106647.

Isik, B.S., Altay, F., & Capanoglu, E. (2018). The uniaxial and coaxial encapsulations of sour cherry (*Prunus cerasus L.*). *Food Chemistry*, 265, 260-273.

Jiang, T., Carbone, E. J., & Lo, K. W. (2015). Progress in Polymer Science Electrospinning of polymer nanofibers for tissue regeneration. *Progress in Polymer Science*, *46*, 1–24.

Jiang, G., Zhang, S., Qin, X. (2013). High through put of quality nanofibers via one stepped pyramid-shaped spinneret. *Materials Letters*, 106, 56-58.

Krogstad, E. A., & Woodrow, K. A. (2014). Manufacturing scale-up of electrospun poly (vinyl alcohol) fibers containing tenofovir for vaginal drug delivery. *International Journal of Pharmaceutics*, 475(1-2), 282-291.

Kijeńska, E., Prabhakaran, p.m., Swieszkowski, W., Kurzydlowski, K.J., Ramakrishna, S. (2014). Interaction of Schwann cells with laminin encapsulated PLCL core–shell nanofibers for nerve tissue engineering. *European Polymer Journal*, 50, 30-38.

Koosha, M., Hamid Mirzadeh, H. (2015). Electrospinning, mechanical properties, and cell behavior study of chitosan/PVA nanofibers. *Society For Biomateriales*, 3081-3093.

Kumar, T.S.M., Kumar K.S., Rajini, N., Siengchin, S., Ayrilmis, N., Rajulu, A.V. (2019). A comprehensive review of electrospun nanofibers: Food and packaging perspective. *Composites Part B*, 176, 107074.

Li, Z., Kang, H., Chen, N., Liu, Z., Li, P., Li, W., Zhang, C., Cao, C., Liu, R., Huang, Y. (2014). Controlled release of liposome-encapsulated Naproxen fromcore-sheath electrospun nanofibers. *Carbohydrate Polymers*, 111, 18-24.

Li, D., McCann, J., & Xia, Y. (2005). Use of electrospinning to directly fabricate hollow nanofibers with functionalized inner and outer surfaces. *Small*, 1, 83-86.

Li, L., & Hsieh, Y.-L. (2006). Chitosan bicomponent nanofibers and nanoporous fibers. *Carbohydrate Research*, 341, 374 – 381.

Liao, Y., Loh, C-H., Tian, M., Wang, R., Fane, G.A. (2018). Progress in electrospun polymeric nanofibrous membranes for water treatment: Fabrication, modification and applications. *Progress in Polymer Science*, 77, 69-94.

Methaapanon, R., Chutchakul, K., & Pavarajarn, V. (2019). Photocatalytic zinc oxide on flexible polyacrylonitrile nanofibers via sol–gel coaxial electrospinning. *Ceramics International*.

Mirjalili, M., & Zohoori, S. (2016). Review for application of electrospinning and electrospun nanofibers technology in textile industry. *J Nanostruct Chem*, 6, 207-213.

Nagihan, O., Pınar, T., & Filiz, A. (2014). Affecting parameters on electrospinning process and characterization of electrospun gelatin nanofibers. *Food Hydrocolloids 39*, 19-26.

Niu, H., Lin, T., & Wang, X. (2009). Needleless Electrospinning. I. A Comparison of Cylinder and Disk Nozzles. *Journal ofAppliedPolymer Science*, 114, 3524-3530.

Noyan, C.B.E., Onder, E., Sarier, N., Arat, R. (2018). Development of heat storing poly(acrylonitrile) nanofibers by coaxial electrospinning. *Thermochimica Acta*, 662, 135-148.

Nguyen, T.T.T., Chung, O.H., & Park, J.S. (2011). Coaxial electrospun poly(lactic acid)/chitosan (core/shell) composite nanofibers and their antibacterial activity. *Carbohydrate Polymer*, 86, 1799-1806. Radacsi, N., Giapis, P.K., Ovari, G., Szabó-Révész, P., Ambrus, R. (2019). Electrospun nanofiber-based niflumic acid capsules with superiorphysicochemical properties. *Journal of Pharmaceutical and Biomedical Analysis,* 166, 371-378.

Rojas, A., Velasquez, E., Garrido, L., Galotto, M.J., Dicastillo, L.C. (2020). Design of active electrospun mats with single and core-shell structures to achieve different curcumin release kinetics. *Journal of Food Engineering*. 273.

Roya, S., Alireza, S., Zohreh, M., Samadi, F. Y., Elham, I.(2016). Biocompatible Electrospinning Chitosan Nanofibers: A Novel Delivery System with Superior Local Cancer Therapy. *Carbohydrate Polymers.*

Pant, B., Park, M & Park, S-J. (2019). Drug Delivery Applications of Core-Sheath Nanofibers Prepared by Coaxial Electrospinning: A Review. *pharmaceutics,* 11,305.

Patil, J.V., Mali, S.S., Kamble, S.A., Hong, K.C., Kim, H.J., Patil, S.P. (2017). Electrospinning: A versatile technique for making of 1D growth of nanostructured nanofibers and its applications: an experimental approach. *Applied Surface Science*.

Peng, H., Xiao, L., Sun, K., Ma, G., Wei, G., Lei, Z. (2019). Preparation of a cheap and environmentally friendly separator by coaxial electrospinning toward suppressing self-discharge of supercapacitors. *Journal of Power Sources,* 435.

Quin, Z., Zhang, P., Wu, Z., Yin, M., Geng, Y., Pan, K. (2018). Coaxial electrospinning for flexible uniform white-light-emiting porous fibrous membrane. *Materials & Desing*, 145(5), 175-181.

Sahay, R., Thavasi, V., & Ramakrishna, S. (2011). Design modifications in electrospinning setup for advanced applications. *Journal of nanomaterials*, 1-17.

Tang, Y., Chen, L., Zhao, K., Wu, Z., Wang, Y., & Tan, Q. (2016). Fabrication of PLGA/HA (core)-collagen/amoxicillin (shell) nanofiber membranes through coaxial electrospinning for guided tissue regeneration. *Composites Science and Technology*, 125, 100–107.

Theron, S.A., Yarin, A.L., Zussman, E, & Kroll, E. (2005). Multiple jets in electrospinning: experiment and modeling. P*olymer*, 46, 2889-2899.

Tomaszewski, W, & Szadkowski, M. (2005), Investigation of Electrospinning with the Use of a Multi-jet Electrospinning Head. *Fibres & Textiles in Eastern Europe*, 13(4), 22-26.

Varabhas, J,S., Chase, G.G., Reneker, D.H. (2008). Electrospun nanofibers from a porous hollow tuve. *Polymer*, 49, 4226-4229.

Vass, p., Szabó, E., Domokos,A., Hirsch, E., Galata, D., Farkas, B., Démuth, B., Andersen, K,S., Vigh, T., Verreck, G., Marosi, G., Nagy, K.Z. (2019). Scale-up of electrospinning technology: Applications in the pharmaceutical industry. *WIREs Nanomedicine and Nanobiotechnology*.

Vyslouzilova, L., Buzgo, M., Pokorny, P., Chvojka, J., Mickova, A., Rampichova, M., Amler, E. (2017). Needleless coaxial electrospinning: A novel approach to mass production of coaxial nanofibers. *International Journal of Pharmaceutics*, 516(1–2), 293–300.

Wang, C., Yan, K-W., Lin, Y-D, & Hsieh, C.H.P. (2010). Biodegradable Core/Shell Fibers by Coaxial Electrospinning: Processing, Fiber Characterization, and Its Application in Sustained Drug Release. *Macromolecules*, 43, 6389-6397.

Wang, L., Zhang, C., Gao, F., & Pan, G. (2016). Needleless electrospinning for scaled-up production of ultrafine chitosan hybrid nanofibers used for air filtration, RSC Adv, 6 (107), 105988-105995.

Wu, Y., He, G., Wu, X., Yuan, Q., Gong, X., Zhen, D., Sun, B. (2019). Confinement of functionalized graphene oxide in sulfonated poly (ether ether ketone) nanofibers by coaxial electrospinning for polymer electrolyte membranes. *International Journal of Hidrogen Energy*, 44, 7494.7504.

Yan, E., Fan, Y., Sun, Z., Gao, J., Hao, X., Pei, S., Wang, C., Sun, L., Zhang, D. (2014). Biocompatible core–shell electrospun nanofibers as potential application for chemotherapy against ovary cancer. *Materials Science and Engineering C*, 41, 217-223.

Yarin, A., (2011). Coaxial electrospinning and emulsion electrospinning of core–shell fibers. *Polym. Adv. Technol*. 22, 310–317.

Yao, Z. C., Gao, Y., Chang, M. W., Ahmad, Z., & Li, J. S. (2016). Regulating poly-caprolactone fiber characteristics in-situ during one-step coaxial electrospinning via enveloping liquids. *Materials Letters*, 183, 202–206.

Yoon, J., Yang, H-S., Lee, B-S, & Yu, W-R. (2018). Recent Progress in Coaxial Electrospinning: New Parameters, Various Structures, and Wide Applications. *Advanced Materials*, 30, 1704765.

Yu, D.-G., Xu, Y., Li, Z., Du, L.-P., Zhao, B.-G., & Wang, X. (2014). Coaxial electrospinning with mixed solvents: From flat to round eudragit L100 nanofibers for better colon-targeted sustained drug release profiles. *Journal of Nanomaterials*, 8.

Zhang, Y., Ouyang, H., Lim, C. T., Ramakrishna, S., & Huang, Z.-M. (2004). Electrospinning of Gelatin Fibers and Gelatin/PCL Composite Fibrous Sacffolds. *Interscience*, 156 - 165.

Zhang, H., Qin, X., Wu, J., He, Y.-B., Du, H., Li, B., Kang, F., (2015). Electrospun core–shell silicon/carbon fibers with an internal honeycomb-like conductive carbon framework as an anode for lithium ion batteries. *J. Mater. Chem. A.* 3, 7112–7120.

Zhang, M., Huang, X., Xin, H., Li, D., Zhao, Y., Shi, L., Lin, Y., Yu, J., Yu, Z., Zhu, C., Xu, J. (2019). Coaxial electrospinning synthesis hollow Mo2C@C core-shell nanofibers for high-performance and long-term lithium-ion batteries. *Applied Surface Science*, 473, 352-358.

Zhou, F-L., Gong, R-H., & Porat, I. (2009). Polymeric Nanofibers via Flat Spinneret Electrospinning. *Polymer Engineering and Science*, 2475-2481.

Chapter 9 Green infrastructure: An ally to improve urban runoff management in semi-arid areas

Capítulo 9 Infraestructura verde: Una aliada para mejorar la gestión de escorrentías urbanas en zonas semiáridas

LIZÁRRAGA-MENDIOLA, Liliana†*, VÁZQUEZ-RODRÍGUEZ, Gabriela A. and BIGURRA-ALZATI, Carlos Alfredo

Academic Area of Engineering and Architecture, Universidad Autónoma del Estado de Hidalgo
Academic Area of Chemistry, Universidad Autónoma del Estado de Hidalgo
Academic Area of Engineering and Architecture, Universidad Autónoma del Estado de Hidalgo

ID 1st Author: *Liliana, Lizárraga-Mendiola* / **ORC ID:** 0000-0001-6320-8923, **CVU CONACYT:** 99262

ID 1st Co-author: *Gabriela Alejandra, Vázquez-Rodríguez* / **ORC ID:** 0000-0001-8351-8451, **CVU CONACYT:** 25767

ID 2nd Co-author: *Carlos Alfredo, Bigurra-Alzati* / **ORC ID:** 0000-0001-9740-9483, **CVU CONACYT:** 352163

DOI: 10.35429/H.2021.6.125.146

L. Lizárraga, G. Vázquez and C. Bigurra

*mendiola@uaeh.edu.mx

A. Marroquín, J. Olivares, M. Ramírez and L. Cruz (Coord) Engineering and Technology. Handbooks-©ECORFAN-México, Querétaro, 2021.

Abstract

The growth of cities negatively alters the urban hydrological cycle, and causes problems such as the reduction of their permeable surfaces, increases in temperature that affect the thermal comfort of buildings, large volumes of urban runoff that produce floods, and its contamination. This work highlights the hydrological, hydraulic, and ecosystem advantages of green infrastructure as a strategy of climate change adaptation in cities with a semi-arid climate. Case studies published in international journals, design criteria in technical manuals, national and international standards, and regulations were reviewed. The types of green infrastructure most studied and implemented in various regions with a semi-arid climate were selected, and the most frequently applied criteria and recommendations were chosen. It was possible to determine the most appropriate design and construction parameters for their adaptation in spaces already provided with gray infrastructure, where they can be applied as complementary works that help to solve problems of water shortages to the population, as well as damage to infrastructure due to floods, aquifer overexploitation and pollution.

Water scarcity, Floods, Sustainable infrastructure

Resumen

El crecimiento de las ciudades altera negativamente el ciclo hidrológico urbano, y ocasiona problemáticas tales como la reducción de sus superficies permeables, aumentos en la temperatura que afectan el confort térmico de las edificaciones, grandes volúmenes de escorrentía urbana que producen inundaciones, así como su contaminación. En este trabajo se destacan las principales ventajas hidrológicas, hidráulicas y ecosistémicas de la infraestructura verde, como una estrategia de adaptación al cambio climático en ciudades con clima semiárido. Se revisaron casos de estudio publicados en revistas internacionales, criterios de diseño en manuales técnicos, normas y reglamentos nacionales e internacionales. Se seleccionaron los tipos de infraestructura verde más estudiados e implementados en diversas regiones con clima semiárido y se eligieron los criterios y recomendaciones más frecuentemente aplicados. Fue posible determinar los parámetros de diseño y construcción más apropiados para su adaptación en espacios que ya cuentan con infraestructura gris, donde se pueden aplicar como obras complementarias que ayuden a resolver problemáticas de desabasto de agua a la población, así como daños a la infraestructura por inundaciones, sobreexplotación de acuíferos y contaminación.

Escasez hídrica, Inundaciones, Infraestructura sostenible

1 Introduction

Nearly one billion people living in arid or semi-arid areas of the planet are at risk due to water scarcity problems (UN, n.d.). An arid zone is defined as a region where water supply is insufficient because precipitation and atmospheric humidity are lower than the global annual average of 840 mm (González-Medrano, 2012). Other authors define semi-arid zones as those with precipitation between 250-500 mm (Lane and Nichols, 1999). In Mexico, the average annual precipitation is 780 mm and some authors consider that about 63% of the national territory has some level of aridity; in addition, these areas are inhabited by about 41% of the total population (Díaz-Padilla *et al*., 2011).

The rainy season mainly comprises the months of June to September; however, about 49% of these rains occur in the southeastern region of the country, while the central-northern region experiences significant droughts (CONAGUA, 2018). The constant population growth has also decreased water availability; in 1950 it was 18,000 m^3/inhabitant/a, while by 2015 this was reduced to only 20.5% (3,692 m^3/inhabitant/a) (CONAGUA, 2018). Similarly, a large part of the country experiences a high degree of water pressure (40-100%); this has caused that, at present, about 9 million people do not have access to drinking water, while 10.4 million do not have access to sewerage services (INEGI, 2015).

This scarcity situation makes it necessary to look for more water supply sources to meet the population's demand; however, alternative options to conventional infrastructure must also be considered, in order to mitigate the problems of evaporation, overexploitation, scarcity, contamination and low availability that exist today. Green infrastructure offers a series of options designed to mitigate the impacts caused by the natural risks associated with climate change.

Among its main advantages are environmental (conservation of resources and biodiversity), social (construction of water drains or green spaces, which generate an environment that promotes outdoor coexistence) and economic (job creation, increased property appreciation) (Austin, 2017). Overall, this type of infrastructure represents benefits by providing more efficient water management, as well as additional benefits to those of gray or conventional infrastructure. The adaptation of this type of infrastructure seeks to mimic the conditions that the environment had prior to its urbanization, where the soil surface and vegetation had the capacity to absorb rainwater, evapotranspire it, infiltrate it, and recharge aquifers, among other natural functions (UN-HABITAT, 2018). In contrast, we are familiar with gray infrastructure (that construction that serves as a base for urban activities, their services, technical means and facilities), which generally fulfill a single function: supplying drinking water to the population, channeling wastewater through sewage works, improving wastewater quality through treatment plants, disposing of solid waste in landfills, or mobilizing the population through communication and transportation routes, among others (NWRM, 2014). Currently, it has been demonstrated that this type of infrastructure is insufficient to meet the needs of a constantly growing population with a sustainable vision.

One of the alternatives to mitigate the consequences of urban growth and the negative effects it represents is to introduce green infrastructure in cities. Among the most common examples are permeable pavement (Liu *et al*., 2014; Jia *et al*., 2015), bioretention systems or rain gardens (Chapman and Horner, 2010), infiltration trenches (Ahiablame *et al*., 2012) rainwater harvesting on rooftops (Martin-Mikle *et al*., 2015), as well as green roofs and green walls (Jia *et al*., 2015; Martin-Mikle et al., 2015). The implementation of green infrastructure is an effective tool for climate change adaptation (Melo dos Santos *et al*., 2019). Its use in urbanized environments with semi-arid climate can help restore up to 82% of the hydrological balance (Feng *et al*., 2016). In arid sites such as Arizona in the United States, green infrastructure was adapted with xeric vegetation and sustainable irrigation practices; the positive effect of these measures achieved a saving of $0.77 \pm 0.05 \pm 0.05 \times 108$ m^3 of water (Yang and Wang, 2017) and an increase in water availability for the population (Guertin *et al*., 2015). Choosing this type of strategies can annually reduce urban runoff (35-45%; Feng *et al*., 2016) and restore evapotranspiration (18-25%; Li and Davis, 2009; Feng *et al*., 2016); moreover, infiltration is favored and ponding is decreased (84%; Braswell *et al*., 2018); they have the capacity to remove pollutants through natural processes (Kamali *et al*., 2017); they provide ecological benefits (Li and Davis, 2009); they are an option for domestic self-consumption and waste discharge management (Melo dos Santos and Farias, 2017); they improve the thermal and acoustic insulation of buildings (Reyes *et al*., 2016), among others.

The objective of this work is to review the positive effects of green infrastructure as an adaptation strategy in cities with semi-arid climates where the hydrological cycle has been negatively altered due to urbanization. Its main hydrological and ecosystemic functions, most commonly recommended design criteria, physical factors necessary for its adaptation in previously urbanized environments, as well as its hydraulic efficiency to mitigate flooding and water scarcity problems are defined. The scope of this work is limited to the effects of urban surface runoff and its management through examples of green infrastructure in semi-arid climate zones.

2 Main approaches to green infrastructure

Green infrastructure is defined as an emerging urban planning and design concept (Dige, 2015) that contributes to the resilience of urban ecosystems by providing services to maintain or restore ecological and hydrological functions (Zölch *et al*., 2017). Its main applications include reducing runoff from impervious areas (Martin-Mikle *et al*., 2015), facilitating infiltration and increasing evapotranspiration (Zahmatkesh *et al*., 2015), replicating water balance to preserve local ecosystem integrity (Feng *et al*., 2016), and improving infiltrated water quality (Obropta *et al*., 2018), to name a few. Among their main attractions are their low cost compared to gray infrastructure works (Jia *et al*., 2015) and their ability to adapt to a previously urbanized environment. Its variety of applications is wide, as it can be adapted from the micro-scale (a building) to the macro-scale (watershed or city). This depends, among other things, on the function they perform, the space available, as well as the budget and the management of users and authorities for their implementation. The most common examples are shown in Figure 9.1.

Figure 9.1 Most common green infrastructure applications

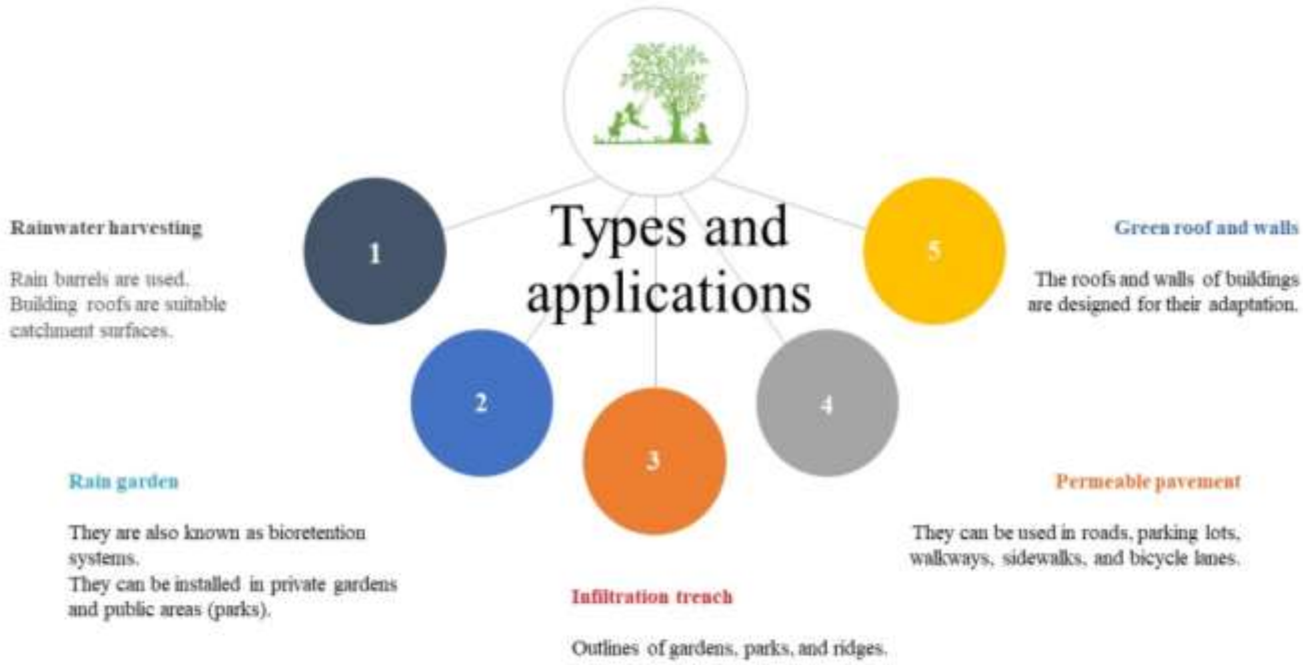

Source of reference: Image prepared by the authors

The green infrastructure also has several hydrological functions that help to improve the restoration capacity of the water cycle. The composition of materials and construction elements used is simple and practical to install. Table 9.1 defines their basic components, as well as the most well-known hydrological functions.

Table 9.1 Composition and hydrological functions of the green infrastructure.

Ranking	Composition	Hydrological function	Author
Permeable pavement	Aggregates (gravels), cement and water	Infiltrate and reduce runoff	Liu *et al*. (2014); Jia *et al*. (2015)
	Photocatalytic film on its surface	Improve the quality of infiltrated water	Martin-Mikle *et al*. (2015); Zahmatkesh *et al*. (2015); Ortega-Villar *et al*. (2019)
Rain garden	Coarse aggregate layer at the bottom, medium aggregate layer in the middle layer, soil and vegetation layer on its surface	Retention and infiltration of runoff	Chapman and Horner (2010)
		Reducing the amount of pollutants	Zahmatkesh *et al*. (2015); Zúñiga-Estrada *et al*. (2020)
		Temporarily storing and treating a volume of runoff water and improving its quality	Winston *et al*. (2016); Zölch *et al.* (2017); Eaton (2018); Tavakol-Davani *et al*. (2019)
Rainwater harvesting	Tanks for storing rainwater that is normally used for non-drinking purposes	Public supply	Martin-Mikle *et al*. (2015)
Green roofs and walls	They have waterproofing at the base, anti-root layer, intermediate layer to reduce saturation, soil substrate and vegetation on its surface	Reduce nutrients and sediments	Martin-Mikle *et al*. (2015)
		Reducing the amount of runoff and pollutants	Jia *et al*. (2015); Tavakol-Davani *et al*. (2019)
		Increase evapotranspiration	Zölch *et al*. (2017)
Infiltration trench	A layer of fine aggregate on the bottom and a layer of coarse aggregate on its surface. It is used parallel to walkways, sidewalks and medians. May or may not have vegetation	Reduce runoff, increase infiltration and filtration, and reduce pollution	Ahiablame *et al*. (2012); Lizárraga-Mendiola *et al*. (2017)

Source of reference: Table prepared by the authors

2.1 Adaptation of green infrastructure in urban spaces

It is necessary to adapt existing infrastructure in cities to reduce the vulnerability of the population to water scarcity and flooding, particularly in areas where rainfall is scarce (Liu and Russo, 2021). Strategies for better urban runoff management have been employed for years (Chao *et al*., 2015). Green infrastructure is widely considered in urban and regional planning processes in different parts of the world (Li and Davis, 2009; Melo dos Santos and Farias, 2017; Martí *et al*., 2020; Tirpak *et al*., 2021). This is composed of a variety of alternatives, from street trees, green walls and roofs on buildings, parks and playgrounds, and permeable pavements, walkways and parking lots, among many other examples (US EPA, 1999). The benefits are broad, as they not only contribute to restoring the urban hydrological cycle, but also promote the wellbeing of the population, the reintroduction of local animal and plant species, and increase the value of real estate, to name a few (Li and Davis, 2009). The following is a description of the most commonly used types of green infrastructure. The focus of this paper is to highlight mainly the benefits on the urban hydrological cycle, such as flood and water shortage mitigation.

2.1.1 Permeable pavement

Main features and functions

There are several types of permeable pavement, including cobblestones, adopasto, gravel pavement, porous asphalt and permeable concrete (Wanielista *et al*., 2007). Pervious concrete is widely used in roads, walkways and bicycle paths and is basically composed of three layers: a bearing surface sufficiently permeable to allow water to enter through its voids, a base layer of fine granular material that favors the optimal conditioning of the bearing surface, and a sub-base layer with coarse granular material that facilitates water infiltration into the subsoil (Wanielista *et al*., 2007). Its interconnected porous structure favors the reduction of surface runoff through physical processes such as infiltration.
(Figure 9.2).

Figure 9.2 Common configuration of a permeable pavement

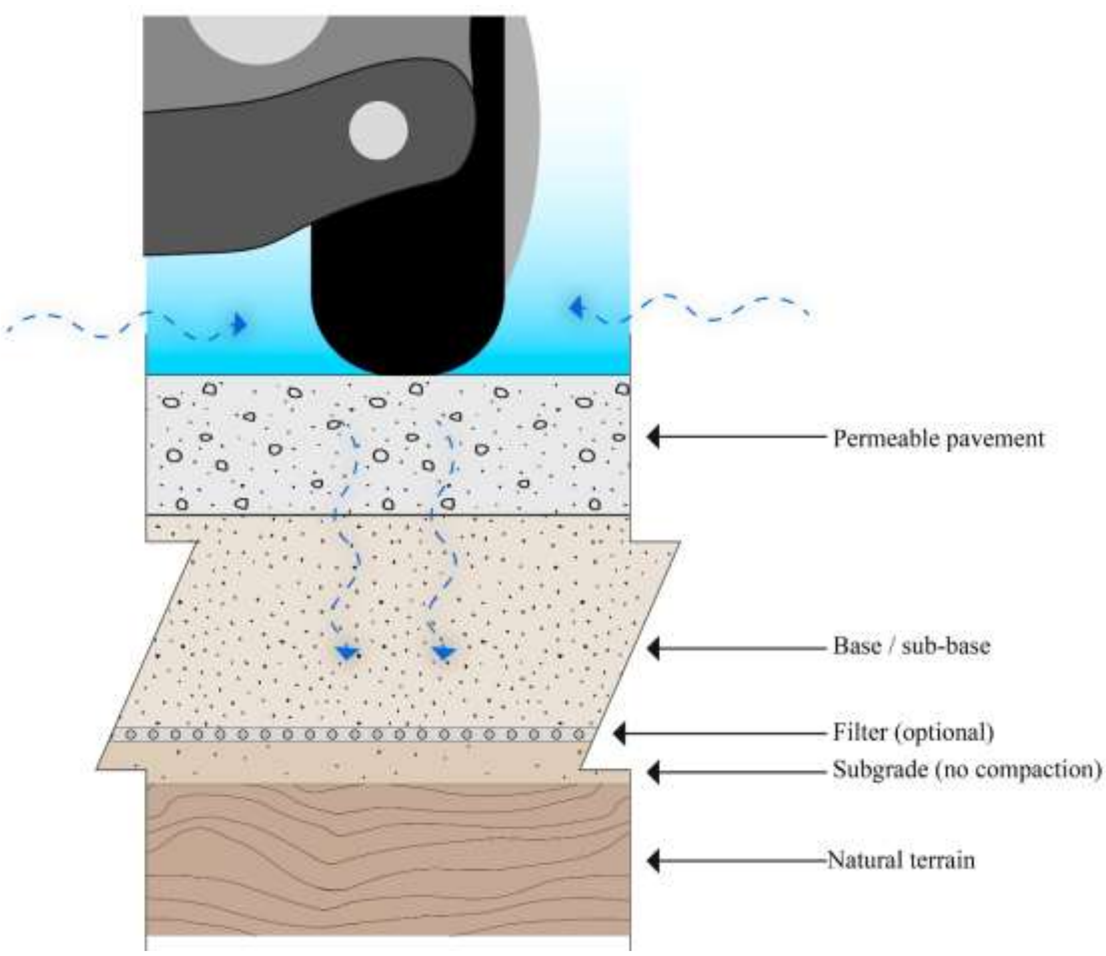

Source of reference: Own image

Its average porosity varies between 15 and 25% (NRMCA, 2010). Although it does not have a strength like conventional concrete, the water/cement ratio (0.28-0.40) provides sufficient bearing capacity for light traffic roads (US EPA, 1999; Yahia and Kabagire, 2014). Its strength depends in part on the porosity of the material, ranging from 44 to 15 MPa for pavements with lower and higher porosity, respectively (Chandrappa and Biligiri, 2016). A low compressive strength (compared to that of a conventional concrete) requires a pavement with higher thickness to help distribute the vehicular load. In a regular pavement the recommended thickness is 10 cm, while in this type of green infrastructure it is 12.5 cm or higher (Wanielista *et al*., 2007). The most commonly used granulometry contains coarse aggregates in a volume between 50-65%, with particle diameters varying between 19-9.5 mm (NRMCA, 2010), although other authors suggest between 2-8 mm (Deo and Neithalath, 2010).

Physical factors required for design and installation

Commonly, these pavements are adapted on soils with good permeability (low clay content, <30%), gentle slope (<5%) and in areas with light traffic (US EPA, 1999). However, in the case of sites with clay soil (low hydraulic conductivity), they have also proven to be efficient in the removal of pollutants and urban runoff (Braswell *et al*., 2018) although their application is uncommon (Dreelin *et al*., 2006). Moreover, when there are low rainfall events (< 8 mm) they can be even more efficient than during heavy rainfall, reducing up to 84% of surface runoff (Braswell *et a*l., 2018). Factors such as pavement age or periodicity of maintenance influence its hydraulic capacity; however, the recommended contributing impervious area ratio for best hydraulic performance is < 5 (Selbig *et al*., 2019). The use of technologies to improve its pollutant removal capacity can also slightly affect its infiltration coefficient; Liang *et al*. (2019) found that, although not significant, the use of titanium dioxide nanoparticles slightly reduced the permeability of permeable pavement, although without deteriorating its hydraulic efficiency.

Hydrologic/hydraulic efficiency

Permeable pavements are characterized because all the layers that compose them are capable of infiltrating runoff; in addition, their internal structure serves as a reservoir to store water and minimize the negative impacts of runoff (Saadeh *et al*., 2019). Their hydraulic behavior is determined by the mix and pavement design, as well as maintenance during operation, making it complex to simultaneously optimize their mechanical and hydraulic properties (Xie *et al*., 2019). It has been reported, for example, that there is a 50% decrease in its strength for every 10% increase in porosity, so a balance must be found to obtain a material that is mechanically and hydraulically efficient (Chandrappa and Biligiri, 2016). Its infiltration capacity (0.1-2 cm/s) is associated with the aggregate size and its compaction level, so it is not recommended to include fine aggregates (Chandrappa and Biligiri, 2016). Their physical characteristics help filter pollutants carried by urban runoff (Wanielista *et al*., 2007). However, sediment accumulation in the pores can reduce their permeability by up to 95% over time and this decreases their hydraulic performance, durability and functionality (Sandoval *et al*., 2020). It has been found that after 5 years, pavement permeability tends to decrease up to 40% due to the clogging of its pores by sediment accumulation. Given the above, it is advisable to provide annual maintenance to prolong its original permeability for a longer period of time (Sandoval *et al*., 2020).

Pollutant removal capacity

They have the capacity to retain runoff water pollutants such as total suspended solids (TSS), nitrates (NO_3^-), nitrites (NO_2^-), ammonium (NH_4^+), phosphates (PO_4^{-3}), and other pollutants (Kamali *et al*., 2017). (Kamali *et al*., 2017). It is believed that the decrease in dissolved phosphorus (P) is due to its interaction with calcium (Ca) and magnesium (Mg) available in concrete, as they precipitate it as phosphate. (Hassan *et al*., 2017). It was also found that pavements remove suspended metals better (such as *Pb, Al* and *Fe*) than the soluble ones (such as *Cu, Zn* y *Mn*) (Selbig *et al*., 2019). Its main purifying mechanisms are filtration and sedimentation, since most of the particles are retained in the first centimeters of the pavement (Selbig *et al*., 2019). However, after some time its treatment capacity tends to decrease, possibly due to a loss in its adsorption capacity due to problems of clogging of its pores (Zhang *et al.*, 2018).

Technologies have also been used for urban runoff treatment such as the incorporation of photocatalytic coatings, e.g., based on nanoparticles of TiO_2, for the removal of various pollutants from runoff water (Liang *et al*., 2019). Photocatalytic oxidation occurs on the surface of permeable pavement in contact with ultraviolet light (Hassan *et al*., 2017). Then, Xu *et al*. (2020) determined that a permeable pavement with a granulometry between 5-10 mm impregnated with nanoparticles of TiO_2 had a greater capacity for oxidation of *NO* than one with larger particles. In another study, nanoparticles of Fe_2O_3 as a coating were found to be capable of removing *Mn* and various microbiological indicators due to oxidation processes (Ortega-Villar *et al*., 2019).

2.1.2 Rain gardens

Main features and functions

They are also known as bioretention systems, biofilters or swales (Le Costumer *et al*., 2009). They are widely used in urban environments to improve their quality and hydrological impacts on infrastructure (Vijayaraghavan *et al*., 2021). They are able to reduce runoff, mitigate its pollutants and provide aesthetic and ecological benefits (Li and Davis, 2009). They favor the development of local flora and fauna, improve water quality and infiltrate stormwater runoff, thus mitigating waterlogging problems (Tirpak *et al.*, 2021). Although they can have different sizes and shapes, they are mainly composed of vegetation on a substrate layer, fine (sand) and coarse (gravel) granular material; occasionally, they can include drainage at their base to increase their hydraulic conductivity (Vijayaraghavan *et al*., 2021) (Figure 9.3). The granulometry of the filter media must drain quickly, but at the same time, it must allow sufficient retention time for the treatment of runoff and vegetation growth (Le Costumer *et al*., 2009).

Figure 9.3 Common configuration of a rain garden

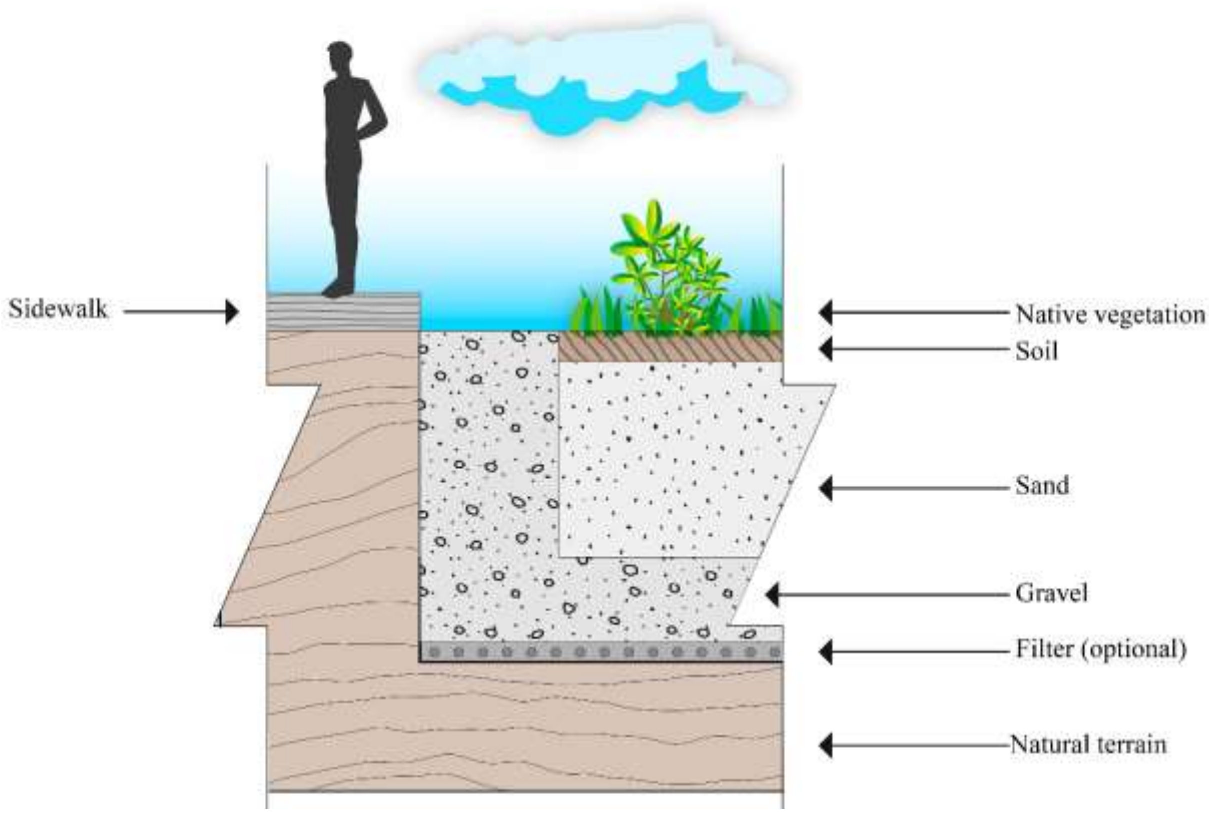

Source of reference: Own image

Physical factors required for design and installation

They are a very versatile type of green infrastructure; however, it is important to consider the catchment area and the type of pollutants they will infiltrate, since selecting the most efficient design will depend on this (Tirpak et al., 2021).

It is possible to combine their shape, size, filtering materials and the type of vegetation, adapt facilities to partially store the infiltrated water or increase its hydraulic conductivity. On the other hand, in climates with low rainfall it is advisable to increase the density of native vegetation in this type of infrastructure, since they have the capacity to absorb pollutants through plants and microbial communities that proliferate in their soil (Houdeschel *et al*., 2012). Likewise, it is advisable to previously characterize the filtering materials in order to improve their decontaminant treatment capacity and predict negative interactions with runoff water (Zúñiga-Estrada *et al*., 2020). Some examples used are gravels of granitic composition with very low dissolving capacity (Caldelas *et al*., 2021) as well as pebbles, quartz sand, slag, loess and activated carbon due to their high porosity and adsorption capacity (Zhang *et al*., 2021a).

Hydrologic/hydraulic efficiency

Their hydrological performance depends on many factors, such as design configuration, location, average annual precipitation, potential evapotranspiration, ratio of catchment area to rain garden area, subsoil infiltration rate, as well as the composition of the growing substrate (Skorobogatov *et al*., 2020). The pore size of the filter media is also thought to influence water availability to plants, so the presence of mesopores (0.2 to 60 µm) is desirable (Skorobogatov *et al*., 2020). Its permeability may decrease as incoming sediment accumulates and clogs the pores of the material; however, vegetation roots play an important role in counteracting this effect (New Jersey Department of Environmental Protection, 2004). It is recommended that its hydraulic conductivity be at least 12.5 mm/h (ARC, 2003), although other sources recommend between 50-200 mm/h (Melbourne Water, 2005) and 4-6 mm/min (Zhang *et al*., 2021b).

Depending on the type of vegetation selected, their roots have the ability to promote the passage of water and air through the pores, mainly in the surface layers. Houdeschel *et al.* (2012) found that grasses can neutralize clogging due to sediment accumulation in this type of infrastructure. Le Costumer *et al*. (2012) demonstrated that plants with thick roots maintain their infiltration capacity and also delay the clogging of their pores with sediments. However, regardless of these benefits, the selection of vegetation should take into account other factors such as its adaptation to the local climate, its phytoremediation potential, sorption capacity, high biomass production and extensive root systems, among others (Vijayaraghavan *et al.*, 2021). Another important hydrological function in rain gardens is evapotranspiration, which can account for up to 19% of intercepted urban runoff, even when the ratio of catchment area to garden area is 1:0.045 (Li and Davis, 2009). In another study, it was found that when this ratio is 2.5%, its retention capacity increases up to 88% (Le Costumer *et al*., 2012).

Pollutant removal capacity

Rain gardens are effective in treating suspended sediments, heavy metals, nutrients and organic compounds (Vijayaraghavan *et al*., 2021). Water quality improves through a complex combination of natural processes that take place in the filter material, such as adsorption, precipitation, microbial biodegradation, photodegradation, volatilization and absorption through plants (Caldelas *et al*., 2021). As for the materials selected for backfilling, those commonly used (soil with organic matter, sand, clay loam and clayey sand) have a limited capacity to treat dissolved contaminants, which tend to infiltrate into the subsoil (Tirpak *et al*., 2021). Studies have proven their ability to reduce the presence of nutrients (N and P), metals and metalloids, as well as microplastics (Smyth *et al*., 2021). The presence of microplastics in urban runoff is considered to come from various anthropogenic sources such as tire and road wear, plastics, paints, construction materials, industrial waste, among others. Their concentration tends to be higher (66-191 particles/L) during the first rains after prolonged periods of drought (Piñon-Colin *et al*., 2020). When they enter a rain garden, retention of up to 84% is possible (Smyth *et al*., 2021).

2.1.3 Rainwater harvesting

Main features and functions

The collection, storage and use of rainwater in urban areas can have a positive impact on the public supply system, since it would not only facilitate the reduction in the demand and use of drinking water, but also mitigate the volume of urban runoff that occasionally causes flooding and negative damage to infrastructure (Melo dos Santos and Farias, 2017).

However, it is important to take into account that captured rainwater requires a first rain separator and treatment prior to its reuse, since the catchment surfaces or rooftops may have dirt, leaves, bird feces, insects and garbage that can contaminate the water, as well as particles in the atmosphere (WHO, 2011). The collection capacity of the rooftop will depend, among other factors, on the available area, its slope, type of material, as well as the amount of precipitation (Jing *et al*., 2017). In sites with semi-arid climates, the temporal variability of rainfall and the aforementioned factors affect the harvestable volume; however, it will depend on the purposes for which it is intended to fully or partially meet the necessary demand (Abdulla and Al-Shareef, 2009; Ali *et al*., 2020).

Physical factors required for design and installation

It is necessary to have an available catchment surface (rooftops), minimum slope of 2%, materials such as concrete or sheet metal (Secretaría de Obras y Servicios del Gobierno de Distrito Federal, 2008); gutters and pipes (PVC, aluminum, galvanized steel) for collection, the first rainfall separator tank, as well as a storage tank with filter (CONAGUA, 2016).

Regardless of the roof material and slope, some designers consider 20% annual losses due to splashing, evaporation and collection failures (Abdulla and Al-Shareef, 2009). Its efficiency will depend on the temporal distribution of rainfall, water demand, the available catchment area (rooftop) and the size of the separator tank, mainly (Ali *et al*., 2020) (Figure 9.4).

Figure 9.4 Common configuration of a rain harvesting system

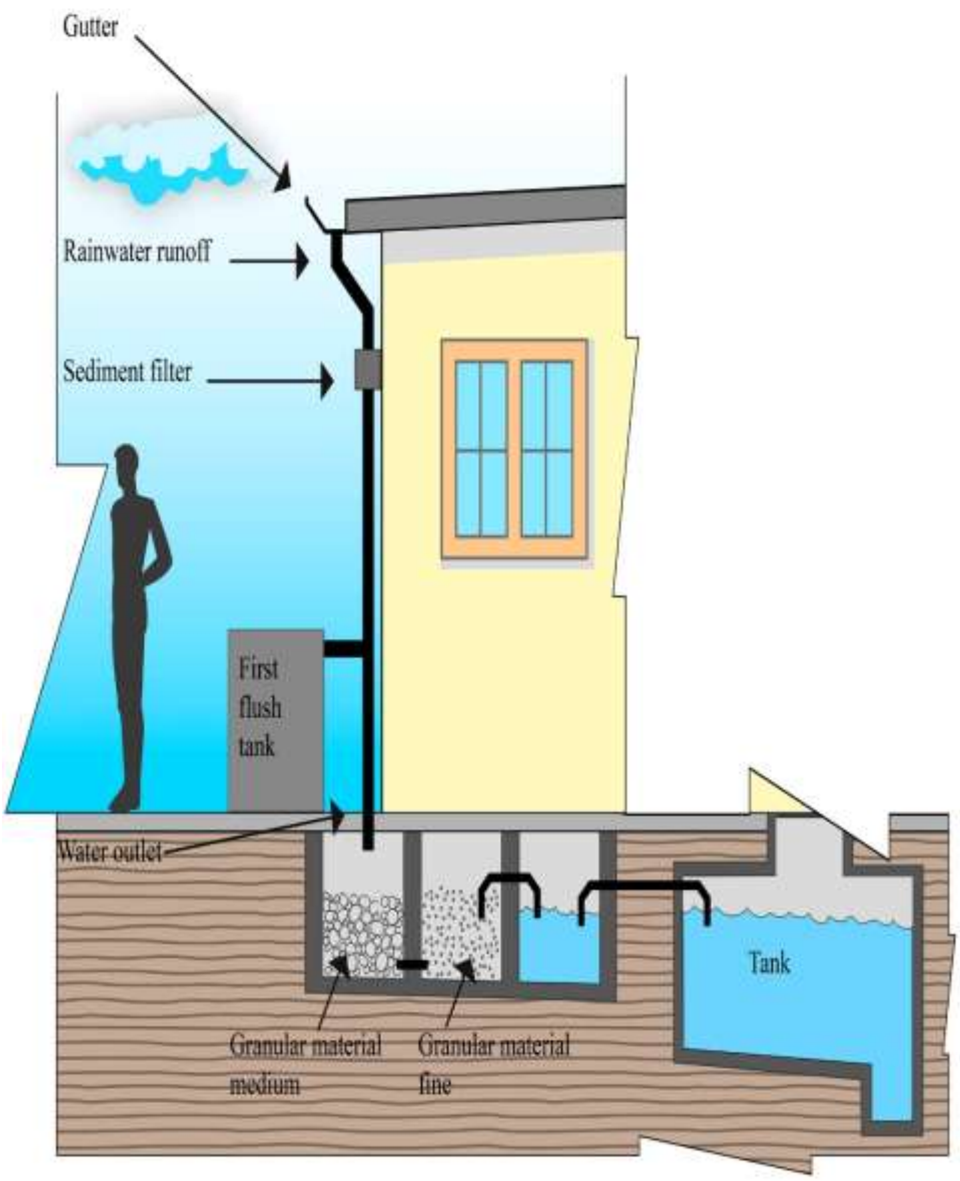

Source of reference: Own image

Hydrologic/hydraulic efficiency

In semi-arid climate zones (< 800 mm) rooftop rainwater harvesting systems are more efficient if they have storage capacities greater than 20 m^3 (Jing *et al*., 2017) and 60 m^3 (Ali *et al*., 2020), although they have a lower cost-benefit ratio than 1 (Jing *et al*., 2017; Ali *et al*., 2020). With large storage volumes and extended periods of rainfall during the year (more than 6 months), it is possible to meet domestic demand more efficiently (Abu-Zreig *et al*., 2019) and reverse the cost-benefit ratio. To obtain the desirable tank size, it is important that cost, reliability, technical feasibility and user interest are in balance to ensure sustainability (Alim *et al*., 2020). In a study conducted in a logistics company located in Mexico City, it was found that the installation of these systems is technically and economically feasible, since the cost-benefit ratio was 1.9 with a recovery rate of 5 years (López-Zavala *et al*., 2018).

Pollutant removal capacity

The quality of the rainwater that is stored is usually higher than that of the first rainfall separator tank (described in the previous section), so it is essential to have this treatment prior to its final storage (Mao *et al*., 2021). Also, water quality improves after the first rains, as this is when the roof surface is washed (Zhang *et al.,* 2014). On concrete surfaces (one of the most commonly used materials in Mexico), as well as on roofs with metal sheets, the presence of total suspended solids is common, as well as K^+, Ca^{2+}, Si^{4+}, *Al* y *Fe* (Méndez *et al*., 2011; Zhang *et al*., 2014). The presence of microorganisms has also been reported (*Legionella*, *Escherichia coli* $O157{:}H7$) (Bae *et al*., 2019). Without an adequate treatment system, its consumption is recommended only for non-potable purposes (Mao *et al*., 2021), so at least filtration and disinfection are suggested (Méndez *et al*., 2011).

2.1.4 Green roofs

Main features and functions

Green roofs can significantly reduce urban runoff volumes through two hydrological processes, rain retention (subsequently lost through evapotranspiration) and runoff detention (through transient storage of rainfall as it infiltrates due to the hydraulic conductivity of the substrate) (De-Ville et al., 2018) (Figure 9.5). Among its known advantages are its ability to reduce the concentration of atmospheric CO_2 and provide an urban aesthetic approach. (Gong *et al*., 2021).

Figure 9.5 Common configuration of a green roof

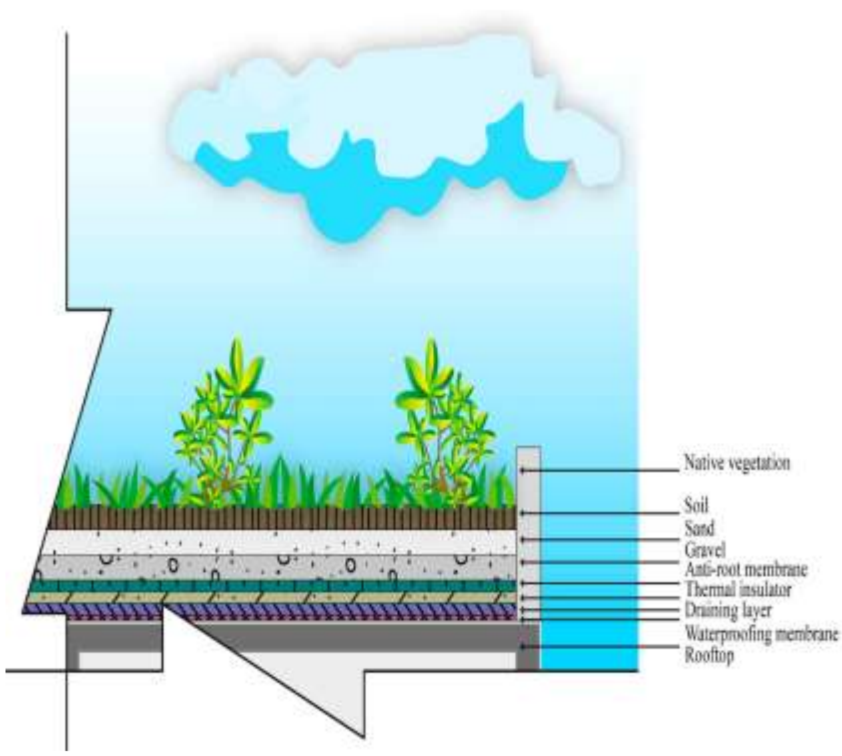

Source of reference: Own image

In addition, they extend the useful life of the roof and improve the thermal and acoustic insulation of the building (Reyes *et al*., 2016; Melo dos Santos *et al*., 2019). Green roofs with 10 cm deep substrates have a buffering effect on changes in temperature in the root zone (up to 13 °C lower than ambient temperature) (Reyes *et al*., 2016), while a substrate with 15 cm depth increases its runoff attenuation capacity (Zhang *et al*., 2021b). In places with semi-arid climates, they may reduce 2.2 °C (Melo dos Santos *et al.*, 2019) and up to 5.3 °C (Reyes *et al*., 2016) the interior temperature of the building, compared to a regular roof. In this type of climate, atmospheric conditions in spring and summer expose green roofs to evaporation, high solar radiation and air temperature. Therefore, the selection of plants is crucial to facilitate the retention of moisture in the substrate, since the flow of water that infiltrates depends on the type of roots (Zhang *et al*., 2019). This promotes better moisture retention throughout the year, which is important in arid and semi-arid climates where sustainable irrigation conditions are required.

Physical factors required for design and installation

These surfaces consist of a series of layers such as a waterproofing membrane over the deck or roof, a drainage system, anti-root layer and filtering material (if necessary) to be placed under and over the drainage, respectively, as well as a layer of substrate and plants (Reyes *et al*., 2016). In addition to the hydraulic conductivity and weight of the substrate, its absorption capacity (Melo dos Santos *et al*., 2019) and a low bulk density should also be taken into account to avoid structural damage to the roof (Zhang *et al*., 2021b). The thickness of the substrate can vary from a few cm to one meter. Depending on the type of rooftop, substrate depth, and irrigation needs of the selected vegetation, there are two types of green roofs: extensive and intensive. Extensive-type green roofs have a substrate layer 2 to 20 cm deep, require minimal or no irrigation, and are generally planted with moss, succulents, grasses, and some herbaceous plants (Reyes *et al*., 2016). Those of the intensive type are more than 20 cm deep, are often designed as gardens for human use and require irrigation and maintenance. The former are adaptable to any type of building (single-family house, building), while the latter require more specific structural conditions and are dependent on irrigation (Reyes *et al*., 2016).

Hydrologic/hydraulic efficiency

Green roofs have higher retention capacity in arid and semi-arid climate sites (67%, Sims *et al*., 2016; 81%, Zhang *et al*., 2021a); furthermore, the use of plants such as the different species of *Sedum*, require little water to subsist and can increase their retention capacity by 89 to 95%. (Zhang *et al*., 2019). It has been reported that the use of mixed vegetation can improve both plant survival (especially in low rainfall conditions) and the retention capacity of a green roof (Gong *et al*., 2021). Substrates with low hydraulic conductivity (0.46 mm/min) show higher moisture detention than those with higher hydraulic conductivity and higher porosity (Zhang *et al*., 2021a). It has also been pointed out that the moisture condition antecedent to the onset of a rainfall event defines its retention efficiency, while rainfall above 45 mm can reduce its efficiency to 16-29% (Sims *et al*., 2016). On the other hand, although temperature has a direct effect on substrate moisture retention, those with thicknesses greater than 10 cm have a buffering effect (Reyes *et al*., 2016). Regarding their potential to mitigate urban runoff, they are capable of reducing it by up to 50% with respect to other impervious areas (Buffam *et al*., 2016).

Pollutant removal capacity

Green roofs are an alternative for absorbing and storing carbon in plants and soils and, therefore, reducing the high concentration levels of carbon dioxide in the soil CO_2 atmospheric in cities (Zhang *et al*., 2021a). Similar to natural ecosystems, this type of infrastructure can undergo seasonal changes in the quality of filtered water, due to factors such as plant development, microbial activity, or other temperature- or light-dependent factors, antecedent humidity, and so on (Buffam *et al*., 2016). They can also degrade the water quality by leaching nutrients (*P, C, N*) and metals (*Cu* and *Fe*) during the rainy season, so it is important to reduce the amount of runoff that will be diverted into the local drainage system (Buffam *et al*., 2016). As for runoff treatment, the adsorption process could be the main factor in reducing nutrient concentration, especially when there is low rainfall (Gong *et al*., 2021). For example, it was found that low concentrations of ammonium ion may be due to its binding to negatively charged organic matter, clays through adsorption or ion exchange, as well as N fixation in the plant; in the case of P, the decrease in its concentration may be associated with physical retention in the substrate (Gong *et al*., 2021).

Other processes such as microbial mineralization of organic matter, desorption or weathering, rather than plant uptake or hydrological variation between storms, are mechanisms controlling the quality of filtered water (Buffam *et al*., 2016).

2.1.5 Green walls

Main features and functions

They are also known as vertical gardens. They can be installed on any vertical surface (building walls), so they take up little space horizontally and add aesthetic value to the real estate (Prodanovic *et al*., 2020). Green walls provide thermal insulation to the buildings in which they are installed, cool the surrounding microclimate, provide acoustic damping and improve air quality (Prodanovic *et al*., 2019). This type of infrastructure requires high amounts of irrigation water in areas with a semi-arid climate (up to 20 L/m^2), which often makes them unsustainable for water-stressed regions (Prodanovic *et al*., 2019). Fortunately, there is the practice of reusing gray water generated in buildings (sink, washing machine or shower) for irrigation, which makes them part of the solution to address water scarcity issues (Prodanovic *et al*., 2020).

Physical factors required for design and installation

In the case of green walls that are irrigated with gray water, it is important that their design includes a filter media that functions as a treatment system to purify pollutants during infiltration (Prodanovic et *al*., 2020). Regarding the filter media used, the mixture (1:2) of perlite and coconut fiber is common (Jørgensen *et al*., 2018), as this mixture is highly permeable and has shown to have a high capacity to remove pollutants from graywater used in irrigation. The filter material must have sufficient macroporosity (>60 μm) to achieve a hydraulic conductivity sufficient for water to flow downward by gravity and then spread with the help of capillary action through mesopores (0.2-60 μm) and micropores (<0.2 μm) (Jim, 2015) (Figura 9.6).

Figure 9.6 Common configuration of a green wall

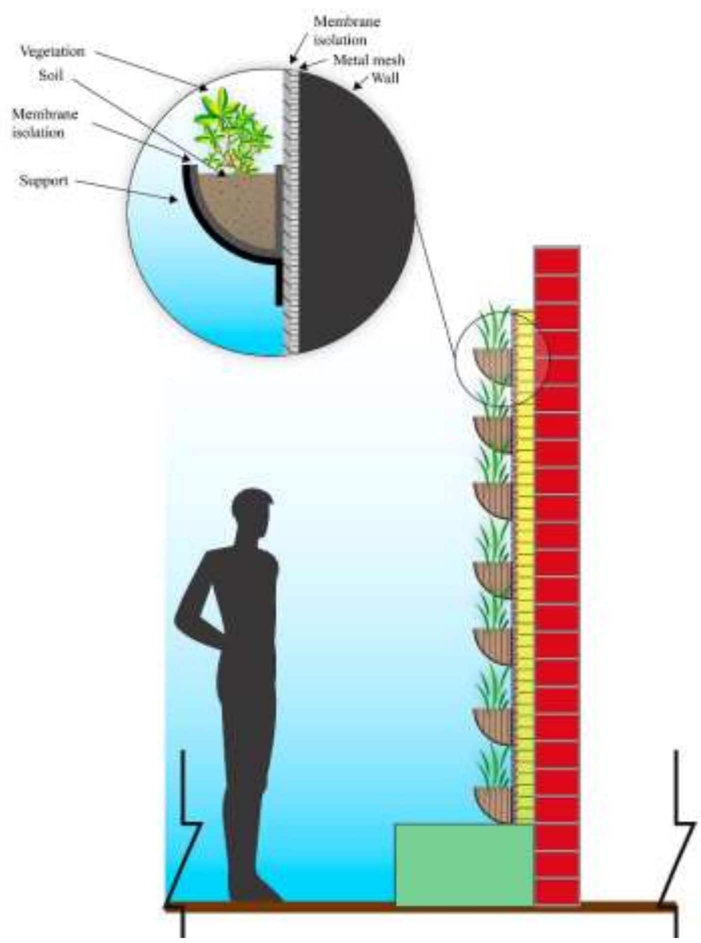

Source of Reference: Own Image

Hydrologic/hydraulic efficiency

It is common to see green walls installed with pots (where irrigation and plant growth occur in isolation) and as continuous blocks (there may be a combination of plants and irrigation is applied from the highest elevation and runs through the entire system to its bottom) (Prodanovic *et al*., 2020).

Block-installed green walls have been found to be more resilient to drought conditions, as they tend to retain moisture due to less surface area exposed to the elements. In addition, the selection of sufficiently porous filter material will favor plant absorption and evaporation, as it allows for better water distribution in the substrate (Prodanovic *et al*., 2019).

The time of the year, which defines the amount of rainfall received, temperature and relative humidity, play an important role in the hydrological balance of the green wall. In the rainy season, evaporation can account for 35-50% of water loss (Prodanovic *et al*., 2019). In the upper part of the wall, evapotranspiration and water retention may be mainly due to the fact that in this zone the plants have greater exposure to the sun and use a greater amount of water to increase their metabolic activity; this also means that it is in this zone where they have greater growth with respect to the lower part of the wall (Dal Ferro *et al*., 2021).

Pollutant removal capacity

Both the filtering material and the vegetation selected in this type of infrastructure play an important role in water treatment. Plants such as *Mentha aquatica L., Oenanthe javanica DC.* and *Lysimachia nummularia L.,* have been efficient in the removal of organic pollutants and nutrients from graywater (Dal Ferro *et al*., 2021). In another study, species of ornamental plants (*lirios de Canna, Lonicera japonica*, vid ornamental) eliminated some contaminants (N > 80%, P entre 13% y 99) (Fowdar *et al*., 2017). On the other hand, the selection of filtering materials favors both infiltration and treatment of pollutants. Coconut fiber, perlite, vermiculite, gravels and sands of high hydraulic conductivity have been used as decontamination treatment systems (Prodanovic *et al*., 2017). Those materials with lower hydraulic conductivity, such as perlite and coconut fiber, showed higher treatment capacity, possibly due to longer retention time and physical-chemical processes (Prodanovic *et al*., 2020). This indicates that green walls are not only an option for reinserting vegetation in limited urban spaces, but are also an option for reusing and treating wastewater, thus reducing the amount of water that is discharged into the sewage system.

2.1.6 Infiltration trench

Main features and functions

This type of infrastructure is very simple to build; in cities they can be installed in areas adjacent to roads, sidewalks and green areas, either in public spaces or private gardens, since they do not require large areas for their adaptation. It consists of a shallow excavation with a minimum slope (2%) and a level bottom surface; its surface has an overflow area (Bureau of Watershed Management, 2006). It is filled with sand on top of the natural ground and coarse aggregates and perforated pipe may be placed to facilitate further infiltration into the subsoil vertically and laterally (NWRM, 2015). On the superficial part it contains a layer of soil and may include vegetation (Figure 9.7). It can be adapted as a complementary drainage work to the storm sewer system or as a surplus infiltration area (e.g., the volume of rainwater that was not stored for reuse). As a constraint, it is important to take into account the depth to groundwater before trench design, as a shallow water table can negatively affect its recharge capacity (Locatelli *et al*., 2015).

Figure 9.7 Common configuration of an infiltration trench

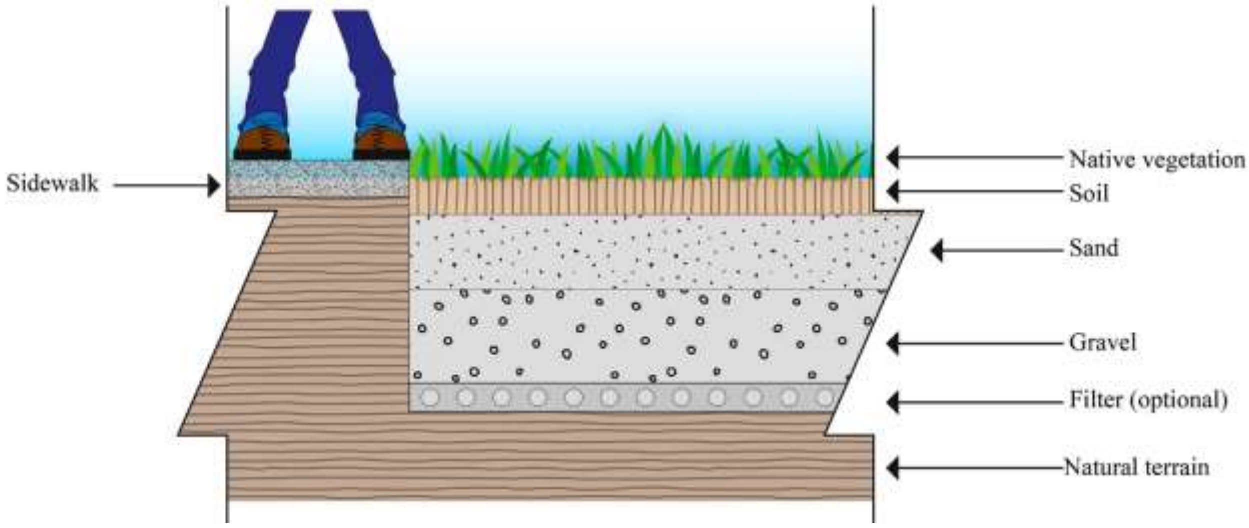

Source of reference: Own Image

Physical factors required for design and installation

In contact with the natural soil, perforated pipe is installed to increase its infiltration capacity. It is recommended that its width not exceed 240 cm; aggregates (gravels with sizes of 2.5-5 cm and void volume of 40%, ASTM-C29) are placed at a maximum depth of 180 cm. A 15 cm layer of soil and native vegetation with low water requirements can be deposited on this surface (Bureau of Watershed Management, 2006). They are usually long, narrow structures that rely primarily on their infiltration capacity to reduce runoff (Ebrahimian *et al*., 2021). In one study, a ditch was designed with a 20:1 ratio with respect to its impervious area, with a capacity to absorb 23 mm rainfall. It was found that its hydraulic efficiency was adequate even for higher rainfall (36 mm), since the surrounding soil was able to absorb more infiltration volume, so its oversizing is common (Ebrahimian *et al*., 2021).

Hydrologic/hydraulic efficiency

Its greatest hydraulic efficiency is observed under light rainfall conditions, since it favors infiltration and recharge. Its design should allow the ditch to be emptied within 72 hours after the rainfall event (Bureau of Watershed Management, 2006). Another factor to consider is hydraulic conductivity, as this will determine the capacity of the trench to manage infiltration of urban runoff (Locatelli *et al*., 2015). The type of material used plays an important role in the hydraulic conductivity value, as a sandy loam soil will behave more efficiently than a silty clay loam type, for example, mainly due to its porosity (Locatelli *et al*., 2015). It is important to have adequate maintenance on a regular basis, otherwise, the clogging of their pores due to sediment carried by infiltrated urban runoff can reduce their hydraulic efficiency (Bergman *et al*., 2011). Like other types of infrastructure, infiltration trenches can also increase their hydraulic efficiency (in periods of low water or low rainfall) or decrease it due to their antecedent moisture content (periods of continuous rainfall) (Ebrahimian *et al*., 2021). Locatelli *et al*. (2015) found that annual seasonal changes can affect their runoff reduction capacity by 10-15%, while permeabilities of $8.2\text{x}10^{-7}$ m/s produce a catchment volume of 68-87%. If there is higher porosity (silty sands), its permeability may increase. ($4\text{x}10^{-5}$ m/s) and the volume of uptake, too (up to 92%).

Pollutant removal capacity

This type of infrastructure is used to remove suspended solids, coliforms, organic pollutants and some soluble forms of metals and nutrients from urban runoff (EPA, 1999). Seasonal changes can alter the geochemical and hydraulic behavior of infiltration ditches, particularly those built on the sides of roads, since they receive, among other things, pollutants from industrial activities and vehicular traffic (Ebrahimian *et al*., 2021). In one study it was determined that during the rainy season there was an increase in the concentration of some dissolved metals (Fe and Mn), while some nutrients decreased; this was possibly due to the washing of the surrounding impervious surfaces (Mullins *et al*., 2020).

Also, when large amounts of runoff are received and the water table is shallow, saturation of the filter material may increase and form anaerobic zones, leading to some heterotrophic bacteria rapidly consuming the little oxygen available (Machusick *et al*., 2011). This behavior facilitates the mobilization of some metals and metalloids through the reduction of metal oxides (Mullins *et al*., 2020).

2.2 Mitigation of water scarcity

It is evident that water scarcity affects a large part of the population living in arid and semi-arid areas, either due to prolonged droughts or poor management (Yang and Wang, 2017). This paper reviews green infrastructure alternatives to mitigate this problem, identifying that rainwater harvesting on rooftops can positively and directly impact users, by collecting *in situ* and have it available almost immediately. Among its main advantages are that most buildings can collect it; it is only necessary to have a minimum slope, adequate surfaces to avoid contamination or unnecessary losses, as well as periodic maintenance. As for its storage and treatment prior to consumption, it will depend on the space available, as well as the user's budget for its installation, since, as mentioned by Ali *et al*. (2020), the larger the collection and storage area, the greater the availability of water for self-consumption. Table 9.2 shows examples studied in different parts of the world with semi-arid climates.

Table 9.2 Rainfall distribution and rainwater availability in different semiarid regions

.

Location	Annual precipitation (mm)	Annual precipitation (mm/m^2)	Annual availability (m^3)	Author
Brazil	800	9.83	15.61	Melo dos Santos and Farías (2017)
Jordan	300	1	0.56	Abdulla and Al-Shareef (2009)
	446.5	0.44	N/D	Abu-Zreig *et al*. (2019)
Pakistan	295	1.05	3.39	Ali *et al*. (2020)
China	600	1.66	N/D	Jing *et al*. (2017)

Source of reference: Table prepared by the authors

As can be seen in Table 9.2, in semi-arid regions there are important variations in the amount of annual precipitation. While in those regions with higher precipitation (800 mm/year) it is possible to have large volumes of water available for self-consumption, in those regions with lower precipitation (800 mm/year) it is possible to have large volumes of water available for self-consumption (15.61 m^3), in sites with very low rainfall (295 mm/a) the available volume is reduced 4.6 times. Seasonal periods, the duration of rainfall events, as well as their intensity, possibly influence the amount of water that can be collected through rooftops in these areas (Melo dos Santos and Farias, 2017). However, in those sites where there are water scarcity problems, they are an alternative option to reduce dependence on the public supply system and achieve better management of drinking water.

2.3 Reduction of urban runoff

All of the examples of green infrastructure discussed in this chapter help reduce urban runoff through different processes, and their hydraulic efficiency tends to be greatest when light rainfall occurs (Bureau of Watershed Management, 2006). Some types do this through detention by infiltration (permeable pavement, rain gardens, infiltration trenches) and storage (rainwater harvesting), others through retention and evapotranspiration (green roofs, green walls). Their advantages include facilitating the recharge of aquifers in waterproofed spaces, reducing the temperature in buildings and their surroundings, and reducing waterlogging and damage to infrastructure. If complemented with storage facilities, they can help to recover part of the infiltrated volume and use it for non-potable purposes such as irrigation of public parks and gardens (Prodanovic *et al*., 2020). Factors such as the impermeable area, the appropriate selection of materials with good hydraulic conductivity and capacity to reduce pollutants, the space available for their construction, among others, determine their efficiency in mitigating flooding problems and increasing the recharge of groundwater sources. Among the positive ecosystemic effects are the reinsertion of native plants and the removal of contaminants through different physical, chemical and microbiological processes. Periodic maintenance is essential to avoid clogging of pores and the accumulation of sediments, organic matter and other debris. Moreover, the selection of vegetation should take into account both its adaptation to local hydrological conditions, as well as its phytoremediation potential (Buffam *et al*., 2016; Vijayaraghavan *et al*., 2021).

Acknowledgment

This work was not financed by any institution.

Conclusions

The examples of green infrastructure most frequently used to mitigate water scarcity and flooding problems in cities with semi-arid climates were reviewed. The main design criteria required for their installation were highlighted, such as available space, slope, type of surface and materials to be used during their construction. In addition, their capacity to retain and detain urban runoff, infiltrate it into the subsoil, evapotranspirate it, purify the pollutants it acquires during its trajectory (in the atmosphere and on the urban surface), as well as its reuse for supply purposes were highlighted. Although their hydraulic and environmental potential may be limited, if properly designed and constructed, they are a sustainable option to complement the capacity of existing gray infrastructure and mitigate problems of water shortages, overexploitation and flooding. It is recommended that planners and designers take into account the appropriate choice of the site, the composition of the materials and the selection of the vegetation to be used, since this will determine their efficiency. Although in Mexico there are national standards and local regulations that take into account aspects of green infrastructure, it is still necessary to promote the main sustainable benefits it offers to the population, especially those living in places with semi-arid climates.

References

Abdulla F.A., Al-Shareef A.W. (2009). Roof rainwater harvesting systems for household water supply in Jordan. *Desalination,* 243, 195-207. Doi:10.1016/j.desal.2008.05.013

Abu-Zreigh M., Ababneh F., Abdullah F. (2019). Assessment of rooftop rainwater harvesting in northern Jordan. *Physics and Chemistry of the Earth*, Parts A/B/C, vol. 114, 102794. Doi:10.1016/j.pce.2019.08.002

Ahiablame L.M., Engel B.A., Chaubey I. (2012). Effectiveness of Low Impact Development Practices: Literature Review and Suggestions for Future Research. *Water Air and Soil Pollution*, 223, 4253-4273. Doi: 10.1007/s11270-012-1189-2

Ali S., Zhang S., Yue T. (2020). Environmental and economic assessment of rainwater harvesting systems under five climatic conditions of Pakistan. *Journal of Cleaner Production*, vol. 259 (20), 120829. Doi: 10.1016/j.jclepro.2020.120829

Alim M.A., Rahman A., Tao Z., Samali B., Khan M.M., Shirin S. (2020). Suitability of roof harvested rainwater for potential potable water production: A scoping review. *Journal of Cleaner Production,* vol. 248 (1), 119226. Doi: 10.1016/j.jclepro.2019.119226

ARC (2003). *Stormwater Management Devices*: Design Guidelines Manual, Auckland Regional Council, Auckland, New Zealand.

ASTM C29 / C29M-17a, *Standard Test Method for Bulk Density ("Unit Weight") and Voids in Aggregate,* ASTM International, West Conshohocken, PA, 2017. Doi: 10.1520/C0029_C0029M-17A

Austin, G. (2017). *Infraestructura verde para la planeación del paisaje*. Interacción humana y sistemas naturales. Editorial Trillas, primera edición en español. ISBN: 978-607-17-2997-2.

Bae S., Maestre J.P., Kinney K.A., Kirisits M.J. (2019). An examination of the microbial community and occurrence of potential human pathogens in rainwater harvested from different roofing materials. *Water Research,* vol. 159, 406-413. Doi: 10.1016/j.watres.2019.05.029

Bergman M., Hedegaard M.R., Petersen M.F., Binning P., Mark O., Mikkelsen P.S. (2011). Evaluation of two stormwater infiltration trenches in central Copenhagen after 15 years of operation. *Water Science & Technology*, vol. 63(10), 2279-2286. Doi: 10.2166/wst.2011.158

Braswell A.S., Winston R.J., Hung W.F. (2018). Hydrologic and water quality performance of permeable pavement with internal water storage over a clay soil in Durham, North Carolina. Journal of Environmental Management, vol. 224, 277-287. Doi: 10.1016/j.jenvman.2018.07.040

Buffam I., Mitchel M.E., Durtsche R.D. (2016). Environmental drivers of seasonal variation in green roof runoff water quality. *Ecological Engineering*, vol. 91, 506-514. Doi: 10.1016/j.ecoleng.2016.02.044

Bureau of Watershed Management (2006). *Pennsylvania Stormwater Best Management Practices Manual*. Department of Environmental Protection, document number 363-0300-002. December 30, 2006, 685 p. https://pecpa.org/wp-content/uploads/Stormwater-BMP-Manual.pdf

Caldelas C., Gurí R., Araus J.L., Sorolla A. (2021). Effect of ZnO nanoparticles on Zn, Cu, and Pb dissolution in a green bioretention system for urban stormwater remediation. *Chemosphere*, https://doi.org/10.1016/j.chemosphere.2021.131045

Chandrappa A.K., Biligiri K.P. (2016). Pervious concrete as a sustainable pavement material-Research findings and future prospects: A state-of-the-art review. *Construction and Building Materials*, 111, 262-274. Doi: 10.1016/j.conbuildmat.2016.02.054

Chang M., McBroom M.W., Beasley R.S. (2004). Roofing as a source of nonpoint water pollution. *Journal of Environmental Management*, 73(4), 307-315. Doi: 10.1016/j.jenvman.2004.06.014

Chao P.R., Umapathi S., Sa W. (2015). Water consumption characteristics at a sustainable residential development with rainwater-sourced hot water supply. *Journal of Cleaner Production*, 109, 190-202. Doi: 10.1016/j.jclepro.2015.04.091

Chapman, C., Horner, R.R. (2010). Performance assessment of a street-drainage bioretention system. *Water Environmental Research*, 82, 109–119. Doi: 10.2175/106143009X426112

CONAGUA. (2016). *Lineamientos Técnicos: Sistema de captación de agua de lluvia con fines de abasto de agua potable a nivel vivienda*. Programas de Agua Potable. Versión 1.0, abril de 2016. 42 p.
CONAGUA (2018). *Estadísticas del Agua en México*. Comisión Nacional del Agua y Secretaría de Medio Ambiente y Recursos Naturales, edición 2018. 306 p.

Dal Ferro N., De Mattia C., Gandini M.A., Maucieri C., Stevanato P., Squartini A., Borin M. (2021). Green walls to treat kitchen greywater in urban areas: Performance from a pilot-scale experiment. *Science of the Total Environment*, vol. 757, 144189. Doi: 10.1016/j.scitotenv.2020.144189
Deo O., Neithalath N. (2010). Compressive behavior of pervious concretes and a quantification of the influence of random pore structure features. *Materials Science Engineering*, A 528, 402-412. Doi: 10.1016/j.msea.2010.09.024

De-Ville S., Menon M., Stovin V. (2018). Temporal variations in the potential hydrological performance of extensive green roof systems. *Journal of Hydrology*, vol. 558, 564-578. Doi: 10.1016/j.jhydrol.2018.01.055

Dige, G. (2015). *Infraestructura verde: una vida mejor mediante soluciones naturales*. European Environment Agency Newsletter, issue no. 3, 15 de septiembre de 2015. https://www.eea.europa.eu/es/articles/infraestructura-verde-una-vida-mejor

Dreelin E.A., Fowler L., Carroll C.R. (2006). A test of porous pavement effectiveness on clay soils during natural storm events. Water Research, vol. 40 (4), 799-805. https://doi.org/10.1016/j.watres.2005.12.002

Díaz-Padilla G., Sánchez-Cohen I., Guajardo-Panes R.A., Del-Ángel-Pérez A.L., Ruíz-Corral A., Medina-García G., Ibarra-Castillo D. (2011). Mapeo del índice de aridez y su distribución poblacional en México. *Revista Chapingo Serie Ciencias Forestales y del Ambiente*, vol. 17, número especial enero, 267-275. Doi: 10.5154/r.rchscfa.2010.09.069

Eaton, T.T. (2018). Approach and case-study of green infrastructure screening analysis for urban stormwater control. *Journal of Environmental Management*, 209, 495–504. Doi: 10.1016/j.jenvman.2017.12.068

Ebrahimian A., Sokolovskaya N., Wadzuk B. (2021). Modeling dynamic performance of urban infiltration trench systems: Methodology and a case study in Philadelphia. *Journal of Hydrology*, vol. 594, 125938. Doi: 10.1016/j.jhydrol.2020.125938

Environmental Protection Agency, EPA (1999). *Storm Water Technology Fact Sheet. Infiltration Trench.* EPA 832-F-99-019, September 1999, Washington, D.C.

Feng Y., Burian S., Pomeroy C. (2016). Potential of green infrastructure to restore the predevelopment water budget of a semi-arid urban catchment. *Journal of Hydrology*, vol. 542, 744-755. Doi: 10.1016/j.jhydrol.2016.09.044

Fowdar H.S., Hatt B.E., Breen P., Cook P.L.M., Deletic A. (2017). Designing living walls for greywater treatment. *Water Research*, vol. 110, 218-232. Doi: 10.1016/j.watres.2016.12.018

Guertin D.P., Korgaonkar Y., Burns S., Barlow J., Unkrich C., Goodrich D.C., Kepner W. (2015). Evaluation of Green Infrastructure Designs Using the Automated Geospatial Watershed Assessment Tool. *Watershed Management Symposium*, agosto 5–7, 2015. Reston, VA

Gong Y., Zhang X., Li H., Zhang X., He S., Miao Y. (2021). A comparison of the growth status, rainfall retention and purification effects of four green roof plant species. *Journal of Environmental Management*, vol. 278, part 1, 111451. Doi: 10.1016/j.jenvman.2020.111451

González-Medrano F. (2012). *Las zonas áridas y semiáridas de México y su vegetación*. Instituto Nacional de Ecología, México. 173 p. ISBN: 9786077908692

Hassan M.R., Zain M.F.M., Hamid R., Kaish A.B.M.A., Nahar S. (2017). A comprehensive study on sustainable photocatalytic pervious concrete for storm water pollution mitigation: A review. *Materials Today: Proceedings* 4, 9773-9776. Doi: 10.1016/j.matpr.2017.06.265

Houdeschel C.D., Pomeroy C.A., Hultine K.R. (2012). Bioretention design for xeric climates based on ecological principles. *Journal of American Water Association*, 48, 1178-1190. Doi: 10.1111/j.1752-1688.2012.00678.x

INEGI (2015). *Datos estadísticos nacionales*. Temas sobre Medio Ambiente y Agua. Base de datos del Instituto Nacional de Estadística Geografía e Informática.

Jia H., Yao H., Tang Y., Yu S.L., Field R., Tafuri A.N. (2015). LID-BMPs planning for urban runoff control and the case study in China. *Journal of Environmental Management*, 149, 65-76. Doi: 10.1016/j.jenvman.2014.10.003

Jim C.Y. (2015). Greenwall classification and critical design-management assessments. *Ecological Engineering*, vol. 77, 348-362. Doi: 10.1016/j.ecoleng.2015.01.021

Jing X., Zhang S., Zhang J., Wang Y., Wang Y. (2017). Assessing efficiency and economic viability of rainwater harvesting systems for meeting non-potable water demands in four climatic zones of China. *Resources, Conservation and Recycling*, vol. 126, 74-85. Doi: 10.1016/j.resconrec.2017.07.027

Jørgensen L., Thorup-Kristensen K., Dresbll D.B. (2018). Against the wall-root growth and competition in four perennial winter hardy plant species grown in living walls. *Urban Forestry and Urban Greening*, 29, 293-302. Doi: 10.1016/j.ufug.2017.12.012

Kamali M., Delkash M., Tajrishy M. (2017). Evaluation of permeable pavement responses to urban surface runoff. *Journal of Environmental Management*, vol. 187(1), 43-53. Doi: 10.1016/j.jenvman.2016.11.027

Lane L.J., Nichols M.H. (1999). *Semi-arid climates and terrain*. En: Environmental Geology. Encyclopedia of Earth Science. Springer, Dordrecht. Doi: 10.1007/1-4020-4494-1_300

Le Costumer S., Fletcher T.D., Deletic A., Barraud S., Lewis J.F. (2009). Hydraulic performance of biofilter systems for stormwater management: Influences of design and operation. *Journal of Hydrology*, vol. 376(1-2), 16-23. Doi: 10.1016/j.jhydrol.2009.07.012

Le Costumer S., Fletcher T.D., Deletic A., Barraud S., Poelsma P. (2012). The influence of design parameters on clogging of stormwater biofilters: a large-scale column study. *Water Research*, 46, 6743-6752. Doi: 10.1016/j.watres.2012.01.026

Li H., Davis A.P. (2009). Water quality improvement through reductions of pollutant loads using bioretention. *Journal of Environmental Engineering*, 135, 567-576. Doi: 10.1061/(ASCE)EE.1943-7870.0000026

Li J., Liu Z., Jiang C., Li Y., Li H., Xia J. (2021). Optimization design of key parameters for bioretention cells with mixed filter media via HYDRUS-1D model and regression analysis. *Ecological Engineering*, vol. 164 (1), 106206. Doi: 10.1016/j.ecoleng.2021.106206

Liang X., Cui S., Li H., Abdelhady A., Wang H., Zhou H. (2019). Removal effect on stormwater runoff pollution of porous concrete treated with nanometer titanium dioxide. Transportation Research Part D: *Transport and Environment*, vol. 73, 34-45. Doi: 10.1016/j.trd.2019.06.001

Liu, W., Chen, W., Peng, C. (2014). Assessing the effectiveness of green infrastructures on urban flooding reduction: A community scale study. *Ecological Modelling*, 291, 6–14. Doi: 10.1016/j.ecolmodel.2014.07.012

Liu O.Y., Russo A. (2021). Assessing the contribution of urban green spaces in green infrastructure strategy planning for urban ecosystem conditions and services. *Sustainable Cities and Society*, vol. 68, 102772. Doi: 10.1016/j.scs.2021.102772

Lizárraga-Mendiola L., Vázquez-Rodríguez G.A., Lucho-Constantino C.A., Bigurra-Alzati C.A., Beltrán-Hernández R.I., Ortiz-Hernández J.E., López-León L.D. (2017). Hydrological Design of Two Low-Impact Development Techniques in a Semi-Arid Climate Zone of Central Mexico. *Water*, vol. 9(8), 561. Doi: 10.3390/w9080561

Locatelli L., Mark O., Mikkelsen P.S., Arnbjerg-Nielsen K., Wong T., Binning P.J. (2015). Determining the extent of groundwater interference on the performance of infiltration trenches. *Journal of Hydrology*, vol. 529, Part 3, 1360-1372. Doi: doi.org/10.1016/j.jhydrol.2015.08.047
López-Zavala M.A., Prieto M.J.C., Rojas C.A.R. (2018). Rainwater harvesting as an alternative for water supply in regions with high water stress. *Water Science and Technology*. *Water Supply*, 18(6), 1946-1955. Doi: 10.2166/ws.2018.018

Machusick M., Welker A., Traver R. (2011). Groundwater mounding at a storm-water infiltration BMP. *Journal of Irrigation Drainage Engineering*, 137(1), 154-160. Doi: 10.1061/(ASCE)IR.1943-4774.0000184

Mao J., Xia B., Zhou Y., Bi F., Zhang X., Zhang W., Xia S. (2021). Effect of roof materials and weather patterns on the quality of harvested rainwater in Shanghai, China. *Journal of Cleaner Production*, vol. 279, 123419. Doi: 10.1016/j.jclepro.2020.123419

Martí P., García-Mayor C., Nolasco-Cirugeda A., Serrano-Estrada L. (2020). Green infrastructure planning: Unveiling meaningful spaces through Foursquare users' preferences. *Land Use Policy*, vol. 97, 104641. Doi: 10.1016/j.landusepol.2020.104641

Martin-Mikle C.J., de Beurs K.M., Julian J.P., Mayer P.M. (2015). Identifying priority sites for low impact development (LID) in a mixed-use watershed. *Landscape and Urban Planning*, vol. 140, 29-41. Doi: 10.1016/j.landurbplan.2015.04.002

Melbourne Water (2005). *Water Sensitive Urban Design (WSUD).* Engineering Procedures: Stormwater. CSIRO Publishing, Melbourne.

Melo dos Santos S., Farías M.M.M.W.E.C. (2017). Potential for rainwater harvesting in a dry climate: Assessments in a semiarid region in northeast Brazil. *Journal of Cleaner Production*, vol. 164(15), 1007-1015. Doi: 10.1016/j.jclepro.2017.06.251

Melo dos Santos S., Fernandes Ferreira Silva J., Chaves dos Santos G., Martins Torres de Macedo P., Gavazza S. (2019). Integrating conventional and green roofs for mitigating thermal discomfort and water scarcity in urban areas. *Journal of Cleaner Production,* vol. 219, 639-648. Doi: 10.1016/j.jclepro.2019.01.068

Mendez C.B., Klenzendorf J.B., Afshar B.R., Simmons M.T., Barrett M.E., Kinney K.A., Kirisits M.J. (2011). The effect of roofing material on the quality of harvested rainwater. *Water Research*, vol. 45(5), 2049-2059. Doi: 10.1016/j.watres.2010.12.015

Mullins A.R., Brain D.J., Pfeil-McCullough E., Hopkins K.G., Lavin S., Copeland E. (2020). Seasonal drivers of chemical and hydrological patterns in roadside infiltration-based green infrastructure. *Science of the Total Environment*, vol. 714, 136503. Doi: 10.1016/j.scitotenv.2020.136503

National Ready Mix Concrete Association, NRMCA (2010). NRMCA-Concrete in Practice-38 (CIP-38).

New Jersey Department of Environmental Protection (2004). *New jersey Stormwater Best Management Practices Manual*. Trenton, NJ.

Nnadi E.O., Newman A.P., Coupe S.J., Mbanaso F.U. (2015). Stormwater harvesting for irrigation purposes: An investigation of chemical quality of water recycled in pervious pavement system. *Journal of Environmental Management*, vol. 147(1), 246-256. Doi: 10.1016/j.jenvman.2014.08.020

Natural Water Retention Measures, NWRM (2014). *Una guía para apoyar la elección, el diseño y la implementación de las medidas naturales retención de agua Europa.* Comisión Europea. Dirección General de Medio Ambiente. Bruselas. 98 p. http://nwrm.eu/guide-es/files/assets/basic-html/index.html#2

Natural Water Retention Measures, NWRM (2015). *U8. Infiltration trenches*. European Commission, 14 p. http://nwrm.eu/sites/default/files/nwrm_ressources/u8_-_infiltration_trenches.pdf

Obropta C.C., Del Monaco N. (2018). Reducing Directly Connected Impervious Areas with Green Stormwater Infrastructure. *Journal of Sustainable Water Built Environment*, vol. 4(1): 05017004. Doi: 10.1061/JSWBAY.0000833.

ONU, s.f. *Ordenación de los ecosistemas frágiles: Lucha contra la desertificación y la sequía*. Cumbre para la Tierra, capítulo 12. https://www.un.org/spanish/esa/sustdev/agenda21/agenda21spchapter12.htm

ONU HABITAT (2018a). *Ciudades resilientes*. Nueva Agenda Urbana de la ONU. Publicado en octubre de 2018.

Organización Mundial de la Salud, OMS (2011). *Guidelines for drinking-water quality*. 4ta edición, WHO Library Cataloguing-in-Publication Data.

Ortega-Villar R., Lizárraga-Mendiola L., Coronel-Olivares C., López-León L.D., Bigurra-Alzati C., Vázquez-Rodríguez G.A. (2019). Effect of photocatalytic Fe_2O_3 nanoparticles on urban runoff pollutant removal by permeable concrete. *Journal of Environmental Management*, vol. 242, 487-495. Doi: 10.1016/j.jenvman.2019.04.104

Piñon-Colin T., Rodríguez-Jimenez R., Rogel-Hernández E., Álvarez-Andrade A., Wakida F.T. (2020). Microplastics in stormwater runoff in a semiarid region, Tijuana, Mexico. *Science of the Total Environment*, vol. 704, 135411. Doi: 10.1016/j.scitotenv.2019.135411

Prodanovic V., Hatt B., McCarthy D., Zhang K., Deletic A. (2017). Green walls for greywater reuse: Understanding the role of media on pollutant removal. *Ecological Engineering*, vol. 102, 625-635. Doi: 10.1016/j.ecoleng.2017.02.045

Prodanovic V., Wang A., Deletic A. (2019). Assessing water retention and correlation to climate conditions of five plant species in greywater treating green walls. *Water Research*, vol. 167, 115092. Doi: 10.1016/j.watres.2019.115092

Prodanovic V., Hatt B., McCarthy D., Deletic A. (2020). Green wall height and design optimisation for effective greywater pollution treatment and reuse. *Journal of Environmental Management*, vol. 261, 110173. Doi: 10.1016/j.jenvman.2020.110173

Reyes R., Bustamante W., Gironás J., Pastén P.A., Rojas V., Suárez F., Vera S., Victorero F., Bonilla C.A. (2016). Effect of substrate depth and roof layers on green roof temperature and water requirements in a semi-arid climate. *Ecological Engineering*, vol. 97, 624-632. Doi: 10.1016/j.ecoleng.2016.10.025

Saadeh S., Ralla A., Al-Zubi Y., Wu R., Harvey J. (2019). Application of fully permeable pavements as a sustainable approach for mitigation of stormwater runoff. *International Journal of Transportation Science and Technology*, vol. 8(4), 338-350. Doi: 10.1016/j.ijtst.2019.02.001

Sandoval G.F.B., Galobardes I., Campos de Moura A., Toralles B.M. (2020). Hydraulic behavior variation of pervious concrete due to clogging. *Case Studies in Construction Materials*, vol. 13, e00354. Doi: 10.1016/j.cscm.2020.e00354

Secretaría de Obras y Servicios del Gobierno del Distrito Federal. (2008). *Normas De Construcción de la Administración Pública del Distrito Federal Construcción e Instalaciones*. Obra Civil en Edificaciones. http://cgservicios.df.gob.mx/prontuario/vigente/r314501.pdf

Selbig W.R., Buer N., Danz M.E. (2019). Stormwater-quality performance of lined permeable pavement systems. *Journal of Environmental Management*, vol. 251, 109510. Doi: 10.1016/j.jenvman.2019.109510

Sims A.W., Robinson C.E., Smart C.C., Voogt J.A., Hay G.J., Lundholm J.T., Powers B., O´Carroll D.M. (2016). Retention performance of green roofs in three different climate regions. *Journal of Hydrology*, vol. 542, 115-124. Doi: 10.1016/j.jhydrol.2016.08.055

Skorobogatov A., He J., Chu A., Valeo C., van Duin B. (2020). The impact of media, plants and their interactions on bioretention performance: A review. *Science of the Total Environment*, vol. 715(1), 136918. Doi: 10.1016/j.scitotenv.2020.136918

Smyth K., Drake J., Li Y., Rochman C., Van-Seters T., Passeport E. (2021). Bioretention cells remove microplastics from urban stormwater. *Water Research*, vol. 191(1), 116785. Doi: 10.1016/j.watres.2020.116785

Tavakol-Davani H., Tavakol-Davani H., Burian S.J., McPherson B.J., Barber M.E. (2019). Green infrastructure optimization to achieve predevelopment conditions of a semiarid urban catchment. *Environmental Science Water Research & Technology*, 5, 1157-1171. Doi: 10.1039/c8ew00789f

Tirpak R.A., Afrooz A.R.M.N., Winston R.J., Valenca R., Schiff K., Mohanty S.K. (2021). Conventional and amended bioretention soil media for targeted pollutant treatment: A critical review to guide the state of the practice. *Water Research*, vol. 189(1), 116648. Doi: 10.1016/j.watres.2020.116648

U.S. Environmental Protection Agency (US EPA, 1999). *Storm Water Technology Fact Sheet: Porous Pavement*. EPA 832-F-99-023.

Vijayaraghavan K., Biswal B.K., Adam M.G., Soh S.H., Tsen-Tieng D.L., Davis A.P., Chew S.H., Tan P.Y., Babovic V., Balasubramanian R. (2021). Bioretention systems for stormwater management: Recent advances and future prospects. *Journal of Environmental Management*, vol. 292, 112766. Doi: 10.1016/j.jenvman.2021.112766

Wanielista M., Chopra M., Spence J., Ballock C. (2007). *Hydraulic performance assessment of pervious concrete pavements for stormwater management credit*. Final report, University of Central Florida. 81 p. https://rmc-foundation.org/wp-content/uploads/2017/07/PerformanceAssessmenFBD13pdf.pdf

Winston R.J., Dorsey J.D., Hunt W.F. (2016). Quantifying volume reduction and peak flow mitigation for three bioretention cells in clay soils in northeast Ohio. *Science of the Total Environment*, 553, 83-95. Doi: 10.1016/j.scitotenv.2016.02.081

Xie N., Akin M., Shi X. (2019). Permeable concrete pavements: A review of environmental benefits and durability. *Journal of Cleaner Production*, 210, 1605-1621. Doi: 10.1016/j.jclepro.2018.11.134

Xu Y., Jin R., Hu L., Li B., Chen W., Shen J., Wu P., Fang J. (2020). Studying the mix design and investigating the photocatalytic performance of pervious concrete containing TiO_2-Soaked recycled aggregates. *Journal of Cleaner Production*, vol. 248, 119281. Doi: 10.1016/j.jclepro.2019.119281

Yahia A., Kabagire D. (2014). New approach to proportion pervious concrete. *Construction and Building Materials*, 62, 38-46. Doi: 10.1016/j.conbuildmat.2014.03.025

Yang J., Wang Z.H. (2017). Planning for a sustainable desert city: The potential water buffering capacity of urban green infrastructure. *Landscape and Urban Planning*, vol. 167, 339-347. Doi: 10.1016/j.landurbplan.2017.07.014

Zahmatkesh Z., Burian S.J., Karamouz M., ASCE F., Tavakol-Davani, Goharian E. (2015). Low-Impact Development Practices to Mitigate Climate Change Effects on Urban Stormwater Runoff: Case Study of New York City. *Journal of Irrigation Drainage Engineering*, 141(1), 04014043. Doi: 10.1061/(ASCE)IR.1943-4774.0000770

Zhang Q., Wang X., Hou P., Wan W., Li R., Ren Y., Ouyang Z. (2014). Quality and seasonal variation of rainwater harvested from concrete, asphalt, ceramic tile and green roofs in Chongqing, China. *Journal of Environmental Management*, vol. 132, 178-187. Doi: 10.1016/j.jenvman.2013.11.009

Zhang K., Yong F., McCarthy D.T., Deletic A. (2018). Predicting long term removal of heavy metals from porous pavements for stormwater treatment. *Water Research*, vol. 142(1), 236-245. Doi: 10.1016/j.watres.2018.05.038

Zhang Z., Szota C., Fletcher T.D., Williams N.S.G., Farrell C. (2019). Green roof storage capacity can be more important than evapotranspiration for retention performance. *Journal of Environmental Management*, vol. 232, 404-412. Doi: 10.1016/j.jenvman.2018.11.070

Zhang L., Lu Q., Ding Y., Wu J. (2021a). A procedure to design road bioretention soil media based on runoff reduction and pollutant removal performance. *Journal of Cleaner Production*, vol. 287, 125524. Doi: 10.1016/j.jclepro.2020.125524

Zhang S., Lin Z., Zhang S., Ge D. (2021b). Stormwater retention and detention performance of green roofs with different substrates: Observational data and hydrological simulations. *Journal of Environmental Management*, vol. 291, 112682. Doi: 10.1016/j.jenvman.2021.112682

Zölch T., Henze L., Keilholz P., Pauleit S. (2017). Regulating urban surface runoff through nature-based solutions – An assessment at the micro-scale. *Environmental Research*, 157, 135-144. Doi: 10.1016/j.envres.2017.05.023

Zúñiga-Estrada M.A., Vázquez-Rodríguez G.A., Ramírez-Cardona M., Lizárraga-Mendiola L. (2020). Mineralogical evidence of unfavorable geochemical interactions between urban runoff pollutants and filter materials in low-impact systems. *Journal of Hazardous Materials*, 390, 122136. Doi: 10.1016/j.jhazmat.2020.122136

Chapter 10 Microencapsulation of acachul (*Ardisia Compressa)* extract by spray drying using diferente polymeric materials as encapsulating agents

Capítulo 10 Microencapsulación de extractos de acachul (*Ardisia Compressa*) mediante secado por aspersión utilizando diferentes materiales poliméricos como agentes encapsulantes

SANTACRUZ-VÁZQUEZ, Claudia†* & SANTACRUZ-VÁZQUEZ, Verónica

Benemérita Universidad Autónoma de Puebla. Faculty of Chemical Engineering. Departamento de Alimentos. Boulevard 18 Sur y Av. San Claudio. Ciudad Universitaria. Puebla, Pue. México

ID 1st Author: *Claudia, Santacruz-Vázquez* /**ORC ID**: 0000-0001-6660-469X, **CVU CONACYT**: 70094

ID 1er Co-author: *Verónica, Santacruz-Vázquez* / **ORC ID**: 0000-0003-0527-5815, **CVU CONACYT**: 70091

DOI: 10.35429/H.2021.6.147.159

C. Santacruz & V. Santacruz

claudia.santacruz@correobuap.mx

A. Marroquín, J. Olivares, M. Ramírez and L. Cruz (Coord) Engineering and Technology. Handbooks-©ECORFAN-México, Querétaro, 2021.

Abstract

The microencapsulation process is a technique whose purpose is to protect liquid, solid and gaseous compounds susceptible to thermal, light or oxidative deterioration, among other factors. The particular substance may be individually coated with an encapsulating material to protect it from the environment, from the reaction with other compounds or to prevent oxidation reactions from light or oxygen present in its surroundings. There is a wide variety of biopolymeric materials used as barrier materials for encapsulation. Among the materials that serve as encapsulating or entraining agents are carbohydrates, lipids, proteins and polymers, while the active or encapsulated compounds may be antimicrobials, pigments, vitamins, minerals or microorganisms. Therefore there is a need to find the best option, to encapsulate the desired active ingredients using different biopolymeric materials as barrier materials. Whence, in the present work, the effect and characteristics from acachul (*Ardisia Compressa*) pigments were determined, encapsulated them using maltodextrin, gum arabic and a combination of gum arabic- maltodextrin in a 1:1 ratio as encapsulating agents. Determining that acachul (*Ardisia Compressa*) pigments were better encapsulated when maltodextrin was utilized as the encapsulating agent.

Microencapsulation, Pigments, Encapsulation agents, Acachul

Resumen

El proceso de microencapsulación es una técnica que tiene como finalidad proteger, líquidos, sólidos y gaseosos susceptibles al deterioro térmico, lumínico, oxidativo, entre otros. La sustancia en particular puede ser cubierta de manera individual con un material encapsulante para protegerla del ambiente, de la reacción con otros compuestos o para impedir que sufran reacciones de oxidación debido a la luz o al oxígeno presentes en su entorno. Existe una gran variedad de materiales biopolímericos como materiales de barrera utilizados para la encapsulación. Entre los materiales que sirven como agentes encapsulantes o de arrastre se encuentran los carbohidratos, lípidos, proteínas y polímeros, mientras que los agentes activos o encapsulados pueden ser antimicrobianos, pigmentos, vitaminas, minerales o microorganísmos. Por lo que existe la necesidad de encontrar la mejor opción, para encapsular los ingredientes activos deseados utilizando diferentes materiales biopoliméricos como materiales de barrera. Por lo que en el presente trabajo, se determinó el efecto y características que presentan los pigmentos de acachul (*Ardisia Compressa*). Encapsulados al utilizar maltodextrina, goma arábiga y una combinación de goma arábiga-maltodextrina en proporción 1:1 como agentes encapsulantes. Determinando que los pigmentos de acachul (*Ardisia Compressa*) fueron mejor encapsulados al utilizar maltodextrina como agente encapsulante.

Microencapsulación, Pigmentos, Agentes encapsulantes, Achachul

1 Introducción

Nowadays, consumers demand nutritious and functional products that also contribute to consumer health. For such reason, food and coloring industries have been subject to making changes in reformulation of their products and searching for new alternatives that do not affect consumers health maintaining the desired characteristics of food. For this reason, natural pigments of vegetable origin (carotenoids, chlorophylls, phenolic pigments: flavonoids, anthocyanins, tannins, and betalains) have been chosen as substitutes for artificial colors. In addition to the above, Mexico has a wide range of plant sources with attractive colors that are due to the presence of compounds (anthocyanins) found in the epidermal tissues of flowers and fruits mainly, which provide red, orange, blue and purple colors. By geographical location, in north of Puebla State an endemic fruit called Acachul (*Ardisia compressa*) is produced, which is cultivated in the municipalities of Xicotepec, Tlaxco, Zihuatehutla, Tlacuilotepec, Jalpan and Pahuatlán all of them belonging to northern zone of Puebla State, Mexico (SAGARPA, 2018). This fruit is not entirety exploited, being commonly used as raw material for elaboration of artisan wines, thereby opening a field of application for obtaining natural coloring, having with it an economic and social benefit for producers of Acachul fruit expanding the market and encouraging its production to prevent this endemic crop from being lost by giving it a new added value and greater use.

Therefore, importance of this research lies fundamentally in using polymeric agents as protective coatings of interest compounds (anthocyanins) and by means of spray drying used as a micro-encapsulation technique to obtain a natural powder pigment and thuscarrying out its physicochemical characterization, determining stability conditions for its application in food systems.

2 Theoretical Fundaments

2.1 Acachul (*Ardisia compressa*)

In northern region of Puebla State, Acachul bush (*Ardisia compressa*) is cultivated, which is a plant that is still in its natural agro-ecosystem. The municipalities Xicotepec, Tlaxco, Zihuatehutla, Tlacuilotepec, Jalpan and Pahuatlán are the main producers with a production of 60 tons per year, including 30 hectares area for this activity (SAGRAPA, 2018).

Acachul (*Ardisia compressa*) belongs to *Myrsinaceae* family, it is described as a shrub 1 to 3 m high, it has round or elliptical-lanceolate leaves of 10 to 20 cm, with entire or serulated edge, with smooth textures above and below. Flowers are pinkish-white in color and produce edible globose fruit. The seed or wild fruit is similar to a bunch of grapes, which contains a single seed, its flavor is sour-sweet, similar in size to blueberry, one of its main characteristics is that it has a high content of anthocyanin compounds and can be used to obtaining a natural pigment (Vázquez., *et al*. 2019, Vázquez., *et al.* 2021).

2.2 Pigments

Color is an important factor in determining the attractiveness of most foods, color is often used as an index of freshness and good condition. Unfortunately, color can change during processing, storage, or preparation, thereby reducing food quality. So controlling, changing and stabilizing food color is one of the main goals of food scientists and technologists.

2.3 Anthocyanins

Anthocyanins, alike flavonoids and betalains, are water-soluble pigments with glycoside characteristics, they are made up of an anthocyanidin molecule, which is aglycone, to which a sugar is attached through a β-glucosidic bond. Basic chemical structure of these aglycones is the flavillium ion, which consists of two aromatic groups: a benzopyryl (A) and a phenolic ring (B); Due to its trivalent position of oxygen, flavillium normally functions as a cation (Aguilera, *et al.* 2011). Currently about 20 anthocyanins are known, the most important of which are perlargonidin, delphinidin, cyanidin, petunidin, peonidin and malvidin. It is very common that an anthocyanidin interacts with more than one carbohydrate to form different anthocyanins (Barragán, *et al*., 2018). Anthocyanins have become an interesting option for food industry, as possible substitutes for synthetic colorants. Additionally, these substances exhibit an added value due to their antioxidant and cytotoxic capacity (Cassidy, 2018). In addition to the above, the expanded interest in anthocyanic compounds has become known, knowing that they play an important role in reducing coronary heart disease, cancer, diabetes, anti-inflammatory effects and improvement of visual acuity. Likewise, they are considered potential agents in obtaining products with added value for human consumption (Garzón, 2008; Nardini & Garaguso, 2020). Consequently, demand for acquiring these compounds has increased, which leads to search for new techniques for obtaining anthocyanins on large scale, which is why the use of spray drying has been directed mainly; which has led to studies of separation, structural characterization and quantification of obtained anthocyanins (Guerra and Ortega, 2006).

2.3.1 Color and stability of anthocyanins

One of best known and most widespread functions of anthocyanins is to provide flowers with color, making them more attractive to pollinators. Considerable effort has been made to explain color variations exhibited by anthocyanins in plants; various factors such as concentration and nature of anthocyanidin, equilibrium forms of anthocyanidin, glycosylation or acylation, nature and concentration of co-pigmentation, metal complexes, intra- and intermolecular association mechanisms, and the influence of external factors such as pH, salts, among others, have been shown to have a certain impact on coloration of anthocyanins.

Role of anthocyanins and flavones to provide angiosperm flowers with a stable blue color has been recently studied, finding that anthocyanin with the greatest presence is delphinidin, and that co-pigmentation with a specific flavone was most common mechanism to transform the mauve color of delphinidin glycosides to blue hues. One of the first systematic reports on the role of pH in chemical stability of anthocyanins, found that anthocyanins slightly diluted at typical pH values of various foods, in a range of 3 to 6, resulted in being almost completely hydrated to obtain Colorless carbinol pseudobases, while the flavyl ion exists mostly at pH values below 2.0 (Nollet & Toldrá, 2013).

2.3.2 Anthocyanin degradation mechanisms

Aside from typical factors, species, agronomic and environmental factors, which affect anthocyanin content in fruits, its processing prior to consumption significantly influences total content in final product. Thermal processing is one of the most common processes, involving heating to temperatures between 50 and 150 ° C, depending on pH of the product and desired shelf life. Given their potential, technical or benefits they could bring to human health, chemical stability of anthocyanins is a focus point for many assays and analyzes.

As scrutinized, it has been observed that anthocyanins stability depends not only on processing temperature, but also on intrinsic properties of the product such as its pH, storage temperature, chemical structure and anthocyanin concentration, as well as presence of light, oxygen, enzymes, proteins, and metal ions.

2.3.3 Nutritional and health aspects related to anthocyanins

Interest in anthocyanins for use as nutritional supplements in the daily diet of humans has increased. It is postulated that regular consumption of anthocyanins and other polyphenols from fruits, vegetables, wines, jellies, and preserves, is associated with a possible reduction in risk of chronic diseases such as cancer, cardiovascular diseases, viral inhibition, and Alzheimer's (Rangel Huerta *et al.,* 2015) Anthocyanins, as well as other flavonoids, are considered important nutraceuticals due to their antioxidant effects, which give them a potential role in prevention of various diseases related to oxidative stress. There are several studies channelized to identify that anthocyanins and other flavonoids present in food have effects in the diet, analyzing their bioavailability, their metabolism, pharmacokinetics of their action, and safety of their consumption.

Current knowledge about molecular actions of anthocyanins to chemoprevent cancer is divided into: antioxidat mechanism, molecular mechanisms of anticarcinogenesis, and molecular mechanism that involves the induction of apoptosis of tumor cells (Khoo, *et al*., 2017)

2.3.4 Anthocyanins as food coloring

In addition to interest about the effects of anthocyanins on human health, there is a widespread interest in using them as food colorants. Due to the fact that these are obtained from natural sources, consumers show a certain proclivity towards this type of substances compared to synthetic colorants, which, at the same time, have limitations established by corresponding legislation. Extensive studies related to common food colorants, derived from anthocyanins, qualitative and quantitative aspects of anthocyanins used in food, and their physicochemical properties (color characteristics and stability), have been carried out along over years regarding information on the subject of application of these compounds.In cases where anthocyanins are present as part of the ingredients of the product, they undergo various transformations that lead such product acquires typical colors. Commonly, colorants that are sought to be substituted with use of anthocyanins are those that present shades between red and purple. However, biggest problem related to their use is pH control in products where they are applied, their susceptibility to thermal processing and low stability during storage. Existing legislations do not indicate specific sources from which anthocyanins, to be used as colorants, must be extracted, they simply define acceptable procedures for their extraction. Extractions carried out with acidified water, methane and ethanol are those that present a greater acceptance for this purpose. Extracts obtained by these methods are known to also contain sugars, tannins, minerals and other interfering compounds. Anthocyanin fraction, even though it can be recovered from various types of fruits and vegetables, commonly grapes, strawberry, black currant, purple cabbage and others, for economic reasons, is obtained mainly from by-products derived from the wine industry, especially the peel of grape.

A well-known commercial compound, derived from this latter matrix, distributed and used globally in Europe, Asia, and North America, is enocyanin. Extracts of black carrots, known to reach concentrations of 1,700 mg / kg of fresh product, as well as dried and deodorized extracts of purple cabbage, are also widely used in beverages, candies, ice cream, jellies and jams, in addition to light drinks (Nollet & Toldrá, 2013).

3. Methodology to be developed

3.1. Project development location

Development of this research was carried out in the city of Puebla de Zaragoza, Puebla, in the Food Laboratory facilities FIQ4 / 105 of the Chemical Engineering Department and University Center for Entailment and Technology Transfer (CUVyTT) of the Benemérita Universidad Autónoma de Puebla (BUAP).

3.2. Collection of biological material

Acachul *(Ardisia Compressa)* in a commercial maturity state, was collected in municipality of Xicotepec de Juárez, located in northwestern part of Puebla state. Fruits were stored in hermetic polyethylene bags labeled with date and place, after harvesting they were stored at -4 ° C until use for experimentation.

3.3 Characterization of fresh Acachul fruit

3.3.1 Determination of total soluble solids (TSS)

Determination of TSS was resolved in fruit stored at -4 ° C, methodology consisted of pressing a piece of fruit to extract a few drops of juice, considering the equatorial zone of fruit. Using a model PAL-1 digital refractometer at 20 ° C, prism of the refractometer was supported in a fixed place to ensure that juice is distributed evenly.

3.3.2 Color determination

Colorimetry is a non-destructive physical method widely used to determine color of a sample. To measure color (color saturation) a calibrated Hunterlab Model D25A-9000 colorimeter was used, it provides the achromatic parameters or coordinates L * wich is luminosity or clarity and represents whether a color is dark, gray or light, varying from zero to a black up to 100 for white and the chromatic coordinates a * and b * form a plane perpendicular to L *, a * coordinate corresponds to red if a *> 0, or green if a * <0. The b * coordinate corresponds to yellow if b *> 0, and blue if b * <0.

3.3.3 pH Determination

pH was determined using a digital potentiometer pH-meter brand Conductronic model pH10, previously calibrated, using buffer solutions (pH = 4 and pH = 7), 6 g of fruit were taken and homogenized with 10 mL distilled water. All measurements were carried out in triplicate and result was expressed as average value of determinations.

3.3.4 Preliminary treatment of Acachul fruit

Acachul fruit *(Ardisia Compressa)* was previously washed and sanitized using chlorine at 100 ppm, forthcoming seed was manually separated from the pulp. Subsequently, quantity to be occupied was weighed on a precision electronic balance. To obtain juice of acachul fruit, a Hamilton Beach juice extractor model: 67608 was used, to which 10% (w / v) of encapsulating agents were incorporated with respect to the amount of juice obtained, for which Three samples were prepared with two different biopolymers (Gum arabic brand Fabpsa and Maltodextrin 10D Meyer) and a combination of both in relation (1: 1), incorporation of encapsulating agents was carried out slowly by stirring, using an electronic stirrer model: 102 at 7500 rpm speed following by a vacuum filtration, using a kitasato flask, filter paper, Buchner funnel, vacuum pump, to eliminate the larger pulp residues that could clog nozzles of spray dryer atomizer

3.4 Microencapsulation by spray drying

To encapsulate desired active ingredient (natural acachul pigments), different biopolymeric materials were used as barrier materials, in different proportions, having three treatments as mentioned below in Table 10.1.

Table 10.1 Encapsulating agent used in experimentation

Treatment	Encapsulating agent	Proportion tested
A	Maltodextrin	10% weigth in volume
B	Arabic Gum	10% weigth in volume
C	Arabic Gum- Maltodextrin	10% weigth in volume in proportion 1:1

For spray drying, a Prendo brand spray dryer with serial number 1212IA900054A (Mexico) was utilized, which uses a parallel flow pressure nozzle atomizer. Using different encapsulating agents as barrier materials, such as maltodextrin, arabic gum, and a combination of maltodextrin and arabic gum. Samples were placed for feeding through a peristaltic pump, where drying consists of atomizing the juice generating small droplets, which are microencapsulated by a hot air stream. Being independent variables to control the inlet temperature (140 ° C), feed flow of the sample (3 mL / min), air flow of 10 l / min at a pressure of 5 mm Hg. At the moment in which the drops of acachul juice come into contact with hot air, temperature balance and partial vapor pressure between liquid and gas phases is established. Therefore heat transfer takes place from air to the product as a result of temperature difference while water transfer takes place in the opposite direction due to vapor pressure difference, after that, droplets evaporation is carried out at constant temperature and at partial pressure of water vapor. When water content of droplet reaches a critical value, a dry crust forms on droplet surface, drying rate decreases rapidly and becomes dependent on rate of water diffusion through crust. Drying is theoretically finished when particle temperature is the same as that of the air, passing encapsulated product to a collector. Product (powder) dried by spraying and encapsulated by using different encapsulating agents, was stored in amber vials incorporating N2, which provides an inert atmosphere to avoid reactions of biological material during storage (figure 10.1).

Figure 10.1 Microencapsulation by spray drying

3.5 Characterization of natural pigment

3.5.1 Determination of water activity (a_W)

a_W was determined in an AquaLab equipment, model series 3TE, determination consisted of placing pigment in sample tray, introducing sample and then turning knob to the left to place it in reading position, afterwards withdrawing sample when equipment alarm activates with an intermittent sound.

3.5.2 Water content determination

Water content was determined in an Ohaus brand thermobalance, model MB45 which uses halogen as a heating source, equipment works on the basis of thermogravimetric principle: at the beginning of measurement, moisture analyzer determines sample weight, sample is heated by means of the halogen drying unit and moisture evaporates. During drying operation equipment continuously determines sample weight and presents the result expressed in % of moisture content. Therefore, 0.5 g of sample were placed reaching a temperature of 150 ° C for determination.

3.5.3 Color determination

Color was determined in a Hunterlab model D25A-9000 colorimeter, which was previously calibrated. From the reflection spectra, color coordinates of CIELab system were obtained, each color reading represents the average of three readings made L *, a * and b *. Subsequently, with values obtained from the coordinates, color index (IC *) is determined as a reference of tonality acquired by the simple.

3.5.4 Scanning electron microscopy (SEM)

To evaluate the quality of encapsulated product and the shape of particles obtained, a Jeol JSM-5900LV brand scanning electron microscope, Scanning Electron Microscopy, was used. Samples were placed in sample holder with the help of double-sided carbon tape.
However, as it is a material of biological nature, it was coated with gold (Au) under vacuum in a DENTON VACUUM model DESK V equipment, which gives conductive property to samples, they are protected from collapse by vacuum generated and breakage by the incidence of electrons beam. Particles were studied at magnifications ranging from 1000X to 20,000X.

3.5.5 Determination of total anthocyanins by spectrophotometry

To evaluate the total anthocyanin content of Acachul *(Ardisia compressa)* in all three treatments (a, b and c), a Pharo Merck spectrophotometer was used, scanning at a wavelength from 200 to 600 nm range in which anthocyanins are identified. . Pigment content was calculated as cyanidin-3-glucoside, using an extinction coefficient of 26900 and molecular weight of 449.2, using formula (1) for anthocyanidin quantification.

$$AT\left(\frac{mg}{100g}\right) = \frac{A \cdot PM \cdot FD \cdot 1000}{w \cdot \epsilon} \quad (1)$$

Where: A: is the absorbance; MW: molecular weight; FD: dilution factor; w: sample weight occupied; E: molar extinction coefficient; AT: total anthocyanins expressed in milligrams per 100 grams of fresh fruit.

For samples preparation, a solution of methanol: water: formic acid (70: 28: 2) was used for anthocyanins extraction.

Procedure consisted of weighing 1 g of pigment and depositing it in a mortar, subsequently, 30 mL of acidified methanol was added for further extraction and solubilization, thus obtaining a mother solution. From this solution, 1mL is taken which is added again to 9 mL of acidified methanol solution as well as FD 10 (this was performed for all three treatments), making a scan of 200-600 nm, using distilled water as a blank.

3.5.6 Hygroscopicity determination

Closed systems were used with saturated solutions of different salts that generate different relative humidities at a temperature of 20 ° C, according to what was described in 1980 by Rockland and Nishi. Procedure was carried out for three different treatments, which consisted of placing 0.2 g of sample obtained from each treatment in closed desiccators. Thereafter, closed containers were stored during six days in an extraction hood at 22 ° C temperature and 88% relative humidity, determining the value of water activity (a_w) before and after established time.

Table 10.2 Relative humidity generated by different salts used to determine hygroscopicity at 20 ° C.

Salt	Relative Humity (%) at 20°C
Sodium Hidroxide	8.9
Magnesium Cloride	33.0
Sodium Cloride	75.5
Potassium Sulfate	97.5

3.5.7 Density determination

The method was follow through as described by Papadakis (2006), using a Denver Instrument model TP-214 digital scale (previously calibrated), a 10 mL cylinder, xylene and the sample. Methodology that will be described below was carried out on three treatments. 0.5g of xylene was placed in a 10 mL graduated cylinder, then 0.2 of the pigment was added, this is tapped lightly on work table 10 times at a height of 10 cm. Once the solute has been completely diluted, density is determined. Density is calculated by dividing powder mass between final volume occupied in test tube, formula (2).

$$D = {}^{m}/_{v}. \tag{2}$$

Where: D = density; m: mass; v: volume.

3.5.8 Reconstitution Test

To maintain the efficiency of spray drying process, it is important to ensure that final product will have a rapid and complete rehydration in different media, be it aqueous or in some other type of solvent. For reconstitution or rehydration it involves four conditions: ability to moisturize, ability to submerge, agility to disperse into independent particles in solvent, solubilization. For these conditions, morphology of particles plays an important role in terms of rehydration capacity in spray-dried products. Particles have less rough surfaces and greater sphericity, which gives a smaller surface for water absorption, compared to products that present greater roughness and therefore greater surface available for water absorption. Reconstitution test was carried out using a beaker with a 120 mL aqueous solution (H_2O), and 2 g of pigment (powder), at temperatures of 25, 30, 50 and 80 ° C, determining precipitation time of powder in water. This measurement will indicate the time required to wet samples of natural pigment powder in its entirety. Determination of immersion time was made by using a Casio brand digital chronometer (Model 1121. Manufactured in Mexico).

4 Results

4.1 Physicochemical characterization of fruit and encapsulated pigment

Table 10.3 shows average values and standard deviation of pH, soluble solid content (°Bx) moisture content (%) of fresh acachul fruit *(Ardisia compressa)* stored at a refrigeration temperature of -4 °C

Table 10.3 Physicochemical characterization of Acachul *(Ardisia compressa)*

pH	ºBrix	Moisture Content (%) (%)
3.48 ± 0.72	7.8 ± 0.3	77.45± 2.92

4.2 Characterization of Acachul pigment *(Ardisia compressa)* obtained by spray drying

Table 4 shows water activity and moisture content (%) of powdered acachul fruit once spray drying has been carried out, using an inlet air temperature of 140 ° C, with a feed of (3 mL / min) and 5mm Hg air pressure. Results indicate that regardless of polymeric material used to encapsulate the product, acachul is a product with a water activity of around (0.348 ± 0.004), and a variable moisture content depending on the encapsulating agent to be used. So it can be said that stability of encapsulated pigment depends on the encapsulating agent to be used. As can be seen in Table 10.4, it is observed that treatment C when using maltodextrin as an encapsulating agent, moisture content of product is 7.8%, a moisture content lower than that obtained when using treatment A or B.

Furthermore, it is considered that the product encapsulated with maltodextrin, has a lower proliferation capacity of deteriorative microorganisms compared to other treatments.

Table 10.4 Results of Water Activity (a_w) and moisture (%) of powdered acachul fruit

Treatment	(a_w)	Moisture Content (%)
A	0.364 ± 0.009	12.01 ± 0.14
B	0.323 ± 0.004	14.41 ± 0.39
C	0.358 ± 0.004	07.80 ± 0.27

4.2.1 Color determination

Cielab color parameters (L, a, b) of powdered acachul obtained from spray drying, when using different encapsulating agents, are presented in Table 10.5, being these parameters the following.

Table 10.5 Color parameters of CIELab system and color index (IC *) obtained from the treatments (A, B and C) obtained by spray drying

Colorimetry	Treatment		
	A	B	C
L*	43.02 ± 0.02	43.12 ± 0.01	38.82 ± 0.01
a*	31.40 ± 0.03	29.52 ± 0.03	30.86 ± 0.1
b*	-3.78 ± 0.06	-4.68 ± 0.09	-3.80 ± 0.08
IC*	-192.94 ± 3.5	-146.18 ± 2.94	-209.80 ± 3.77

4.2.2 Scanning electron microscopy (SEM) of powders

In figure 10.2, morphology of microcapsules can be observed in treatments (A, B and C) that were used to microencapsulate anthocyanins at a concentration of 10% at a temperature of 140 ° C. Microcapsules are of variable size and shape, that is to say, there are capsules with a smooth spherical shape and capsules with a dented or irregular surface. Variation in particle size ranges from 2,209 µm to 21,715 µm. Even in the size variation it was not isotropic.

Figure 10.2 Scanning electron microscopy photomicrographs of acachul pigment microcapsules from Acachul *(Ardisia Compressa),* obtained by spray drying for the different treatments.

Treatment A	**a)**1000x	**b)** 5000x **c)** 10000x
Treatment B	**d)** 1000x	**e)** 5000x **f)** 10000x
Treatment C	**g)** 1000x	**h)** 5000x **i)** 10000x

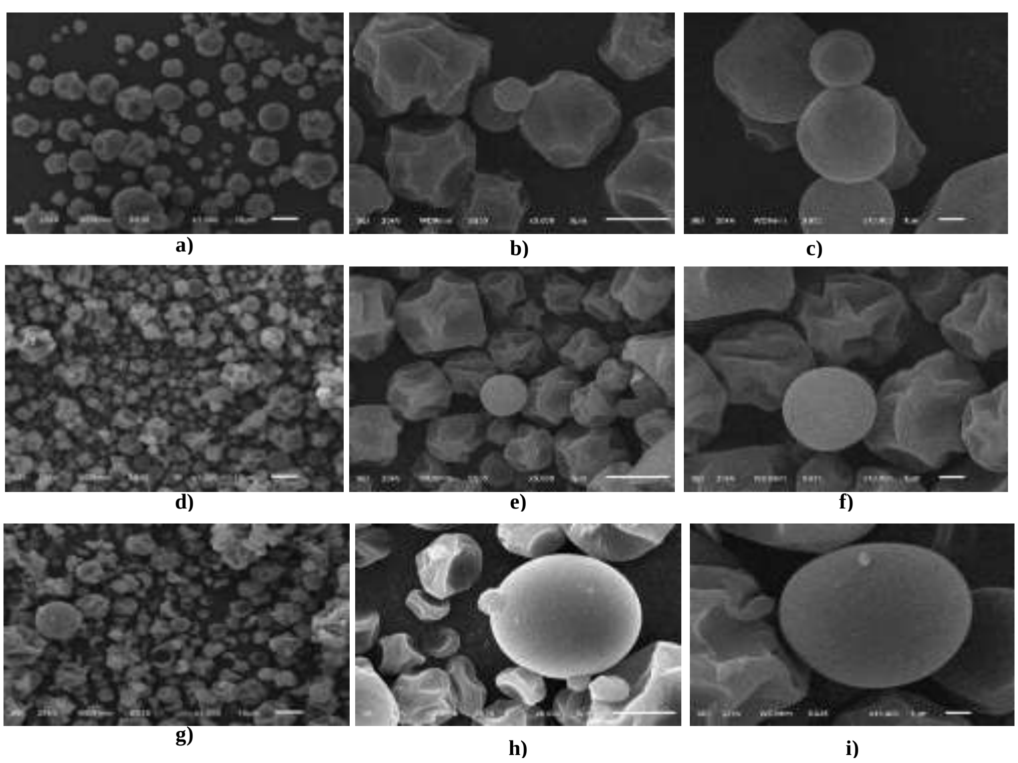

Treatments B and C present spherical particles with smooth surfaces and semi-uniform sizes, observing anisotropic shapes, that is, irregular shapes on the surface, this behavior is due to the fact that particles present deformation and fracture in their structure, attributable to vacuum generated in scanning electron microscope observation chamber for electron beam scanning. Formation of dents on capsule surface can be attributed to contraction of particles during drying, due to drastic loss of moisture followed by cooling. In general, for three treatments carried out, it is observed that particles do not reach a size at the nanometric level, since there are particles with size greater than 1 µm.

4.2.3 Determination of total anthocyanins (TA)

Determination of total anthocyanins was accomplish at (λ) 523nm wavelength. Wavelength that presents response at 523 nm corresponding to cyanidin-3-glucoside (Total anthocyanin content) expressed in mg per 100 g of fresh fruit. Results of absorbance and total anthocyanins (AT) for fresh fruit and treatments A, B and C, are presented in Table 10.6.

Table 10.6 Absorbance results (A) obtained by spectrophotometry to determine total content of anthocyanins (AT)

Treatment	λ nm	A	AT (mg/100 g)
A	523	0.4434	82.76
B	523	0.4986	93.57
C	523	0.3232	60.62
Fresh fruit	523	0.8392	157.53

4.2.4. Hygroscopicity

A measure of the degree of hydration of the sample under different moisture content atmospheres is the determination of the hygroscopicity under different atmospheres of relative moisture content, represented by isotherms of the different encapsulation treatments at storage temperature at 20 ° C. As can be seen in graphic 10.1, it is observed that treatment

A presents a higher hygroscopicity condition than treatments B and C, a behavior that is attributable to the fact that in treatment B (Encapsulated with Gum Arabic), water molecules intertwine with product components due to formation of hydrogen bonds in competition with water solute bonds due to the fact that the polar groups –OH and H behave as active sorption centers. According to results obtained, it could be considered that the product should be kept at a relative moisture content of less than 33% at room temperature to prevent deterioration reactions and prevent the product from hydrating, showing the appearance of wet powder or with agglomerate formation characteristics due to hydration of powdered product, which will affect its stability and reduce its shelf life significantly.

Graphic 10.1

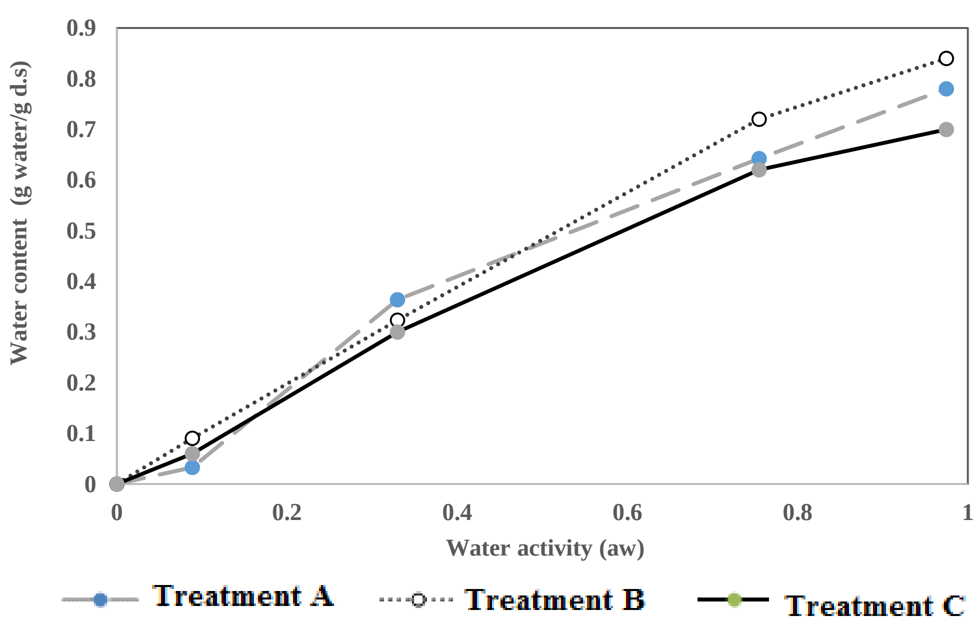

4.2.5. Reconstitution

Reconstitution time of dehydrated powder pigment in an aqueous medium to determine the behavior of the dehydrated product when it is subjected to rehydration with water, was carried out at rehydration water temperatures of 25, 30, 50 and 80 ° C, results that are presented in Table 10.7.

Table 10.7 Pigment reconstitution time obtained by spray drying with different encapsulating agents

Temperature (ºC)	Treatment A	Treatment B	Treatment C
25	24	24	27
30	22	23	26
50	21	22	23
80	9	21	14

As can be seen from Table 10.7, it is observed that time to effect the dissolution of the powdered pigment is inversely proportional to time used in the reconstitution. This behavior is attributable to the fact that surface tension of water decreases with temperature, since the cohesion forces decrease with increasing water temperature. Influence of the external environment is due to the fact that the molecules of the environment exert attractive actions on the molecules located on the surface of the liquid, counteracting the actions of the molecules of the liquid.

4.2.6 Apparent density

Apparent density of obtained product is the ratio of mass and its volume, including the volume contribution of the empty space between particles. Consequently, apparent density depends on both density of the powder particles and the spatial distribution of particles in the powder bed. Properties that determine apparent density of powdered pigment depend on preparation, encapsulating agent used and sample storage, that is to say on the way of handling. Particles can be compacted to have a variable range of apparent densities; however, slightest disturbance to powder bed can cause a change in apparent density. Obtained results are presented in Table 10.8.

Table 10.8 Apparent density of powder pigment when using different encapsulating agents

Treatment	Apparent density (g/ml)
A	1
B	1
C	0.5

From the above table it can be observed that density of encapsulated powder with maltodextrin: arabic gum, has a lower density than when using other encapsulating agents, behavior attributable to the occurrence that empty space between particles is less than when using other encapsulating agents.

Acknowledgment

We are grateful for facilities granted to University Center for Linkage and Technology Transfer (CUVyTT) of Benemérita Universidad Autónoma de Puebla for conducting scanning electron microscopy studies.

Conclusions

Anthocyanins, although they can be recovered from various types of fruits and vegetables, commonly grapes, strawberries, black currants, purple cabbage and others, for economic reasons, are obtained mainly from by-products derived from wine industry, especially the grape peel, therewithal it can be considered that acachul can be a good alternative to obtain these pigments. Analysis of acachul anthocyanin content, reveal to have a significantly high anthocyanin content compared to that reported for other fruits and by other authors, which can make acachul an important source for obtaining this type of pigments, especially to obtain extracts with potential for application as food colorants.

References

Aguilera, M.; Reza, M.C.; Chew, R.G., *et al*. (2011). *Functional Properties of Anthocyanin's. En: Revista de ciencias biológicas y de la salud, 2,* pp. 16-22.

Barragán Condori, M., Aro Aro, J. M., Meléndez, H., Justiniano, V., & Cartagena Cutipa, R. (2018). Antocianinas, compuestos fenólicos y capacidad antioxidante del mio-mio (*Coriaria ruscifolia* L). *Revista de Investigaciones Altoandinas*,*20*(4), 419-428.

Castagnini J. M. (2014). Estudio del proceso de obtención de zumo de arándanos y su utilización como ingrediente para la obtención de un alimento funcional por impregnación a vacío. Instituto Universitario de Ingeniería de alimentos para el desarrollo, Universidad Politécnica de Valencia, España. 175 p.

Cassidy, A. (2018). Berry anthocyanin intake and cardiovascular health. *Molecular aspects of medicine*,*61*, 76-82.

Cömert, E. D., Mogol, B. A., & Gökmen, V. (2020). Relationship between color and antioxidant capacity of fruits and vegetables. *Current Research in Food Science*, 2, 1-10

Ersus, S., y Yurdagel, U. (2007). Microencapsulation of anthocyanin pigments of black carrot (*Daucus Carota L.)* by spray drier. *Journal Food Engineering* (pp. 805-812). España: Elsevier.

Escalona, S. (2005). *Encapsulados de luteina-enocianina y su aplicación en alimentos.* Tesis de licenciatura, Facultad de Ciencias Químicas, Universidad de Chile, Santiago de Chile.

Garzón, G.A. (2008). Las antocianinas como colorantes naturales y compuestos bioactvios. En: Revista *Scielo, 3*, pp. 27- 36.

Guerra, M., y Ortega, G. (2006). Separación, caracterización estructural y cuantificación de antocianinas mediante métodos químicos-físicos. En: *Revista Redalyc.org, 2,* pp. 35-44.

Giuliani, A., Cerretani, L. Cichelli A. 2016. Colors: Properties and Determination of Natural Pigments. Encyclopedia of Food and Health. 273–283.

Hong, S. H., Heo, J.-I., Kim, J.-H., Kwon, S.-O., Yeo, K.-M., Bakowska-Barczak, A. M., Kang, Y.-H. (2013). Antidiabetic and Beta cell-protection activities of purple corn anthocyanins. *Biomolecules & therapeutics*, *21*(4), 284.

Khoo, H. E., A. Azlan, S. T. Tang, S. M. Lim. (2017). Anthocyanidins and anthocyanins: colored pigments as food, pharmaceutical ingredients, and potential health benefits. Review. Food Nutr. Res. 61 (1361779): 1-21

Nardini, M., & Garaguso, I. (2020). Characterization of bioactive compounds and antioxidant activity of fruit beers. *Food chemistry*. *305*, 125437

Nollet, L. M., & Toldrá, F. (2013). *Food Analysis by HPLC* (Third ed.). Boca Raton, Florida, United States of America: CRC Press Taylor & Francis Group.

Rangel-Huerta, O. D., Pastor-Villaescusa, B., Aguilera, C. M., & Gil, A. (2015). A systematic review of the efficacy of bioactive compounds in cardiovascular disease: phenolic compounds. *Nutrients*, 7(7), 5177-5216.

Rockland, L.B. y Nishi, S.K. (1980). Influence of water activity on food product quality and stability. *Food Tech* (pp. 42-51). New York, New York. Marcel Dekker.

Papadakis, E., y Gardeli, C. Tzia C. (2006). Spray Drying of juice concentrate. *Drying Technology*: An International Journal (pp. 173-180). Atenas, Grecia: Taylor

SAGARPA. (2018). Comité Nacional del sistema producto VID. . En: *Secretaria de Desarrollo Rural.*

Vázquez-Sánchez A.Y., Aguilar-Zárate, P., Muñiz-Márquez D. B., Wong-Paz J. E., Romeo-Rojas, J. A. Ascacio-Valdes, G., Martínez-Avila., G. C. G. (2019). Effect of ultrasound treatment on the extraction of antioxidants from *Ardisia compressa* Kunth fruits and identification of phytochemicals by HPLC-ESIMS. Heliyon 5 1-7.

Vázquez-Sánchez, A. Y., Corfield, R., Sosa, N., Salvatori, D., & Schebor, C. (2021). Physicochemical, functional, and sensory characterization of apple leathers enriched with acáchul (*Ardisia compressa Kunth*) powder. *LWT*, *146*, 111472.

[[Title in Times New Roman and Bold No. 14 in English and Spanish]

Surname (IN UPPERCASE), Name 1st Author†*, Surname (IN UPPERCASE), Name 1st Coauthor, Surname (IN UPPERCASE), Name 2nd Coauthor and Surname (IN UPPERCASE), Name 3rd Coauthor

Institution of Affiliation of the Author including dependency (in Times New Roman No.10 and Italics)

International Identification of Science - Technology and Innovation

ID 1st Author: (ORC ID - Researcher ID Thomson, arXiv Author ID - PubMed Author ID - Open ID) and CVU 1st author: (Scholar-PNPC or SNI-CONACYT) (No.10 Times New Roman)

ID 1st Coauthor: (ORC ID - Researcher ID Thomson, arXiv Author ID - PubMed Author ID - Open ID) and CVU 1st coauthor: (Scholar or SNI) (No.10 Times New Roman)

ID 2nd Coauthor: (ORC ID - Researcher ID Thomson, arXiv Author ID - PubMed Author ID - Open ID) and CVU 2nd coauthor: (Scholar or SNI) (No.10 Times New Roman)

ID 3rd Coauthor: (ORC ID - Researcher ID Thomson, arXiv Author ID - PubMed Author ID - Open ID) and CVU 3rd coauthor: (Scholar or SNI) (No.10 Times New Roman)

(Report Submission Date: Month, Day, and Year); Accepted (Insert date of Acceptance: Use Only ECORFAN)

Citation: First letter (IN UPPERCASE) of the Name of the 1st Author. Surname, First letter (IN UPPERCASE) of the First Coauthor's Name. Surname, First letter (IN UPPERCASE) of the Name of the 2nd Co-author. Surname, First letter (IN UPPERCASE) of the Name of the 3rd Co-author. Last name

Institutional mail [Times New Roman No.10]

First letter (IN UPPERCASE) of the Name Publishers. Surnames (eds.) Title of the Handbook [Times New Roman No.10], Selected Topics of the corresponding area © ECORFAN- Subsidiary, Year.

Abstract (In English, 150-200 words)

Text written in Times New Roman No.12, single space

Keywords (In English)

Indicate 3 keywords in Times New Roman and Bold No. 12

1 Introduction

Text in Times New Roman No.12, single space.

General explanation of the subject and explain why it is important.

What is your added value with respect to other techniques?

Clearly focus each of its features

Clearly explain the problem to be solved and the central hypothesis.

Explanation of sections Chapter.

Development of headings and subheadings of the chapter with subsequent numbers

[Title No.12 in Times New Roman, single spaced and bold]

Products in development No.12 Times New Roman, single spaced.

Including graphs, figures and tables-Editable

In the Chapter content any graphic, table and figure should be editable formats that can change size, type and number of letter, for the purposes of edition, these must be high quality, not pixelated and should be noticeable even reducing image scale.

[Indicating the title at the bottom with No.10 and Times New Roman Bold]

Table 1.1 Title

Variable	**Descripción**	**Valor**
V_V	Volumen de Venta	20000
P_V	Postura de venta	490.61
V_C	Volumen de Compra	20000
P_c	Postura de Compra	485.39
P^{Uh}	Precio último Hecho	491.61
V_o	Volumen Operado	1241979
P_u	Precio/Utilidad	0
P^{VL}	Precio/Valor Libro	0
U_a	Utilidad p/Acción	0
V^{La}	Valor Libro p/Acción	0

Source (in italics)
Should not be images-everything must be editable.

Figure 1.1 Title

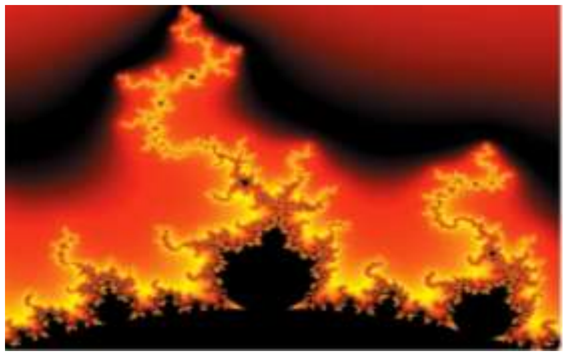

Source (in italics)

Should not be images-everything must be editable.

Graphic 1.1 Title

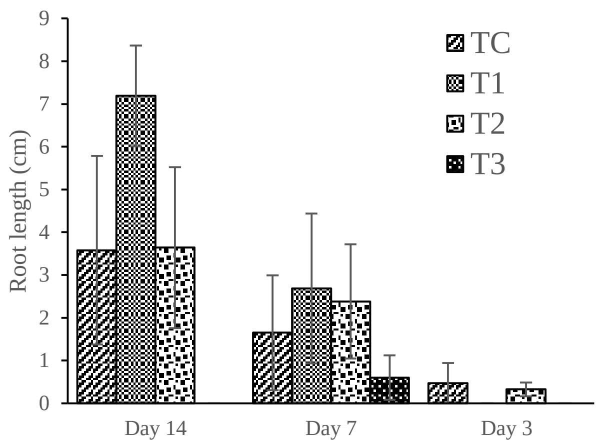

Source (in italics)

Should not be images-everything must be editable.

Each chapter shall present separately in **3 folders**: a) Figures, b) Charts and c) Tables in .JPG format, indicating the number and sequential Bold Title.

For the use of equations, noted as follows:

$$\int_{lim^{-1}}^{lim^{1}} = \int \frac{lim^{1}}{lim^{-1}} = \left[\frac{1\,(-1)}{lim}\right]^{2} = \frac{(0)^{2}}{lim} = \sqrt{lim} = 0 = 0 \rightarrow \propto \quad (1)$$

Must be editable and number aligned on the right side.

Methodology

Develop give the meaning of the variables in linear writing and important is the comparison of the used criteria.

Results

The results shall be by section of the Chapter.

Annexes

Tables and adequate sources

Thanks

Indicate if they were financed by any institution, University or company.

Conclusions

Explain clearly the results and possibilities of improvement.

References

Use APA system. Should not be numbered, nor with bullets, however if necessary numbering will be because reference or mention is made somewhere in the Chapter.

Use Roman Alphabet, all references you have used must be in the Roman Alphabet, even if you have quoted an Chapter, book in any of the official languages of the United Nations (English, French, German, Chinese, Russian, Portuguese, Italian, Spanish, Arabic), you must write the reference in Roman script and not in any of the official languages.

Technical Specifications

Each chapter must submit your dates into a Word document (.docx):

Handbooks title
Chapter title
Abstract
Keywords

Proceedings sections, for example:

1. Introduction
2. Description of the method
3. Analysis from the regression demand curve
4. Results
5. Thanks
6. Conclusions
7. References

Author Name (s)
Email Correspondence to Author
References

Intellectual Property Requirements for editing:

-Authentic Signature in Color of Originality Format Author and Coauthors
-Authentic Signature in Color of the Acceptance Format of Author and Coauthors

Reservation of Editorial Policy

ECORFAN Handbooks se reserva el derecho de hacer los cambios editoriales requeridos para adecuar la Obra Científica a la Política Editorial del ECORFAN Handbooks. Una vez aceptada la Obra Científica en su versión final, el ECORFAN Handbooks enviará al autor las pruebas para su revisión. ECORFAN® únicamente aceptará la corrección de erratas y errores u omisiones provenientes del proceso de edición de la revista reservándose en su totalidad los derechos de autor y difusión de contenido. No se aceptarán supresiones, sustituciones o añadidos que alteren la formación de la Obra Científica.

Code of Ethics - Good Practices and Declaration of Solution to Editorial Conflicts

Declaration of Originality and unpublished character of the Scientific Work, of Authorship, on the obtaining of data and interpretation of results, Acknowledgments, Conflict of interests, Assignment of rights and distribution

The ECORFAN-Mexico, S.C Directorate asserts to the Authors of the Scientific Work that its content must be original, unpublished and of Scientific, Technological and Innovation content to be submitted for evaluation.

The Authors signing the Scientific Work must be the same that have contributed to its conception, realization and development, as well as the obtaining of data, interpretation of the results, its writing and revision. The Correspondent Author of the proposed Scientific Work will request the form that follows.

Title of the Scientific Work:

– The sending of a Scientific Work to ECORFAN Handbooks emanates the commitment of the author not to submit it simultaneously to the consideration of other serial publications for it must complement the Format of Originality for its Scientific Work, unless it is rejected by the Arbitration Committee, may be withdrawn.

– None of the data presented in this Scientific Work has been plagiarized or invented. The original data are clearly distinguishable from those already published. And you have knowledge of the test in PLAGSCAN if a level of plagiarism is detected Positive will not proceed to arbitrate.

– References are cited on which the information contained in the Scientific Work is based, as well as theories and data from other previously published Scientific Works.

– The authors sign the Authorization Form for their Scientific Work to be disseminated by means that ECORFAN-Mexico, S.C. in its Holding Mexico consider relevant for the dissemination and dissemination of its Scientific Work by giving up its Scientific Work Rights.

– The consent of those who have provided unpublished data obtained by verbal or written communication has been obtained, and such communication and authorship are adequately identified.

– The Author and Co-Authors who sign this work have participated in its planning, design and execution, as well as in the interpretation of the results. They also critically reviewed the paper, approved its final version and agreed with its publication.

– No signature responsible for the work has been omitted and the criteria of Scientific Authorization are satisfied.

– The results of this Scientific Work have been interpreted objectively. Any result contrary to the point of view of those who sign is exposed and discussed in the Scientific Work.

Copyright and Access

The publication of this Scientific Work entails the transfer of the copyright to ECORFAN-Mexico, SC in its Mexico Holding for its ECORFAN Handbooks, which reserves the right to distribute on the Web the published version of the Scientific Work and the making available of the Scientific Work in this format supposes for its Authors the fulfillment of what is established in the Law of Science and Technology of the United States of Mexico, regarding the obligation to allow access to the results of Scientific Research.

Title of the Scientific Work:

Name and surnames of the Contact Author and the Coauthors	Signature
1.	
2.	
3.	
4.	

Principles of Ethics and Declaration of Solution to Editorial Conflicts

Publisher Responsibilities

The Publisher undertakes to guarantee the confidentiality of the evaluation process, it may not disclose to the Arbitrators the identity of the Authors, nor may it reveal the identity of the Arbitrators at any time.

The Editor assumes the responsibility of properly informing the Author of the phase of the editorial process in which the text is sent, as well as the resolutions of Double Blind Arbitration.

The Editor must evaluate the manuscripts and their intellectual content without distinction of race, gender, sexual orientation, religious beliefs, ethnicity, nationality, or the political philosophy of the Authors.

The Editor and his editing team of ECORFAN® Holdings will not disclose any information about the Scientific Work sent to anyone other than the corresponding Author.

The Editor must make fair and impartial decisions and ensure a fair peer arbitration process.

Responsibilities of the Editorial Board

The description of the processes of peer review is made known by the Editorial Board in order that the Authors know the evaluation criteria and will always be willing to justify any controversy in the evaluation process. In case of Detection of Plagiarism to the Scientific Work the Committee notifies the Authors for Violation to the Right of Scientific, Technological and Innovation Authorization.

Responsibilities of the Arbitration Committee

The Arbitrators undertake to notify about any unethical conduct by the Authors and to indicate all the information that may be reason to reject the publication of the Scientific Work. In addition, they must commit to keep confidential information related to the Scientific Work that they evaluate.

Any manuscript received for your arbitration must be treated as confidential, must not be displayed or discussed with other experts, except with the permission of the Editor.

The Referees should conduct themselves objectively, any personal criticism of the Author is inappropriate.

The Arbitrators must express their points of view with clear and valid arguments that contribute to the Scientific, Technological and Innovation of the Author.

The Arbitrators should not evaluate the manuscripts in which they have conflicts of interest and that they have been notified to the Editor before submitting the Scientific Work to evaluation.

Responsibilities of Authors

Authors must ensure that their Scientific Works are the product of their original work and that the data have been obtained in an ethical manner.

Authors must ensure they have not been previously published or are not being considered in another serial publication.

Authors must strictly follow the rules for the publication of Scientific Works defined by the Editorial Board.

Authors should consider that plagiarism in all its forms constitutes unethical editorial conduct and is unacceptable, consequently any manuscript that incurs plagiarism will be removed and not considered for publication.

Authors should cite publications that have been influential in the nature of the Scientific Work submitted to arbitration.

Information services

Indexing - Bases and Repositories

RESEARCH GATE (Germany)
MENDELEY (Bibliographic References Manager)
GOOGLE SCHOLAR (Citation indices-Google)
REDIB Ibero-American Network of Innovation and Scientific Knowledge-CSIC

Publishing Services

Citation and Index Identification H
Management of Originality Format and Authorization
Testing of Handbooks with PLAGSCAN
Evaluation of Scientific Work
Issuance of Certificate of Arbitration
Edition of Scientific Work
Web layout
Indexing and Repository
Publication of Scientific Work
Certificate of Scientific Work
Editing Service Billing

Editorial Policy and Management

143 – 50 Itzopan, Ecatepec de Morelos–Mexico. Phones: +52 1 55 6159 2296, +52 1 55 1260 0355, +52 1 55 6034 9181; Email: contact@ecorfan.org www.ecorfan.org

ISBN 978-607-8695-58-4

www.ecorfan.org